Preimplation Diagnosis for Single-Gene Disorders

3

Single-gene disorders are the first group of indications for which preimplantation genetic diagnosis (PGD) was originally introduced 21 years ago, with the purpose of performing genetic testing before pregnancy, in order to establish only unaffected pregnancies and avoid the need for pregnancy termination, which is the major limitation of traditional prenatal diagnosis [1, 2]. Despite the requirement for ovarian hyperstimulation and in vitro fertilization (IVF), needed to perform genetic testing of oocyte or embryo prior to transfer, PGD has been accepted in most parts of the world [3, 4]. At least 10,000 PGD cycles were performed for single-gene disorders and, as will be shown below, is presently offered for some indications that have never been practiced in prenatal diagnosis, such as late-onset diseases with genetic predisposition, and preimplantation HLA typing, making PGD not only an alternative but also a complement to prenatal diagnosis [5–8]. The progress of PGD has been extensively reviewed, so the present book will mainly concentrate on those aspects of PGD that are useful for reproductive medicine and genetics practices, including available PGD approaches for different groups of genetic disorders, their accuracy, and major indications compared to prenatal diagnosis, and present practical details useful for the realization of PGD for each of the conditions described.

Indications for PGD were initially similar to those practiced in prenatal diagnosis and applied for those at-risk couples that could not accept pregnancy termination, expected in 25–50% of cases following prenatal diagnosis, depending on the mode of inheritance. However, these indications have been extended beyond those for prenatal diagnosis, and currently include the conditions with a low penetrance, late-onset disorders with genetic predisposition, and HLA typing with or without testing for causative genes [8]. The list of disorders, for which PGD has been applied, according to our experience, now comprises close to 300 conditions (Table 3.1), with most frequent ones still being cystic fibrosis (CFTR), hemoglobin disorders, and some of the dynamic mutations, such as myotonic dystrophy. Initially, the choice between prenatal diagnosis and PGD mainly depended on the patient's attitude to termination of pregnancy, which is strongly influenced by social and religious factors, but steadily it is becoming a part of family planning for couples at risk to ensure having only unaffected pregnancy, especially when there is a risk of having offspring with severe late-onset common disorders with a strong genetic predisposition [8]. However, the majority of patients are still unaware of the availability of PGD, due to a relative novelty of the procedure. So there is an obvious need for increasing awareness of PGD both for couples at risk and the medical profession, who require information about benefits, accuracy, safety, and expected risks of the procedure.

Tables 3.2 and 3.3 present our overall data of 2,158 PGD cycles for single-gene disorders, which is the world's largest experience in one center. A total of 938 of these cycles were performed by PB approach, involving the retrieval and testing

A. Kuliev, *Practical Preimplantation Genetic Diagnosis*,
DOI 10.1007/978-1-4471-4090-0_3, © Springer-Verlag London 2012

Table 3.1 List of diseases and genes for which PGD was performed

Disease	MIM number	Inheritance	Gene name/ symbol	Protein name	Location
Achondroplasia (ACH)	100800	AD	FGFR3	Fibroblast growth factor receptor 3 [Precursor]	4 p16.3
Acyl-CoA dehydrogenase, medium-chain, deficiency	201450	AR	ACADM	Acyl-CoA dehydrogenase, medium-chain specific, mitochondrial [Precursor]	1p31
Acyl-CoA dehydrogenase, very long-chain (ACADVL)	609575	AR	ACADVL	Acyl-coenzyme A dehydrogenase, very long chain	17p13-p11
Adenosine deaminase deficiency (ADA)	102700	AR	ADA	Adenosine deaminase	20q13.11
Adenomatous polyposis of the colon (APC)	175100	AD	APC	Adenomatous polyposis coli protein	5q21-q22
Adrenoleukodystrophy (ALD)	300100	XL	ABCD1	Adrenoleukodystrophy protein	Xq28
Agammaglobulinemia, X-linked (XLA)	300755	XL	BTK	Bruton agammaglobuline-mia tyrosine kinase	Xq21.3-q22
Aicardi-Goutieres syndrome 1 (AGS1)	225750	AR	TREX1	Three prime repair exonuclease 1	3p21.31
Aicardi-Goutieres syndrome 5 (AGS5)	612952	AR	SAMHD1	SAM domain and HD domain 1	20pter-q12
Albinism, ocular, type I (OA1)	300500	XL	OA1	G-protein coupled receptor 143	Xp22.3
Alopecia universalis congenita (ALUNC)	203655	AR	HR	Hairless protein	8p21.2
Alpers diffuse degeneration of cerebral gray matter with hepatic cirrhosis	203700	AR	POLG	Mitochondrial DNA polymerase gamma	15q25
Alpha 1 antitrypsin deficiency (AAT)	107400	AR	SERPINA1	Alpha-1-antitrypsin [Precursor]	14q32.1
Alport syndrome, X-linked (ATS)	301050	XL	AMMECR1	AMME syndrome candidate gene 1 protein	Xq22.3
Alzheimer disease 3	607822	AD	PSEN1	Presenilin 1	14q24.3
Alzheimer disease 4	606889	AD	PSEN2	Presenilin 2 (Alzheimer disease 4)	1q31-q42
Amyloidosis I, hereditary neuropathic	176300	AD	TTR	Transthyretin [Precursor]	18q11.2-q12.1
Amyotrophic lateral sclerosis 1 (ALS1)	105400	AD	SOD1	Superoxide dismutase 1, soluble	21q22.11
Androgen receptor (AR) (testicular feminization; spinal and bulbar muscular atrophy; Kennedy disease)	313700	XL	AR	AR protein	Xq11-q12
Aneuploidies by STR genotyping					
Angelman syndrome	105830	AD	UBE3A	Ubiquitin protein ligase E3A	15q11.2
Angioedema, hereditary (HAE)	106100	AD	SERPING1	Plasma protease C1 inhibitor precursor	11q11-q13.1
Argininosuccinic aciduria	207900	AR	ASL	Argininosuccinate lyase	7cen-q11.2
Arthrogryposis, distal, type 2B (DA2B)	601680	AD	TNNT3	Troponin T type 3 (skeletal, fast)	11p15.5

Table 3.1 (continued)

Disease	MIM number	Inheritance	Gene name/ symbol	Protein name	Location
Ataxia-telangiectasia (AT)	208900	AR	ATM	Serine-protein kinase ATM	11q22-q23
Basal cell nevus syndrome (BCNS; Gorlin)	109400	AD	PTCH	Patched protein homolog 1	9q22.1-31
Beta-hydroxyisobutyryl CoA deacylase, deficiency	250620	AR	HIBCH	3-Hydroxyisobutyryl-coenzyme A hydrolase	2q32.2
Blepharophimosis, ptosis, and epicanthus inversus (BPES)	110100	AD	FOXL2	Forkhead box protein L2.	3 q23
Blood group – Kell-Cellano system	110900	AD	KEL	Kell blood group glycoprotein	7q33
Brachydactyly, type B1 (BDB1)	113000	AD	ROR2	Receptor tyrosine kinase-like orphan receptor 2	9q22
Brain tumor, posterior fossa of infancy, familial	601607	AD	SMARCB1	SWI/SNF related, matrix associated, actin dependent regulator of chromatin subfamily B member	22q11.2
Breast cancer, familial	113705	AD	BRCA1	Breast cancer type 1 susceptibility protein	17q21
Breast-ovarian cancer, familial, susceptibility to	612555	AD	BRCA2	Breast cancer 2	13q12.3
Canavan disease	271900	AR	ASPA	Aspartoacylase	17pter-p13
Carbamoyl phosphate synthetase I (CPS I) deficiency	237300	AR	CPS1	Carbamoyl-phosphate synthase 1, mitochondrial	2q35
Cardioencephalomyopathy, fatal infantile, due to cytochrome c oxidase deficiency	604377	AR	SCO2	SCO cytochrome oxidase deficient homolog 2 (yeast)	22q13.33
Cardiomyopathy, dilated, 1A (CMD1A)	115200	AD	LMNA	Lamin A/C	1q21.2
Cardiomyopathy, dilated, 1DD (CMD1DD)	613172	AD	RBM20	RNA binding motif protein 20	10q25.2
Cardiomyopathy, familial hypertrophic, 1 (CMH1)	192600	AD	MYH7	Myosin, heavy chain 7, cardiac muscle, beta	14q12
Cardiomyopathy, familial hypertrophic, 4 (CMH4)	115197	AD	MYBPC3	Myosin binding protein C, cardiac	11p11.2
Cardiomyopathy, familial hypertrophic, 7 (CMH7)	613690	AD	TNNI3	Troponin I type 3 (cardiac)	19q13.4
Carnitine deficiency, systemic primary (CDSP)	212140	AR	SLC22A5	Solute carrier family 22 (organic cation/carnitine transporter), member 5	5q31
Carnitine deficiency, systemic primary (CDSP)	212140	AR	SLC2A10	Solute carrier family 2 (facilitated glucose transporter), member 10	20q13.1
Carnitine palmitoyltransferase II deficiency, lethal neonatal	608836	AR	CPT2	Carnitine palmitoyltransferase 2	1p32
Ceroid lipofuscinosis, neuronal 2, late infantile (CLN2)	204500	AR	CLN2	Tripeptidyl-peptidase I [Precursor]	11p15

(continued)

Table 3.1 (continued)

Disease	MIM number	Inheritance	Gene name/ symbol	Protein name	Location
Charcot-Marie-Tooth disease, axonal, type 2E	607684	AD	NEFL	Neurofilament triplet L protein	8p21
Charcot-Marie-Tooth disease, demyelinating, type 1A (CMT1A)	118220	AD	PMP22	Peripheral myelin protein 22	17p12
Charcot-Marie-Tooth disease, demyelinating, type 1B (CMT1B)	118200	AD	MPZ	Myelin P0 protein [Precursor]	1q23.3
Charcot-Marie-Tooth disease, X-linked, 1 (CMTX1)	302800	XL	GJB1	Gap junction beta-1 protein	Xq13.1
Cholestasis, progressive familial intrahepatic 2	603201	AR	ABCB11	ATP-binding cassette, sub-family B (MDR/TAP), member 11	2q24
Chondrodysplasia punctata 1, X-linked recessive (CDPX1)	302950	XL	ARSE	Arylsulfatase E	Xp22.3
Choroideremia (CHM)	303100	XL	CHM	Rab proteins geranylgeranyltransferase component A 1	Xq21.2
Ciliary dyskinesia, primary, 3 (CILD3)	608644	AR	DNAH5	Dynein, axonemal, heavy chain 5	5p15.2
Citrullinemia, classic	215700	AR	ASS1	Argininosuccinate synthase 1	9q34.1
Coenzyme Q10 deficiency	607426	AR	COQ2	Coenzyme Q2 homolog, prenyltransferase	4q21.23
Cohen syndrome (COH1)	216550	AR	VPS13B	Vacuolar protein sorting 13 homolog B	8q22.2
Collagen, type IV, alpha-5 (COL4A5)	303630	XL	COL4A5	Collagen, type IV, alpha 5	Xq22.3
Colorectal cancer, hereditary nonpolyposis, type 1 (HNPCC1)	120435	AD	MSH2	DNA mismatch repair protein Msh2	2p 2-p21
Colorectal cancer, hereditary nonpolyposis, type 1 (HNPCC1)	600678	AD	MSH6	mutS homolog 6 (*E. coli*)	2p16
Colorectal cancer, hereditary nonpolyposis, type 2 (HNPCC2)	609310	AD	MLH1	DNA mismatch repair protein Mlh1	3 p21.3
Congenital adrenal hyperplasia (CAH)	201910	AR	CYP21A2	Cytochrome P450 XXIB	6 p21.3
Congenital disorder of glycosylation, type I (CDG1A)	212065	AR	PMM2	Phosphomannomutase 2	16p13.3-p13.2
Corneal dystrophy, Avellino type (CDA)	607541	AD	TGFB1	Keratoepithelin	5q31
Craniofacial dysostosis, type I (CFD1)	123500	AD	FGFR2	Fibroblast growth factor receptor 2 [Precursor]	10q26.13
Currarino syndrome	176450	AD	HLXB9	Homeobox protein HB9	7q36
Cutis laxa, autosomal recessive, type I	219100	AR	FBLN4	EGF-containing fibulin-like extracellular matrix protein 2	11q13

Table 3.1 (continued)

Disease	MIM number	Inheritance	Gene name/ symbol	Protein name	Location
Cystic fibrosis (CF)	219700	AR	CFTR	Cystic fibrosis transmembrane conductance regulator	7q31.2
Cystinosis, nephropathic (CTNS)	219800	AR	CTNS	Cystinosin	17p13
Darier-White disease (DAR)	124200	AD	ATP2A2	Sarcoplasmic/endoplasmic reticulum calcium ATPase 2	12q23-q24.1
D-bifunctional protein deficiency	261515	AR	HSD17B4	Hydroxysteroid (17-beta) dehydrogenase 4	5q21
Deafness, neurosensory, autosomal recessive 1 (DFNB1)	220290	AR	GJB2	Gap junction protein connexin-26	13q11-q12
Diamond-Blackfan anemia (DBA)	105650	AD	RPS19	40S ribosomal protein S19	19q13.2
Dihydroxyadenine urolithiasis	102600	AD	APRT	Adenine phosphoribosyltransferase	16q24
Donohue syndrome	246200	AR	INSR	Insulin receptor	19p13.3-p13.2
Dyskeratosis congenita, autosomal dominant, 1 (DKCA1)	127550	AD	TINF2	TERF1 (TRF1)-interacting nuclear factor 2	14q12
Dystonia 1, torsion, autosomal dominant (DYT1)	128100	AD	TOR1A	Torsin family 1, member A (torsin A)	9q34
Dystrophia myotonica 1	160900	AD	DMPK	Myotonin-protein kinase	19q13.2-q13.3
Early-onset familial Alzheimer disease	104760	AD	APP	Amyloid beta A4 protein [Precursor]	21q21.3
Ectodermal dysplasia, anhidrotic	224900	AR	EDAR	Tumor necrosis factor receptor superfamily member EDAR [Precursor]	2q 11-q13
Ectodermal dysplasia, hypohidrotic, X-linked (XHED)	305100	XL	EDA	Ectodysplasin A	Xq12-q13.1
Ectrodactyly, ectodermal dysplasia, and cleft lip/palate syndrome 1 (EEC1)	129900	AD	p63	Tumor protein 63	7q11.2-q21.3
Ehlers-Danlos syndrome, type I	130000	AD	COL5A1	Collagen, type V, alpha 1	9q34.2-q34.3
Ehlers-Danlos syndrome, type IV	130050	AD	COL3A1	Collagen, type III, alpha 1	2q31
Ehlers-Danlos syndrome, type VI	225400	AR	PLOD1	Procollagen-lysine 1, 2-oxoglutarate 5-dioxygenase 1	1p36.22
Ehlers-Danlos syndrome, type VIIC	225410	AR	ADAMATS2	ADAM metallopeptidase with thrombospondin type 1 motif, 2	5q35.3
Emery-Dreifuss muscular dystrophy, autosomal recessive (EDMD3)	604929	AR	LMNA	Lamin A/C	1q21.2
Emery-Dreifuss muscular dystrophy, X-linked (EDMD)	310300	XL	EMD	Emerin	Xq28
Epidermolysis bullosa dystrophica, Pasini type	131750	AR	COL7A1	Collagen alpha 1(VII) chain [Precursor]	3 p21.3

(continued)

Table 3.1 (continued)

Disease	MIM number	Inheritance	Gene name/ symbol	Protein name	Location
Epidermolysis bullosa letalis	226650	AR	LAMB3	Laminin, beta 3	1q32
Epidermolysis bullosa simplex with pyloric atresia	612138	AR	PLEC1	Plectin 1, intermediate filament binding protein 500kDa	8q24
Epidermolysis bullosa, junctional, Herlitz type	226700	AR	LAMA3	Laminin, alpha 3	18q11.2
Epileptic encephalopathy, early infantile, 2	300672	XL	CDKL5	Cyclin-dependent kinase-like 5	Xp22
Epiphyseal dysplasia, multiple, 1 (EDM1)	132400	AD	COMP	Cartilage oligomeric matrix protein [Precursor]	19p13.1
Exostoses, multiple, type I	133700	AD	EXT1	Exostosin-1	8q24.11-q24.13
Exostoses, multiple, type II	133701	AD	EXT2	Exostosin 2	11p12-p11
Fabry disease	301500	XL	GLA	Alpha-galactosidase A [Precursor]	Xq22
Facioscapulohumeral muscular dystrophy 1a (FSHMD1a)	158900	AD	FRG1	FRG1 protein	4 q35
Familial Mediterranean fever gene (MEFV)	608107	AR	MEFV	Mediterranean fever protein	16p13
Fanconi anemia, complementation group C (FANCC)	227645	AR	FANCC	Fanconi anemia group C protein	9q22.3
Fanconi anemia, complementation group D2 (FANCD2)	227650	AR	FANCD2	Fanconi anemia, complementation group D2	3p26
Fanconi anemia, complementation group E (FANCE)	600901	AR	FANCE	Fanconi anemia, complementation group E	6p22-p21
Fanconi anemia, complementation group F (FANCF)	603467	AR	FANCF	Fanconi anemia group F protein	11p15
Fanconi anemia, complementation group G	602956	AR	FANCG	DNA-repair protein XRCC9	9p13
Fanconi anemia, complementation group I (FANCI)	609053	AR	FANCI	Fanconi anemia, complementation group I	15q26.1
Fanconi anemia, complementation group J	609054	AR	BRIP1	Fanconi anemia group J protein	17q22
Fancony anemia, complementation group A; FANCA	227650	AR	FANCA	Fanconi anemia group A protein	16q24.3
Fragile site mental retardation 1	309550	XL	FMR1	Fragile X mental retardation 1 protein	Xq27.3
Fragile site, folic acid type, rare, FRA(X)(q28) (FRAXE)	309548	XL	FMR2	Fragile X mental retardation 2 protein	Xq28
Fraser syndrome	219000	AR	FRAS1	Fraser syndrome 1 protein	4q21.21
Friedreich ataxia 1 (FRDA)	229300	AR	FRDA	Frataxin, mitochondrial precursor	9q13
Galactosemia	230400	AR	GALT	Galactose-1-phosphate Uridylyltransferase	9p13
Gangliosidosis, generalized GM1, type I	230500	AR	GLB1	Galactosidase, beta 1	3p21.33

Table 3.1 (continued)

Disease	MIM number	Inheritance	Gene name/ symbol	Protein name	Location
Gastric cancer, hereditary diffuse (HDGC)	137215	AD	CDH1	Cadherin 1, type 1, E-cadherin	16q22.1
Gaucher disease, type I	230800	AR	GBA	Glucosylceramidase [Precursor]	1q21
Geroderma osteodysplasticum (GO)	231070	AR	SCYL1BP1	SCY1-like 1 binding protein 1	1q24.2
Gerstmann-Straussler disease (GSD)	137440	AD	PRNP	Prion protein	20p13
Glaucoma 3, primary congenital, A (GLC3A)	231300	AR	CYP1B1	Cytochrome P450, family 1, subfamily B, polypeptide 1	2p21
Glucose transport defect, blood–brain barrier	606777	AD	SLC2A1	Solute carrier family 2 (facilitated glucose transporter), member 1	1p35-p31.3
Glucose-6-phosphate dehydrogenase (G6PD)	305900	XL	G6PD	Glucose-6-phosphate dehydrogenase	Xq28
Glutaric acidemia I	231670	AR	GCDH	Glutaryl-coenzyme A dehydrogenase	19p13.2
Glycogen storage disease I	232200	AR	G6PC	Glucose-6-phosphatase, catalytic subunit	17q21
Glycogen storage disease II	232300	AR	GAA	Glucosidase, alpha; acid	17q25.2-q25.3
Glycogen storage disease type VI	232700	AR	PYGL	Glycogen phosphorylase, liver form	14q21-q22
Granulomatous disease, chronic	233710	AR	NCF2	Neutrophil cytosolic factor 2	1q25
Granulomatous disease, chronic, X-linked (CGD)	306400	XL	CYBB	Cytochrome b-245, beta polypeptide	Xp21.1
Griscelli syndrome with hemophagocytic syndrome, type 2 (GS2)	607624	AR	RAB27A	RAB27A, member RAS oncogene family	15q15-q21.1
Hemochromatosis (HFE)	235200	AR	HFE	Hemochromatosis	6p21.3
Hemoglobin–alpha locus 1 (HBA1)	141800	AR	HBA1	Hemoglobin alpha chain	16pter-p13.3
Hemoglobin–alpha locus 2 (HBA2)	141850	AR	HBA2	Hemoglobin alpha subunit	16pter-p13.3
Hemoglobin–beta locus (HBB)	141900	AR	HBB	Hemoglobin beta chain	11p15.5
Hemophagocytic lymphohistiocytosis, familial, 2	603553	AR	PRF1	Perforin 1 [Precursor]	10q22
Hemophagocytic lymphohistiocytosis, familial, 3 (FHL3)	608898	AR	UNC13D	unc-13 homolog D	17q25.1
Hemophagocytic lymphohistiocytosis, familial, 4 (FHL4)	603552	AR	STX11	Syntaxin 11	6q24.2
Hemophilia A	306700	XL	F8	Coagulation factor VIII [Precursor]	Xq28
Hemophilia B	306900	XL	F9	Coagulation factor IX [Precursor]	Xq27.1-q27.2
Hereditary motor and sensory neuropathy VI	601152	AD	MFN2	Mitofusin 2	1p36.22

(continued)

Table 3.1 (continued)

Disease	MIM number	Inheritance	Gene name/ symbol	Protein name	Location
HLA matching genotyping					6 q21.3
Holt-Oram syndrome (HOS)	142900	AD	TBX5	T-box 5	12q24.1
Homocystinuria due to deficiency of N(5,10)-methylenetetrahydrofolate reductase activity	236250	AR	MTHFR	Methylenetetrahydrofolate reductase	1p36.3
Hoyeraal-Hreidarsson syndrome (HHS)	300240	XL	DKC1	H/ACA ribonucleoprotein complex subunit 4	Xq28
Huntington disease (HD)	143100	AD	HTT	Huntingtin	4 p16.3
Hurler syndrome	607014	AR	IDUA	Alpha-L-iduronidase [Precursor]	4 p16.3
Hyalinosis, infantile systemic	236490	AR	ANTXR2	Anthrax toxin receptor 2	4q21
Hydrocephalus, X-linked (L1CAM)	308840	XL	L1CAM	Neural cell adhesion molecule L1 [Precursor]	Xq28
Hyperglycinemia, nonketotic (NKH)	605899	AR	AMT	Aminomethyltransferase	3p21.2-p21.1
Hyperglycinemia, nonketotic (NKH)	605899	AR	GLDC	Glycine dehydrogenase	9p22
Hyper-IgE recurrent infection syndrome	147060	AD	STAT3	Signal transducer and activator of transcription 3 (acute-phase response factor)	17q21.31
Hyperinsulinemic hypoglycemia, familial, 1 (HHF1)	256450	AR	ABCC8	ATP-binding cassette, sub-family C (CFTR/MRP), member 8	11p15.1
Hypomagnesemia, renal, with ocular involvement	248190	AR	CLDN16	Claudin 16	3q28
Hypophosphatasia, infantile	241500	AR	ALPL	Alkaline phosphatase, tissue-nonspecific isozyme [Precursor]	1p36.1-34
Hypophosphatemic rickets, X-linked dominant	307800	XL	PHEX	Phosphate regulating endopeptidase homolog	Xp22.2-p22.1
Ichthyosis follicularis, atrichia, and photophobia syndrome	308205	XL	MBTPS2	Membrane-bound transcription factor peptidase, site 2	Xp22.13
Ichthyosis, lamellar, 1 (LI1)	190195	AD	TGM1	Transglutaminase 1 (K polypeptide epidermal type I, protein-glutamine gamma-glutamyltransferase)	14q11.2
Ichthyosis, lamellar, 2 (LI2)	601277	AR	ABCA12	ATP-binding cassette, sub-family A (ABC1), member 12	2q34
Immunodeficiency due to defect in CD3-zeta	610163	AR	CD247	CD247 molecule	1q22-q23
Immunodeficiency with hyper-IgM, type 1 (HIGM1)	308230	XL	CD40LG	Tumor necrosis factor ligand superfamily member 5	Xq26
Immunodysregulation, polyendocrinopathy, and enteropathy, X-linked (IPEX)	304790	XL	FOXP3	Forkhead box P3	Xp11.23-q13.3
Incontinentia pigmenti (IP)	308300	XL	IKBKG	NF-kappa-B essential modulator	Xq28

Table 3.1 (continued)

Disease	MIM number	Inheritance	Gene name/ symbol	Protein name	Location
Isovaleric acidemia (IVA)	243500	AR	IVD	Isovaleryl coenzyme A dehydrogenase	15q14-q15
Joubert syndrome 3 (JBTS3)	608629	AR	AHI1	Abelson helper integration site 1	6q23.3
Joubert syndrome 6 (JBTS6)	610688	AR	TMEM67	Transmembrane protein 67	8q22.1
Juvenile myelomonocytic leukemia (JMML)	607785	AD	NRAS	Neuroblastoma RAS viral (v-ras) oncogene homolog	1p13.2
Kallmann syndrome 2	147950	AD	FGFR1	Fibroblast growth factor receptor 1	8p11.2-p11.1
Krabbe disease	245200	AR	GALC	Galactocerebrosidase [Precursor]	14q31
Leber congenital amaurosis 2 (LCA2)	204100	AR	RPE65	Retinal pigment epithelium-specific protein 65kDa	1p31
Leber congenital amaurosis 6	605446	AR	RPGRIP1	Retinitis pigmentosa GTPase regulator interacting protein 1	14q11
Leigh syndrome (LS)	185620	AR	SURF1	Surfeit locus protein 1	9q34.2
Leri-Weill dyschondrosteosis (LWD)	127300	XL	SHOX	Short stature homeobox	Xp22.33;Yp11.3
Leukoencephalopathy with vanishing white matter (VWM)	603896	AR	EIF2B2	Translation initiation factor eIF-2B beta subunit	14q24
Leukoencephalopathy with vanishing white matter (VWM)	603896	AR	EIF2B4	Eukaryotic translation initiation factor 2B, subunit 4 delta, 67kDa	2p23.3
Leukoencephalopathy with vanishing white matter (VWM)	603896	AR	EIF2B5	Eukaryotic translation initiation factor 2B, subunit 5 epsilon, 82kDa	3q27.1
Li-Fraumeni syndrome 1 (LFS1)	151623	AD	TP53	Cellular tumor antigen p53	17p13.1
Lipoid congenital adrenal hyperplasia	201710	AR	STAR	Steroidogenic acute regulatory protein	8p11.2
Loeys-Dietz syndrome (LDS)	609192	AD	TGFBR2	Transforming growth factor, beta receptor II (70/80kDa)	3p22
Long-chain 3-hydroxyacyl-CoA dehydrogenase deficiency (HADHA)	600890	AR	HADHA	Trifunctional enzyme alpha subunit, mitochondrial [Precursor]	2p 3
Lymphedema-distichiasis syndrome	153400	AD	FOXC2	Forkhead box C2	16q24.1
Machado-Joseph disease (MJD)	109150	AD	ATX3	Machado-Joseph disease protein 1	14q24.3-q31
Marfan syndrome (MFS)	154700	AD	FBN1	Fibrillin 1 [Precursor]	15q21.1
Meckel syndrome, type 4 (MKS4)	611134	AR	CEP290	Centrosomal protein 290kDa	12q21.32
Meckel syndrome, type 6 (MKS6)	612284	AR	CC2D2A	coiled-coil and C2 domain containing 2A	4p15.32
Metachromatic leukodystrophy	250100	AR	ARSA	Arylsulfatase A [Precursor]	22q13.31-qter
Metaphyseal chondrodysplasia, Schmid type (MCDS)	156500	AD	COL10A1	Collagen, type X, alpha 1	6q21-q22

(continued)

Table 3.1 (continued)

Disease	MIM number	Inheritance	Gene name/ symbol	Protein name	Location
Methylmalonic aciduria	251000	AR	MUT	Methylmalonyl CoA mutase	6p12.3
Microcephaly 3, primary, autosomal recessive (MCPH3)	604804	AR	CDK5RAP2	CDK5 regulatory subunit associated protein 2	9q33.2
Microcoria-congenital nephrosis syndrome	609049	AR	LAMB2	Laminin beta-2	3p21
Microphthalmia, isolated 2 (MCOP2)	610093	AR	VSX2	Visual system homeobox 2	14q24.3
Microtubule-associated protein tau (MAPT)	157140	AD	MAPT	Microtubule-associated protein tau	17q21.1
Migraine, familial hemiplegic, 1 (FHM1)	141500	AD	CACNA1A	Calcium channel, voltage-dependent, P/Q type, alpha 1A subunit	19p13.2-p13.1
Morquio syndrome, nonkeratosulfate-excreting type	252300	AR	GALNS	Galactosamine (N-acetyl)-6-sulfate sulfatase	16q24.3
Mosaic variegated aneuploidy syndrome 1 (MVA1)	257300	AR	BUB1B	Budding uninhibited by benzimidazoles 1 homolog beta	15q15
Mucopolysaccharidosis type II (Hunter) Hunter-McAlpine craniosynostosis syndrome	309900	AD	IDS	Iduronate 2-sulfatase [Precursor]	Xq28
Mucopolysaccharidosis type IIIa	252900	AR	SGSH	N-sulfoglucosamine sulfohydrolase	17q25.3
Mucopolysaccharidosis type VI	253200	AR	ARSB	arylsulfatase B	5q11-q13
Multiple acyl-CoA dehydrogenase deficiency (MADD)	231680	AR	ETFA	Electron-transfer-flavoprotein, alpha polypeptide	15q23-q25
Multiple endocrine neoplasia, type I (MEN1)	131100	AD	MEN1	Multiple endocrine neoplasia I	11q13.1
Multiple endocrine neoplasia, type IIA (MEN2A)	171400	AD	RET	Ret proto-oncogene	10q11.2
Muscular dystrophy, becker type (BMD)	300376	XL	DMD	Dystrophin	Xq21.2
Muscular dystrophy, congenital merosin-deficient, 1A (MDC1A)	607855	AR	LAMA2	Laminin, alpha 2	6q22-q23
Muscular dystrophy, Duchenne type (DMD)	310200	XL	DMD	Dystrophin	Xq21.2
Myoclonic epilepsy of Lafora	254780	AR	NHLRC1	E3 ubiquitin-protein ligase	6p22.3
Myopathy, myofibrillar, desmin-related	601419	AD	DES	Desmin	2q35
Myotonia congenita, autosomal dominant	160800	AD	CLCN1	Chloride channel 1, skeletal muscle	7q32-qter|7q35
Myotonic dystrophy 2 (DM2)	602668	AD	CNBP	CCHC-type zinc finger, nucleic acid binding protein	3q21

Table 3.1 (continued)

Disease	MIM number	Inheritance	Gene name/ symbol	Protein name	Location
Myotubular myopathy 1 (MTM1)	310400	XL	MTM1	Myotubularin	Xq28
N-acetylglutamate synthase deficiency	237310	AR	NAGS	N-acetylglutamate synthase	17q21.31
Nail-patella syndrome (NPS)	161200	AD	LMX1B	LIM homeobox transcription factor 1, beta	9q34
Nephrogenic syndrome of inappropriate antidiuresis	300539	XL	AVPR2	Arginine vasopressin receptor 2	Xq28
Nephrosis 1, congenital, Finnish type (NPHS1)	256300	AR	NPHS1	Nephrosis 1, congenital, Finnish type (nephrin)	19q13.1
Neuraminidase deficiency	256550	AR	NEU1	Sialidase 1 (lysosomal sialidase)	6p21.3
Neurofibromatosis, type I (NF1)	162200	AD	NF1	Neurofibromin	17q11.2
Neurofibromatosis, type II (NF2)	101000	AD	NF2	Merlin	22q12.2
Neuropathy, hereditary sensory and autonomic, type I (HSAN1)	162400	AD	SPTLC1	Serine palmitoyltransferase, long chain base subunit 1	9q22.1-q22.3
Neuropathy, hereditary sensory and autonomic, type III (HSAN3)	223900	AR	IKBKAP	Kinase complex-associated protein	9q31
Niemann-Pick disease, type A	257200	AR	SMPD1	Sphingomyelin phosphodiesterase 1, acid lysosomal	11p15.4-p15.1
Niemann-Pick disease, type C1 (NPC1)	257220	AR	NPC1	Niemann-Pick C1 protein	18q11-q12
Noonan syndrome 1 (NS1)	163950	AD	PTPN11	Protein tyrosine phosphatase, non-receptor type 11	12q24
Noonan syndrome 3 (NS3)	609942	AD	KRAS	v-Ki-ras2 Kirsten rat sarcoma viral oncogene homolog	12p12.1
Noonan syndrome 4 (NS4)	610733	AD	SOS1	Son of sevenless homolog 1	2p22-p21
Norrie disease (NDP)	310600	XL	NDP	Norrin	Xp11.4-p11.3
Oculocutaneous albinism, type I (OCA1)	203100	AR	TYR	Tyrosinase [Precursor]	11q14-q21
Oculocutaneous albinism, type II (OCA2)	203200	AD	OCA2	P protein	15q11.2-q12
Omenn syndrome	603554	AD	RAG1	V(D)J recombination-activating protein 1	11p13
Optic atrophy 1 (OPA1)	165500	AD	OPA1	Dynamin-like 120 kDa protein, mitochondrial [Precursor]	3 q28-q29
Ornithine transcarbamylase deficiency	311250	XL	OTC	Ornithine carbamoyltransferase, mitochondrial [Precursor]	Xp21.1
Osteogenesis imperfecta congenita (OIC)	166200	AD	COL1A1	Collagen alpha 1(I) chain [Precursor]	17q21.31-q22
Osteogenesis imperfecta congenita (OIC)	166200	AD	COL1A2	Collagen alpha 2(I) chain [Precursor]	7q22.1

(continued)

Table 3.1 (continued)

Disease	MIM number	Inheritance	Gene name/ symbol	Protein name	Location
Osteogenesis imperfecta, type IX	259440	AR	PPIB	Peptidylprolyl isomerase B (cyclophilin B)	15q21-q22
Osteopetrosis, autosomal recessive	259700	AR	TCIRG1	Vacuolar proton translocating ATPase 116 kDa subunit a isoform 3	11q13.4-q13.5.
Pachygyria with mental retardation, seizures	600176	AR	WDR62	WD repeat domain 62	19q13.12
Pancreatitis, hereditary (PCTT)	167800	AD	PRSS1	Protease, serine, 1 (trypsin 1)	7q32-qter|7q34
Pelizaeus-Merzbacher-like disease (PMLD)	311601	XL	PLP1	Myelin proteolipid protein	Xq22
Periodic fever, familial, autosomal dominant	142680	AD	TNFRSF1A	Tumor necrosis factor receptor superfamily	12p13.2
Peutz-Jeghers syndrome (PJS)	175200	AD	STK11	Serine/threonine kinase 11	19p13.3
Pfeiffer syndrome	101600	AD	FGFR1	Fibroblast growth factor receptor 1	8p11.2-p11.1
Phenylketonuria	261600	AR	PAH	Phenylalanine-4-hydroxylase	12q22-q24.2
Polycystic kidney disease 1 (PKD1)	601313	AD	PKD1	Polycystin 1 precursor	16P13.3
Polycystic kidney disease 2 (PKD2)	173910	AD	PKD2	Polycystin 2	4 q22.1
Polycystic kidney disease, autosomal recessive (ARPKD)	263200	AR	PKHD1	Polycystic kidney and hepatic disease 1 [Precursor]	6 p12.3
Popliteal pterygium syndrome (PPS)	119500	AD	IRF6	Interferon regulatory factor 6	1q32-q41
Porphyria, congenital erythropoietic	263700	AR	UROS	Uroporphyrinogen III synthase	10q26.2
Propionic acidemia	232000	AR	PCCA	Propionyl coenzyme A carboxylase, alpha polypeptide	13q32
Propionic acidemia	606054	AR	PCCB	Propionyl coenzyme A carboxylase, beta polypeptide	3q21-q22
Prosaposin deficiency (PSAPD)	611721	AR	PSAP	Prosaposin	10q21-q22
Pseudohypoparathyroidism, type IA (PHP1A)	103580	AD	GNAS	Guanine nucleotide binding protein (G protein)	20q13.3
Pseudohypoparathyroidism, type IB (PHP1B)	603233	AD	GNAS	GNAS complex locus	20q13.3
Pseudovaginal perineoscrotal hypospadias	264600	AR	SRD5A2	Steroid-5-alpha-reductase, alpha polypeptide 2	2p23.1
Pyridoxamine 5-prime-phosphate oxidase deficiency	610090	AR	PNPO	Pyridoxamine 5′-phosphate oxidase	17q21.32
Pyruvate kinase deficiency of red cells	266200	AD	PKLR	Pyruvate kinase, liver and RBC	1q21
Restrictive dermopathy, lethal	275210	AR	ZMPSTE24	Zinc metallopeptidase	1p34

Table 3.1 (continued)

Disease	MIM number	Inheritance	Gene name/ symbol	Protein name	Location
Retinitis pigmentosa 4 (RP4);	180380	AD	RHO	Rhodopsin	3q21-q24
Retinitis pigmentosa 3 (RP3)	300389	XL	RPGR	Retinitis pigmentosa GTPase regulator	Xp21.1
Retinoblastoma (RB1)	180200	AD	RB1	Retinoblastoma-associated protein	13q14.1-q14.2
Retinoschisis 1, X-linked, juvenile (RS1)	312700	XL	RS1	Retinoschisin 1	Xp22.13
Rett syndrome (RTT)	312750	XL	MECP2	Methyl-CpG-binding protein 2	Xq28
Rhesus blood group, CcEe antigens (RHCE)	111700	AD	RHCE	CcEe antigens	1p36.2-p34
Rhesus blood group, D antigen (RHD)	111680	AD	RHD	D antigen	1p36.11
Saethre-Chotzen syndrome (SCS)	101400	AD	TWIST1	Twist homolog 1 (Drosophila)	7p21.2
Sandhoff disease	268800	AR	HEXB	Beta-hexosaminidase beta chain [Precursor]	5q13
Severe combined immunodeficiency	601457	AR	RAG2	Recombination activating gene 2	11p13
Severe combined immunodeficiency, X-linked (SCIDX1)	300400	XL	IL2RG	Interleukin 2 receptor, gamma	Xq13.1
Shwachman-Diamond syndrome (SDS)	260400	AR	SBDS	Shwachman-Bodian-Diamond syndrome protein	7q11.21
Sickle cell anemia	603903	AR	HBB	Hemoglobin beta chain	11p15.5
Smith-Lemli-Opitz syndrome (SLOS)	270400	AR	DHCR7	7-dehydrocholesterol reductase	11q12-q13
Sonic hedgehog (SHH)	600725	AD	SHH	Sonic hedgehog protein [Precursor]	7q36
Sotos syndrome	117550	AD	NSD1	Nuclear receptor binding SET domain protein 1	5q35.2-q35.3
Spastic paraplegia 3, autosomal dominant	182600	AD	ATL1	Atlastin GTPase 1	14q22.1
Spastic paraplegia 4, autosomal dominant (SPG4)	182601	AD	SPAST	Spastin	2p24-p21
Spinal muscular atrophy, distal, autosomal recessive	604320	AR	IGHMBP2	Immunoglobulin mu binding protein 2	11q13.3
Spinal muscular atrophy, type I (SMA1)	253300	AD	SMN1	Survival motor neuron protein	5q12.2-q13.3
Spinocerebellar ataxia 1 (SCA1)	164400	AD	ATXN1	Ataxin 1	6p23
Spinocerebellar ataxia 2 (SCA2)	183090	AD	ATX2	SCA2 protein	12q24
Spinocerebellar ataxia 6 (SCA6)	183086	AD	CACNA1A	Voltage-dependent P/Q-type calcium channel alpha-1A subunit	19p13
Spinocerebellar ataxia 7 (SCA7)	164500	AD	SCA7	Ataxin-7	3 p21.1-p12
Spinocerebellar ataxia, autosomal recessive 1	606002	AR	SETX	Senataxin	9q34.13

(continued)

Table 3.1 (continued)

Disease	MIM number	Inheritance	Gene name/ symbol	Protein name	Location
Stickler syndrome, type I (STL1)	108300	AD	COL2A1	Collagen, type II, alpha 1	12q13.11-q13.2
Stickler syndrome, type II (STL2)	604841	AD	COL11A1	Collagen, type XI, alpha 1	1p21
Succinic semialdehyde dehydrogenase deficiency	271980	AR	ALDH5A1	Succinate semialdehyde dehydrogenase, mitochondrial [Precursor]	6 p22
Surfactant metabolism dysfunction, pulmonary, 3 (SMDP3)	610921	AR	ABCA3	ATP-binding cassette, sub-family A (ABC1), member 3	16p13.3
Symphalangism, proximal (SYM1)	185800	AD	NOG	Noggin [Precursor]	17q22
Tay-Sachs disease (TSD)	272800	AR	HEXA	Beta-hexosaminidase alpha chain [Precursor]	15q23-q24
Thrombasthenia of Glanzmann and Naegeli	273800	AR	ITGA2B	Integrin, alpha 2b	17q21.32
Thrombotic thrombocytopenic purpura, congenital (TTP)	274150	AR	ADAMTS13	ADAM metallopeptidase with thrombospondin type 1 motif, 13	9q34
Torsion dystonia 1, autosomal dominant (DYT1)	128100	AD	DYT1	Torsin A [Precursor]	9q34
Treacher Collins-Franceschetti syndrome (TCOF)	154500	AD	TCOF1	Treacle protein	5q32-q33.1
Tuberous sclerosis type 1	191100	AD	TSC1	Hamartin	9q34
Tuberous sclerosis type 2	191100	AD	TSC2	Tuberin	16p13.3
Tyrosinemia, type I	276700	AR	FAH	Fumarylacetoacetate hydrolase (fumarylacetoacetase)	15q23-q25
Ulnar-mammary syndrome (UMS)	181450	AD	TBX3	T-box 3	12q24.1
Von Hippel-Lindau syndrome (VHL)	193300	AD	VHL	Von Hippel-Lindau disease tumor suppressor	3 p26-p25
Waardenburg syndrome, type 2A (WS2A)	193510	AD	MITF	Microphthalmia-associated transcription factor	3p14.2-p14.1
Wiskott-Aldrich syndrome (WAS)	301000	XL	WAS	Wiskott-Aldrich syndrome protein	Xp11.23-p11.22
Wolfram syndrome 1 (WFS1)	222300	AR	WFS1	Wolframin	4p16
Wolman disease	278000	AR	LIPA	Lipase A, lysosomal acid, cholesterol esterase	10q23.2-q23.3
Zellweger syndrome (ZS)	214100	AR	PEX1	Peroxisome biogenesis factor 1	7q21-q22
Zellweger syndrome (ZS)	214100	AR	PEX3	Peroxisomal biogenesis factor 3	6q24.2
Zellweger syndrome (ZS)	214100	AR	PXMP3	Peroxisomal membrane protein 3, 35kDa	8q21.1

Table 3.2 Clinical outcome of 2,158 PGD cycles for Mendelian disorders

Cells tested	Patient	Cycle	Embryo transfers	Number of embryos transferred	Pregnancy	Birth
PB	131	237	188	379	72 (38.3%)	64
PB + BL	422	701	602	1,199	255 (41.4%)	278
Subtotal	*553*	*938*	*790*	*1,578*	*327*	*342*
BL + BC	*653*	*1,220*	*988*	*1,859*	*406*	*389*
Total	*1,206*	*2,158*	*1,778*	*3,437*	*733 (41.2%)*	*731*

PB polar body, BL blastomere, *BC* blastocyst

Table 3.3 Clinical outcome of PGD for Mendelian disorders performed by PB approach

	Cycles	ET	# Embryos transferred	Pregnancy	Birth
Autosomal-recessive					
Polar bodies	115	94	199	33	32
Polar bodies + blastomere/blastocyst	389	334	683	135	155
Subtotal	504	428	882	168	187
Autosomal-dominant					
Polar bodies +	46	37	78	20	17
blastomere/blastocyst	118	105	207	45	47
Subtotal	164	142	285	65	64
X-linked					
Polar bodies +	76	57	102	19	15
blastomere/blastocyst	194	163	309	75	76
Subtotal	270	220	411	94	91
Total	938	790	1,578 (1.99)	327 (41.4%)	342

of 9,036 oocytes, of which 7,653 (97.6%) were with both PB1 and PB2 available for analysis, with the results of sequential PB1 and PB2 testing obtained in 7,841 (97.6%) of these oocytes. This made it possible to preselect for transfer as many as 1,578 embryos originating from these oocytes (1.99 per transfer on an average) in 790 (84.2%) cycles, resulting in 327 pregnancies (41.4%) and the birth of 342 healthy children.

The remaining 1,220 PGD cycles were performed by blastomere or blastocyst biopsy, resulting in the transfer of 1,829 unaffected embryos in 988 cycles, yielding 406 clinical pregnancies and the birth of 389 healthy children. Overall, 2,158 cycles were performed for 1,206 patients at risk of producing offspring with single-gene disorders, which resulted in preselection and transfer of 3,437 unaffected embryos in 1,778 cycles (approximately two embryos per cycle), yielding 731 unaffected pregnancies (41.2% pregnancy rate per transfer) and the birth of 731 apparently healthy children.

3.1 Autosomal-Recessive Diseases

In our experience, more than half of the PGD cycles were performed for autosomal-recessive conditions, with 504 of them using the PB approach (Tables 3.2 and 3.3). The most common indications for PGD were *CFTR and hemoglobin disorders* (HBB), performed for an increasing number of mutations presented in Figs. 3.1 and 3.2.

3.1.1 Hemoglobinopathies

Testing for hemoglobin disorders currently represents the world's largest experience in PGD. For example, in some communities, such as in Cyprus, Greece, and Turkey, PGD is becoming a routine procedure for couples carrying thalassemia mutations who cannot accept prenatal diagnosis and termination of pregnancy [9–11]. Introduced for the first time in 1996 in Cyprus, only 40 PGD cycles for hemoglobin disorders

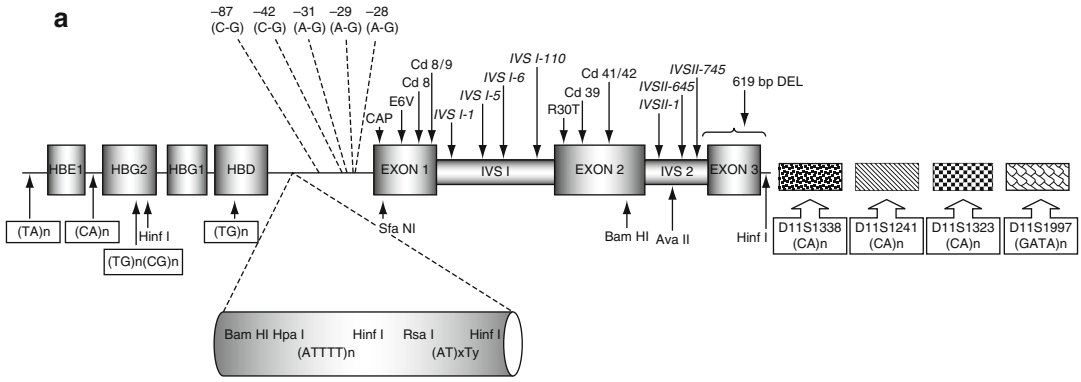

b Polymorphic markers

List of mutations:

RNA Processing mutations:	Transcriptional mutations:	Nonfunctional mRNA:
IVSI–1 (G–A)	–87 (C–G)	Codon 8 (–AA)
IVSI–1 (G–T)	–42 (C–G)	Codon 39 (C–T)
IVSI–5 (G–C)	–31 (A–G)	Codon 41/42 (–CTTT)
IVSI–5 (G–T)	–29 (A–G)	
IVSI–5 (G–A)	–28 (A–G)	
IVSI–6 (T–C)	E 6V (Sickle cell anemia)	
IVSI–110 (G–A)	R30T	
IVS2–1 (G–A)	Deletion:	Cap site:
IVS2–654 (C–T)	619 bp	+1 (A–C)
IVS2–745 (C–G)		+2 (T–C)

Fig. 3.1 Mutations in beta-globin gene for which PGD was performed and polymorphic markers used in multiplex PCR analysis. Map of human beta-globin gene, showing sites and location of mutations (**a**), and linked polymorphic markers used for avoiding misdiagnosis (**b**). List of mutations is also presented in the *lower panel*

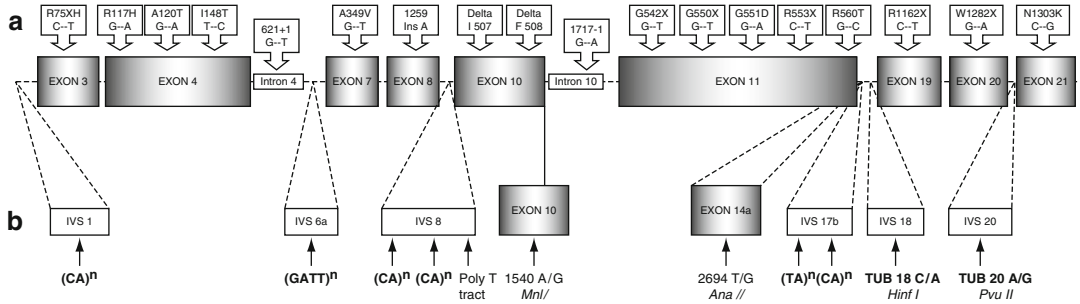

a (Upper level). Mutations in CFTR gene
b (Bottom level). Polymorphic markers in CFTR gene

Fig. 3.2 Mutations in CFTR gene, for which PGD was performed and polymorphic markers used in multiplex PCR analysis. Map of CFTR gene, showing sites and location of mutations (**a**), and polymorphic markers used for avoiding misdiagnosis (**b**)

were performed before the year 2000, with hundreds of cycles performed since then. At the present time, the proportion of PGD cases for hemoglobin disorders in our overall PGD experience of over 2,158 PGD cycles for single-gene disorders is as high as one-quarter.

To improve accuracy of diagnosis of PGD for hemoglobin disorders a set of polymorphic markers, listed in Fig. 3.1, were used, which makes it realistic to select at least three closely linked informative markers in any case performed to analyze simultaneously with mutation testing.

Table 3.4 Clinical outcome of PGD for hemoglobinopathies

Mutation	Number of patients	Number of cycles	Number of transfers	Number of embryos transferred	Pregnancy	Births
IVS-I-1 (*G*>*A*)	9	18	13	20	2	3
IVS-I-5 (*G*>*C*)	10	16	11	17	3	2
IVS-I-6 (*T*>*C*)	21	39	35	71	17	19
IVS-I-110 (G>A)	61	100	88	202	26	24
IVS-II-1 (*G*>*A*)	4	9	5	8	1	2
IVS-II-745 (C>G)	9	23	20	42	3	2
Codon 6 (−A)	1	1	1	3	0	0
Codon 5 (−*CT*)	3	3	2	3	1	1
Codon 8 (−AA)	12	20	17	26	3	4
Codon 39 (C>T)	10	16	14	26	6	7
HB O-Arab [β121(GH4)Glu→Lys]	1	1	1	2	0	0
Codons 41/42 (−TCTT)	7	1	4	10	1	1
−29 (A>G)	1	1	1	1	0	0
−87 (C>G)	1	2	2	2	0	0
Cap +1(*A*>*C*)	2	3	2	2	0	0
HB Monroe [β30(B12)Arg→Thr]	1	12	9	13	0	0
HBB −619 bp deletion	6	13	11	19	2	3
Sicilian delta-beta 0 Thal-deletion of 13378 nts from the delta gene to beta gene	1	4	4	9	1	2
Filipino beta 0 −45 kb deletion	1	1	0	0	0	0
Hb S [β6(A3)Glu→Val]	59	90	80	169	32	32
Hb E [β26(B8)Glu→Lys]	1	2	1	1	0	0
Hb C [β6(A3)Glu→Lys]	1	1	1	2	1	1
α-Thal (45 kb deletion)	4	9	9	17	2	2
Total	226	395	331	665 (2%)	102 (31%)	105

A total of 395 PGD cycles were performed for 226 couples at risk of bearing children with hemoglobin (Hb) disorders. This included nine PGD cycles for alpha-thalassemia (α-thal), 296 for β-thal, and 90 for sickle cell disease. A total of 144 of these cycles were performed in combination with HLA typing to select unaffected embryos as potential donors for stem cell transplantation (see Chap. 4).

Of 395 clinical cycles performed, unaffected embryos for transfer were available in 331 (83.81%), resulting in 102 (30.8%) clinical pregnancies and the birth of 105 healthy children. Because the majority of cases as mentioned were done for Eastern Mediterranean patients, approximately half of the cases were performed for IVS I-110 mutation, which is the most common thalassemia mutation in the Mediterranean region (Table 3.4).

While PGD cycles were mainly performed for heterozygous carriers, eight cycles were done for couples with homozygous or compound heterozygous male or female patients at 50% risk of bearing an affected offspring. In these couples, PGD involved testing for either three different mutations or, in the majority of cases, for two different mutations or the same maternal and paternal mutation. Analysis in these cases was done either simultaneously or in sequence by testing the maternal mutation in PB1 and PB2 and the paternal one in blastomeres.

While beta-globin gene mutations were tested in the majority of cases, α-thal mutations involving a 45 kb deletion were tested in nine cycles performed for four couples, resulting in preselection and transfer of 17 unaffected embryos in nine cycles, yielding two clinical pregnancies and the birth of two unaffected children,

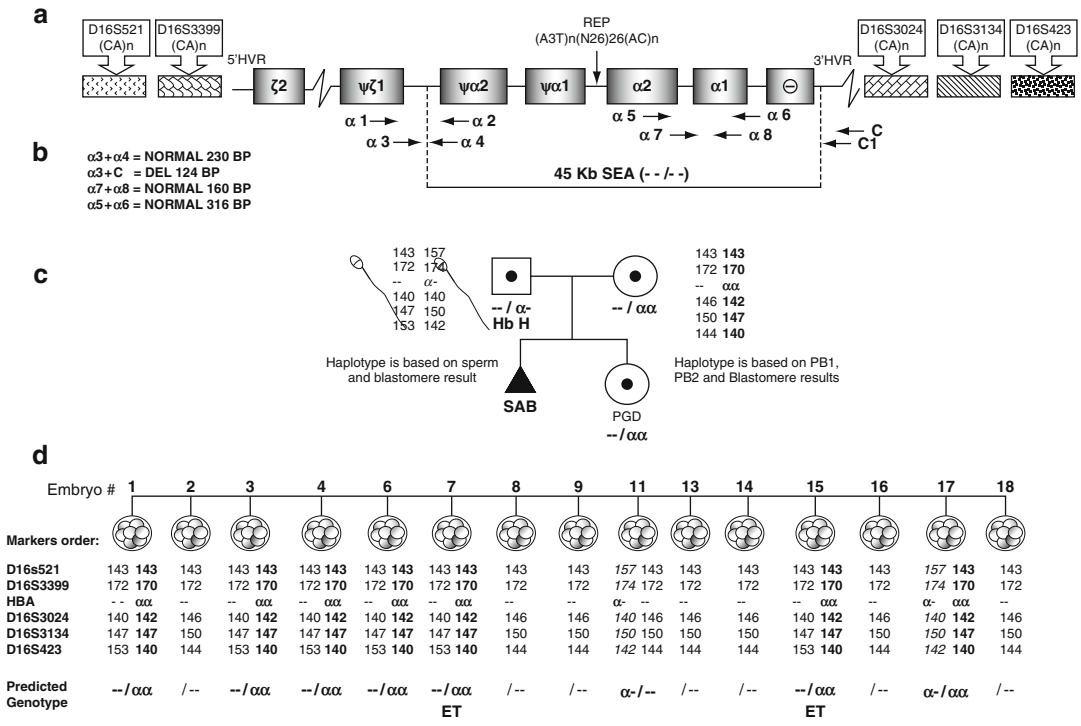

Fig. 3.3 PGD for alpha thalassemia. (**a**) Map of human alpha-globin gene, showing the position of 45 Kb SEA deletion and polymorphic markers used in multiplex PCR analysis; (**b**) size of fragments; (**c**) family pedigree showing both parents carrying SEA deletion, the father also having HbH disease; parental haplotypes are also shown, with paternal haplotypes obtained from sperm testing, and maternal haplotypes obtained from PB1 and PB2 analysis; (**d**) results of testing of 15 embryos showing the presence of 6 heterozygous embryos for deletion, of which 2 were transferred back to the patients

confirmed to be free from hydrops fetalis. To avoid misdiagnosis, the haplotype analysis for five polymorphic markers was performed, with confirmatory testing on the nontransferred embryos showing a correct diagnosis.

The example of PGD for α-thalassemia is presented in Fig. 3.3. As seen from this figure, both parents are carriers of this mutation, with the father having also hemoglobin H disease. The couple had one previous pregnancy resulting in spontaneous abortion, caused by hydrops fetalis. To avoid misdiagnosis the haplotype analysis with at least five polymorphic markers involved was performed. Of 15 embryos tested, 8 were affected, with the remaining 7 carrying one copy of the deleted α-globin gene, of which 2 (embryos #7 and #15) were transferred, with the mutant embryos confirmed to be affected, showing the reliability of the approach.

3.1.2 Cystic Fibrosis (CFTR)

CFTR has been the major indication from the very beginning of the application of PGD [12–15], and this is currently a routine procedure, which has been done in our experience of approximately 400 cases, involving testing for more than two dozens of different mutations in the CFTR gene (Fig. 3.2). Testing for CFTR mutation is usually performed simultaneously with at least three strongly linked polymorphic markers, which may realistically be selected from a set of 11 available markers listed in Fig. 3.2. In our experience of PGD for CFTR, unaffected embryo transfer was possible in almost 90% of initiated cycles, resulting in 44% clinical pregnancies and the birth unaffected children.

Because of the high prevalence of CFTR mutations, there might be a need to test

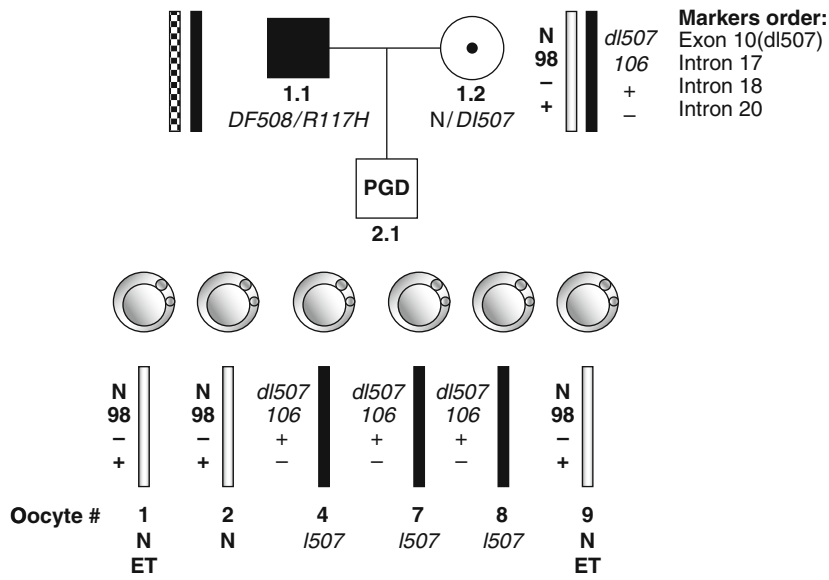

Fig. 3.4 PGD for a couple with three different mutations in CFTR gene. (*Top*) The mother (1.2) is a carrier of the delta I507 mutation in CFTR gene. The father (1.1) is affected with *CF* and had delta F508 and R117H mutations in CFTR gene. (*Bottom*) PGD was performed by sequential PB1 and PB2 analysis. The mother is informative for three inside CFTR gene polymorphic markers (introns 17, 18, and 20). Multiplex heminested PCR of PB1 and PB2 revealed three normal (#1, #2, and #9) and three affected oocytes (#4, #7 and #8). Embryos #1 and #9 were transferred and a healthy boy was born

simultaneously for two or three CFTR mutations in the same reaction, as presented in Fig. 3.4. As can be seen from the pedigree, PGD for this couple seems to be the only choice, as the father is a double heterozygote for DF508 and R117H, and the mother is a carrier of the D1507 mutation in the CFTR gene. To avoid testing for three different mutations in blastomeres, taking into consideration approximately 20% risk for ADO for each of the three alleles, which may lead to a potential misdiagnosis, PB1 and PB2 testing was performed to limit the testing to the preselection of the mutation-free oocytes. As can be seen from Fig. 3.4, testing for DI507 maternal mutation, simultaneously with four closely linked markers, allowed the identification of three mutation-free oocytes from the six oocytes available for testing. Two of these embryos resulting from oocytes #1 and #9 with acceptable development potential were transferred, yielding a singleton pregnancy and the birth of a healthy boy, confirmed to be an unaffected carrier of the paternal mutation.

3.1.3 Familial Disautonomia (FD)

Although other autosomal-recessive disorders are much rarer (listed in Table 3.1), overall, they have become the established indicators for PGD in genetic practices. The practical implications of PGD for these rare recessive disorders may be demonstrated by the examples of PGD for familial dysautonomia (FD) and spinal muscular atrophy (SMA), presented below.

FD is an autosomal-recessive disorder, associated with the mutation affecting the donor splice site of intron 20 of the IKBKAP gene, assigned to chromosome 9q31 [16, 17]. It is the most common congenital sensory neuropathy present in 1/3,600 live births in Ashkenazi Jews. FD is present at birth with characteristic features, including the absence of fungiform papillae on the tongue, absence of flare after injection of intradermal histamine, decreased or absent deep-tendon reflexes, and absence of overflow of emotional tears. This is a devastating and debilitating disorder characterized by the poor development and progressive

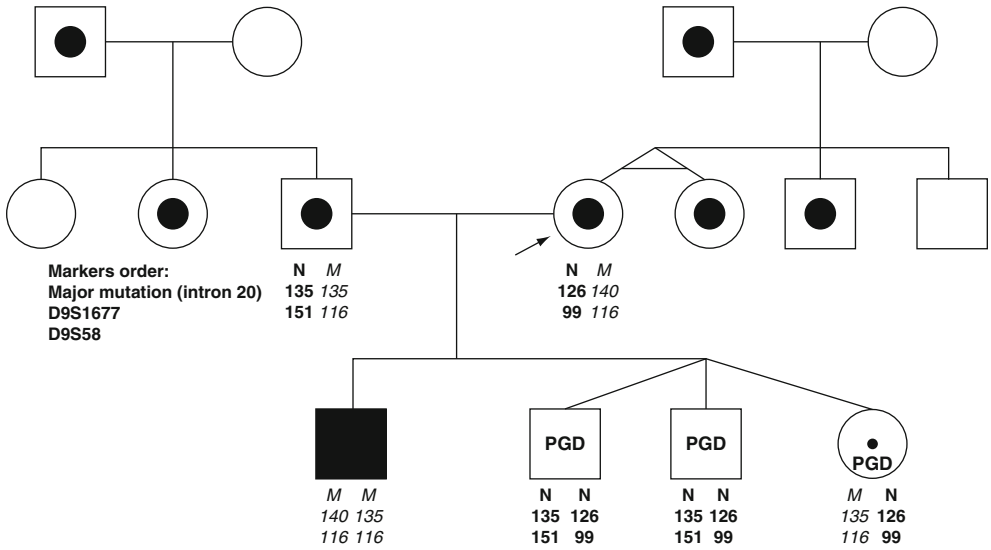

Fig. 3.5 Family Pedigree of the couple undergoing PGD for familial dysautonomia (*FD*). The father is a carrier of mutation of the donor splice site of intron 20 of the IKBKAP gene, which is linked to 135 bp repeat of D9S1677, and 116 bp repeat of D9S58, while the normal allele is linked to 135 and 151 bp repeats of the same polymorphic markers respectively. The mother is also a carrier of the same mutation, linked to 140 and 116 bp repeats, the normal gene being linked to 126 and 99 bp repeats respectively. As seen from this panel, the paternal and maternal sisters and maternal brother are also carriers of the mutation, which was inherited from the paternal father and maternal mother, respectively. Reproductive outcomes of this couple, including one previous affected child with FD and unaffected triplets born following PGD, are shown at the *bottom*

degeneration of the sensory and autonomous nervous system, gastrointestinal and respiratory dysfunctions, vomiting crisis, excessive sweating, and postural hypotension. Despite a remarkable variability of the disease phenotype within and between families, expected to derive from different mutations producing inactivation of the gene, a single major mutation has been described [18]. It is also of interest that a single T→C change at the base pair 6 of the splice donor site, which is probably responsible for 99% of cases of FD, was shown to result in the skipping of exon 20 (74 bp) from the IKBKAP mRNA only in the brain tissue, with varying level of the gene expression in other tissues. This may explain the severe progressive degeneration of the sensory and autonomous nervous system, leading to continued neuronal depletion with age and early death. The product of the IKBKAP gene is a part of a multiprotein complex, hypothesized to play a role in general transcriptional regulation, so the complete inactivation of the gene might cause a lethal phenotype at any stage of embryonic development [18]. The remarkable variability of the disease phenotype may be explained by the presence of a partially functional gene product in some tissues, including the brain, because even a small amount of the encoded protein expressed at critical developmental stages might permit sufficient neuronal survival. In addition, a very rare minor FD missence mutation was described (G→C change at base pair 17 in exon 19 of the gene), which is associated with a mild phenotype in patients with heterozygous status for the major mutation [18].

Despite the above progress in understanding the nature and pathogenesis of the disease, FD is still fatal, with no effective management available at the present time, making PGD a useful option for those at-risk couples that cannot accept prenatal diagnosis and termination of pregnancy as an option for avoiding FD in their offspring. One of such couples presented for PGD with one previous child diagnosed to be affected with FD. Both parents have an Ashkenazi Jew ancestor and, as seen from the pedigree (Fig. 3.5), are carriers of the gene for FD, based on marker analysis, which has been available for all members of the extended family [19].

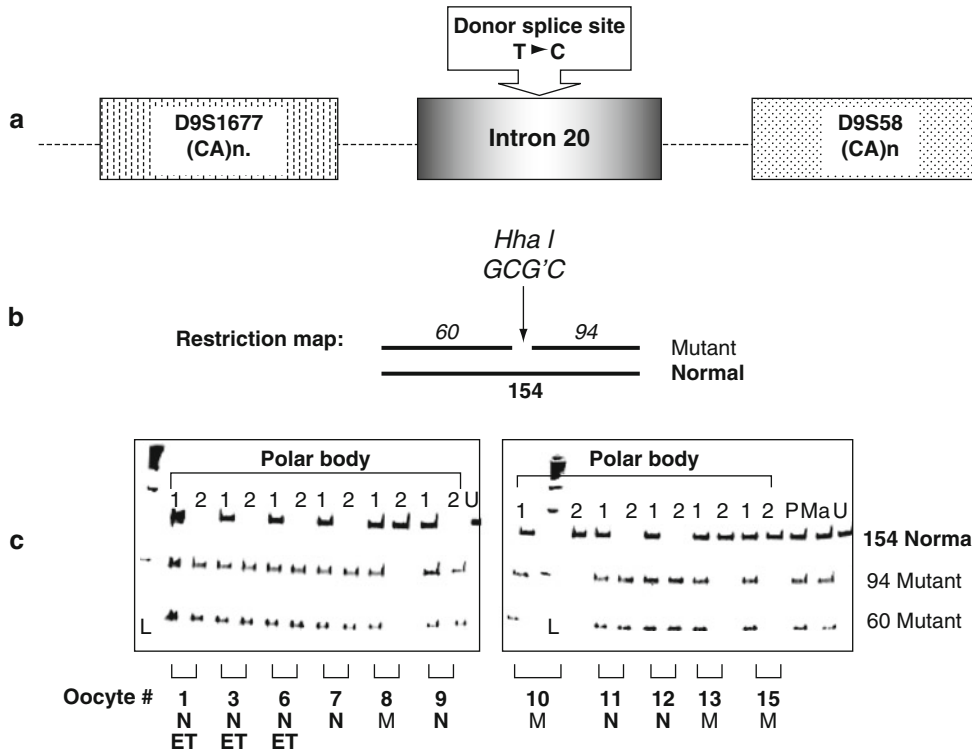

Fig. 3.6 Preimplantation genetic diagnosis for major mutation in IKBKAP gene, causing FD. (**a**) Position of major splice donor mutation T– C in IKBKAP gene and linked markers. (**b**) Restriction map. Major mutation creates restriction site for *Hha*I enzyme. (**c**) PB analysis of normal and mutant sequences of IKBKAP gene. Of 11 oocytes tested, 7 were mutation-free based on heterozygous PB1 and affected PB2, of which oocytes #1, #3, and #6 were transferred resulting in unaffected triplets. *L* 100 bp ladder, *N* normal, *M* mutant, *ET* embryo transfer, *U* undigested PCR product, *Ma* maternal genotype, *P* paternal genotype

A PGD cycle was performed using a standard IVF protocol coupled with micromanipulation procedures for PB sampling, described above in Chap. 2. PB1 and PB2 were removed following maturation and fertilization of the oocytes, and tested by the multiplex nested PCR analysis, involving mutation testing simultaneously with different linked markers as described above. The mutation analysis involved the detection of T to C change in the donor splice site of intron 20, based on HhaI restriction digestion, which does not cut the normal allele, while creating two fragments of 60 and 94 bp in the mutant allele (Fig. 3.6).

As described in Chap. 2, there may be three genetic possibilities for the PB1 genotype from a heterozygous mother. If no crossover occurs, PB1 will be homozygous (either normal or mutant), but in the event of a crossover, PB1 will be heterozygous. If crossover does not occur and the PB1 is homozygous for the mutant gene, the oocyte must contain two copies of the normal gene and any embryo resulting from this oocyte can be transferred, but this was not the case in any of the oocytes shown in Fig. 3.6. If the PB1 is homozygous for the normal gene, the maternal contribution to the embryo must be the mutant gene, which was also not the case as seen from Fig. 3.6. In both of these occasions the extruded PB2 will have identical genotype to oocyte (opposite to genotype of PB1). In the event of crossover that has been observed in all cases shown in Fig. 3.6, PB1 is heterozygous and the analysis of PB2 is required to predict which maternal allele have been extruded with PB2 and which left in the maternal pronucleus following fertilization. Accordingly, if the normal gene is extruded with PB2 (e.g., PB2 is

hemizygous normal), the resulting maternal contribution to the embryos is the mutant gene, and in reverse if the mutant gene is extruded with PB2 (e.g., PB2 is hemizygous mutant), the resulting maternal contribution to the embryos is the normal gene. It is furthermore possible that even the oocytes predicted as mutant may further form unaffected heterozygous embryos, following fertilization by a mutation-free sperm. Therefore, with insufficient number of mutation-free oocytes, preselected by PB1 and PB2 sequential analysis, further testing of the resulting embryos may allow the identification of heterozygous unaffected carrier embryos for transfer.

The preselection of mutation-free oocytes was performed based on the simultaneous mutation detection and linked marker analysis, involving two strongly linked markers D9S58 and D9S1677, which were shown not to be involved in recombination in the analysis of 435 FD chromosomes [19]. Therefore, prior to PGD, a single sperm testing was performed to identify the paternal haplotypes, which were as follows: the mutant allele was linked to 116 bp, and the normal to 151 bp repeat of the D9S58 marker, while the D9S1677 marker was not informative. The maternal haplotypes were established based on PB analysis as follows: the mutant allele was linked to 116 bp repeat of the D9S58 marker, and 140 bp repeat of the D9S1677 marker, while the normal allele to 140 bp repeat of the D9S58 marker and 126 bp repeat of the D9S1677 marker (Fig. 3.5). Primer sequences and reaction conditions are presented in Table 3.5.

A single PGD cycle was performed, with 15 oocytes available for testing, of which 11 were with the information for both PB1 and PB2. Of these 11 oocytes, 4 were predicted to be mutant based on the heterozygous PB1 and hemizygous normal (mutation-free) PB2 (oocytes #8, #10, #13, and #15), while the remaining 7 oocytes were free of the mutant gene, as evidenced by the heterozygous PB1 and hemizygous mutant PB2. These results were in agreement with both markers, except for oocytes #7 and #11, in which ADO of D9S1677 allele linked to the mutant gene was observed. Three embryos resulting from the above seven oocytes (embryos #1, #3, #6; Fig. 3.6), with the mutation-free status confirmed by both markers, reaching the blastocyst stage, were transferred back to the patient, yielding a triplet pregnancy and the birth of three unaffected children, including two homozygous normal and one heterozygous carrier. Two of the other embryos resulting from normal oocytes did not form blastocysts and the other two were further tested because of ADO of one of the markers (oocytes #7 and #11).

Three of four embryos deriving from the mutant oocytes were shown to be heterozygous carriers of the mutant gene, and one homozygous mutant. One of the embryos deriving from normal oocytes was confirmed to be homozygous for normal gene and the other was a heterozygous carrier. These embryos, as well as other three embryos, which appeared to be heterozygous carriers, were frozen and are available for transfer in the future cycles, should the couple wish to have another unaffected child. Of course the above normal noncarrier embryo could be given preference in transfer, but because a possible detrimental effect of removing blastomeres from cleaving embryos cannot be completely excluded, we gave priority to the three non-biopsied embryos resulting from the mutation-free oocytes. However, when more data are collected on the possible effect of different biopsy procedures on the outcome of pregnancy, and the accuracy of blastomere analysis is further improved, the possibility for parents to choose implanting normal or carrier embryos should be explored.

These results and further similar cases performed by the present time demonstrate a diagnostic accuracy of PGD for FD by sequential PB1and PB2 analysis, as the follow-up analysis of the embryos, resulting from either mutant or normal (mutation-free) oocytes, was in agreement with the sequential PB1 and PB2 analysis in all the embryos tested, which is in accordance with the extensive data on the sequential PB1 and PB2 analysis, described above in Chap. 2. Although, as mentioned, ideally at least three linked markers are considered necessary to completely exclude the risk for misdiagnosis

Table 3.5 Primers and PCR conditions used in PGD for FD

Gene/polymorphism	Upper primer	Lower primer	Anneal T_m (°C)
Intron 20 major mutation (T-C) *Hha I restriction* heminested PCR	Outside 5′ GTTGTTCATCATCGAGCCC 3′	5′ CTGATTGATGATATAGGTAATGAGG 3″	62–55
	Inside 5′ GTTGTTCATCATCGAGCCC 3′	5′ GCTTTTCATAATTTTAAGTTCTCG 3′	55
D9S1677	Outside 5′ TGGCTGTTTTGAGAAGT 3′	5′ TGGGAGGATGAGTTGAG 3′	62–55
	Inside 5′ Hex ATGTAACCTGTCTCCACTG 3′	5′ CTGGGCAACATAGCAAG 3′	57
D9S58	Outside 5′ AAGCAATCCTCGCACCTCAG 3′	5′ CCAGGAGTTTGAGACCAGCC 3′	62–55
	Inside 5′ FamCCTGAGTAGCCGGGACTATA 3′	5′ TAGGCAACACATCAAGATCCT 3′	57

due to ADO, the use of the two linked markers or even one in the present study was reliable, because it was possible to follow both normal and mutant alleles through the first and second meiotic divisions in all but four oocytes, in which either no PB2 was available due to failure of fertilization or PB2 failed to amplify. In other words, the presence of both mutant and normal alleles in PB1 following meiosis I, and the detection of the mutant allele extruded with PB2 following meiosis II, leaves no doubt of the mutation-free status of the maternal pronucleus, even if no linked markers are available for testing. However, the testing of sufficient number of linked markers would be absolutely essential if PB1 appears to be homozygous mutant, to exclude the possible ADO of the normal allele, because the failure of detecting ADO could lead to the opposite interpretation of the results of PB2. With undetected ADO in PB1, the presence of normal allele in PB2 will erroneously suggest the normal (mutation-free) status of the resulting oocyte, which has apparently a mutant status.

The presented experience of PGD for FD demonstrates the clinical relevance of PGD in those couples that cannot accept prenatal diagnosis and termination of pregnancy [20]. Because of the high prevalence of FD in Ashkenazi Jews, with carrier frequency of 1 in 32, this approach may have practical implications, so the at-risk couples require information about the availability of PGD. The presented PGD design for FD may probably be applied without extensive preparatory work in different couples, due to the fact that a single major mutation is involved, although a sufficient number of informative linked markers should be selected, a variety of which are readily available.

As also shown by the above example of FD, it may be predicted that PGD may in future be applied for gene expression abnormalities, which might be limited to a particular tissue or particular stage of embryonic development. This may also allow preselecting the embryos with best potential to establish a viable pregnancy, based on the progress on the understanding of stage-specific gene expression.

3.1.4 Spinal Muscular Atrophy (SMA)

PGD for SMA still presents a real complexity [21, 22]. SMA is another relatively rare autosomal-recessive disorder with a newborn prevalence of 1/10,000 and a carrier frequency of 1 in 40–60 individuals. All types of SMA are caused by mutations in the survival motor neuron gene (SMN) locus mapped on chromosome 5q11.2–13 [16]. The SMN gene is present in two highly homologous copies, SMN1 and SMN2, of which homozygous loss of functional survival motor neuron 1 (SMN1) alleles results in SMA, while homozygous absence of SMN2 gives no clinical phenotype. Since 95% of SMA patients lack both copies of SMN1 in exon 7, PGD for SMA is based on the avoidance of SMN1 homozygous deletions, which is complex because of the sequence similarity between the SMN1 and SMN2 genes, requiring simultaneous linkage analysis involving STR markers. To test for paternal SMN1 and SMN2 deletion patterns on each chromosome by blastomere analysis, single sperm testing was required to establish the linkage between normal and deleted alleles with multicopy marker D15S1556 on the promoter region of both gene copies.

The example of PGD for SMA is presented in Fig. 3.7, which shows PGD for SMA performed for a couple with both parents carrying the deletion in the SMN1 gene. Paternal haplotypes were predicted by multiplex heminested PCR analysis in single sperm, and maternal ones by sequential PB1 and PB2 analysis. Of 16 embryos tested for deletion and 4 linked markers (primers are listed in Table 3.6), 2 embryos were mutant, 10 were predicted to be heterozygous for the deletion in SMN1 gene, and 2 with only one copy of the normal gene present. In addition, at least three STRs were amplified on each chromosome for aneupolidy testing of chromosomes 13, 16, 18, 21, and 22, which revealed five chromosomally abnormal embryos, including trisomy 13, monosomy 18, double trisomy 18 and 21, double monosomy 18 and 21, and triple monosomy 13, 16, and 22 (embryo #8, #10, #9, #14, and #13, respectively). Abnormalities predicted by PCR were confirmed

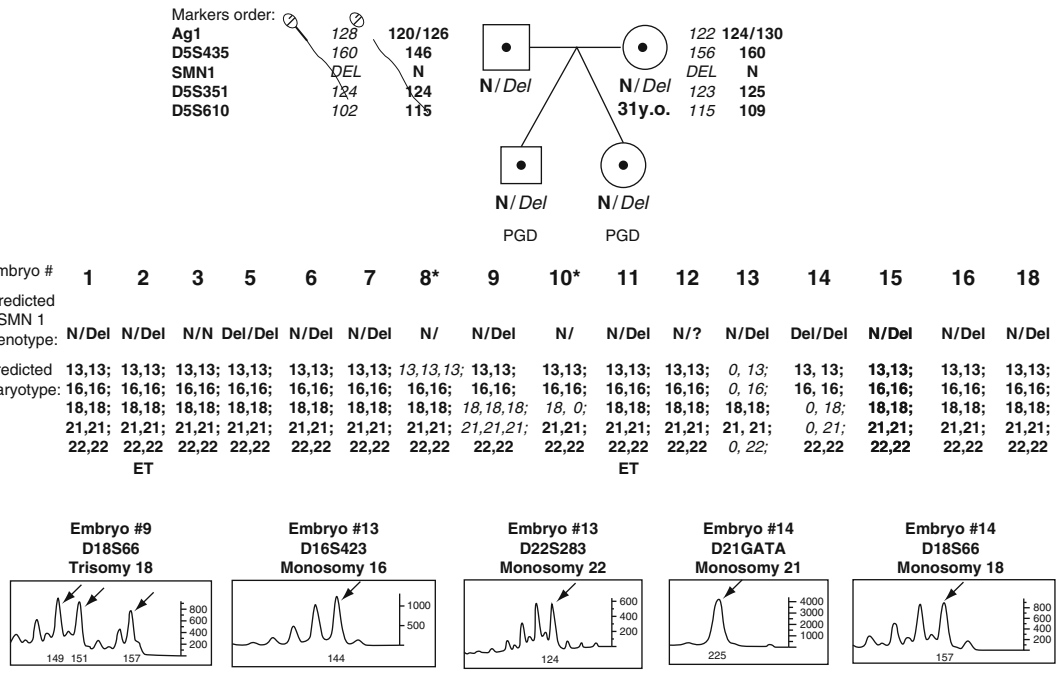

Fig. 3.7 Combined PGD for spinal muscular atrophy (*SMA*) and aneuploidy. (*Top*) Pedigree of the family undergoing PGD for SMA. Both parents are the carriers of the deletion in SMN1 gene. Paternal haplotype was predicted by multiplex heminested single-sperm PCR analysis. Maternal haplotype was established by sequential PB1 and PB2 analysis. As a result of IVF–PGD cycle healthy twins were born. Positions of polymorphic markers linked to SMN1 gene and applied for improving accuracy of the mutation analysis are shown next to the paternal haplotypes. (*Middle*) Oocytes #3, #8, and #11 were predicted to be normal by polar body (*PB*) analysis. The embryos resulting from these oocytes were subjected to aneuploidy testing using five chromosome-specific probes. Trisomy for chromosome 13 was detected in embryo #8 and monosomy 18 in embryo #10. Blastomeres from the remaining 13 embryos were subjected to multiplex heminested PCR to perform simultaneous mutation, linked polymorphic marker, and aneuploidy analysis for chromosomes 13, 16, 18, 21, and 22. Of these, embryos #5 and #14 were affected, while embryos #1, #2, #6, #7, #9, #11, #13, #15, #16, and #18 were predicted to be heterozygous for the deletion in SMN1 gene. At least three short tandem repeats (STRs) were amplified on each chromosome for aneupolidy testing, which revealed monosomy13, 16, and 22 in embryo #13, monosomy 18 and 21 in embryo #14 and trisomy 18 and 21 in embryo # 9. Chromosomal abnormalities predicted by PCR were confirmed by whole embryo fixation and FISH analysis. Embryos #2 and #18 were transferred and healthy twins were born. All unaffected and chromosomally normal blastocysts were frozen for future cycles. (*Bottom*) Examples of chromosomal abnormalities (monosomy and trisomy) detected by PCR of different STRs. *N* normal allele, *Del* deletion, *ET* embryo transfer, *FISH* fluorescent in situ hybridization

by whole embryo fixation and FISH analysis. Embryos #2 and #11 were transferred, and healthy twins were born. All unaffected and chromosomally normal blastocysts were frozen for future family use.

The data also show the importance of simultaneous testing for aneuploidy, to avoid misdiagnosis and also to avoid the transfer of chromosomally abnormal embryos, destined to be lost in pre- or post-implantation development.

3.2 Autosomal-Dominant Disorders

Autosomal-dominant conditions are important candidates for PGD, as couples have a 50% risk of producing an affected child. PGD for autosomal-dominant disorders represents under one-fifth of our experience, which was extremely accurate and effective in detection and transfer of mutation-free embryos (Table 3.3).

Table 3.6 Primers and PCR conditions used in PGD for SMA

Gene/polymorphism	Upper primer	Lower primer	Annealing T_m (°C)
SMN (detection of Exon 7 deletion by *Hinf I or Dra I digestion*)	Outside		62–45
	5′ TGCAGCCTAATAATTGTTTTCTTTG 3′	5′ CCAACCAGTTAAGTATGAGAATTCTAG 3′	
	Inside for *Hinf I* :		55
	5′ CTTCCTTTTATTTTCCTTACAGGGATT 3′	5′ GTAGGGATGTAGATTAACCTTTTATCT 3′	
	Inside for *Dra I* [3]:	Inside for *Dra I* [2]:	55
	5′ AAATGTCTTGTGAAACAAAATGC 3′	5′ CCTTCCTTCTTTTTGATTTTGTTT 3′	
SMN (detection of Exon 8 deletion by *Dde I digestion*)	Outside		62–45
	5′ GTGGAATGGGTAACTCTTCTTGA 3′	5′ TAAACTACAACACCCTTCTCACAG 3′	
	Inside		48
	5′ TAATAACCAAATGCAATGTGAAAT 3′	5′ TAAACTACAACACCCTTCTCACAG 3′	
D5S1556 promotor area (heminested)	Outside		62–45
	5′ TCCTTCCTGCCCCCATG 3′	5′ TCGGCATGTTGCTTAGGC 3′	
	Inside		55
	5′ FamAAATTCCTAGTAGGAGCTTACATTTAC 3′	5′ TCGGCATGTTGCTTAGGC 3′	
D5S435 (heminested)	Outside		62–45
	5′ TTCCTCCATTGACAACTCCTT 3′	5′ CCTTAGATAGGGTTGATTTACACA 3′	
	Inside		55
	5′ HexGTCAAGAGCACAGTTTGGAGTG 3′	5′ CCTTAGATAGGGTTGATTTACACA 3′	
D5S351 (nested)	Outside		62–45
	5′ GAGTTTGAAGACCAGTCTATGG 3′	5′ GAGCATTGCCACTTTAGCC 3′	
	Inside		55
	5′ FamCACAGCGAGACCCCGTC 3′	5′ CCCGTGGAAGAAAGGCTAT 3′	
D5S610 (heminested)	Outside		62–45
	5′ TCCAGTGAATTTTCATTTCAGATAC 3′	5′ CAAGTGACCCTCCCACCTT 3′	
	Inside		55
	5′ TCCAGTGAATTTTCATTTCAGATAC 3′	5′ HexCCAGCCTAAACTGAACTTTCAAAG 3′	

Autosomal-dominant conditions for which PGD was performed are presented in Table 3.1, and the examples of two of them, early-onset *primary torsion dystonia* (*PTD*) and *Charcot-Marie-Tooth disease* (*CMT*), are described below.

3.2.1 Primary Torsion Dystonia (PTD)

Primary torsion dystonia (PTD) is caused in the majority of cases by a 3 bp deletion of the DYT1gene, located on chromosome 9q34 [16, 17, 23–25]. This is actually the most severe and common form of hereditary movement disorders, present in 1/15,000 live births, characterized by sustained twisting contractures that begin in an arm or leg between 4 and 44 years, spreading to other limbs within about 5 years. Although the phenotypic expression of the disease is similar in all ethnic populations, the highest prevalence was reported among Ashkenazi Jews. Despite a low penetrance (30–40%), the disease phenotype varies greatly between families. In contrast to other neurodegenerative disorders, PTD does not show any distinct neuropathology. A 3 bp deletion in the coding sequence of the DYT1 gene is believed to result in a loss of a pair of glutamic acid residues in a conserved region of an ATP-binding protein torsin A, which has resemblance to the heat-shock proteins, and may lead to imbalance of neuronal transmission in the basal ganglia implicated in dystonia. As low levels of dopaminergic metabolites in the cerebrospinal fluid of these patients show no response to dopa, it is probably caused by a defect in release rather than synthesis of dopamine.

The remarkable phenotypic variability of the disease may be explained by the interaction of the 3 bp deletion with modifying genetic, such as polymorphic, variations in torsin A or mutations in the associated proteins, or with environmental factors, such as trauma, high body temperature, or exposure to toxic agents. Although understanding these relationships may allow elucidating neuronal mechanisms underlying loss of movement control, there is no effective treatment as yet available. This makes PGD a useful option for those at-risk couples that cannot accept prenatal diagnosis and termination of pregnancy as an option for avoiding PTD in their offspring.

Two couple presented for PGD, both with the affected paternal partners carrying the DYT1 3 bp deletion. In one of the couples, the mutation was inherited from the paternal father (Fig. 3.8), whose four sons were affected. In the other, the male partner inherited the mutation from the mother, who did not have any other children (Fig. 3.9).

PGD cycles were performed using blastomere biopsy, and tested by the multiplex nested PCR analysis, involving the DYT1 mutation testing simultaneously with a set of linked polymorphic markers. The mutation analysis involved the detection of GAG deletion in the coding sequence of the DYT1 gene, based on either fragment-size analysis using capillary elecrophoresis or BSeRI restriction digestion, which creates three fragments of 161, 24, and 8 bp in the normal allele (Fig. 3.10), in contrast to only two fragments of 185 and 8 bp in the mutant gene.

Three closely linked markers, D9S62, D9S63, and ASS (intron 14), which were shown not to be involved in recombination with the DYT1 gene [23, 25–27], were used in the multiplex nested PCR system. To identify the paternal haplotypes, a single sperm testing was performed prior to PGD, which showed the linkage of the mutant allele in both couples to 121, 157, and 134 bp; the normal paternal allele in the first couple was linked to128, 140, and 124 bp, and in the second to 123, 155, and 130 bp repeat of D9S62, D9S63, and ASS markers, respectively. The maternal haplotypes were in the first couple 123/123, 149/155, and 128/124 bp, and in the second 123/123, 140/155, and 126/136 bp repeats of D9S62, D9S63, and ASS markers, respectively. Primer sequences and reaction conditions are presented in Table 3.7.

The embryos derived from the oocytes free of DYT1 3 bp deletion, in agreement with the information about the above polymorphic markers, were preselected for transfer back to patients, while those predicted to be mutant or with insufficient marker information were exposed to confirmatory analysis using genomic DNA from these embryos to evaluate the accuracy of single-cell-based PGD.

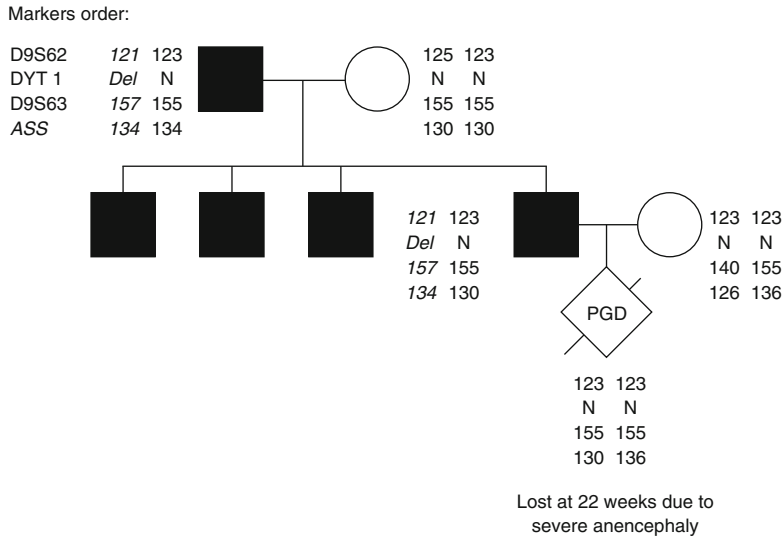

Fig. 3.8 PGD for a couple at risk for torsion dystonia 1 resulting in miscarriage of an unaffected child with anencephaly. (*Upper panel*) Patient's parents, showing that he inherited 3 bp deletion of DYT1 gene from his father. (*Middle panel*) The father is a carrier of a 3 bp deletion of DYT1 gene, which is linked to 121, 157, and 134 bp repeats of D9S62, D9S63, and ASS markers, respectively, while the normal allele is linked to 123, 155, and 130 pb repeats of the same polymorphic markers, respectively. The mother is normal, with one normal DYT1 allele linked to 123, 140, and 126 and the other to 123, 155, and 136 pb repeats of D9S62, D9S63, and ASS markers, respectively. As seen from this panel, three paternal brothers are also affected obligate carriers of a 3 bp deletion of DYT1 gene, inherited from their father. (*Lower panel*) Reproductive outcomes of this couple, following PGD showing the 3 bp deletion-free fetus, which was terminated due to anencephaly

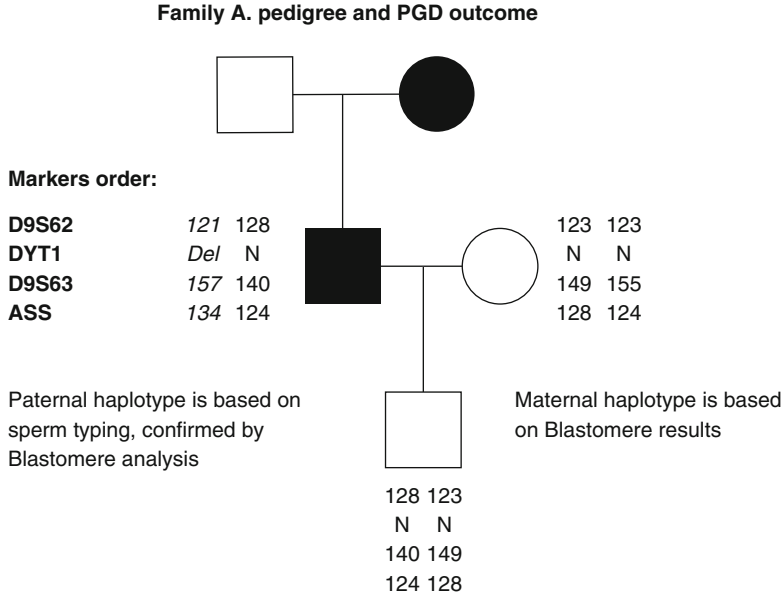

Fig. 3.9 Pedigree of a couple whose PGD for DYT1 resulted in the birth of a mutation-free baby. (*Upper panel*) Patient's parents, showing that he inherited 3 bp deletion of DYT1 gene from his father. (*Middle panel*) The father is a carrier of a 3 bp deletion of DYT1 gene, which is linked to 121, 157, and 134 bp repeats of D9S62, D9S63, and ASS markers, respectively, while the normal allele is linked to 128, 140, and 124 bp repeats of the same polymorphic markers, respectively. The mother is normal, with one normal DYT1 allele linked to 123, 150, and 128 and the other to 123, 155, and 124 bp repeats of D9S62, D9S63, and ASS markers, respectively. As seen from the upper panel the mutation was inherited from the paternal mother, with no other family members available in the pedigree. (*Lower panel*) Reproductive outcomes following PGD, showing the 3 bp deletion-free baby, which is in agreement with polymorphic markers, also suggesting the presence of both paternal and maternal normal genes. This embryo originates from the transfer of embryo #6, as shown in Fig. 3.10

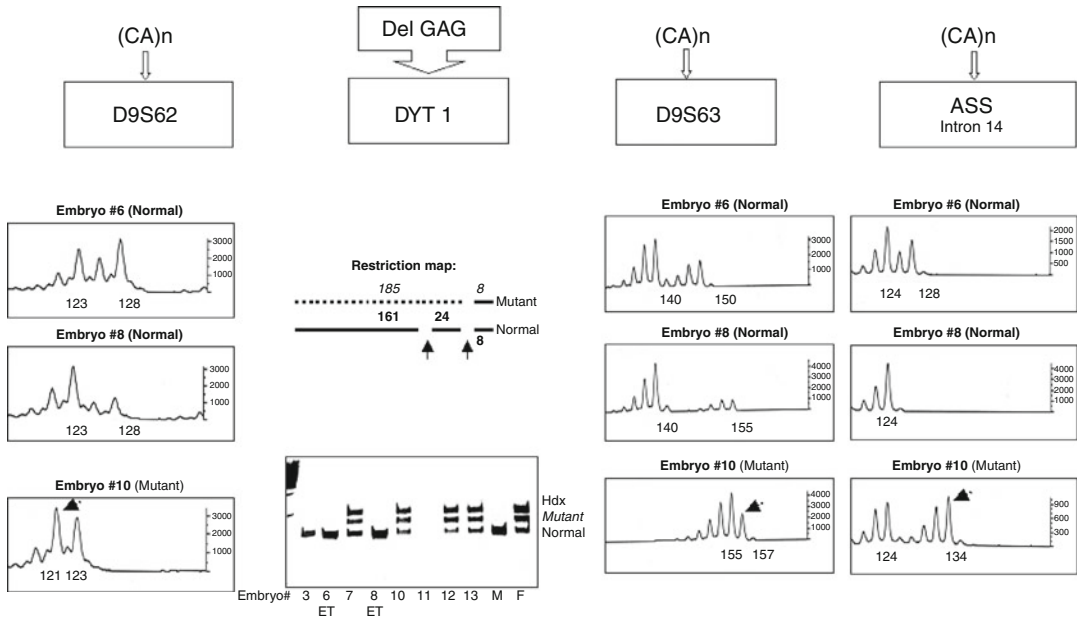

Fig. 3.10 Preimplantation diagnosis for GAG deletion of DYT1 gene, resulting in the birth of mutation-free baby. Capillary electrophoregrams of fluorescently labeled PCR products of linked markers D9S62 (*first from the left*), D9S63 (*third from the left*), and ASS (*first from the right*), scored by Genotyper TM. The data of genotyping of only three embryos are shown as examples, including two transferred normal (embryos #6 and #8) and one affected (embryo #10) embryo. Paternally derived 128, 140, and 124 dinucleotides indicative of the DYT1 mutation are evident in blastomeres of embryos #6 and #8, together with the presence of maternal normal alleles. (*Second panel from the left*) The location (*top*) of the mutation in DYT1, restriction map for Dse RI digestion (*second panel from the top*), creating three fragments of 161, 24, and 8 bp in the normal allele, in contrast to only two fragments of 185 and 8 bp in the mutant gene. However, because this required a long incubation and high amount of enzymes, fluorescent genotyping was also performed (*bottom of this panel*). (*Middle section of the same panel*) The polyacrylamide gel electrophoregram of Dse RI-digested PCR products of 8 blastomeres from one of the cycles of PGD, paternal DNA from sperm (P), and maternal (normal) DNA. Hdx – the extra fragment in the heterozygous mutant embryos as a result of heteroduplex formation. (*Bottom section of this panel*) Capillary electrophoregrams of fluorescently labeled PCR products of some of the above blastomeres, including two normal (embryos #6 and #8) and one affected (embryo #10). Paternally derived GAG deletion shown by an arrow is evident in embryo #10, which is absent in embryos #6 and #8, in agreement with the linked marker analysis (*see relevant panels on the left and right*). These embryos inherited the paternal normal chromosome, but may be distinguished from each other by the inheritance of different maternal chromosomes, allowing the identification of the origin of the resulting mutation-free baby (see Fig. 3.9)

Three PGD cycles were performed including two for the first and one for the second couple, with a total of 19 embryos available for testing, of which 17 were with sufficient information on the mutation and marker analysis to predict the embryos' genotype. Of these 17 embryos, 9 were predicted to contain a 3 bp deletion, while the remaining 8 were free of the mutant gene, as also confirmed by the polymorphic markers. Six of these embryos, which reached the blastocyst stage, were transferred back to the patients, two in each of the three cycles, yielding a singleton DYT1 mutation-free pregnancy in two of them.

In one couple, only the second cycle resulted in a clinical pregnancy in which eight embryos were available for testing (Fig. 3.10). Although the biopsied blastomere of one of these embryos (embryo #3) was free of the paternal mutant gene, no other paternally derived alleles were present, suggesting that this cell contained only maternal alleles, probably due to monosomy 9. In the other embryo (embryo #11) one of the biopsied blastomeres showed no amplification, so the second

Table 3.7 Primers for detection of GAG deletion in DYT1 gene and linked polymorphic markers

Gene/polymorphism	Upper primer	Lower primer	Annealing T_m (°C)
DYT 1 (del GAG) (heminested)	Outside		62–55
	5′ GCACAGCAGCTTAATTGACC 3′	5′ CGTAGTAATAATCTAACTTGGTGAA 3′	
	Inside		56
	5′ GCACAGCAGCTTAATTGACC 3′	5′ Hex TTTATCTGAGAAAACTCTCTCCTCT 3′	
D9S62 (heminested)	Outside		62–55
	5′ ACCTGTAATCCCAGTTGCT 3′	5′ TCACTTCTGACCCTCCTATCT 3′	
	Inside		56
	5′ Hex GGCAACAGGGCAAGACT 3′	5′ TCACTTCTGACCCTCCTATCT 3′	
D9S63 (heminested)	Outside		62–55
	5′ ATTCTGTGGGGGAATTATG 3′	5′ TTATAATGCCGGTCAACC 3′	
	Inside		56
	5′ Fam CACAAAAGAAAGTCACAATCC 3′	5′ TTATAATGCCGGTCAACC 3′	
ASS Intron 14 (CA)n (heminested)	Outside		62–55
	5′ GGGAGCTATAAAAATGACAAT 3′	5′ TTAACAGGCTGTCTGGCA 3′	
	Inside		56
	5′ GGGAGCTATAAAAATGACAAT 3′	5′ Fam TAGGTCCGAAAACACAAAG 3′	

blastomere was removed, but did not show amplification of the DYT1 gene and ASS marker either, together with ADO of the D9S62 paternal allele. Despite this blastomere being informative for the D9S63 marker, which suggested the presence of both paternal and maternal normal alleles, the corresponding embryo was not transferred, to avoid the risk for misdiagnosis, associated with the use of a single linked marker. Four of the remaining six embryos were predicted to be mutant (embryos #7, #10, #12, and #13), evidenced by the presence of the DYT1 3 bp deletion and all three markers linked to the mutant gene (Fig. 3.10). The remaining two embryos (embryos #6 and #8) were free of 3 bp deletion, with all three markers not only excluding a possible ADO of the mutation, but also confirming the presence of both maternal and paternal normal alleles. These two embryos were transferred back to the patient resulting in the birth of a mutation-free boy. As can be seen from the inherited maternal normal chromosome, this baby originates from the transfer of embryo #6 (Figs. 3.9 and 3.10).

In the second patient, only four embryos were available for testing, two of which showed the presence of the DYT1 3 bp deletion confirmed by all three linked polymorphic markers. Of the remaining two embryos with no evidence for the presence of DYT1 3 bp deletion, the marker analysis also showed the presence of both paternal and maternal normal alleles, despite ADO of one of the paternal polymorphic markers in one of these embryos. The transfer of these embryos yielded a singleton pregnancy, which was terminated at 22 weeks of pregnancy due to a severe anencephaly (Fig. 3.8). The results of the mutation and marker analysis in the abortion material showed that the resulting fetus was free of mutation, with all three markers confirming the presence of both paternal and maternal normal alleles.

The presented results represent the first experience of PGD for TDY1, demonstrating the clinical usefulness of PGD in those couples that cannot accept prenatal diagnosis and termination of pregnancy. Because a single unique 3 bp deletion is involved in more than 70% cases of early-onset PTD, the presented PGD design for DYT1 mutation may probably be applied without extensive preparatory work in different couples, taking also into consideration the limited number of founder mutations [25]. As seen from the sperm haplotype analysis of our patients with GAG deletion of the DYT1 gene, the same haplotypes appeared to surround the DYT1 gene. The availability of a sufficient number of highly variable and closely linked markers also allows testing for the mutation simultaneously with at least three markers, to exclude misdiagnosis due to ADO, which may exceed 10% in blastomere analysis [28]. Because PTD is an autosomal-dominant disorder, to ensure a reliable preselection of mutation-free embryos for transfer, PGD should include the detection of both paternal and maternal normal alleles in addition to the exclusion GAG deletion, which may be masked by ADO. This also allows identification of individual embryos that was implanted, as usually two or embryos are transferred. As mentioned, the baby resulting from the transfer of two mutation-free embryos in one of the PGD cycles described has actually originated from the implantation of embryo #6 [29].

Our data also showed that the above microsatellite markers used in this study were also useful in detection of the chromosomal number containing the DYT1 gene in single blastomeres, without which the accuracy of the predicted embryo genotype might not be sufficient. For example, without such information the embryo #3 in one of the couples (Fig. 3.10) could have wrongly been predicted to be normal, which in fact contained no paternal linked markers either. This, therefore, may have suggested the presence of only maternal chromosome 9 due to mosaicism in this embryo, which in fact might have otherwise contained the paternal chromosome 9 with DYT1 mutation, so being affected.

Although prenatal diagnosis for PTD is also available, PGD may seem to be a more attractive option. The fact that approximately 70% of the offspring will not develop the disease in the obligate carriers of the mutation makes the decision of what to do in the case of a mutation carrier is very difficult for the parents.

As for the neonatal outcome, the presented case with anencephaly detected in the second trimester of pregnancy is probably not related to the procedure. As will be described in Chap. 6, the analysis of the outcome of many thousands of PGD cases showed that the prevalence of congenital malformations (5%) was not different from the population prevalence. It is too early to analyze the prevalence of specific types of congenital malformations, but it has been demonstrated that the prevalence of anencephaly and other neural-tube defects may be efficiently prevented by folic acid supplementation before pregnancy (see Chap. 1), so this should be recommended to all patients requesting PGD, as this is one of those rare occasions when the pregnancy is planned well ahead.

3.2.2 Charcot-Marie-Tooth Disease (CMT)

Charcot-Marie-Tooth disease (CMT) represents a clinically and genetically heterogeneous group of hereditary peripheral neuropathies, affecting approximately 1 in 2,500 in the United States. Although prenatal diagnosis is available, it may lead to termination of pregnancy, which is not acceptable for many couples. PGD has previously been applied in five couples with CMT1A, representing the most frequent autosomal-dominant type of CMT caused by 1.5 Mb tandem duplication including dosage-sensitive gene for peripheral myelin protein 22 (PMP22) on chromosome 17p11.2–12, presenting complexity of diagnosis requiring the application of multiple polymorphic markers [30]. PCR design for PGD of this condition involved the application of 13 highly polymorphic microsatellite markers, located within the duplicated area and closely linked to the PMP22 gene, some showing three alleles in patients with CMT1A duplication.

We performed PGD for CMT type 1A and 1B, with both paternally and maternally derived mutations. In those with paternally derived duplication, single-sperm analysis was performed to determine normal and mutant haplotypes. In the PGD cycles with maternal mutation, both PB1 and PB2 and blastomeres were analyzed, using markers D17S1357, D17S2229, D17S2226, D17S2225, D17S839, D17S2224, D17S2221, D17S2220, D17S291, D17S2219, D17S2218, D17S2217, and D17S2216, which were amplified in a multiplex heminested PCR system, followed by fragment analysis on an ABI 3100 analyzer. These cycles resulted in the transfer of the embryos free of PMP 22 duplication, yielding unaffected pregnancies and the birth of unaffected children.

In the other PGD cycle performed for maternally derived autosomal-dominant CMT-type 2E mutation in the light polypeptide neurofilament protein gene (NEFL), testing of oocytes by PB1 and PB2 and also blastomeres was performed for the presence of the mutation P8R, simultaneously with microsatellite marker D8S137, which resulted in the transfer of two unaffected embryos and the birth of a child with a normal NEFL gene. PGD was also performed for the X-linked forms of CMT, caused by mutations in connexin-32 gene (Cx32), for which 28 oocytes were tested by sequential PB1 and PB2 for the presence of the V95M mutation in the Cx32 gene, simultaneously with STRs (DXS453, DXS8052, DXS8030, DXS559, DXS441), and resulted in the transfer of four mutation-free embryos failing to yield a clinical pregnancy. The example of PGD for paternally derived CMT1A is presented in Fig. 3.11, showing the outcome of testing of ten embryos by blastomere analysis using ten linked markers (primers and reaction conditions are listed in Table 3.8). Five unaffected embryos were identified, two of which were transferred resulting in the birth of a healthy child, demonstrating the reliability and accuracy of PGD designs applied to PGD for CMT, although misdiagnosis in PGD for CMT was also reported, which was due to errors in linkage analysis in preparation to PGD (see below).

As can be seen in Table 3.3, 164 PGD cycles for dominant disorders were performed by the PB approach although the majority of these cases (118 cycles) still needed a follow-up sequential blastomere or blastocyst biopsy. As the mutation rate for dominant conditions is higher than for recessive and X-linked disorders,

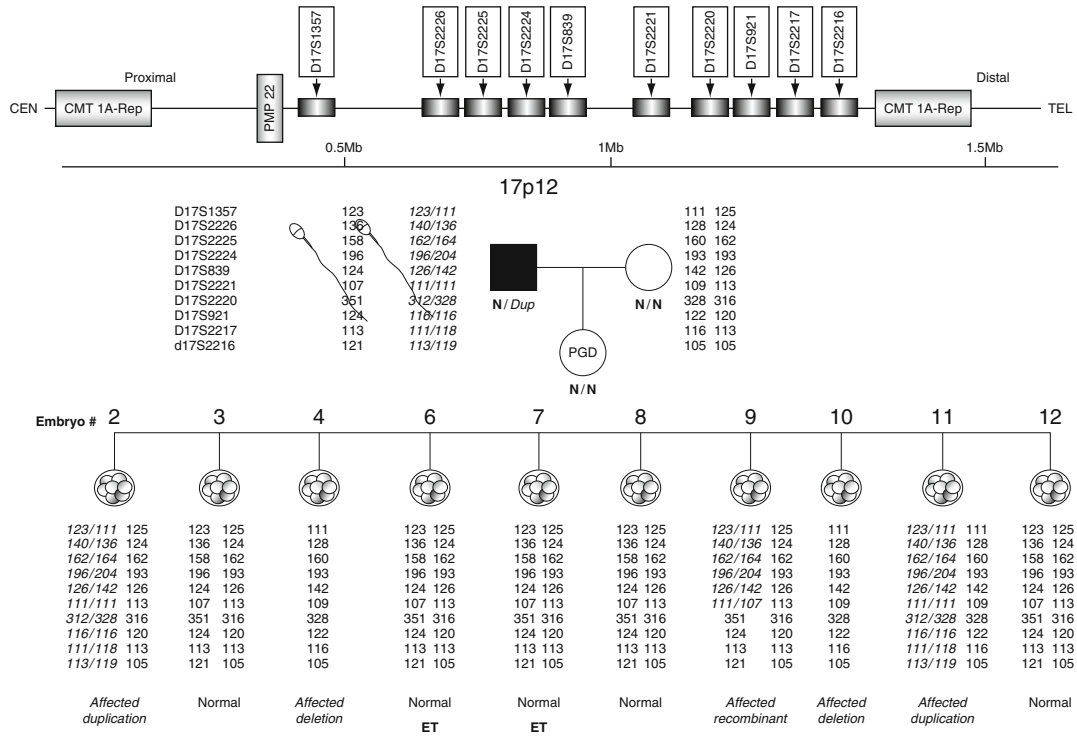

Fig. 3.11 PGD for CMT1A resulted in the birth of a healthy baby. (*Upper panel*) Schematic representation of 1.5 Mb tandem duplication including dosage-sensitive gene for peripheral myelin protein 22 (PMP22) and linked markers, showing the complexity of the diagnosis. (*Middle panel*) Family pedigree, showing the affected father with duplication and the results of haplotype analysis established through sperm testing in the father and blastomere analysis in the mother. (*Lower panel*) Results of multiplex PCR analysis for ten markers, which identified five duplication-free unaffected embryos and five affected ones, including two with duplication, one recombinant containing partial duplication, and two with deletion. Two of the unaffected embryos were transferred resulting in the birth of an unaffected child

some of the PGD cycles for dominant disorders caused by *de novo* mutations will be presented in Sect. 3.6.

3.3 X-Linked Disorders

Almost half of the PGD cycles for single-gene disorders were done for X-linked conditions, the most straightforward indication from the very beginning of the introduction of PGD, either using PCR or FISH technique. Initially this was done by gender determination not only because the sequence information was not always available, but also because it was technically straightforward to identify female embryos by DNA analysis or FISH technique, despite the obvious cost of discarding 50% of healthy male embryos. So the couples at risk may choose either prenatal diagnosis at the cost of the risk for pregnancy termination, or PGD by gender determination at the cost of discarding 50% of male embryos. However, because X-linked disorders are maternally derived the most attractive option may be preselection of mutation-free oocytes through testing for specific causative mutations in PB1 and PB2. This allows avoiding any further testing of the resulting embryos, which may be transferred irrespective of gender or any contribution from the male partner.

PGD for the X-linked disorders was first attempted more than 20 years ago, and has been performed by gender determination [1]. Gender determination was initially done by single-cell

Table 3.8 Primers and PCR conditions for PGD of CMT1 by linkage analysis

Gene/polymorphism	Upper primer	Lower primer	Annealing T_m (°C)
D17S2216 (Heminested)	Outside		62–45
	5′ TGGCAAAGAATAAGAAGGAAAGA 3′	5′ GTGTCTTGGACTCATTCGGAGACCCTT 3′	
	Inside		53
	5′ TGGCAAAGAATAAGAAGGAAAGA 3′	5′ Hex GACAGGCACGGGATTAGGA 3′	
D17S2217 (Heminested)	Outside		62–45
	5′ TCATATGCCCAGTGCCCACTC 3′	5′ GTGTCTTACACAGAGTTGATGAAAATCACTAA 3′	
	Inside		55
	5′ TCATATGCCCAGTGCCCACTC 3′	5′ FamCTTGTCCTGTTTCTCTCCTGGTTTC 3′	
D17S2218 (Heminested)	Outside		62–45
	5′ TTACAGAAGGACAAGGTAGCAAT 3′	5′ CTAAATGCTTGTGGATTAGTTGTA 3′	
	Inside		55
	5′ TTACAGAAGGACAAGGTAGCAAT 3′	5′ HexGTTGTATATTGGATTGGACCCTT 3′	
D17S2219 (Heminested)	Outside		62–45
	5′ GTGTCTTTGCTTTGCCAAGATTAC 3′	5′ CAACTGTAACACATAAAAGATGAGTTG 3′	
	Inside		55
	5′ GTGTCTTTGCTTTGCCAAGATTAC 3′	5′ FamGGGGCTTAGTCTCCATCTGGT 3′	
D17S2220 (Heminested)	Outside		62–45
	5′ GTGTCTTTGGGCAACAGAGCA 3′	5′ CTAATAATTTTCCATTTGTAACCTTG 3′	
	Inside		48
	5′ GTGTCTTTGGGCAACAGAGCA 3′	5′ FamTTCTCTTGAAACCTCAGTCATCTTT 3′	
D17S2221 (Heminested)	Outside		62–45
	5′ GTGTCTTGAAAATTTCCCACCCAAAG 3′	5′ GCCTCTCCCTGAGTGTCTGGT 3′	
	Inside		55
	5′ GTGTCTTGAAAATTTCCCACCCAAAG 3′	5′ HexGCTGCTGTTCCTTCAAAATGTG3 ′	
D17S839 (Heminested)	Outside		62–45
	5′ AACAACAGCGAAACTCTGTCTCA 3′	5′ CCAAACTTCCAAGTAAGAGAGGG 3′	
	Inside		55
	5′ AACAACAGCGAAACTCTGTCTCA 3′	5′ FamAGAGAGACCCTGGAAGATCAACTAC 3′	
D17S2224 (Heminested)	5′ GTGTCTTGTTCATTCTATCGTCTCAAA 3′	5′ AGCAGAAATGAGAGAGGAGACATTA 3′	62–45
	5′ GTGTCTTGTTCATTCTATCGTCTCAAA 3′	5′ HexTACAAAGGATCATAAGGCTACCATA 3′	55
D17S2225 (Heminested)	5′ TGGTTAAATCTGTACTCATTATGGC 3′	5′ TGTCTTACAGTTGTAGAGGGCTTGTG 3′	62–45
	5′ Hex TTCATGTATCTGGGAGTATTCACG	5′ TGTCTTACAGTTGTAGAGGGCTTGTG 3′	55

Table 3.9 Results and outcomes of PGD for X-linked disorders

Disease	Number of patients	Number of cycles	Cycle by PB	Cycle by PB &BL	Cycle by BL	Number of ET	Number of embryos	Pregnancy	Birth
DMD	8	14	1	12	1	13	36	5	6
CMT 1X	2	2	1	1	0	2	4	0	0
FRA X	29	43	16	24	3	37	86	16	15
Hemophilia A & B	4	5	0	5	0	5	11	2	2
Hyper IgM syndrome	1	2	0	2	0	2	2	1	1
Wiscott-Aldrich	1	1	0	1	0	0	0	0	0
Hydrocephalus	3	8	2	6	0	8	18	0	0
Hunter syndrome	1	2	1	1	0	2	3	1	2
Choroideremia	1	1	1	0	0	1	2	1	1
MTM	1	2	2	0	0	1	3	0	0
Norrie disease	2	4	0	4	0	4	7	0	0
X-ALD	2	3	0	3	0	3	7	1	1
OTC	4	5	3	1	1	5	8	4	4
Pelizaeus-Merzbacher disease	2	2	0	2	0	2	5	1	1
Incontinentia Pigmenti	3	4	0	4	0	4	8	1	1
Alport	1	1	1	0	0	1	2	0	0
Total	*65*	*99*	*28*	*66*	*5*	*90*	*202*	*33*	*34*

PCR analysis, while then it was performed by the FISH technique in interphase cells. Although sufficiently accurate, as mentioned, this approach leads to a discard of 50% of unaffected male embryos, which cannot be accepted by many patients. Thus, there has been a need for specific genetic tests allowing the identification of the unaffected healthy male embryos for transfer as an option to preselect the X-linked mutation-free embryos, irrespective of gender.

In an attempt to preselect the X-linked mutation free embryos for transfer, a sequential PB1 and PB2 analysis was applied as an alternative to gender determination. One of such cases, involving PGD for ornithine transcarbamylase deficiency (OTC), was first reported more than 10 years ago, showing the feasibility of the approach [31].

The couples for whom PGD was applied now include those with previous male offspring affected by Duchenne muscular dystrophy (DMD), Charcot-Marie-Tooth disease X1 (CMTX1), fragile-X syndrome (FMR1), hemophilia A (F8) and B (F9), hyperimmunoglobulin syndrome (HIGM1), Wiscott-Aldrich syndrome (WAS), X-linked hydrocephalus (L1CAM), Hunter syndrome (IDS), choroideremia (CHM), myotubular myotonic dystrophy (MTMD), Norrie disease (NDP), X-linked adrenoleukodystrophy (ALD), ornithine transcarbamylase deficiency (OTC), Pelizaeus-Merzbacher disease (PMLD), incontinentia pigmenti (IP), and Alport disease (ATS). Our preferred approach for these conditions was testing PB1 and PB2, performed in 270 PGD cycles, which resulted in the transfer of 411 embryos originating from mutation-free oocytes, yielding 94 clinical pregnancies and the birth of 91 unaffected children (Table 3.3). The details of the first series of 100 cycles are presented in Table 3.9, showing that the application of all available methods allowed preselection of the embryos for transfer in over 90% of cycles, resulting in 37% pregnancy rate per transfer and the birth of 34 healthy children.

As described in Chap. 2, PB1s were removed at least 3 h after oocyte retrieval (38 h after chorionic gonadothropin (hCG) administration), using micromanipulation procedures described above in Chap. 2. Approximately a dozen oocytes, on an average, were fertilized by intracytoplasmic sperm insertion (ICSI), followed by PB2 removal, approximately 16–18 h after ICSI. Although PB1 and PB2 were removed in

sequence, they were amplified at the same time, using nested multiplex PCR, with the primer designs worked out for each of the conditions mentioned. Primers and PCR conditions for some of these conditions are presented in Table 3.10.

Based on sequential PB1 and PB2 testing, involving the mutation and/or linked marker analysis, results of which were available already on day 1 (approximately 30–32 h after oocyte retrieval), the embryos resulting from the oocytes predicted to be free from maternal mutation were transferred back to the patients on day 3, while those predicted as affected were further tested for confirmation of diagnosis, when available. Approximately 7.7 oocytes per cycle on an average were obtained with PB1 results, which appeared to be heterozygous in 66% and homozygous normal or mutant in 34% of oocytes. PB2 results were available in 79% of these oocytes (6.1 oocytes per cycle on an average), so in the remaining oocytes the genotype prediction was not possible, so additional testing by embryo biopsy was applied.

ADO still remains to be the major problem in avoiding misdiagnosis if undetected, as observed in one of the cases of PGD for FMR1, presented below. ADOs were detected either by the use of the linked markers or by sequential PB1 and PB2 analysis. For example, in the case of PGD for X-linked hydrocephalus, both PB1 and PB2 in one of the oocytes had identical homozygous mutant genotype, suggesting that PB1 was apparently heterozygous, with the normal allele not detected due to ADO. However, at least two embryos in each cycle for this condition were available for transfer, originating from the mutation-free oocytes preselected based on the heterozygous status of PB1 and homozygous mutant PB2, which not only predicted the mutation-free status of the resulting embryos, but also reliably excluded any probability of ADO.

In the PGD cycle for *MTMD* tested by both PB1 and PB2, three unaffected embryos were transferred, originating from the oocytes with heterozygous PB1 and homozygous mutant PB2, or with homozygous mutant PB1 and normal PB2, in which ADO in PB1 was excluded by two linked markers. In PGD cycles for *F8 and F9*, embryos originating from the mutation-free oocytes were also predicted based on heterozygous PB1 and mutant PB2, resulting in clinical pregnancies and the birth of unaffected children with no misdiagnosis.

The largest group of X-linked disorders for which PGD was offered was *FMR1*, which is tested indirectly using linkage analysis, as no test is available for direct analysis of the expanded allele [32]. As the mutant allele for this condition cannot be amplified, the preselection of the mutation-free oocytes was inferred from the presence of the linked markers for the normal allele. Only a few of these cycles were performed by blastomere biopsy alone, with the majority being done either by PB1 and PB2 only or PB1 and PB2 analysis followed by blastomere biopsy, if necessary. Only one misdiagnosis was observed, which was due to undetected ADO. Three embryos were transferred, two deriving from oocytes with heterozygous PB1 and mutant PB2, and one from the oocyte with presumably homozygous mutant PB1, which in fact turned out to be heterozygous because of an undetected ADO of both alleles linked to the normal gene (Fig. 3.12). As only two of four available markers were informative for linkage analysis in this cycle, in the absence of the direct test for the expanded allele, the chance of ADO of the normal allele in this case was predicted to be in the range of over 5%, based on our previous observations described in detail above. The second largest group, for which PGD cycles were performed, was *DMD* resulting in the preselection and transfer of mutation-free embryos in all but one cycle.

One of the first X-linked disorders for which the PB approach was utilized was *OTC* [31]. In this case, of five PGD cycles performed for four couples at risk for producing offspring with *OTC*, unaffected embryos for transfer were predicted in every cycle (1.6 embryos per cycles), resulting in four clinical pregnancies, and the birth of four healthy children free of mutation, following confirmation of PGD by prenatal diagnosis [31]. The preselection of mutation-free oocytes were based on heterozygous PB1 and mutant PB2, except only a few with the homozygous mutant PB1 and normal PB2, but with the linked marker

Table 3.10 Primers to amplify mutation or linked markers for PGD of X-linked diseases

Gene/polymorphism	Upper primer	Lower primer	Anneal T_m (°C)
FMR1 AC1	Outside		62–45
	5′ AGCTGCAAAGAGAAACAGACA 3′	5′ AATATCAGGCCAGGCACA 3′	
	Inside		50
	5′ GTTGATGCTGAACATCCTTATCG 3′	5′ Fam GGCTGAGGCATGATGAGAGTC 3′	
FMR1 AC2	Outside		62–45
	5′ GCCCTAATCAGATTTCCACA 3′	5′ GATGCGGTGGCTCAAG 3′	
	Inside		50
	5′ CAAAAAGAACCCAGATGTGA 3′	5′ Fam GGGAGGATAGCTCAAGCTC 3′	
DXs548	Outside		62–45
	5′ Fam CCTACATCAAAGTCCCAGCA 3′	5′ AAGCCTGCAACCAAACACTG 3′	
	Inside		50
	5′ Fam CCTACATCAAAGTCCCAGCA 3′	5′ GTACATTAGAGTCACCTGTGGTGC 3′	
DXs1193	Outside		62–45
	5′ GCCAAGGCATAGAAGACAAC 3′	5′ TGTCAGCACAAAAGGGCTTA 3′	
	Inside		50
	5′ ATTGTTCATGCAACTCTCCTC 3′	5′ Hex TCATCCAAGCTACTTATTTTAAG 3′	
Factor IX RFLP *MseI*	Outside		62–45
	5′ AGAGGGATAAATACATCAATGGC 3′	5′ AATATATTGTCTCCAGCCTGTAGC 3′	
	Inside		60
	5′ GATAGAGAAACTGGAAGTAGACCC 3′	5′ ATTAGGTCTTTCACAGAGTAGAATTT 3′	
Factor IX RFLP *Mnl I*	Outside		62–45
	5′ TTGTAATACATGTTCCATTTGCC 3′	5′ GGGAATTGACCTGGTTTGG 3′	
	Inside		60
	5′ TTCTAGTGCCATTTCCATGTG 3′	5′ ATCTTCTCCACCAACAACCC 3′	
Factor IX VNTR(50 bp repeat)	Outside		62–45
	5′ GGGACCACTGTCGTATAATGTG 3′	5′ GAAGAGACACTCCTGAACTCTGG 3′	
	Inside		60
	5′ CCAAAATGTCATTGTGCAGC 3′	5′ TCTGAATCATATTTCTCCTTCCC 3′	
MTM1 R241C (loses artificial *HhaI site*)	Outside		62–45
	5′ TTGGATGTGGTGCTAATTAAG 3′	5′ CTCATCATCTTTATTTCGTTTC 3′	
	Inside		55
	5′ CGCAGTGAGATTGCAAGTG 3′	5′ CAAGAGGCTGACTGCA *G* C 3′	

(continued)

Table 3.10 (continued)

Gene/polymorphism	Upper primer	Lower primer	Anneal T_m (°C)
MTM1 DXS1684	Outside		62–45
	5′ AGCACCCAGTAAGAGACTG 3′	5′ TGAATCAATCTATCCATCTCTC 3′	
	Inside		55
	5′ CAGGCCACTACCACTTATG 3′	5′ HexTACTGTTTTCCACTCTAATGC 3′	
X-Hydrocephalus Fr.168 (−C) (loses *Hpa II* site)	Outside		62–45
	5′ GAGTGTCAGCCCGTCTG 3′	5′ AGTAGAGGTTGCCGTTCTG 3′	
	Inside		60
	5′ GTGGCCAAAGGAGACAGTGAA 3′	5′ GAAGACACCCCCGCTAACA 3′	
PLP1 L86P (Msp I cuts mutant)	Outside		62–45
	5′ ATCTATGGAACTGCCTCTTTCTTCT 3′	5′ CGCTCCAAAGAATGAGCTTGAT 3′	
	Inside		60
	5′ ATCTATGGAACTGCCTCTTTCTTCT 3′	5′ GGCCCCCTGTTACCGTTG 3′	
5′ PLP1 (CA)n (Heminested)	Outside		62–45
	5′ GGAAGGGACCTGAAGAAAAAGAT 3′	5′ GCTCTCATTTACCTGGCACACTA 3′	
	Inside		55
	5′ FamGGGGTGATTCTAGTAACCAGGC 3′	5′ GCTCTCATTTACCTGGCACACTA 3′	
DXS8020 (Heminested)	Outside		62–45
	5′ GATGGGTCGGTGATGAGAA 3′	5′ TCAGCATTACAATTCTGTATAGACT 3′	
	Inside		60
	5′ FamGGGAGGTAGAAAAGGGTTGGAAAGG 3′	5′ TCAGCATTACAATTCTGTATAGACT 3′	
DXS8096 (Heminested)	Outside		62–45
	5′ CCTAAGGTTTCCAGATTTAGCA 3′	5′ TGTGAGCCAGTTCTTGAAAAT 3′	
	Inside		55
	5′ FamACATCCAGAGAAACAGAACCAA 3′	5′ TGTGAGCCAGTTCTTGAAAAT 3′	
DXS8089 (Heminested)	Outside		62–45
	5′ ATGAATGGTGCTAGGATTTGG 3′	5′ ATTTTTACATTATGATGTGGTCAAA 3′	
	Inside		60
	5′ ATGAATGGTGCTAGGATTTGG 3′	5′ Fam TTCTTGTATGGCTTCTGGGTC 3′	
DXS1191 (Heminested)	Outside		62–45
	5′ TTGAAGGATGCACACTACAAA 3′	5′ GCCCCGTTTGATGCTTCTA 3′	
	Inside		60
	5′ TTGAAGGATGCACACTACAAA 3′	5′ FamCAGCAGTAAACTGTTTCCCTTT 3′	

Oocyte	Cell Type	DXs1193	DXs548	Predicted Genotype
1	PB1	*154*/**156**	*245*/**247**	*Affected*
	PB2	**156**	**247**	
3	PB1	154/**156**	*245*/**247**	*Affected*
	PB2	**156**	**247**	
5	PB1	154/**156**	*245*/**247**	**Normal**
	PB2	*154*	*245*	
6	PB1	*245*/**247**	*245*/**247**	**Normal**
	PB2	*154*	*247*	
9	PB1	*154**	*245**	**Normal***
	PB2	**156**	**247**	
10	PB1	*245*/**247**	*245*/**247**	*Affected*
	PB2	**156**	**247**	
Cord blood		*154*	*245*	*Affected*

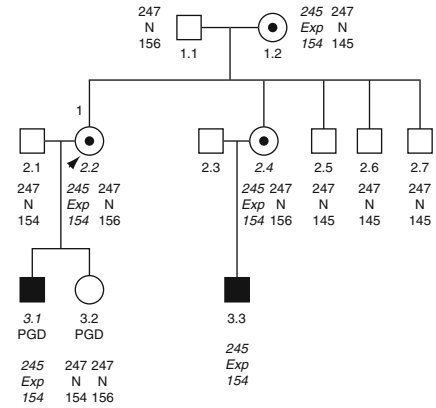

Fig. 3.12 PGD for FRM1 with misdiagnosis due to undetected ADO in the first polar body. Family pedigree (*right*) and PGD results of haplotype analysis for CGG expansion in FMR1 gene using two linked markers (*left*). The mother is a carrier of an expanded allele linked to 154 and 245 markers. Her sister also has an expanded allele inherited from their mother. One of the sisters who presented for PGD is shown by *arrow*. The other sister has an affected son, who carries only an expanded allele (linked to 154 and 245 markers). On the left of the pedigree, an affected child carrying only an expanded allele (linked to 154 and 245 markers) was born following PGD, due to the predicted 5% risk of misdiagnosis, resulting from undetected ADO of the normal allele in PB1 of the corresponding oocyte (shown by * in the table on the *left*), from which the transferred embryo derived. As can be seen from the table, misdiagnosis originates from the undetected ADO of both markers linked to the expanded allele in PB1 of oocyte #9, which was erroneously considered homozygous mutant, while it was actually heterozygous; following the extrusion of PB2 with the normal allele, the maternal contribution to the resulting oocytes should have been considered mutant

information available to confirm the diagnosis. Despite transferring only a single embryo or two in each of these cycles, resulting from the mutation-free oocytes, an extremely positive clinical outcome of PGD for OTC was observed.

It should also be mentioned that, as in PGD for other conditions, an increasing number of patients presenting for PGD are of advance reproductive age, so a combined aneuploidy testing may be expected to be widely applied in the future, which in addition to avoidance of the birth of children with chromosomal disorders may also improve the PGD clinical outcome, as demonstrated in the example of PGD for PMLD, presented below.

PMLD is an X-linked recessive dysmyelinating disorder of the central nervous system that leads to deterioration of coordination, motor ability, and intellectual function, caused by mutation of the proteolipid protein 1 (PLP1) gene located on the long arm of the X (Xq22) chromosome. The gene consists of seven exons of about 15 Kbp, encoding two major proteins PLP1 and DM20, that results from alternative splicing, both serving an important structural component of compact myelin [16, 33].

PMD manifests in infancy or early childhood, with a span of continuum of neurological impairments from nistagmus, delayed motor and cognitive impairment to severe spasticity and ataxia with early mortality from respiratory complication during childhood. Mutations in PLD1 may result in misfolding of the coded proteins, failing to progress through the intracellular processes. This results in their accumulation in the endoplasmic reticulum, which triggers apoptosis, affecting oligodendrocyte survival and myelination. Although several nondisease-causing polymorphisms have

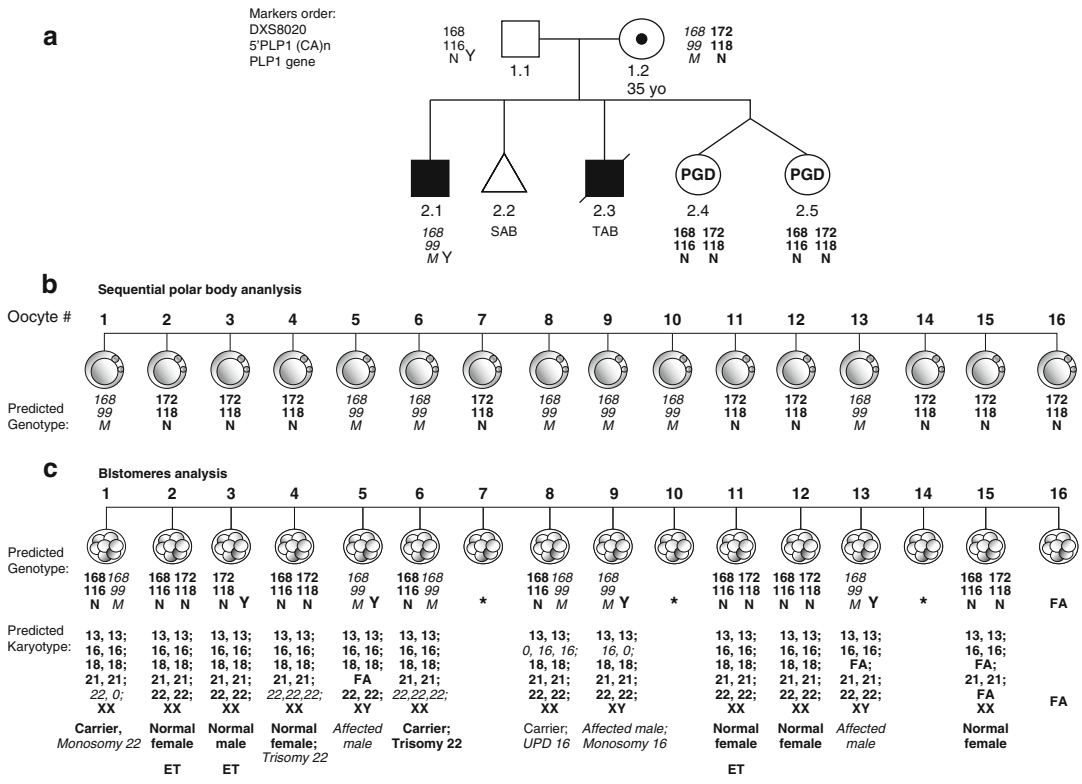

Fig. 3.13 PGD for PMD with aneuploidy testing. (**a**) Pedigree showing that the mother (1.2) is a carrier of L86P mutation in exon 3 of the PLP1 gene, which is linked to 99 bp repeat of 5′ PLP1 (CA)n, and 168 bp repeat of DXS8020, while the normal allele is linked to 118 and 172 bp repeats of the same polymorphic markers, respectively. The father (1.1) is unaffected, carrying the normal PLP1 allele, linked to 116 and 168 bp repeats, respectively. (*Lower panel*) Reproductive outcomes of this couple, including one previous affected child with PMD (2.1), one spontaneous abortion (2.2), and one prenatal diagnosis, resulting in identification of the affected fetus and termination of pregnancy (2.3). *SAB* spontaneous abortion, *TAB* termination of pregnancy following chorionic villus sampling (*CVS*). (**b**) Sequential PB1 and PB2 analysis of 16 oocytes, of which 9 were predicted to be free of L86P mutation in exon 3 of the PLP1 gene, and 7 affected. (**c**) Blastomere analysis for causative gene (*upper panel*) and aneuploidy (*lower panel*), showing 3 mutant embryos (embryos #5, #9, and #13) and 9 unaffected, including 3 heterozygous female embryos. The remaining 4 embryos were inconclusive, including one with failed amplification. Aneuploidy testing revealed 2 embryos with trisomy 22 (embryos #1 and #6), 1 with monosomy 22, 1 with monosomy 16 (embryo #9), and 1 with uniparental disomy 16 (embryo #8). Three unaffected embryos (embryos #2, #3, and #11) were transferred, resulting in the birth of healthy twins. *Not available for testing (the IVF was performed in a different institution in another state and it is assumed that biopsy material was not sent for testing, because embryos did not develop further. For the same reason, the fate of the other two unaffected embryos (embryos #12 and #15) is also unknown, although it is presumed that they were frozen). *FA* failed amplification

been described, at least 100 different mutations in the PLP1 gene are known to be associated with PMD, including duplications, which are the most frequent ones, small insertions, deletions, and single-base substitutions, leading to missence, nonsense, or splicing mutations.

Because no specific treatment for PMD is presently available, prenatal diagnosis is offered as an option for couples at risk to avoid the birth of the affected child [34]. As mentioned above, PGD seems to be particularly attractive for at-risk couples who cannot accept prenatal diagnosis and termination of pregnancy. In addition, because of a wide individual phenotypic variability even within families, the decision about termination of the affected pregnancy may be extremely difficult even for those couples that accept prenatal diagnosis.

The couple presented for PGD had a history of a previous child diagnosed with PMD (Fig. 3.13). The phenotypically normal 35-year-old mother

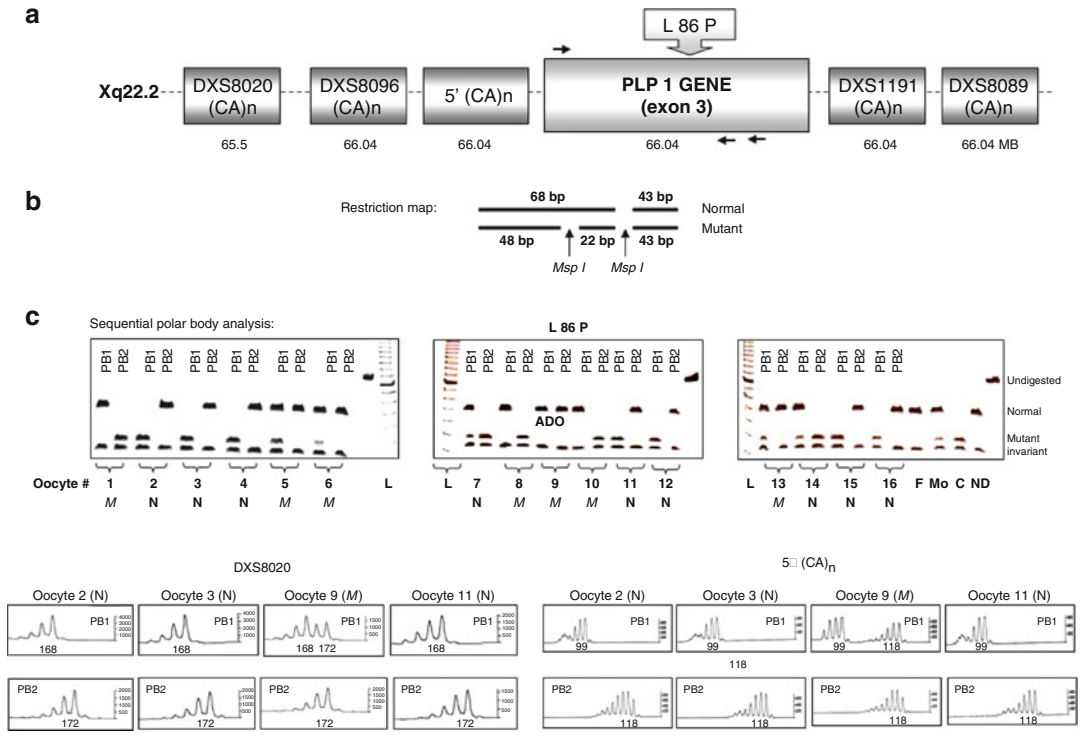

Fig. 3.14 Preimplantation genetic diagnosis for major mutation and polymorphic markers in PMD. (**a**) Position of L86P mutation in PLP1 gene of exon 3 and polymorphic markers. (**b**) Restriction map. The mutation creates restriction site for *Msp*I enzyme. (**c**) PB analysis of normal and mutant sequences of PLP1 gene (*upper panel*). Of 16 oocytes tested, 9 were mutation-free based on heterozygous PB1 and affected PB2 in 2 of them (embryos #7 and #14) and mutant PB1 and normal PB2 in the remaining 7 oocytes. Six embryos were affected, based on heterozygous PB1 and normal PB2 in three of them (embryos #5, #6, and #13) and normal PB1 and mutant PB2 in the remaining three (embryos #1, #8, and #10). ADO of the mutant allele was observed in PB1 analysis of oocyte #9, which is confirmed by both linked polymorphic markers, suggesting the presence of both alleles in PB1 from oocyte #9 (*lower panel*). Linked polymorphic marker analysis confirmed the data of mutation analysis in all the oocytes, including the mutation-free status of oocytes #2, #3, and #11, shown on the *lower panel*; the embryos resulting from these three oocytes were transferred back to the patient resulting in unaffected twins (see Fig. 3.13). L ladder, *N* normal, *M* mutant, *Mo* maternal genotype, *F* paternal genotype, *C* affected child's genotype, *ND* normal (control) DNA

was a carrier of the T257C (L86P) mutation in exon 3 of the PLP1 gene, representing T to C substitution in 257 nucleotide position that results in lysine to proline substitution in 86 position of amino acid sequence of PLP1 protein. As seen from the pedigree (Fig. 3.14), the couples had two more pregnancies, one resulting in spontaneous abortion and the other terminated because the fetus was diagnosed with PMD by chorionic villus sampling (CVS).

The PGD cycle was performed using PB and blastomere analysis, as described above. PB1 and PB2 were removed sequentially following maturation and fertilization of the oocytes, and tested by the multiplex PCR analysis, involving the mutation testing simultaneously with two closely linked polymorphic markers, PLP-intragenic microsatellite PLP5' (CA)n and the nearest flanking extragenic microsatellite DXS8020. The mutation analysis involved the detection of T to C change in nucleotide position 257 of exon 3, based on Msp I restriction digestion, which does not cut the normal allele, while creating two fragments of 48 and 22 bp in the mutant allele (Fig. 3.14). The primers and reaction conditions are presented in Table 3.11.

Because the oocytes predicted as mutant may further form unaffected heterozygous female

Table 3.11 Primers and reaction conditions for PGD of PMD

Gene/ polymorphysm	Accession number	Heterozygosity index	Number of alleles	Upper primer	Lower primer	Annealing T_m (°C)
PLP1 L 86 P (heminested) *Msp I* cuts mutant sequence	NT_011651	NA	NA	Outside: 5′ ATCTATGGAACTGCCTCTTTCTTCT 3′ Inside: 5′ ATCTATGGAACTGCCTCTTTCTTCT 3′	5 CGCTCCAAAGAATGAGCTTGAT 3′ 5′ GATGGTGGTCCTGTAGTCGCC 3′	62–45 60
DXS8020 (heminested)	Z 52328	0.78	9	Outside: 5′ GATGGGTCGGTGATGAGAA 3′ Inside: 5′ *Fam* GGGAGGTAGAAAAGGGTTGGAAAGG 3′	5′ TCAGCATTACAATTCTGTATAGACT 3′ 5′ TCAGCATTACAATTCTGTATAGACT 3′	62–45 55
DXS8096 (heminested)	Z 51652	0.8	12	Outside: 5′ CCTAAGGTTTCCAGATTTAGCA 3′ Inside: 5′ *Fam* ACATCCAGAGAAACAGAACCAA 3′	5′ TGTGAGCCAGTTCTTGAAAAT 3′ 5′ TGTGAGCCAGTTCTTGAAAAT 3′	62–45 55
5′ PLP1 $(CA)_n$ (heminested)	NT_011651	0.56	5	Outside: 5′ GGAAGGGACCTGAAGAAAAAGAT 3′ Inside: 5′ *Fam* GGGGTGATTCTAGTAACCAGGC 3′	5′ GCTCTCATTTACCTGGCACACTA 3′ 5′ GCTCTCATTTACCTGGCACACTA 3′	62–45 55
DXS119 1 (heminested)	Z 23464	0.65	5	Outside: 5′ TTGAAGGATGCACACTACAAA 3′ Inside: 5′ TTGAAGGATGCACACTACAAA 3′	5′ GCCCCGTTTGATGCTTCTA 3′ 5′ *Fam* CAGCAGTAAACTGTTTCCCTTT 3′	62–45 55
DXS8089 (heminested)	Z 51440	0.81	8	Outside: 5′ ATGAATGGTGCTAGGATTTGG 3′ Inside: 5′ ATGAATGGTGCTAGGATTTGG 3′	5′ ATTTTTACATTATGATGTGGTCAAA 3′ 5′ *Fam* TTCTTGTATGGCTTCTGGGTC 3′	62–45 55

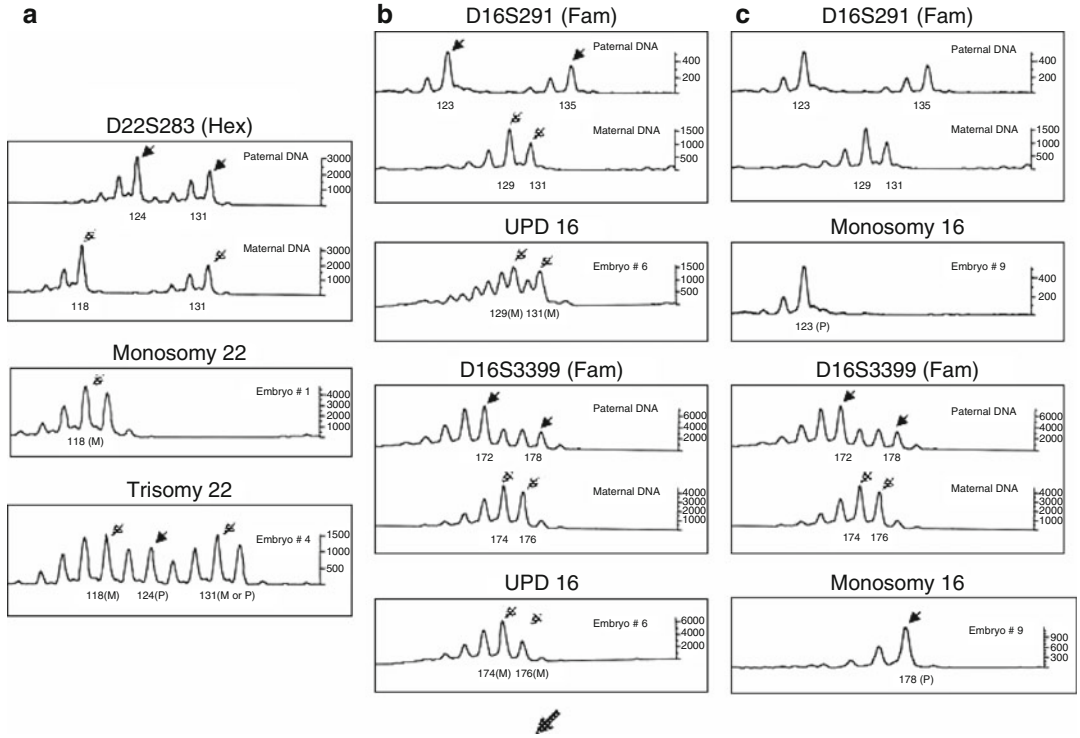

Fig. 3.15 Aneuploidy testing as part of PGD for PMD. (**a**) *Upper panel* shows paternal and maternal haplotypes for D22S283, allowing identification of monosomy 22 in embryo #1, evidenced by only one maternal allele (*middle panel*) and trisomy 22 in embryo #4 (*lower panel*). (**b**) The *first* and *third panels* show paternal and maternal haplotypes for D16S291 and D16S3399, respectively, allowing identification of uniparental disomy 16 in embryo #8, evidenced by only maternal alleles (*second and fourth panels*). (**c**) The *first* and *third panels* show paternal and maternal haplotypes for D16S291 and D16S3399, respectively, allowing identification of monosomy16 in embryo #9, evidenced by only paternal alleles for each marker (*second and fourth panels*)

embryos, following fertilization by a sperm carrying the X chromosome, testing for paternal normal gene in the resulting embryos was also performed. Because the mother was 35 years old, the biopsied blastomeres were also tested for the age-related aneuploidies, for which purpose the copy number of chromosomes 13, 16, 18, 21, 22, X, and Y was identified (Fig. 3.15), using the patterns of alleles that uniquely identify the individual, relying on a multiplex fluorescent PCR of low-template DNA (primers are described in Chap. 2).

The maternal haplotypes, presented in Fig. 3.13, were established based on PB analysis: the mutant allele was linked to 168 bp repeat of DXS8020 and 99 bp repeat of PLP5' (CA) n marker; the normal allele was linked to 172 bp repeat of DXS8020 and 118 bp repeat of PLP5' (CA) n marker. The paternal haplotypes were established based on family blood sample DNA analysis: the normal paternal allele was linked to 168 bp repeat of DXS8020 and 116 bp repeat of PLP5' (CA)n marker.

Of 16 oocytes available for testing in one PGD cycle, 9 were mutation-free based on heterozygous PB1 and affected PB2 in 2 of them (embryos #7 and #14) and mutant PB1 and normal PB2 in the remaining 7 oocytes. Six embryos were affected, based on heterozygous PB1 and normal PB2 in 3 of them (embryos #5, #6, and #13) and normal PB1 and mutant PB2 in the remaining 3 (embryos #1, #8, and #10) (Fig. 3.13). This was in accordance with the two tightly linked polymorphic markers DXS 8020 and 5' (CA) n, as shown in three examples of three normal oocytes (oocytes #2, #3, and #11), in all but one (oocyte

#9), in which both PB1 and PB2 mutation analysis demonstrated the normal genotype, while the marker analysis revealed both normal and mutant alleles in PB1, suggested allele drop out (ADO) of the mutant allele.

Of 13 embryos available for blastomere analysis, 12 were with results, of which 3 were affected (embryos #5, #9, and #13) (Fig. 3.13), 5 chromosomally abnormal, including 2 trisomy 22 (1 of which, embryo #4, is shown in Fig. 3.15), 1 monosomy 22 (embryo #1), 1 monosomy 16 (embryo #9; also affected), and 1 uniparental disomy for chromosome 16 (embryo #8), and 5 unaffected. Three of these embryos, free of mutant gene and aneuploidy (embryos #2, #3, and #12) were transferred, resulting in a twin pregnancy and the birth of two unaffected children, confirmed to be euploid and free of T257C mutation in the PLP1 gene.

The presented case was the first PGD for PMD, demonstrating the realistic option available for couples at risk for producing offspring with the most severe type of PMD, caused by the T257C mutation. However, PGD may be useful also for milder but more frequent types of PMD caused by duplications, the wide variability of clinical manifestations of which may present difficulties in making decision of interruption of the affected pregnancies in prenatal diagnosis.

Because of an advanced reproductive age of the patient in the presented case, aneuploidy testing was also performed, using blastomere analysis to exclude both maternally and paternally derived aneuploidies. As for specific PLP1 mutation testing, which is maternally derived, although this may have been limited solely to oocyte analysis, the embryo testing allowed the identification of those unaffected female embryos which derived from the mutant oocytes detected by PB analysis. For example, embryos #1 and #6 were heterozygous unaffected, despite originating from mutant oocytes; however, embryo #1 appeared to be monosomic for chromosome 22, and embryo #6 trisomic for chromosome 22 (see Figs. 3.13 and 3.15). The fact that 5 of 12 tested embryos were detected to be chromosomally abnormal is in agreement with the expected risk for aneuploidies in patients of advanced reproductive age.

One of the incidental findings shown in Fig. 3.15 was a uniparental disomy of chromosome 16, which cannot be detected without PCR-based aneuploidy testing. Because both of these chromosomes 16 were of maternal origin, the extra chromosome 16 should have derived from the maternal meiosis I, followed by a subsequent trisomy rescue at the cleavage stage, which resulted in an incidental loss of the paternal chromosome 16 and the establishment of uniparental disomy 16 in the heterozygous status for PLP1 mutation in the female embryo. Unfortunately, this embryo could not be tested for the presence of the trisomic cell line, as the IVF was performed in a different institution in another state. It may be expected that the detection of uniparental disomies may in future help in avoiding them from transfer, which may contribute to the avoidance of at least some proportion of imprinting disorders described recently in association with assisted reproductive technologies [35].

With progress in obtaining the sequence information for X-liked disorders, PGD for an increasing number of X-linked disorders may soon be performed by specific diagnosis to avoid discarding 50% of healthy male embryos. On the other hand, as demonstrated above, testing for X-linked genetic disorders may be entirely limited to oocytes, because of the maternal origin of the mutations involved, making useless any further manipulation and testing of the resulting embryos, which may be transferred irrespective of gender or any contribution from the father. PGD using specific diagnosis for X-linked disorders has been reported also based on blastomere biopsy [36].

Presented results further demonstrate the clinical usefulness of PGD for X-linked disorders by a sequential PB1 and PB2 analysis, which resulted in the transfer of the embryos originating from the oocytes predicted to be free from X-linked mutation in 220 of 270 clinical cycles performed (Tables 3.3). As mentioned, these transfers yielded 94 clinical pregnancies, resulting in the birth of 91 healthy unaffected children in all but one case, in which the affected embryo was misdiagnosed to originate from the oocyte with the homozygous mutant PB1, predicted on the basis of only one additional polymorphic marker, which leaves an over 5% chance for misdiagnosis. With two

embryos having been reliably diagnosed for transfer, the couple may have had the reason for accepting such a misdiagnosis risk, so as to have three instead of two embryos for transfer, improving the chances to become pregnant. The results demonstrate once again that the embryos resulting from the oocytes with homozygous mutant PB1should not be transferred unless at least three linked markers are available to exclude the possible heterozygous status of PB1. This is especially relevant to testing for FMR1, which is entirely based on linkage analysis. To exclude completely the risk for misdiagnosis in the embryos resulting from homozygous affected PB1, testing for as many as four linked markers, overall, is required.

In conclusion, the data show that a specific genetic analysis by sequential PB1 and PB2 testing may be a practical option for PGD of X-linked disorders, providing an alternative to PGD by gender determination.

3.4 Homozygous or Double Heterozygous Recessive Conditions

PGD is of special value for dominant conditions and those couples with one homozygous and double heterozygous-affected partner, when only 50% chance of having an unaffected child may be expected. This was first applied for a couple with compound heterozygous male partner affected by *phenylketonuria* (*PKU*), and female partner carrying the third PKU mutation [37].

One in every 10,000 infants in the United States is born with PKU, an inherited metabolic disorder that causes mental retardation if untreated. When infants are fed a strict diet from birth, they have normal development and a normal lifespan. However, a strictly controlled diet must be maintained, especially during pregnancy in female patients, so as to avoid potential detrimental effects on the fetus. Because of considerable progress in screening newborns for PKU and dietary modification treatment, PKU has not often been included in prenatal diagnosis. With the introduction of PGD, which enables couples to have a healthy pregnancy, couples at risk may avoid giving birth to a child who needs a lifelong dietary treatment. PGD may be particularly useful for couples in whom one partner is homozygous or compound heterozygous-affected because there is a 50% chance of producing a child affected with PKU.

As mentioned, the first case of PGD for PKU was performed in a couple with compound heterozygous affected partner presenting for PGD in connection with their first offspring with PKU, and their 50% risk of producing another affected child. The 31-year-old mother was a carrier of the R408W mutation in exon 12 of the phenylalanine hydroxylase (PAH) gene, while the affected father was compound heterozygous for R408 and Y414C mutations in the same exon. Following maturation of oocytes in a standard IVF protocol, PB1s were removed following maturation of oocytes. Then following fertilization of oocytes by ICSI, PB2 were removed using the micromanipulation techniques described in Chap. 2. PB1 and PB2 were amplified by heminested multiplex PCR, using a primer design and primer-melting temperatures, presented in Table 3.12. Restriction digestion of the PCR product for mutation was performed overnight with Sty1 enzyme (Promega), followed by acrylamide gel electrophoresis. To detect possible ADO of mutant or normal allele, two linked markers were amplified simultaneously with the PAH gene, one representing an STR in intron 3, and the other a restriction fragment length polymorphism (RFLP) XmnI in intron 8. To detect potential contamination with extraneous DNA, an additional non-linked VNTR was also amplified.

The embryos resulting from oocytes predicted to contain only normal maternal alleles were cultured into the cleaving 6–8-cell embryos and transferred back to the patient on day 3 after aspiration. The resulting pregnancy was followed up by prenatal diagnosis to confirm the results of PGD. Accordingly, those embryos resulting from oocytes predicted to contain the mutant maternal gene were also analyzed further to investigate the accuracy of the results of the sequential PB1 and PB2 analysis.

Of 15 oocytes available for testing, the results for both PB1 and PB2 were obtained in 11 of

Table 3.12 Primers and reaction conditions used in PGD for PKU

Gene/polymorphism	Upper primer	Lower primer	Annealing T_m (°C)
Y414C Nested PCR (*Pst I* cuts mutant allele)	Outside		62–45
	5′ ATGCCACTGAGAACTCTC 3′	5′ AGTCTTCGATTACTGAGAAA 3′	
	Inside		54
	5′ TACCTTTCTCCAAATGGTG 3′	5′ CCTTTAGGTGTGTAGG*CT*G 3′	
R408W Heminested PCR (*Sty I* cuts mutant allele)	Outside		62–45
	5′ ATGCCACTGAGAACTCTC 3′	5′ AGTCTTCGATTACTGAGAAA′ 3′	
	Inside		54
	5′ TACCTTTCTCCAAATGGTG 3′	5′ AGTCTTCGATTACTGAGAAA 3′	
VNTR Nested PCR	Outside		62–45
	5′ GCTTGAAACTTGAAAGTTGC 3′	5′ GGAAACTTAAGAATCCCATC 3′	
	Inside		56
	5′ CTTGATTTAATCATTTTACAAT 3′	5′ CTCAGAGAAGCACATCTTTT 3′	
SNP (*Xmn I*) Heminested PCR	Outside		62–45
	5′ CTGTACTTGTAAGATGCAGC 3′	5′ GCAGTAACCACACTTCTGAA 3′	
	Inside		58
	5′ CTGTACTTGTAAGATGCAGC 3′	5′ ACTGTCCCAAGCAATCAAAG 3′	
Exon 3 STR $(TCTA)^n$ Heminested PCR	Outside		62–45
	5′ CAAATTGCCAGAACACATA 3′	5′ TCATAAGTGTTCCCAGACA 3′	
	Inside		52
	5′ TGTGGAAAGCAGAAAGAC 3′	5′ TCATAAGTGTTCCCAGACA 3′	

them, allowing a reliable diagnosis. Six oocytes with both PB1 and PB2 data were predicted normal, based on the heterozygous PB1, containing both the normal and mutant maternal alleles, and the mutant PB2, suggesting that no mutant allele was left in the resulting oocytes (Fig. 3.16). Another oocyte was predicted normal based on the presence of the mutant allele in PB1 and the normal allele in PB2. These results were in agreement with the linked marker analysis, showing that the homozygous status of PB1 was not due to ADO of the normal allele. Three oocytes were predicted affected, the diagnosis of two of which were based on the heterozygous status of PB1 and the normal PB2, and one on the homozygous normal status of PB1 and the mutant PB2. ADO of the mutant allele was observed in one oocyte, evidenced by the identical genotype of PB1 and PB2. This was confirmed by the presence of the linked polymorphic markers, suggesting that the resulting oocytes were mutant. The marker analysis also confirmed the mutant status of these three oocytes. ADO was observed in the STR analysis of two oocytes, evidenced by the identical patterns in PB1 and PB2. Three of four embryos resulting from these mutant oocytes were followed up by the mutation and marker analysis, confirming the presence of the mutant allele in all of them. Four of seven embryos resulting from the mutation-free oocytes were selected for transfer back to the patient, yielding a clinical twin pregnancy, confirmed by the chorionic villus sampling (CVS) to be unaffected. Healthy unaffected twins were born, presently of 7 years of age, with normal patterns of mental development.

The presented case was the first experience of PGD for PKU in the experience of PGD for more than 200 different single-gene disorders, which were mainly performed for the at-risk couples with both unaffected partners who were heterozygous carriers of an autosomal-recessive gene mutation, or one with a dominant mutation. Because, in the presented cases, it was a male partner who was compound heterozygous-affected, the PGD strategy was based on the preselection of the maternal mutation-free oocytes using a sequential PB1 and PB2 DNA analysis.

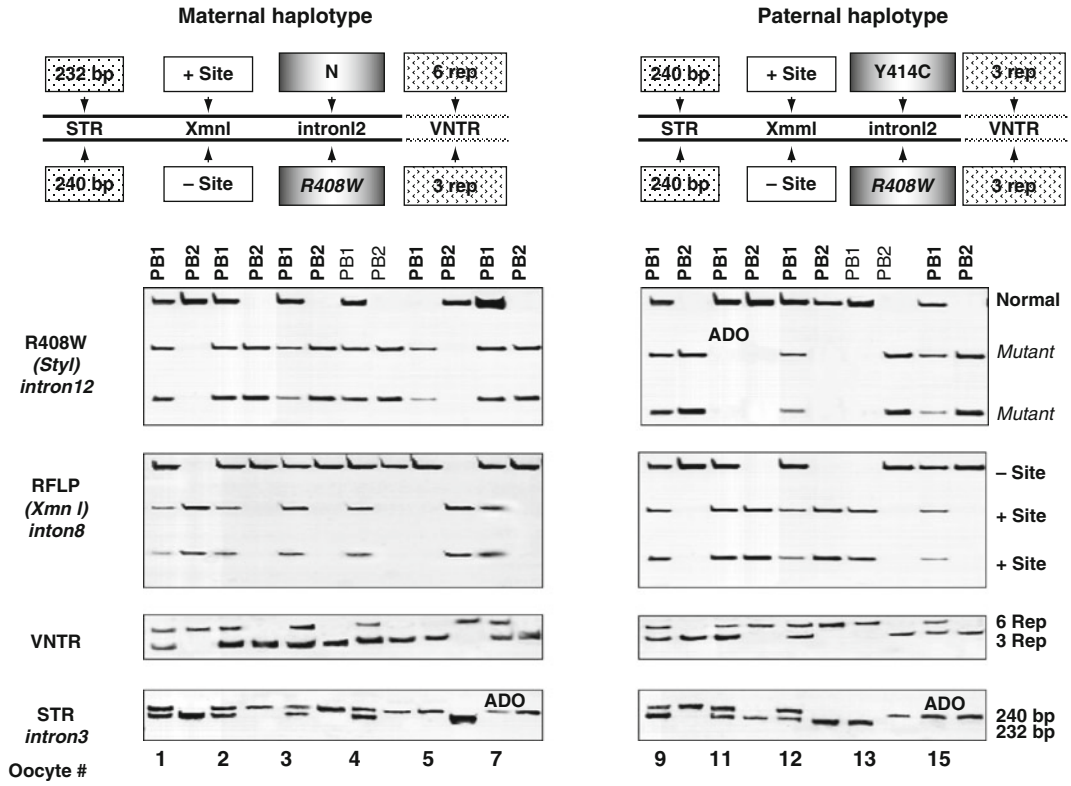

Fig. 3.16 PGD for R408W mutation in phenylalanine hydroxylase gene in a couple with the male partner homozygous affected. (*Upper panel*) Schematic representation of maternal (*left*) and paternal (*right*) haplotypes. Heterozygous mother has R408W mutation linked to short tandem repeats (*STRs*) in intron 3, variable number of tandem repeats (VNTRs) close to 3′ of gene (3 rep), and restriction fragment-length polymorphism (*RFLP*) in intron 8 (−site). Homozygous affected father has two different mutations, one similar to maternal (R408W) mutation, and the other, Y414C mutation, with its own linkage pattern. (*Bottom panel*) Genotyping oocytes by sequential analysis of PB1and PB2 for R408W mutation and informative linked markers – STR, VNTR, and RFLP. All series include PB1 followed by PB2 in the lane to its immediate right, corresponding to 11 oocytes studied (oocytes are numbered at the bottom). As R408W mutation creates restriction site for StyI enzyme, oocytes #2, #3, #4, #7, #9, and #15 were predicted normal based on heterozygous PB1 and homozygous PB2. Oocyte #5 was also predicted normal, but based on homozygous mutant PB1 and normal PB2, which was in agreement with marker analysis, excluding the possibility for ADO in the corresponding PB1. ADO of mutant allele is evident from identical genotype of both PB1 and PB2 in oocyte #11 (confirmed by all three markers), suggesting affected status of this oocyte. Other three affected oocytes were predicted based on heterozygous PB1 and normal PB2 (oocytes #1 and #12), and homozygous normal PB1 and mutant PB2 (oocyte #13). ADO was also detected in oocytes #7 and #15 (identical genotype of PB1 and PB2 for intron 3 STR). These are not in conflict with unaffected genotype of resulting embryos, which were transferred together with two other unaffected embryos (#2 and #4), resulting in twin pregnancy and the birth of two healthy children, following confirmation of PGD by prenatal diagnosis

Based on the multiplex heminested PCR analysis, 6 of 11 oocytes with both PB1 and PB2 results were predicted to contain no mutant allele of the PHA gene. Four embryos resulting from these zygotes were transferred, yielding an unaffected twin pregnancy and the birth of healthy children, following the confirmation of PGD by CVS. The high accuracy of this strategy was obvious from the follow-up study of the embryos resulting from the mutant oocytes, confirming the results of the sequential PB1 and PB2 analysis.

With progress in the treatment of genetic disorders, PGD will have an increasing impact on the decision of the affected and well-treated

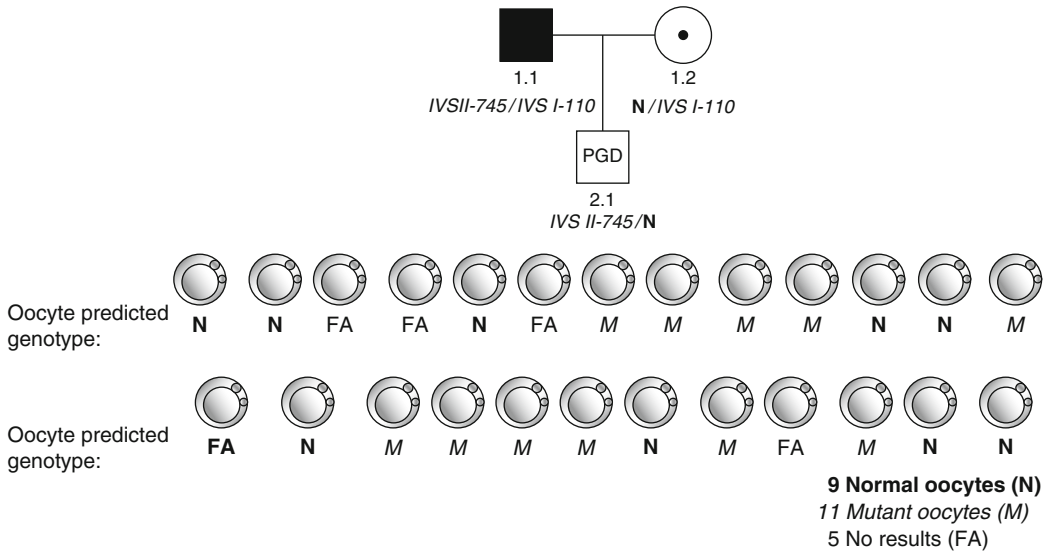

Fig. 3.17 PGD for a couple with double heterozygous affected male partner with thalassemia. (*Top*) Family pedigree with father double-heterozygous IVSI-110 and IVSII-745, and mother carrier of IVSI-110. (*Bottom*) Genotyping of 20 embryos for maternal IVSI-110 mutation by sequential PB1 and PB2, resulting in prediction of 9 mutation-free oocytes

patients to reproduce. For example, the life expectancy has been significantly improved for such common conditions as *CFTR and thalassemias*, which presently may be treated radically by stem cell transplantation. In each of such cases, the strategy depends on whether the affected partner is male or female, because testing may be entirely based on oocytes if the male partner is affected, in contrast to embryo testing when the female partner if affected. We have performed PGD for couples with affected partners with both of these conditions presented below.

In *thalassemia* cases, there may be male factor infertility involved, so the male partners need appropriate treatments before PGD, or testicular biopsy has to be done. This was the case in one of our couples with *male thalassemic partner*, when a sufficient number of oocytes with homozygous mutant or heterozygous PB1 were detected, but no appropriated sperm can be found for fertilization, so matured oocytes were frozen for possible future use after treatment. In the other two cycles because the female partner was affected, blastomere biopsy was utilized, resulting in preselection of a single unaffected embryo for transfer in each cycle, yielding no clinical pregnancy. This was due to a limited number of oocytes obtained from thalassemic female partners. However, in the well-treated patients, the situation may be different as shown in the case with the male affected partner with two different mutations IVSI-110 and IVSII-745 and the female partner with IVSI-110, presented in Fig. 3.17. Of 25 embryos tested, 5 failed to amplify, 11 were mutant, and 9 heterozygous normal, providing a sufficient number of embryos for transfer (to be extended, if necessary).

We also performed PGD for couples, one with female and one with *affected male partner with CF*. In the couple with a maternal affected partner there were three different mutations in the CFTR gene. The mother was affected with *CF* and had two different mutations R117H and G542X. The father was a carrier of 1,717 mutation in the CFTR gene. Paternal haplotypes were established using single-sperm PCR, while maternal linkage was based on DNA amplification of PB1s. The couple had two previous pregnancies, the first one resulting in the spontaneous abortion of twins, and the second pregnancy being terminated following prenatal diagnosis which identified an affected fetus with CFTR. So PGD was performed for three different mutations in the CFTR gene, resulting in an unaffected

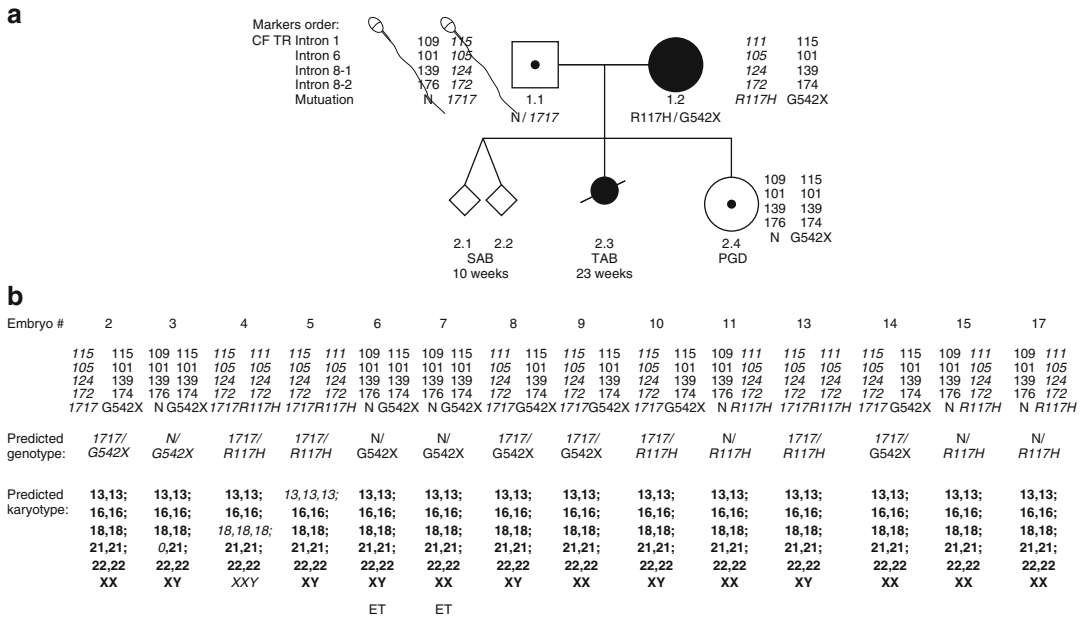

Fig. 3.18 PGD for a couple with female affected double heterozygous partner with two different CFTR mutations combined with aneuploidy testing. (**a**) Family pedigree of a couple with three different mutations in CFTR gene. The mother is affected with cystic fibrosis (*CF*) and had two different mutations (R117H and G542X). The father is a carrier of 1717 mutation in CFTR gene. Paternal haplotype was established by multiplex heminested single-sperm PCR. Maternal linkage was based on DNA amplification of polar bodies. Marker order of the mutations and polymorphic markers in CFTR gene are shown on the *upper left*. The first pregnancy with twins resulted in spontaneous abortion and the second pregnancy in an affected fetus which was terminated; PGD was performed for three different mutations in CFTR gene, resulting in an unaffected pregnancy and the birth of a healthy girl predicted and confirmed to be the carrier of maternal mutation G542X. (**b**) Outcome of PGD cycle for three mutations in CFTR gene combined with age-related aneuploidy testing. Multiplex heminested PCR performed on blastomeres from 14 embryos allowing simultaneous detection of the paternal and maternal CFTR haplotypes and non-syntenic short tandem repeats (STRs) located on chromosomes 13,16,18,21,22, and XY. Six embryos (#3, #6, #7, #11, #15, and #17) were predicted to be carriers based on the presence of the maternal mutation and normal paternal CFTR gene. Monosomy 21 was found in the blastomere from embryo #3, which was excluded from the transfer and freezing. Trisomy 18 and XXY was observed in the blastomere from embryo #4, and trisomy 13 was detected in the blastomere from embryo #5. Embryos #6 and #7 were transferred, resulting in pregnancy and the birth of a healthy girl. DNA analysis of the newborn baby revealed a genetic profile identical to that of embryo #7

pregnancy and the birth of a healthy girl predicted and confirmed to be the carrier of maternal mutation G542X. It is of interest that multiplex PCR performed for three mutations in the CFTR gene in this case was combined with age-related aneuploidy (see below), because of the advanced reproductive age of the mother. Multiplex heminested PCR was performed on blastomeres from 14 embryos allowing simultaneous detection of the paternal and maternal CFTR haplotypes and non-syntenic short tandem repeats (STRs) located on chromosomes 13, 16, 18, 21, 22, and XY. Six embryos were predicted to be carriers based on the presence of the maternal mutation and normal paternal CFTR gene. In addition to avoiding the transfer of the affected double heterozygous embryos, three aneuploid embryos were identified, involving aneuploidy for chromosomes 13, 18, 21, and X and excluded from the transfer and freezing. Two unaffected embryos were transferred resulting in pregnancy and the birth of a healthy girl. DNA analysis of the newborn baby revealed a genetic profile identical to that of embryo #7, evidencing the usefulness and the accuracy of the combined mutations analysis, linkage, and aneuploidy testing in PGD for single-gene disorders in patients with advanced reproductive age (Fig. 3.18).

PGD for another couple with three different mutations in the CFTR gene was performed in which the paternal partner was affected carrying both delta F508 and R117H mutations in the CFTR gene, which was described above (Fig. 3.4).

3.5 Conditions with no Available Direct Mutation Testing

Although the availability of the sequence information is one of the major conditions in undertaking PGD for Mendelian diseases, it is also possible to perform PGD when no exact mutation is known. One of the examples demonstrating feasibility of the approach may be the report of PGD for *autosomal-dominant polycystic kidney disease* (*ADPKD*), caused by either PKD1 or PKD2 genes, for which no direct testing was available, making the linkage analysis the only method of choice.

ADPKD is a common genetic disorder present in 1/1,000 individuals worldwide, which causes progressive cyst formation and may eventually lead to renal failure by late middle age, requiring renal transplantation or dialysis [16]. The overall health implications of ADPKD are obvious from the fact that approximately 10% of all patients in need for renal transplantation or dialysis have this disease. ADPKD is caused by either PKD1 or PKD2 genes, for which no direct testing was available, making the linkage analysis a method of choice [38–40]. Because of an extremely variable expression and the age of onset, much higher in PKD2, only half of the patients carrying these genes may present with severe clinical manifestation and renal failure, making prenatal diagnosis and pregnancy termination highly controversial. PGD may therefore be more attractive for at-risk couples, because an ADPKD-free pregnancy may be established from the onset, without risk for pregnancy termination after prenatal diagnosis.

The majority (85%) of ADPKD is caused by PKD1, assigned to chromosome 16p13.3, the rest being attributed to PKD2, located on chromosome 4q21-q23 [16]. Because both PKD1 and PKD2 are characterized by the enlargement of kidneys due to the formation of bilateral or multiple unilateral fluid-filled cysts, presymptomatic diagnosis is available by abdominal ultrasound examination of young adults at risk, which also allows improving hypertension management in these patients, appearing long before the actual manifestation of renal disease. Although mutation rate is believed to be high, especially in PKD1, approximately half of the cases are still ancestry-related, allowing the diagnosis by linkage analysis. The PKD1 gene contains 46 exons, encoding the membrane protein polycystin 1 involved in cell-to-cell interaction, while PKD2 has at least 15 exons and encodes polycystin 2, which is a channel protein. Both of these proteins interact to produce new calcium-permeable nonselective cation currents, contributing to fluid flow sensation by the primary cilium in renal epithelium. Therefore, a loss or dysfunction of any of these proteins leads to polycystic kidney disease (PKD), due to the inability of cells to sense mechanical cues that normally regulate renal tubular morphology and function.

Because direct mutation testing was not available either for PGD1 or PKD2 in the case presented below, and their clinical manifestations are almost identical, except for the severity and earlier onset of PKD1, the linkage analysis was applied for both of these genes to trace the disease gene from the affected person through the family to the patient. DNA sequencing may be applied for PKD2, but this may not be expected to be useful for the PKD1 gene, because a large part of this gene is a duplication of multiple pseudogenes, which produce mRNA but are not translated.

PGD was performed for a woman with a family history of ADPKD, who inherited the disease from her father with a severe ADPKD and also had a brother with clinical symptoms of ADPKD (Figs. 3.19 and 3.20). Initial linkage analysis could not exclude either PKD1 or PKD2 as a cause of ADPKD in this family, so a set of linked markers have been designed to trace both PKD1 and PKD2 in the same reaction.

A PGD cycle was performed using PB sampling, and blastomere biopsy, described above. PB1 and PB2 were removed in sequence and

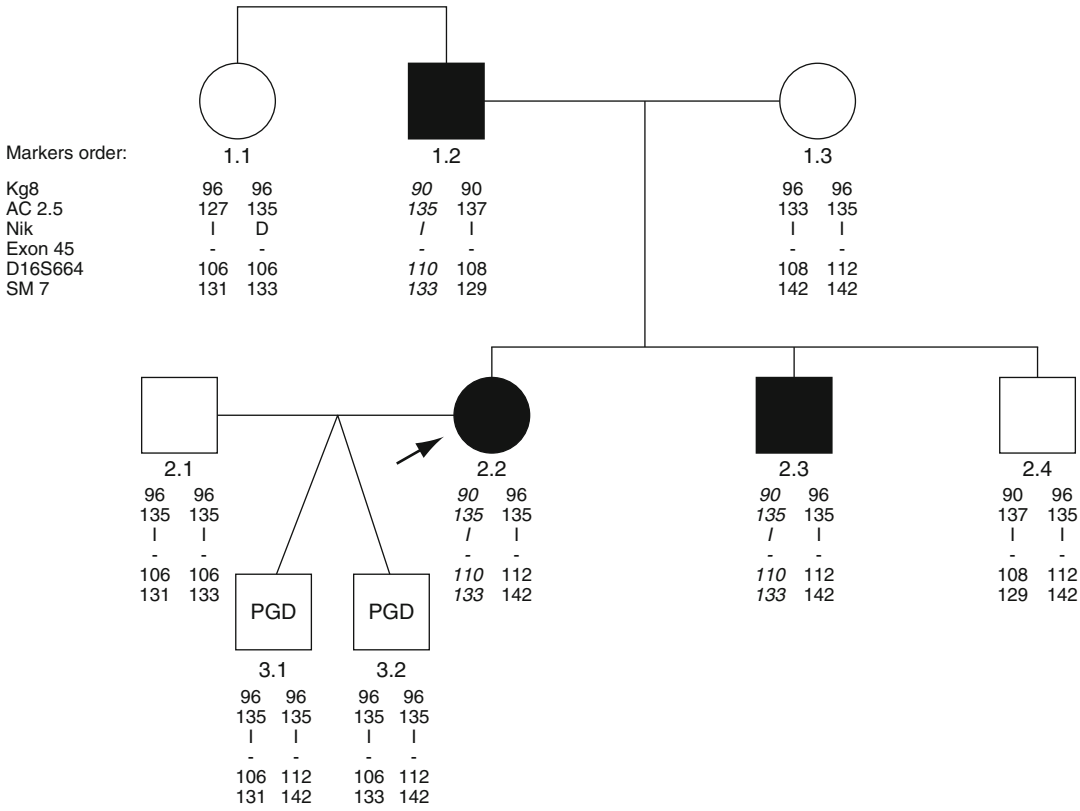

Fig. 3.19 Preimplantation linked marker analysis for PKD-1 resulting in the birth of unaffected twins. (*Upper panel*) ADPKD mutation originated from the affected maternal father (1.2), from whom the patient (2.2) inherited the mutant chromosome 16 (*bold*). Mutation-free chromosomes of maternal mother (1.3) are shown in *non-bold face*. (*Middle panel*) The affected patient (2.2) had one affected brother (2.3), who also inherited the mutant chromosome from his father, and the same normal chromosomes 16 from the mother. Her unaffected husband's (2.1) normal chromosomes 16 differ by one of the markers (131 vs. 133 bp), which makes it possible to identify twins, resulting from PGD (3.1 and 3.2) (*lower panel*)

tested by the multiplex nested PCR analysis, involving the above markers simultaneously in a multiplex heminested system. The preselection of mutation-free oocytes was performed based on the linked marker analysis, involving three closely linked markers to PKD1, Kg8, D16S664, and SM7, and four closely linked markers to PKD2, D4S2922, D4S2458, D4S423, and D4S1557 (primers and reaction conditions are presented in Tables 3.13 and 3.14). The maternal haplotypes were 90, 110, and 133 bp repeats for Kg8, D16S664, and SM7 markers, respectively, to trace PKD1 (Fig. 3.19), and 123, 91, 133, and 100 bp repeat for D4S2922, D4S2458, D4S23, and D4S1557 markers, respectively, to trace the PKD2 gene (Fig. 3.20).

The embryos derived from the oocytes free of PKD1 and PKD2, based on the information about polymorphic markers, were preselected for transfer back to the patient, while those predicted to be mutant or with inconclusive marker information were further tested by blastomere analysis removed from the resulting embryos either to confirm the diagnosis or identify additional mutation-free embryos for transfer.

Of 14 oocytes available for testing, only 11 were with the information for both PB1 and PB2. Two of these oocytes were predicted to contain PKD1 (oocytes #1 and #4), 3 to contain PKD2 (oocytes #2, #8, and #9), 3 neither PKD1 nor PKD2 (oocytes #5, #7, and #10), and 3 inconclusive for one or both genes, due to failed

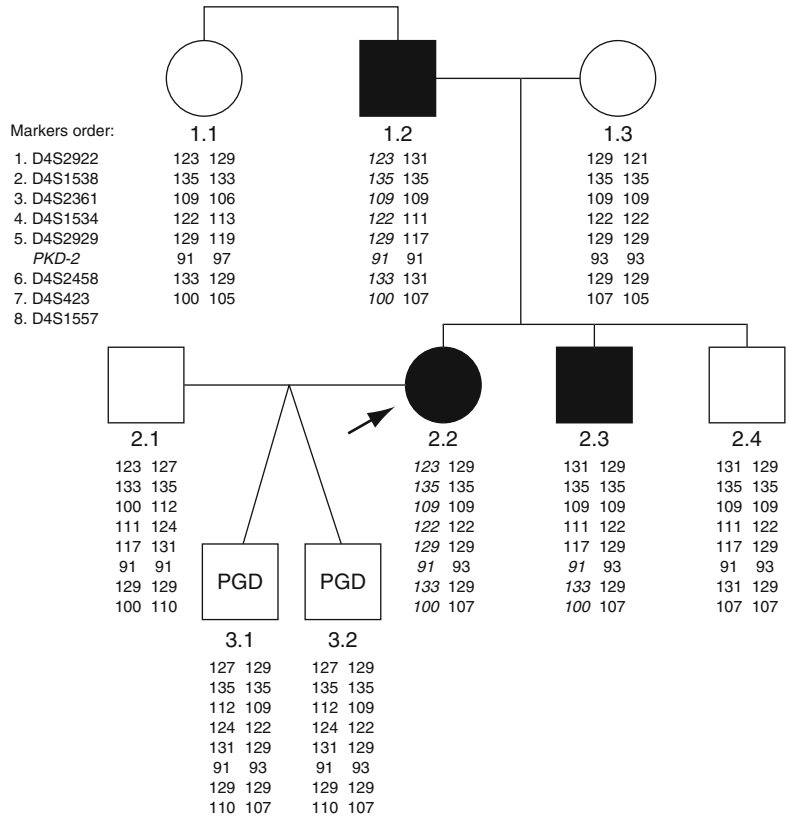

Fig. 3.20 Preimplantation linked marker analysis for PKD-2 (same pedigree as in Fig. 3.19). (*Upper panel*) ADPKD mutation (mutant chromosome 4 is shown in *non-bold face*) originated from the affected maternal father (1.2), from whom the patient (2.2) inherited the mutant chromosome 4 (*non-bold face*). Mutation-free chromosomes of maternal mother (1.3) are shown in *bold face*. (*Middle panel*) The affected patient (2.2) had one affected brother (2.3), who also inherited the mutant chromosome from his father, but following recombination between D4S2929 and D42458, which resulted in a recombinant chromosome 4 (*bold* and *non-bold*), and the same normal chromosomes 16 from his mother. Her unaffected husband's (2.1) normal chromosomes 16 cannot be distinguished due to sharing the same markers, so the fact that the resulting PGD twins are dizygotic cannot be demonstrated (3.1 and 3.2) (*lower panel*)

amplification of PB2 (oocytes #3 and #6) or ADO in PB1 (oocyte #11) (Table 3.15). The latter oocytes, however, were shown to be normal following blastomere analysis, although there was still a probability of recombination between Kg8 marker and PKD1 gene. The other two embryos resulting from oocytes #3 and #6 with inconclusive results were left with insufficient information because the amplification failure of embryo #6, or shared parental markers for PKD2 in embryo #3. Blastomere biopsy from the embryos resulting from the oocytes predicted mutant have been confirmed to be affected, including one (embryo #9), in which according to linkage analysis, neither PKD1 nor PKD2 could be excluded.

Three embryos resulting from oocytes #5, #7, and #10 were transferred, yielding a twin pregnancy and the birth of two children confirmed to be free of both PKD1 and PKD2. As seen from the pattern of markers used to exclude PKD-1, these mutation-free children are dizygotic twins, as they inherited different normal chromosomes 16 from the father. The follow-up analysis of the embryos, resulting from the mutant oocytes, also confirmed the accuracy of sequential PB1 and PB2 by linked marker analysis, which is in accordance with the previously reported data

Table 3.13 Primers for the detection of linked markers to PKD 1 (16p13.3)

Gene/ polymorphism	Upper primer	Lower primer	Annealing T_m (°C)
D16S3252 (Kg 8) nested	Outside		62–45
	5′ CGGCCATGCCCACAGAAG 3′	5′ CCTGGGGGCTGGCTCC 3′	
	Outside		58
	5′ TGCAGCCTCAGTTGTGTTTC 3′	5′ Fam CAGGGTGGAGGAAGGTGAC 3′	
D16S291 (AC2.5) heminested	Outside		62–45
	5′ TGCAGCCTCAGTTGTGTTTC 3′	5′ TGCTGGGATTACAGGCATG 3′	
	Inside		58
	5′ TGCAGCCTCAGTTGTGTTTC 3′	5′ Fam AAGGCTGGCAGAGGAGGTGA 3′	
Nik 2.9 Nested	Outside		62–45
	5′ GGCCCCAGGTCTCTTTCC 3′	5′ TCCGTGAGTTCCACTTGTC 3′	
	Inside		58
	5′ GTGGACGGGCATACATCAGC 3′	5′ CCAGGCCGATGATGTGCAGC 3′	
EXON 45 (*Ava II* & *Bsp1286 I*) Nested	Outside		62–45
	5′ CATCCTGGTAGGTGACTGC 3′	5′ GAACAACTCCACCATCTCG 3′	
	Inside		58
	5′ TACGCCCTCACTGGTGTC 3′	5′ ACAGCTCTCCACGCAAGG 3′	
SM7 Heminested	Outside		62–45
	5′ CTCCGTCTCAAACAAACAAC 3′	5′ TTGTGGCCCAAATATATCA 3′	
	Inside		58
	5′ CTCCGTCTCAAACAAACAAC 3′	5′ Hex TAGTCCTGGTCCCTTCCA 3′	
D16S664 (CW3) Heminested	Outside		62–45
	5′ TCATCGTTAGTGGGAGTCTG 3′	5′ TGCCCGGTCATAAATTG 3′	
	Inside		58
	5′ Fam TCAATGAGATTTCGGGTAA	5′ TGCCCGGTCATAAATTG 3′	

(see Chap. 2). In addition, in cases of inconclusive results by PB analysis, the blastomere biopsy of the resulting embryo may still allow preselecting additional embryos for transfer, as in embryo #11, mentioned above. However, as for avoiding a potential recombination between PKD1 and Kg8 alleles closer linked markers were required, this embryo was frozen for possible future use by the couple.

The presented case was the first PGD for ADPKD [41]. The clinical relevance of PGD for ADPKD is evident from the fact that prenatal diagnosis and termination of pregnancy may not be acceptable for a considerable proportion of ADPKD cases, which might be benign with no clinical manifestation during the whole lifetime.

The practical implication of PGD for ADPKD is also obvious from the high worldwide prevalence of this disease. So the information about the availability of PGD for ADPKD will be useful for practicing physicians, to provide the at-risk couples with appropriate advice regarding the available options for avoiding the risk of producing a child with ADPKD. Because of a straightforward clinical manifestation of the disease and the availability of a simple ultrasound screening, with no need for the mutation identification, the PGD strategy described may be applied without extensive preparatory work, usually required for PGD for many other conditions.

The presented case also demonstrates the feasibility of PGD in cases without exact information on the causative gene involved, and, therefore, may have practical implications for PGD of other conditions, in which the mutation might not be known, but tracing of the mutant chromosome is possible using highly variable linked markers, which presently has much wider clinical implications [42]. Also, because it was not known

Table 3.14 Primers for the detection of linked markers to PKD 2

Gene/polymorphism	Upper primer	Lower primer	Annealing T_m (°C)
D4S2922 (heminested)	Outside		62–45
	5′ AATAATAGAAAACAATCTCCTCA 3′	5′ TACACATCTTCTTTACTCAAACTAC 3′	
	Inside		55
	5′ Hex AGTTCTTCCTCTCCTGCTTAT 3′	5′ TACACATCTTCTTTACTCAAACTAC 3′	
D4S1538 (heminested)	Outside		62–45
	5′ AGCCTGGGTGACAGAGACTC 3′	5′ AACAATAAGTACATAAAAGAATGAAAC 3′	
	Inside		55
	5′ AGCCTGGGTGACAGAGACTC 3′	5′ Hex ATAGAAGCCTCAGTGCCTCTT 3′	
D4S2361 (heminested)	Outside		62–45
	5′ TCCTCCTCCCCACTGAAGT 3′	5′ GCACATGTACCCTAGAACTTAAAG 3′	
	Inside		55
	5′ Fam AAAGCCACGTGACTTTCATTA 3′	5′ GCACATGTACCCTAGAACTTAAAG 3′	
D4S1534 (heminested)	Outside		62–45
	5′ GTATTCAGTTTCAGCCCCATC 3′	5′ CCAAGGTAGAGGAGGGAAGG 3′	
	Inside		55
	5′ HexGTGAATATGCAGGTTACTCCCA 3′	5′ CCAAGGTAGAGGAGGGAAGG 3′	
D4S2929 (heminested)	Outside		62–45
	5′ TGTATTCAGTTTCAGCCCCATC 3′	5′ AGACCAGCCCAAGGTAGAGG 3′	
	Inside		55
	5′ Fam GAATATGCAGGTTACTCCCAGGA 3′	5′ AGACCAGCCCAAGGTAGAGG 3′	
D4S2458 (heminested)	Outside		62–45
	5′ CGAATGTTTCTATGTCATTGGAC 3′	5′ TGTCTTTCATTACAGAGATTCCTTC 3′	
	Inside		55
	5′ CGAATGTTTCTATGTCATTGGAC 3′	5′ Hex CCCCTGTAGCTGCCCTGTA 3′	
D4s423 (heminested)	Outside		62–45
	5′ TATTTGTTTCTCTTGAGTAGTTCCT 3′	5′ TGATCTCTTCTTTGGAAATATAAAT 3′	
	Inside		55
	5′ TATTTGTTTCTCTTGAGTAGTTCCT 3′	5′ Hex GTACATTGCAAAGTCCTCCATC 3′	
D4S1557 (heminested)	5′ TTAATTTCAGACTTTTCTATTTTCA 3′	5′ GGAGATATTGGAAAGGCTGT 3′	62–45
	5′ FamTATATTCTCGATATGAGATTGTGG 3′	5′ GGAGATATTGGAAAGGCTGT 3′	55

Table 3.15 Results of polar body and blastomere testing for PKD 1 and PKD 2 by linked marker analysis

		PKD 1			PKD 2					
Oocyte #	Cell type	Kg8	D16S664	SM7	D4S2922	D4S2458	D4S423	D4S1557	Predicted genotype	ET
1	**PB1**	96	112	142	**123**/129	**ADO**/93	**133**/129	**100**/107	**Oocyte : PKD1 affected**	**NO**
	PB2	**90**	**110**	**133**	**123**	**91**	**133**	**100**	**PKD2 normal**	
2	**PB1**	90/**96**	110/**112**	133/**ADO**	**123**/129	**91**/93	129	**100**	**Oocyte : PKD1 normal**	**NO**
	PB2	90	110	133	**129**	93	129	107	**PKD2 affected**	
3	**PB1**	**90**/96	**110**/112	**133**/ADO	129	**91**/93	**133**/129	**100**/107	Oocyte : PKD1 normal	**NO**
	PB2	FA	**110**	**133**	**123**	**91**	**133**	**100**	PKD2 inconclusive	
	Blast	96/96	106/112	133/142	127/**123**	91/93	129/129	110/107	**Embryo** : PKD1 normal	
									PKD2 inconclusive	
4	**PB1**	**ADO**/96	**110**/112	**ADO**/142	**123**/129	**91**/93	**133**/129	**100**/107	Oocyte : PKD1 affected	**NO**
	PB2	96	112	142	**123**	**91**	**133**	**100**	PKD2 normal	
	Blast	96/**90**	ADO/**110**	133/**133**	123/129	91/93	129/129	100/107	**Embryo** : PKD1 affected	
									PKD2 normal	
5	**PB1**	**90**/96	**110**/112	**133**/ADO	**123**	**91**	**133**	**100**	Oocyte : PKD1 normal	**YES**
	PB2	**90**	**110**	**133**	129	93	129	107	**PKD2 normal**	
6	**PB1**	96	**110**/112	**133**/142	**123**	**91**/93	**133**/129	**100**/107	Oocyte : PKD1 inconclusive	**NO**
	PB2	FA	**110**	**133**	129	**91**	**133**	**100**	PKD2 inconclusive	
	Blast	FA	FA	FA	FA	FA	FA	FA	**Embryo : inconclusive**	
7	**PB1**	**90**/96	**110**/112	**133**/142	**123**/129	**91**/93	**133**/129	**100**/107	**Oocyte : PKD1 normal**	**YES**
	PB2	**90**	**110**	**133**	**123**	**91**	**133**	**100**	**PKD2 normal**	

(continued)

Table 3.15 (continued)

		PKD 1			PKD 2					
Oocyte #	Cell type	Kg8	D16S664	SM7	D4S2922	D4S2458	D4S423	D4S1557	Predicted genotype	ET
8	**PB1**	96	**110**/112	142	**123**/129	**91**/93	**133**/129	**100**/107	Oocyte : PKD1 inconclusive	**NO**
	PB2	FA	**110**	**FA**	129	93	129	107	PKD2 affected	
	Blast	96/[a]	106/112	131/142	127/**123**	91/**91**	129/**133**	110/**100**	Embryo: PKD1 inconclusive **PKD2 affected**	
9	**PB1**	96	**ADO**/112	142	**123**/129	**91**/93	**133**/129	**100**/107	Oocyte : PKD1 inconclusive	**NO**
	PB2	FA	112	**FA**	129	93	129	107	PKD2 affected	
	Blast	96/**90**	106/**110**	133/**133**	123/**123**	91/**91**	ADO/**133**	100/**100**	**Embryo : PKD1 affected** **PKD2 affected**	
10	**PB1**	**90/ADO**	**110**/112	**133**/142	**123**/129	**91**/93	**133**/129	**100**/107	Oocyte : PKD1 normal	**YES**
	PB2	**90**	**110**	**133**	**123**	**91**	**133**	**100**	PKD2 normal	
11	**PB1**	96/[a]	**110**/112	**ADO**/142	**123**	**91**	**133**	**100**	**Oocyte : PKD1 inconclusive**	**YES**
	PB2	**90**	**110**	**133**	129	93	129	107	PKD2 normal	
	Blast	96/[a]	106/112	133/142	123/129	91/93	129/129	100/107	**Embryo**: PKD1 normal **PKD2 normal**	
Affected mother		**90**/96	**110**/112	**133**/142	**123**/129	**91**/93	**133**/129	**100**/107		
Affected maternal brother		**90**/96	**110**/112	**133**/142	**131**/129	**91**/93	**133**/129	**100**/107		
Unaffected father		96/96	106/106	131/133	123/127	91/91	129/129	100/110		

PB1 first polar body, *PB2* second polar body, *Blast* blastomere, *FA* failed amplification, *ADO* allele dropout, *ET* embryo transfer
Bolded number of repeats corresponds to the expected mutant alleles
[a]Means inconclusive results

whether the disease was caused by PKD1 or PKD2, the couple was treated as if both parents were carriers of both PKD1 and PKD2 genes. So the PGD strategy was to exclude the possibility of inheritance of both conditions by tracing markers for PKD1 and PKD2.

The other case, in which we performed concomitant testing for more than one genetic condition, was simultaneous PGD for Charcot-Marie-Tooth (CMT) and Fabry diseases in a couple, with both partners carrying mutations for both of these diseases. Testing was performed by sequential PB1 and PB2 analysis of Fabry disease, followed by embryo biopsy and testing for CMT, which allowed the identification and transfer of an unaffected embryo, which resulted in a triplet pregnancy and the birth of three healthy children, which appeared to be monozygotic triplets. Although the mechanism for the formation of monozygotic triplets is not understood, the data show that concomitant PGD for more than one condition is feasible and may be performed using the combination of different biopsy techniques, allowing the accurate detection of a healthy child free from both of conditions.

A similar approach has previously been described in a childless Ashkenazi Jewish couple, at risk for producing a child with Tay Sacs (TS) and Gaucher disease (GD), with both parents carrying two different mutations in both the β hexosaminidase A (HEX A) and the β glucocerebrosidase (GBD) genes [43]. The authors were able to diagnose six embryos, of which one was wild type for both TS and GD, and three were wild type for GD and carriers of TS, with the remaining two being compound heterozygote for TS. Two of the four transferable embryos which developed into blastocysts were transferred, resulting in a singleton pregnancy and the birth of a healthy child free from both of conditions.

These cases demonstrate the feasibility and advantages of analyzing a large number of markers in a single multiplex reaction allowing the analysis of multiple diseases in cases where couples are carriers of mutations in several genes. This is particularly common in the Ashkenazi Jewish population, in which there are a large number of prevalent autosomal-recessive diseases.

3.6 De Novo Mutations

As presented above, with an increasing number of different genetic disorders for which PGD is being applied each year, PGD may presently be applicable for any inherited disorder for which sequence information or relevant haplotypes are available for the detection by direct mutation analysis or haplotyping in oocytes or embryos [3, 4]. According to the current guidelines, performing PGD requires knowledge of sequence information for Mendelian diseases, but may also be performed when the exact mutation is unknown, through the application of the linkage analysis [3]. As described above, with expanding use of polymorphic markers, the linkage analysis may allow PGD for any genetic disease irrespective of the availability of specific sequence information (see also 42). This approach is more universal, making it possible to track the inheritance of the mutation without actual testing for the gene itself.

However, the above approaches cannot be applied in cases of de novo mutations (DNM) in parent(s) or affected children, as neither origin nor relevant haplotypes are available for tracing the inheritance of this DNM in single cells biopsied from embryos or in oocytes. On the other hand, with the improved awareness of PGD, an increasing number of couples request PGD, without any family history of the genetic disease that has been first diagnosed in one of the parents or in their affected children. So the developments in PGD strategies for the genetic conditions determined by DNM are presented below, which represents the first systematic clinical experience of PGD for over 100 cases with DNM [44].

The PGD strategy was developed for a total of 80 families with 38 different genetic disorders, determined by 33 dominant, 3 recessive, and 2 X-linked DNM (the list of DNM for which this PGD strategy was performed is presented in Table 3.16). The majority of these families (71 of 80) were with dominant mutations, of which 40 were of paternal origin, including 2 cases of gonadal mosaicism, 46 of maternal origin, including 1 with gonadal mosaicism, and 9 detected for the first time only in the affected children. All

Table 3.16 Outcome of PGD for DNM

Disease	Origin of de novo mutation			Number of patients with PGD	Number of cycles	Number of transfers	Number of embryos transferred	Pregnancy	Birth
	Paternal	Maternal	Detected in child						
Autosomal-dominant [33]									
Adenomatous polyposis of the colon (FAP)	1	3		2	7	7	13	1	1
Basal cell nevus syndrome (Gorlin syndrome)	3	1		4	5	4	7	2	2
Brachydactyly (BDB1)	1			1	3	3	4	2	2
Corneal dystrophy		1		0	0	0	0	0	0
Crouson syndrome (CFD1)	1	2		3	5	4	8	3	2
Darier disease (DAR)		1		1	1	1	2	1	1
Diamond–Blackfan anemia (DBA)		2	3	4	9	6	8	3	3
Emery–Dreifuss muscular dystrophy (EDMD2)	2			2	3	2	4	1	1
Epileptic encephalopathy, early infantile			1	1	1	1	2	1	1
Exostoses, multiple (EXT1)	2			2	2	2	5	1	1
Facioscapulohumeral muscular dystrophy (FSHD)	4			3	9	6	9	3	5
Kallmann syndrome (KAL2)		1		1	1	1	2	1	1
Loyes–Dietz syndrome (LDS1A)		1		1	1	1	2	1	1
Malignant rhabdoid tumor (SMARCB1)			1	0	0	0	0	0	0
Marfan syndrome (MFS)	5	3		6	13	12	21	6	4
Metaphyseal dysplasia	1			1	1	1	2	1	1
Multiple endocrine neoplasia, type I (MENI)	1			1	2	2	4	1	1
Multiple endocrine neoplasia, type II (MEN2B)	1			1	1	1	2	0	0
Neurofibromatosis, type I (NF1)	3	13	1	13	24	22	38	11	10
Neurofibromatosis, type II (NF2)	1			1	2	2	4	2	3
Optic atrophy 1 (OPA1)	1	1		0	0	0	0	0	0
Osteogenesis imperfecta I (OI I)	5	5		7	19	11	22	5	6
Peutz–Jeghers syndrome (PJS)		1		1	2	2	3	2	1
Pfeiffer syndrome		1		1	1	1	2	1	1
Retinoblastoma (RB1)	3	3		3	7	7	12	1	1
Rett syndrome (RTT)			1	1	1	1	1	0	0
Sotos syndrome		1		1	1	1	1	1	1
Spinocerebellar ataxia 6 (SCA6)		1		1	2	1	2	0	0
Stickler syndrome (STL1)		1		1	1	1	3	0	0

Treacher–Collins syndrome (TCOF)	1	1		1	1	1	2	1	2
Tuberous sclerosis 1 (TSC1)	1	2		3	7	7	10	3	3
Tuberous sclerosis 2 (TSC2)		1		1	1	1	2	0	0
Von Hippel–Lindau syndrome (VHL)	3			2	3	3	4	2	2
Subtotal	40	46	7	71	136	115	201	57	57
X-linked [2]									
Granulomatous disease, chronic (CGD)		1		1	3	3	4	1	0
Incontinentia pigmenti (IP)		5		5	8	5	8	3	4
Subtotal		6		6	11	8	12	4	4
Autosomal-recessive [3]									
Cystic fibrosis (CF)			1	1	1	1	2	1	2
Fanconi anemia I (FA)			1	1	2	2	2	0	0
Spinal muscular atrophy, type I (SMA)	1			1	1	1	2	1	1
Subtotal	1	0	2	3	4	4	6	2	3
Total [38]	41	52	9	80	151	127 (84%)	219 1.72	63 (49.6%)	64

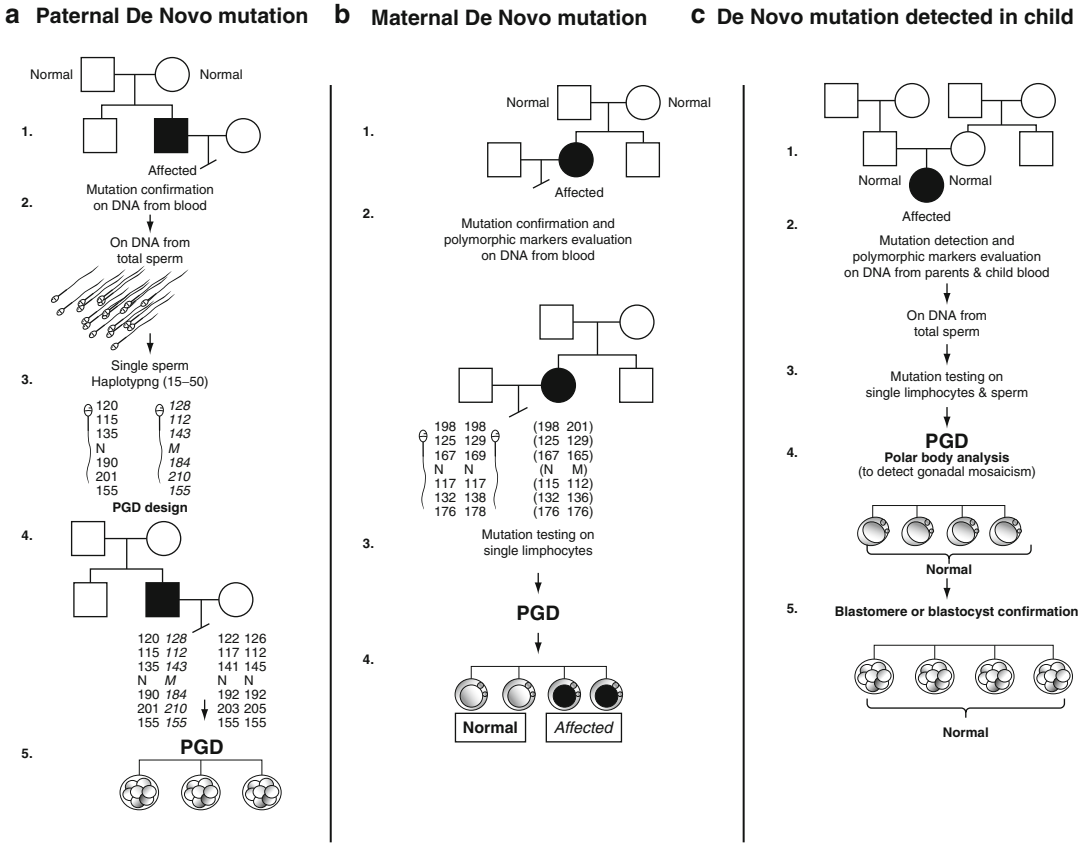

Fig. 3.21 PGD strategies for DNM of different origin. (**a**) Case workout for DNM detected in male partner: (1) Pedigree in two generations. (2) Mutation verification in DNA extracted from blood and total sperm. (3) Amplification of partner's single sperm to establish normal and affected haplotypes required for PGD cycle preparation. (4) Amplification of patient's DNA to identify the most informative markers for PGD. (5) PGD by blastomere or blastocyst biopsy for combined mutation and linkage analysis. (**b**) Case workout for DNM detected in mother (patient): (1) Pedigree in two generations. (2) Mutation verification in DNA extracted from whole blood or cheek swabs and single lymphocytes. Paternal haplotypes are analyzed on a single sperm for more accurate embryo genotype prediction. (3) PGD by PB1 and PB2 analysis to identify DNM-free oocytes and establish maternal haplotypes, followed by blastomere or blastocyst analysis to confirm the diagnosis. (**c**) Case workout for DNM detected first in affected offspring: (1) Pedigree in three generations. (2) Verification of DNM in child's DNA extracted from blood or cheek swabs, and mutation testing on DNA extracted from parents' whole blood and total sperm. (3) Mutation evaluation on single lymphocytes and single-sperm testing to rule out paternal gonadal mosaicism. (4) PGD by polar body analysis to detect potential maternal gonadal mosaicism. (5) Blastomere or blastocyst analysis to confirm the absence of the mutation

three couples with DNM of autosomal-recessive inheritance were of paternal origin, including cystic fibrosis (CFTR), spinal muscular atrophy (SMA) and Fanconi anemia (FA). PGD for 2 X-linked DNM included PGD for chronic granulomatosys and incontinentia pigmenti.

As seen from Fig. 3.21, PGD strategies for these families were different depending on the origin of DNM, and included an extensive DNA analysis of the parents and affected children prior to PGD, with the mutation verification, polymorphic marker evaluation, whole- and single-sperm testing, and PB analysis in order to establish the normal and mutant haplotypes, without which PGD cannot always be performed. In cases of DNM of paternal origin, the DNM was first confirmed on the paternal DNA from blood and total sperm, followed by single-sperm typing to

Table 3.17 Summary of testing and clinical outcome of PGD for DNM

Type of inheritance	Number of patients	Number of cycles	Number of embryo transfers	Number of embryos	Number of pregnancies	Number of births
Autosomal-dominant	71	136	115	198	57	57
X-linked	6	11	8	14	4	4
Autosomal-recessive	3	4	4	7	2	3
Total	80	151	127 (84%)	219 (1.72)	63 (49.6%)	64

determine the proportion of sperm with DNM and relevant normal and mutant haplotypes, as described earlier. For a higher reliability of testing, the relevant maternal linked markers were also detected, to be able to trace for possible shared maternal and paternal markers. To exclude misdiagnosis, PGD involved simultaneous detection of the causative gene, and at least three highly polymorphic markers, closely linked to the gene tested, to ensure detecting preferential amplification and ADO, the main potential causes of PGD misdiagnoses. This involved a multiplex nested PCR analysis, with the initial first round PCR reaction containing all the pairs of outside primers, followed by amplification of separate aliquots of the resulting PCR product with the inside primers specific for each site. Following the nested amplification, PCR products were analyzed either by restriction digesting or direct fragment-size analysis.

In cases of DNM of maternal origin, DNM was first confirmed in maternal blood, and PGD was performed, when possible, by PB analysis, to identify the normal and mutant maternal haplotypes. Also, in order to trace the relevant paternal haplotypes, single-sperm typing was performed, whenever possible, for avoiding misdiagnosis caused by possible shared paternal and maternal markers.

In cases of DNM-detected first in children, the mutation was verified in their whole blood DNA, followed by testing for the mutation in paternal DNA from blood, total and single sperm, if the DNM appears of paternal origin. In DMD of maternal origin, PGD was performed by the PB approach, with confirmation of the diagnosis by embryo biopsy, if necessary.

So, in contrast to previous PGD practice, performing PGD for DNM required extensive preparatory DNA work before performing the actual PGD, with the additional tests including single-sperm analysis and the requirement of performing sequential PB1 and PB2, followed by blastomere or blastocyst analysis, described in detail in Chap. 2. As in previous PGD protocols, the embryos without DNM were transferred in the same cycles, while the affected ones were used for confirmation of diagnosis, at least for in-house cases. Predicted diagnoses were followed up after delivery, while the spare unaffected embryos were frozen for future use by the families.

Overall, 151 PGD cycles for DNM were performed for 80 families under study, resulting in preselection and transfer of 219 (1.72 per cycle) DNM-free embryos in 127 (84%) PGD cycles, yielding 63 (49.6%) unaffected pregnancies and the birth of 64 healthy children, confirmed to be free of DNM tested (Table 3.17).

The largest group was PGD for DNM of autosomal-dominant type, including 136 cycles from 71 patients, which resulted in transfer of 201 DNM-free embryos in 115 cycles, yielding 57 pregnancies and the birth of 53 unaffected children, with 4 ongoing pregnancies by the present time. The most frequent conditions in this group were neurofibromatosis type 1 (NF1) (24 cycles), osteogenesis imperfecta (19 cycles), Marfan syndrome (13 cycles), facioscapularhumoral muscular dystrophy (FSHD) and Blackfan Diamond anemia (BDA) (9 cycles each), familial adenomatous polyposis (FAP), tuberous sclerosis type 1 (TSC1) and retinoblastoma (RB) (7 cycles each), and Gorlin and Crouson syndromes (5 cycles each). From 1 to 3 cycles were performed for the remaining conditions, listed in Table 3.16.

The example of PGD design for DNM of dominant inheritance is presented below for a

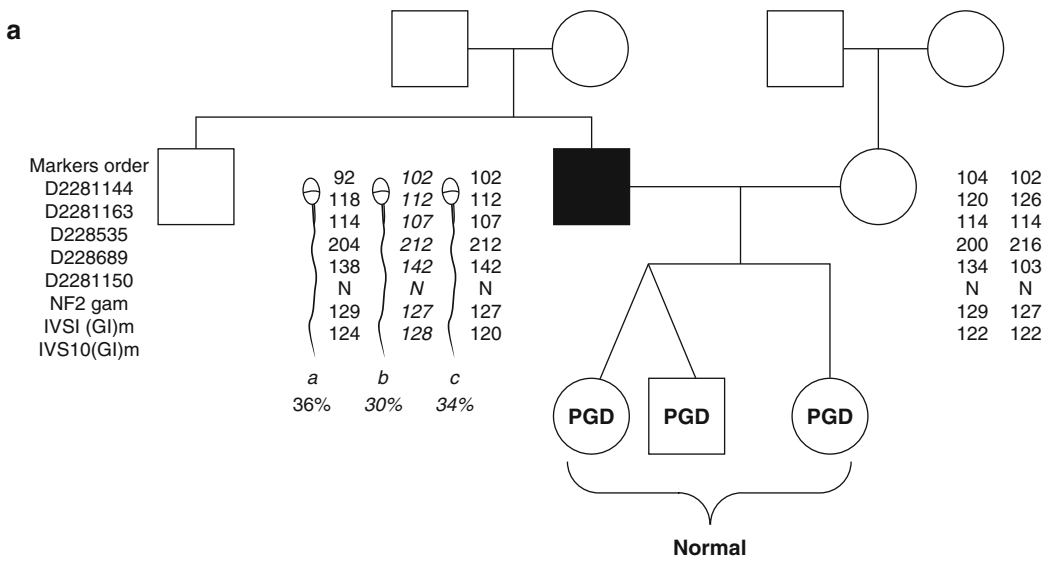

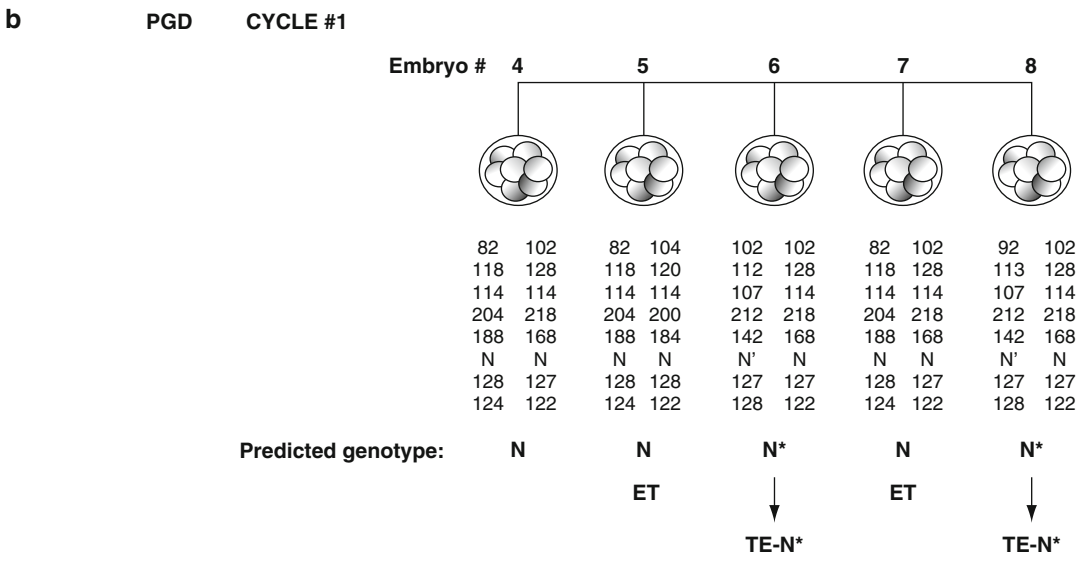

Fig. 3.22 PGD for DNM in NF2 gene (c114+ 2T-C splicing mutation) of paternal origin. (**a**) Family pedigree showing that that DNM in NF2 gene was first detected in the father. Single-sperm analysis via multiplex heminested PCR revealed gonadal mosaicism with three different haplotypes: *a* – normal; *b* – mutant containing c.114+2 T-C allele; and *c* – mutant without c.114+2 T-C allele in NF2. Maternal linkage was based on DNA amplification of blastomeres in PGD cycle. Mutation and marker order is printed in *upper left corner*. (a) Outcome of the first PGD cycle. Blastomeres from five embryos were subjected to combined mutation and linkage analysis by multiplex heminested PCR. Three embryos (#4, #5, and #7) were predicted to be free from the paternal mutation based on the presence of normal sequence (*N*) in NF2 gene and confirmed by linked markers (haplotype *a*). Two embryos (#6 and #8) were predicted to have normal sequence (*N**) on haplotype *c*. The accuracy of this prediction was decreased due to a potential allele dropout (ADO) of the dominant mutation in single blastomere. Trophectoderm (*TE*) biopsy from these embryos confirmed the presence of the normal sequence of NF2 gene. Embryos #5 and #7 were transferred, resulting in an unaffected pregnancy and the birth of a healthy boy and girl confirmed by postnatal testing. (**b**) Outcome of the second PGD cycle. Combined mutation and linkage analysis by multiplex heminested PCR was performed on blastomeres from ten embryos. Mutant haplotype b was detected only in embryo #13. Embryo #6 was missing all the maternal markers, suggesting monosomy of chromosome 22, in which the gene is localized. Although all the remaining embryos were predicted to be normal and free of mutation, only four of them (embryos #3, #4, #9, and #12) were with normal (*N*) paternal haplotype *a*, while embryos #2, #5, #7, and #11 were predicted to have normal sequence (*N**) on the mutant haplotype *c*. Blastocyst biopsy confirmed normal genotypes predicted on blastomeres. Two normal embryos (embryos #3 and #4) were transferred, resulting in clinical pregnancy and the delivery of a healthy girl confirmed by postnatal analysis

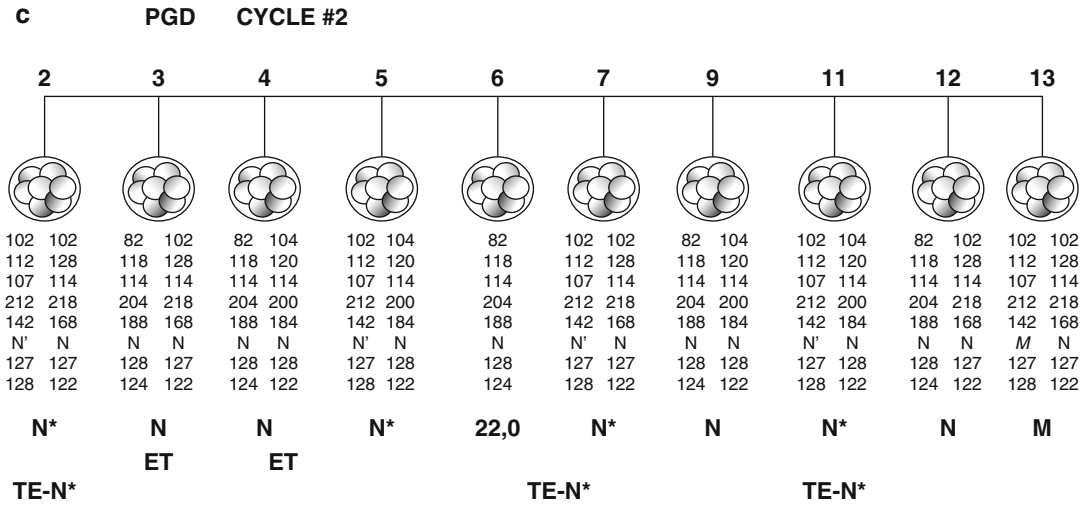

Fig. 3.22 (continued)

couple with NF2 splicing mutation (c114+2T-C) detected in the husband with no previous family history of the disease (Fig. 3.22). DNA analysis in paternal blood confirmed the presence of NF2 splicing mutation (c114+2T-C), while testing of single sperms showed a gonadal mosaicism, represented by three types of sperms corresponding to three different haplotypes. Only 30% of sperms were represented by actual mutant haplotype, while 36% were normal, characterized by normal haplotype, and 34% contained a normal allele in the mutant haplotype.

PGD was based on detecting and avoiding the transfer of embryos with mutant haplotype with or without a mutant gene, while the embryos with normal haplotypes of paternal and maternal origin were transferred. As can be seen from Fig. 3.22, all the five tested embryos from the first PGD cycle may appear unaffected, despite the finding of the mutant haplotype in two of them (embryos #6 and #8), which, however, were missing the mutant gene. The remaining three embryos were with normal paternal and maternal haplotypes, of which two (embryos #5 and #7) were transferred, resulting in a twin pregnancy and the birth of two unaffected children. In the second PGD cycle for this couple, ten embryos were examined, of which only one contained the actual mutant haplotype, while three were with mutant haplotypes without the mutant gene, and the remaining six were with normal haplotypes. Two of these embryos (embryos #3 and #4) were transferred, resulting in a singleton pregnancy and the birth of an unaffected child.

The example of dominant DNM of maternal origin is presented in Fig. 3.23, in which gonadal mosaicism was also detected. DNM in the NF1 gene (intron 17–38 deletion) was first presented in the affected child, and appeared to be originated from the mother, who had three cell populations, represented by three haplotypes, including the normal, mutant with intron 17–38 deletion, and mutant without deletion. So PGD was based on preselection and transfer of the embryos with either normal maternal haplotype or with mutant maternal haplotype lacking intron 17–38 deletion. As seen from Fig. 3.23, of 11 embryos examined, despite the presence of 6 embryos with mutant maternal haplotypes, actually only 2 were affected (embryos #6 and #8), the other 4 (embryos #1, #2, #10, and #12) being unaffected as they contained no inton 17–38 deletion. Of the remaining 5 embryos, 2 were monosomic for the maternal chromosome (embryos #7 and #11), and 3 (embryos #3–5) contained only the normal parental haplotypes. One of these embryos (embryo #3) and the other demonstrating mutant maternal haplotype without deletion (embryo #2) were transferred, resulting in chemical pregnancy (Fig. 3.23).

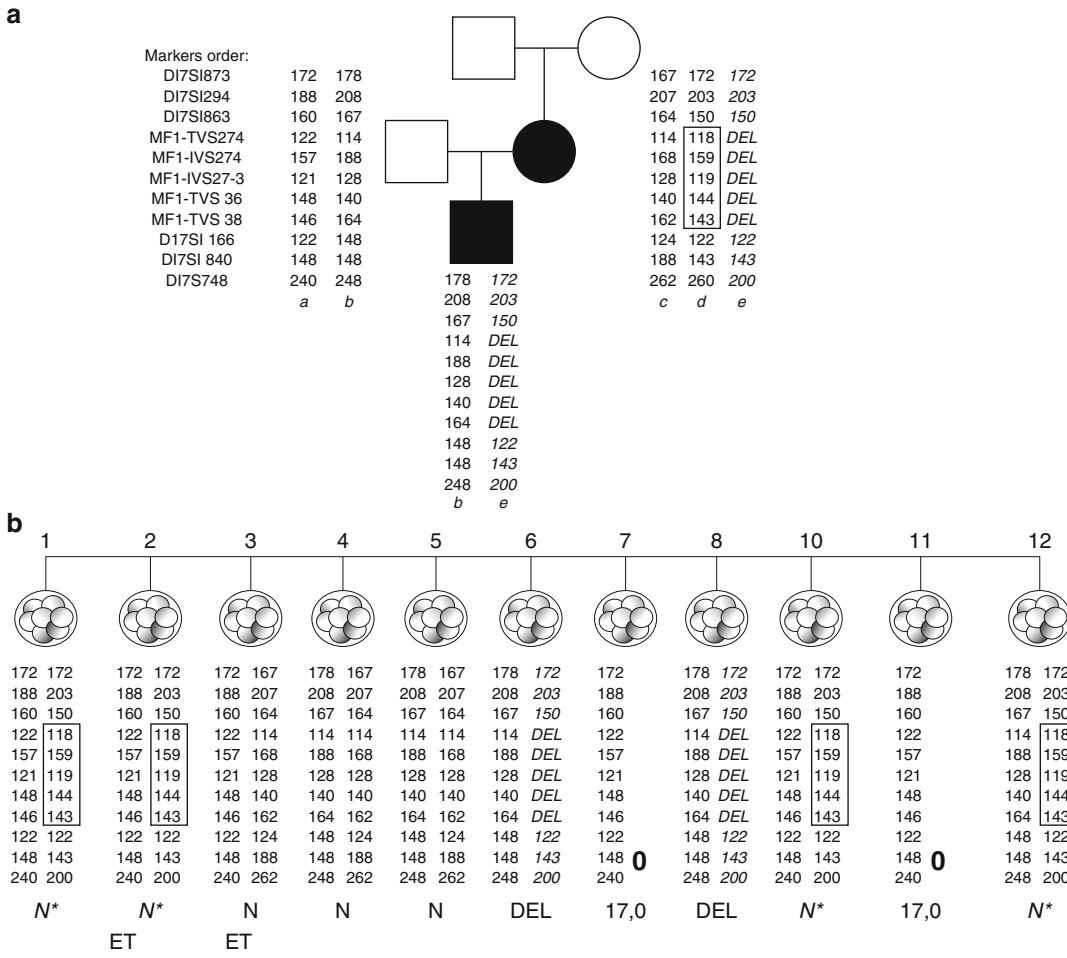

Fig. 3.23 PGD for DMD in NF1 gene (intron 27–38 deletion) of maternal origin. (**a**) Family pedigree of a couple with an affected son carrying deletion of intron 27–38 in the NF1 gene. This deletion was not detected in maternal DNA from whole blood, although two haplotypes (*c*) and (*d*) were present, the latter corresponding to mutant haplotype corresponding to affected son's haplotype, but with no deletion. The expected deleted area on this "benign" chromosome (same haplotype as affected son received from the mother but without deletion) is framed. The actual mutant haplotype (*e*) with deletion was detected on maternal single lymphocytes. Paternal normal haplotypes (*a*) and (*b*) were established based on markers detected on the son's normal chromosome. Position and order of the markers and deletion in NF1 gene are shown on the *upper left*. (**b**) Outcome of PGD cycle, performed by multiplex heminested PCR on blastomeres from 11 embryos. Three embryos (embryos #3, #4, and #5) were predicted normal (*N*) based on the presence of maternal normal haplotype (*c*) and suitable for embryo transfer (*ET*). Four embryos (embryos #1, #2, #10, and #12) inherited the "benign" mutant maternal haplotype (*d*) and were also predicted normal (*N**) and suitable for embryo transfer (*ET*). Of the remaining four embryos, embryos #7 and #11 were predicted to have monosomy of chromosome 17, based on the absence of maternal alleles, while the other two (embryos #6 and #8) were predicted to be affected, based on the absence of maternal markers in deleted area (*DEL*). Two embryos (embryos #2 and #3) were transferred and resulted in a biochemical pregnancy

Only four PGD cycles were performed for DNM of autosomal-recessive type mentioned, including two cycles for *CF*, one for SMA, and one for Fanconi anemia (FA), presented in Fig. 3.24, which resulted in the transfer of seven embryos, yielding two pregnancies and the birth of two unaffected children (Table 3.17).

As presented in Fig. 3.24, DNM for FANC I was first detected in a child who was compound heterozygous for the C750G/E837X mutation.

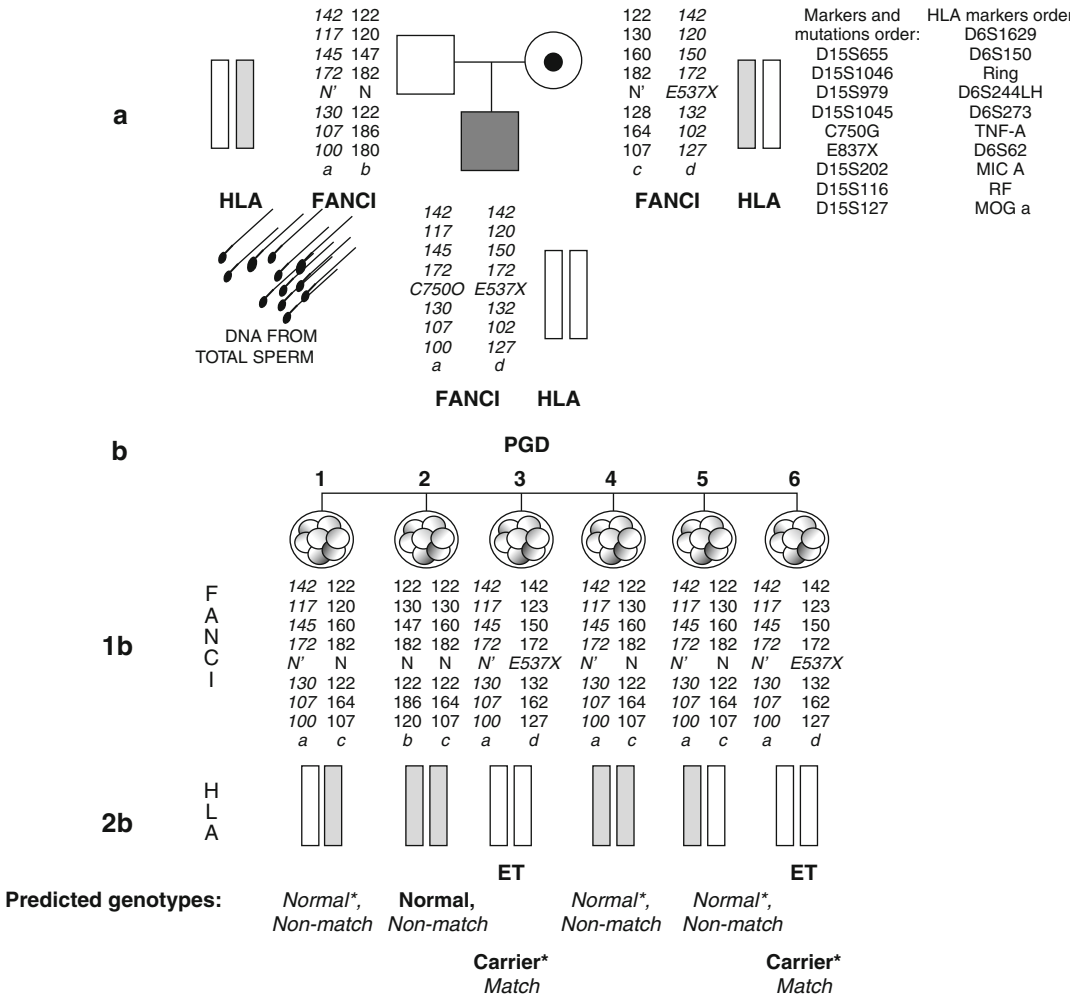

Fig. 3.24 PGD for autosomal-recessive DNM detected first in an affected child who was compound heterozygous for C750G E837X mutations in the FANC I gene, combined with HLA genotyping. (**a**) Family pedigree showing HLA and mutation haplotypes, based on parental and affected child's genomic DNA testing. E837X mutation was detected in the carrier mother, but C750G mutation was absent in DNA extracted from paternal blood or whole-sperm samples. However, both normal and mutant haplotypes were detected in testing of single sperm. White bars represent HLA-matched genotypes. *Gray bars* depict non-matched haplotypes. Mutation and marker orders are printed in the *upper right corner*. (**b**) PGD cycle combined with HLA testing. *1b* – Multiplex heminested and fully nested amplification performed on blastomeres from six embryos did not reveal the paternal mutation (*1b*). Four embryos (embryos #1, #2, #4, and #5) were predicted normal (*N*) based on the absence of both mutations, of which embryos #1, #4, and #5 inherited "benign" paternal haplotype *a*, similar to one of the mutant haplotypes in the affected child, and embryo #2 inherited the normal haplotype *b*. The remaining embryos (#3 and #6) were predicted to be carriers of the maternal mutation E837X, but inherited the paternal haplotype *a*. *2b* – HLA marker analysis demonstrated the presence of two HLA-matched embryos (#3 and #6), which were transferred, but no pregnancy was achieved. *N** – shows benign paternal haplotype *a* similar to the mutant haplotype of the affected child

Testing of both parents for the presence of these mutations showed that the mother was a carrier of the E837X mutation, and characterized by two relevant haplotypes, while no mutation was found either in the paternal blood or whole sperm, despite the presence of both normal and mutant haplotypes in single sperms, which however was lacking the C750G mutation. Because the couple also requested HLA typing for possible stem cell transplantation required for the affected sibling,

the embryos were also tested for HLA haplotypes. As can be seen from Fig. 3.24, of the six embryos tested, only one embryo (embryo #2) inherited both maternal and paternal normal haplotypes, while two were with both paternal and maternal mutant haplotypes (embryos #3 and #6), but were unaffected heterozygous carriers, because the paternal mutant haplotype was missing the expected paternal FANC750G mutation. The remaining three embryos had normal maternal and mutant paternal haplotype, without a mutant gene involved. So all the embryos were actually unaffected, of which two heterozygous carriers appeared to be also an HLA match to the affected child (embryos #3 and #6) and transferred, resulting in no pregnancy.

Eleven PGD cycles were performed for X-linked DNM, including eight for incontinentia pigmenti and three for chronic granulomatosys, resulting in four pregnancies and the birth of four unaffected children (Table 3.17). The results of PGD for chronic granulomatosys, determined by DNM IVS 9+5G-A in the CYBB gene is presented in Fig. 3.25. DNM in this case was first detected in an affected child, who also required HLA-matched stem cell transplantation. So in addition to mutation analysis, HLA typing was performed, together with aneuploidy testing, because the mother was 36 years old.

DNA analysis in maternal blood failed to detect the mutant gene, while both normal and mutant haplotypes were present, despite the latter missing the mutant gene. PGD was performed by sequential PB1 and PB2 analysis in nine oocytes, showing that all the oocytes were normal, although four of them (oocytes #2, #3, #7, and #11) contained the maternal mutant haplotype, without the mutant gene. The testing of the embryos resulting from each of these oocytes confirmed the PB haplotype analysis, showing the lack of the mutant gene. All the embryos were found to be also aneuploidy-free, of which four (embryos #7, #8, #9, and #11) appeared to be also the exact HLA match to the affected sibling. Two of these embryos (embryos #8 and #9) were transferred, resulting in clinical pregnancy, which was spontaneously aborted in the first trimester.

The overall clinical outcome of PGD for DNM showed a success rate as high as 84% of identifying unaffected embryos for transfer (127 of 151 initiated cycles), with the average 1.72 embryos per transfer (219 embryos transferred in 127 cycles), resulting in a 49.6% pregnancy rate (63 clinical pregnancies) and the birth of 59 unaffected children (five pregnancies still ongoing at the time of submission of the paper), with no misdiagnosis observed in the follow-up analysis.

The presented experience is the first cumulative report of PGD for DNM, which could not be performed previously, due to unavailability of family history and lack of any affected family member to identify the origin of mutation and trace the inheritance of the mutant and normal alleles in oocytes and embryos. However, the presented data show that the strategies may be developed in search for the possible origin of DNM and relevant haplotypes as the basis for developing a PGD design for each particular couple with DNM, allowing a highly accurate preselection of oocytes and embryos free from DNM in question.

Although the strategies may differ depending on the type of DNM inheritance, the general approach involves the identification of DNM origin and search for a possible gonadal mosaicism and relevant parental haplotypes. As demonstrated in Fig. 3.21, one of the important steps is single-sperm typing, which was performed in 37 of 80 patients (46.3%). Overall 964 single sperms were tested, with the requirement for testing of at least 15 single sperms per patient, and as many as 50 per patient to exclude a possible gonadal mosaicism. Even if DNM is not identified, single-sperm typing may identify a “benign” mutant haplotype, represented by a mutant haplotype without DNM. The other important requirement is to identify the relevant linked markers in both parents even if only one is a DNM carrier. Although not always possible, PGD by PB approach to detect or confirm the maternal normal and mutant haplotypes is always the method of choice, performed in our material in 54 (35.8%) of 151 cycles.

The implications of gonadal mosaicism for genetic counseling of dominant disorders, such as NF1, TSC1, TSC2, lethal osteogenesis imperfecta, familial adenomatous polyposis, retinoblastoma, and X-linked dominant trait incontinentia

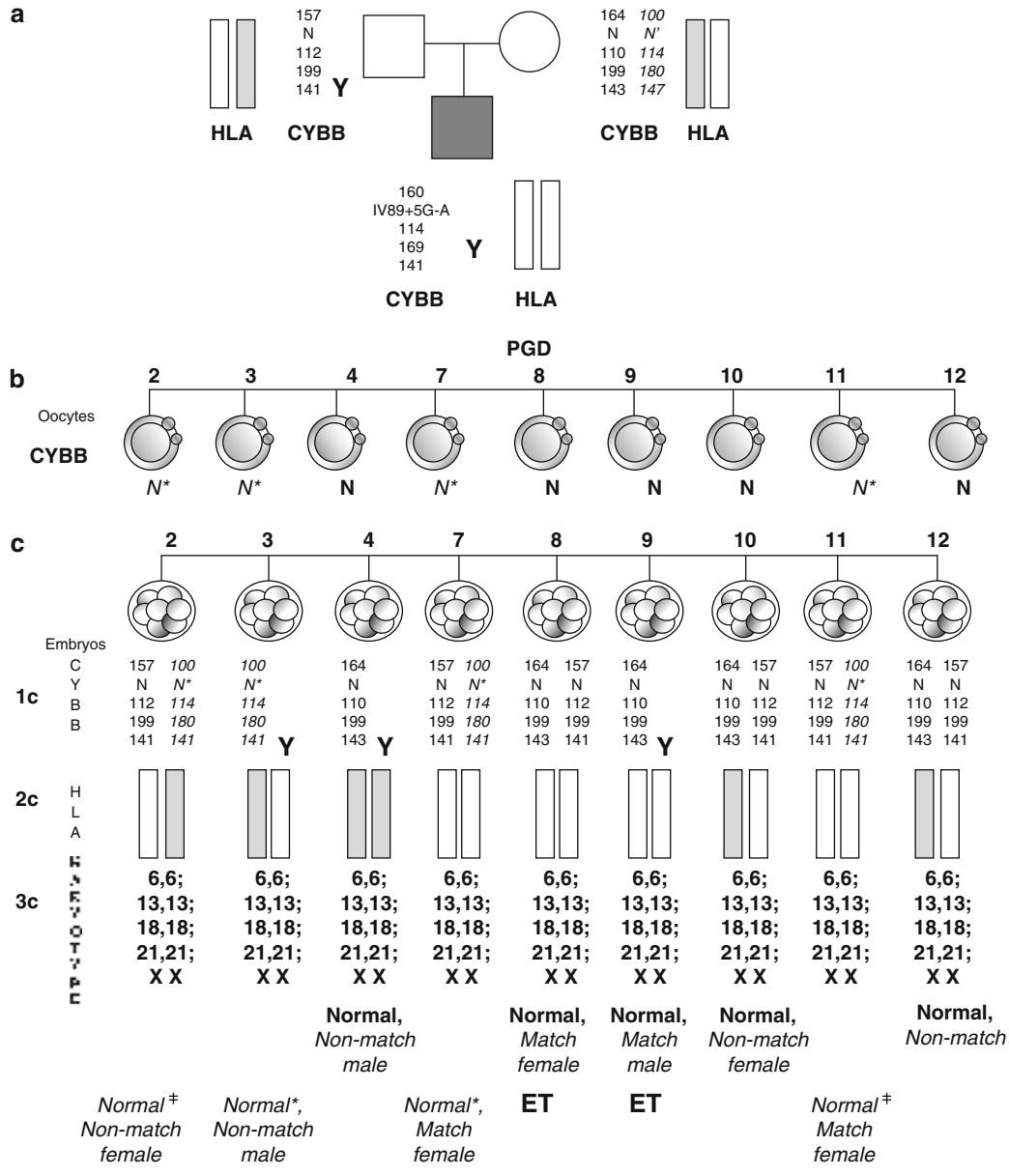

Fig. 3.25 PGD for chronic granulomatous disease, determined by X-linked DNM IVS9+ 5G-A, combined with HLA genotyping and aneuploidy testing. (**a**) Family pedigree showing the mutation and closely linked to CYBB gene markers, and HLA-matched haplotypes depicted as white and non-matched colored in gray. (**b**) Sequential PB1 and PB2 analysis, showing that all the tested oocytes are normal, despite 4 of them containing the "benign" mutant haplotype without IVS9+ 5 mutation (*N**). Multiplex heminested PCR for combined mutation analysis (*1c*), HLA genotyping (*2c*) and karyotyping (*3c*) for six chromosomes by PCR on blastomeres. Two of four embryos (embryos #8 and #9), predicted to be HLA-matched and free of mutation and aneuploidy, were transferred resulting in a singleton pregnancy and the birth of an unaffected child (as indicated in the family pedigree by PGD). *ET* embryo transfer

pigmenti, have been recognized previously [45–50]. Although germinal mosaicism is thought to be common, its presence in families is usually difficult to detect and depends on the gene penetrance. A majority of the newly mutant genes will have mutated during the development of the

affected individual and not during the development of one of the parents' gonads, so testing of the affected child will often reveal mosaicism for the gene in question, but in many cases will remain undetected.

For example, all the oocytes and embryos tested from such cases in our experience appeared to be unaffected, irrespective of the origin of DMN (29 oocytes and 87 embryos). However, this does not mean that PGD is not justified in these cases, because the possibility of a low level of mosaicism in parents' gonads cannot be completely excluded. In our cases of DNM detected first in children, although no mutation was identified in either parent, the presence of mutant haplotypes without the mutant gene was evident, suggesting that there may still be a proportion of germ cells with the mutation remaining undetected. So PGD is indeed indicated in such cases to exclude any possibility of the mutant oocyte and embryo production due to undetected germinal mosaicism.

As expected, the majority of cases involved DNM of dominant inheritance, in agreement with the high mutation rate of dominant disorders. However, almost a similar proportion of DNM of dominant type was either of paternal (45%) or maternal (55%) origin, requiring testing for the presence of DNM in both parents. On the other hand, all the cases of DNM of recessing inheritance were of paternal origin, but the number of cases is not sufficient for conclusions.

It should be mentioned that, despite the complexity of PGD for DNM, the applied strategies appeared to be highly accurate. Based on testing of 631 oocytes by PB analysis and 1,145 embryos by blastomere biopsy, 219 mutation-free embryos were transferred, resulting in extremely high pregnancy rate (49.6%) and the birth of 59 healthy children with no misdiagnosis detected, suggesting 100% accuracy of the applied technique of PGD.

The presented data show that PGD for DNM is an important addition to the practice of PGD for Mendelian diseases, as it makes it now possible to offer PGD to any couple at risk for producing offspring with genetic disease, despite the traditional requirement of family data, which is not always available even in cases with known family history for the disease. So the data demonstrate feasibility of PGD for DNM, which may now be routinely performed with the accuracy of over 99%, using the established PGD strategy.

3.7 Late-Onset Disorders with Genetic Predisposition

The diseases with genetic predisposition have not traditionally been considered an indication for prenatal diagnosis, as this would lead to pregnancy termination, which may hardly be justified on the basis of genetic predisposition alone. On the other hand, the possibility of choosing the embryos free of genetic predisposition for transfer would obviate the need for considering pregnancy termination, as only potentially normal pregnancies are established. PGD for such conditions appeared to be acceptable on ethical grounds because only a limited number of the embryos available from hyperstimulation are selected for transfer.

3.7.1 Inherited Predisposition to Cancer

Cancers are the largest group of conditions with genetic predisposition for which PGD was performed. Our experience (Table 3.18) is currently the world's largest series, involving PGD for 197 PGD cycles performed for 103 couples at risk for producing 20 different inherited cancers, including BRCA 1 and 2, Li-Fraumeni disease, familial adenomatosis polyposis (FAP), familial colorectal cancer, hereditary nonpolyposis coli (HNPCC) (type 1 and 2), Von Hippel-Lindau syndrome (VHL), familial posterior fossa brain tumor (hSNF5), retinoblastoma (RB), neurofibromatosis 1 and 2 (NF1 and NF2), Nevoid basal cell carcinoma (NBCCS) or Gorlin syndrome, tuberous sclerosis (TSC type 1 and type 2), ataxia telangiectasia, and Fanconi anemia (FA). This resulted in the transfer of 284 (1.7 embryos on an average) unaffected embryos in 163 transfer cycles, yielding 66 (40.5%) unaffected pregnancies and

Table 3.18 PGD experience for cancer predisposition

DISEASE	Number of patients	Number of cycles	Number of transfers	Number of embryo transferred	Pregnancies	Births
Ataxia telangiectasia	1	3	2	3	1	1
BCNS (Gorlin)	4	5	4	7	2	2
Brain tumor	1	1	1	1	0	0
BRCA1 &2	19	31	23	39	10	14
Fanconi anemia	17	51	32	52	7	6
FAP	7	20	19	33	4	3
HNPCC 1&2	3	8	8	16	4	5
LFS	4	6	5	9	2	2
MEN 1&2	2	2	2	4	1	2
NF1 & 2	22	40	38	69	18	21
RB1	3	4	4	9	4	3
TSC 1&2	9	13	13	18	5	8
VHL	5	5	4	9	3	4
Peutz–Jegher	1	2	2	3	2	1
Exostosis mult.	5	6	6	12	3	2
Total	103	197	163	284	66	74

the birth of 74 healthy children free from predisposition to those cancers. Some of these data were reported previously [51–53]. All these disorders are relatively rare autosomal-dominant conditions, with prevalence of 1 in 5,000 in the American populations for FAP, 1 in 15,000 for RB, 1 in 36,000 for VHL, and even rarer for others.

The first PGD for inherited predisposition has been performed for couples carrying p53 tumor suppressor gene mutations [53], known to determine a strong predisposition to the majority of cancers, which is described below.

3.7.1.1 p53 Tumor Suppressor Gene Mutations

Two couples presented for PGD, one with the maternally and one with the paternally derived p53 tumor suppressor mutations. The paternal one was a missence mutation due to a transversion of a G to A in exon 5 of the p53 tumor suppressor gene, resulting in a change from Arginine to Histidine at the 175 amino acid residue of the protein [16, 54]. The carrier was a 38-year-old proband with Li-Fraumeni syndrome (LFS), diagnosed with rhabdomyosarcoma of the right shoulder at the age of 2 followed by right upper extremity amputation. At the age of 31, he was also diagnosed with a high-grade leimyosarcoma of the bladder and underwent a radical cystoprostatectomy. His mother was diagnosed with leimyosarcoma at the age of 37 (Fig. 3.26).

In the other couple, the 39-year-old mother with LFS was a carrier of 902insC mutation of the p53 tumor-suppressor gene, representing an insertion of C in exon 8. She was diagnosed with breast cancer at the age of 30, followed by bilateral mastectomy. She also had thyroid cystocarcenoma, which was also removed. Her mother died from a stomach cancer at age 51. One of her sisters diagnosed with breast cancer at 48 followed by mastectomy also died at age 51. Two of her four brothers were diagnosed with bone or brain tumour in their teens (Fig. 3.27).

Prior to PGD cycles, linkage analysis has been performed for each couple in order to establish the maternal and paternal haplotypes, needed for performing a linked marker analysis in addition to mutation testing. Thus, in both cases, a multiplex nested PCR was performed by the testing of the mutations simultaneously with the linked polymorphic markers, representing the short tandem repeats (STR) in intron 1. To establish the paternal haplotypes, a single-sperm analysis was

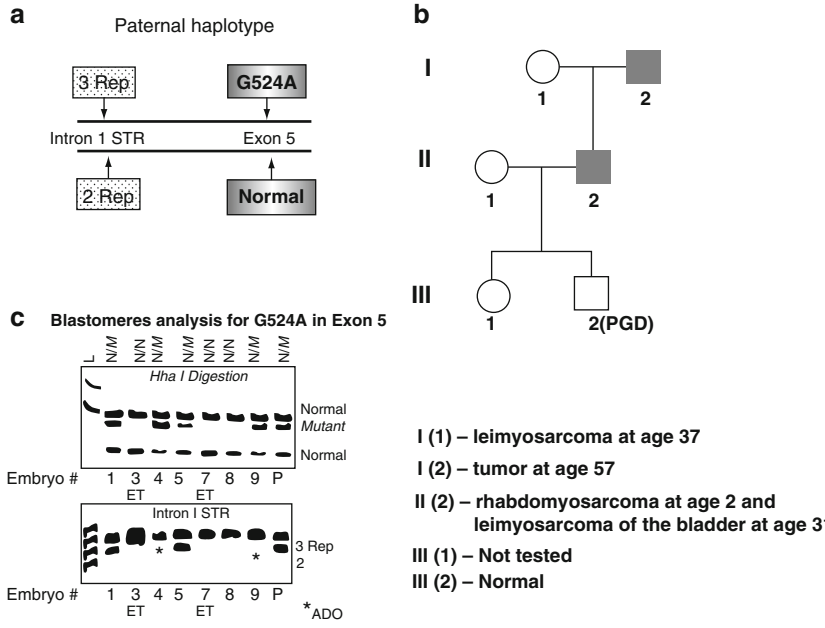

Fig. 3.26 PGD for Paternally Derived Mutation in p53 Tumor Suppressor Gene Mutation. (**a**) Paternal haplotypes are based on single sperm analysis, showing linkage of affected allele to three repeats and normal allele to two repeats in intron 1 STR. (**b**) Family pedigree, also showing a medical history on the bottom. (**c**) Duplex blastomere analysis for G524A mutation in exon 5 and liked STR in intron 1, showing that embryos #1, #4, #5 & #9 are affected, while embryo #3, #7 and #8 are mutation free and suitable for transfer. ADO of three repeats in intron 1 STR was detected in blastomere from embryo#4 and #9

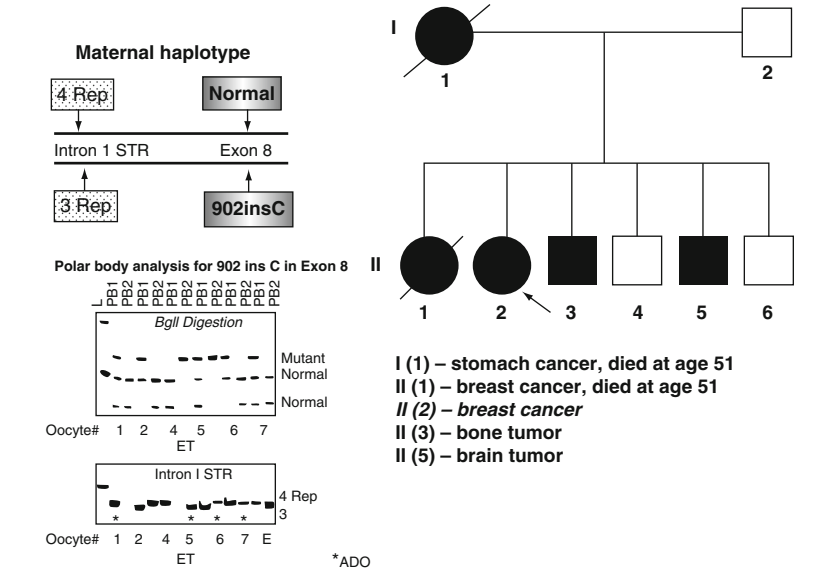

Fig. 3.27 PGD for maternally derived mutation in p53 tumor suppressor gene mutation. (**a**) Maternal haplotypes are based on PB1 and PB2 analysis, showing linkage of affected allele to three repeats and normal allele to four repeats in intron 1 STR. (**b**) Family pedigree, also showing a medical history at the bottom. (**c**) Duplex PB1 and PB2 analysis for 902insC mutation in exon 8 and linked to STR in intron 1, showing that all but one oocyte (oocyte #5) are affected, based on heterozygous PB1 and homozygous normal PB2. Thus, only embryos deriving from oocyte #5 were predicted normal and suitable for transfer, as shown by heterozygous PB1 and affected PB2. ADO of 3 repeats in intron 1 STR linked to 902insC mutation was detected in 4 of 7PB1 studied, all of which were heterozygous in mutation analysis

Table 3.19 Primers and reaction conditions for PGD of p53 tumor suppressor gene mutations

Gene/polymorphism	Upper primer	Lower primer	Annealing T_m (°C)
G524A (−Hha I)	Outside		62–45
	5′ GTGCAGCTGTGGGTTGA 3′	5′ GGAATCAGAGGCCTGGG 3′	
	Inside		56
	5′ CCATGGCCATCTACAAGCA 3′	5′ GGGACCCTGGGCAACC 3′	
902insC (−Bgl I)	Outside		62–5
	5′ AAGAGAATCTCCGCAAGAA 3′	5′ GAGGCAAGGAAAGGTGATAA 3′	
	Inside		60
	5′ GCCTGTCCTGGGAGAGAC 3′	5′ GCTTACCTCGCTTAGTGCG 3′	
(TAAA)n Heminested	Outside		62–45
	5′ CATTTGAATCCGGGAGGAG 3′	5′ ACAAAACATCCCCTACCAAACA 3′	
	Inside		60
	5′ GCCTGGGCAATAAGAGCTG 3′	5′ ACAAAACATCCCCTACCAAACA 3′	

performed, showing a linkage of the affected allele to the three repeats and the normal one to the two repeats. The maternal haplotypes were established by PB1 and PB2 analysis, demonstrating the linkage of the affected allele to the three repeats, and the normal one to the four repeats. The outside and inside primer sequences, the restriction sites, and the primer melting temperature for DNA analysis of both mutations are shown in Table 3.19. The PCR products were identified by restriction digestion, using HhaI for G524A and BglI for 902insC mutation.

Two PGD cycles were performed for each couple as described above. Testing for the maternal 902insC mutation was done by DNA analysis of PB1 and PB2, removed sequentially following maturation and fertilization of oocytes. The paternal G524A mutation was tested by DNA analysis of single blastomeres, removed from the eight-cell embryos. Based on both mutation and STR analysis, unaffected embryos were preselected for transfer back to the patients, while those predicted mutant were exposed to the confirmatory analysis using the genomic DNA from these embryos to evaluate the accuracy of the single-cell-based PGD.

A total of 18 day-3 embryos were tested in the couple with the paternally derived G524A mutation. Eleven embryos were heterozygous, with both alleles of the exon 5 present, while seven contained only the normal allele, in agreement with the STR analysis in intron 1. Figure 3.26 demonstrates the results of the testing of eight embryos in one of the cycles performed for this couple, showing that the embryos #1, #4, #5, and #9 were affected, and the embryos #3, #7, and #8 were unaffected. These results were in agreement with the marker analysis in all but two embryos (embryos #4 and #9), in which the three-repeat STR marker linked to the mutant gene was missing, probably due to ADO, because these embryos were clearly heterozygous according to the mutation analysis.

A total of ten oocytes were tested in two PGD cycles from the couple with the maternally derived 902insC mutation in exon 8. Mutation analysis was performed simultaneously with the linked STR in intron 1, using a sequential PB1 and PB2 analysis. Six oocytes with the available PCR results in both PB1 and PB2 were predicted affected, based on the heterozygous PB1 and normal PB2, and four unaffected, based on the heterozygous PB1 and the mutant PB2. As in the previous case, ADO of the three-repeat marker linked to the 902insC mutation was observed in four of seven heterozygous PB1 (Fig. 3.27).

The unaffected embryos were preselected and transferred back to the patients in each of the four PGD cycles performed for these two couples. Neither transfer yielded clinical pregnancies in the two cycles performed for the maternal mutation 902insC, while one of the transfers resulted in a singleton pregnancy and the birth of a

mutation-free child in a couple with the paternally derived G525A mutation, following the confirmation of PGD by prenatal diagnosis. The follow-up PCR analysis of the embryos predicted affected was possible for the embryos resulting from the six affected oocytes for the maternal mutation 902insC, and showed a concordance with the results of the PB analysis.

In one of our couples, the maternal carrier of the p53 tumor suppressor mutation was 39 years old, thus her elevated age-related risk for aneuploidy may have contributed to the failure of establishing pregnancy in the two subsequent clinical cycles. Although the testing for chromosomal abnormalities could be done for this couple, only one or two embryos, respectively, were available for the transfer in each of the two cycles, preventing further embryo preselection for the age-related aneuploidies. On the contrary, the other patient with the established pregnancy was neither a carrier of the p53 tumor-suppressor mutation, nor had the risk for the age-related aneuploidy.

As seen from the presented cases, indications for PGD are being extended steadily compared to the practice of prenatal diagnosis. This is due to the potential of PGD for the preselection of the mutation-free embryos and the establishment of an unaffected pregnancy, instead of the testing and termination of the pregnancies already in process. In fact, many at-risk couples have had such unfortunate experiences of repeated prenatal diagnoses and termination of affected pregnancies, that they regard PGD as their only hope for having children of their own, despite having to undergo IVF. This has made PGD also attractive for the couples at risk for late-onset disorders with the genetic predisposition, although such conditions have never been an indication even for prenatal diagnosis.

The presented cases demonstrate practical feasibility of PGD for the late-onset disorders, providing a principally new option for a large group of couples who wish to avoid the risk of having children with a strong inherited predisposition to common disorders. The application of PGD for avoiding the establishment of pregnancy with neurofibromatosis is presented below.

3.7.1.2 Neurofibromatosis

Neurofibromatosis (NF) is a common autosomal-dominant neurological disorder, with at least two distinct major forms, including NF type I (NF1), which is more common (1:4,000) and characterized by fibromatous skin tumors with café-au-lait spots, known also as Von Recklinghausen disease, and NF type II (NF2), which is less common (1:100,000) and characterized by bilateral acoustic neuromas, meningeomas, schwannomas, and neurofibromas [16].

The NF1 gene is located on chromosome 17ql 1.2, while the NF2 gene is mapped on chromosome 22q12.2. Alterations in the sequence of these genes affect the tumor suppressor function of their products (neurofibromin and merlin, respectively), leading to a strong predisposition to malignancies. Different mutations in these genes have been described, resulting in a variety of clinical manifestations. Approximately half of these mutations are sporadic [55, 56], with the rest representing germ-line mutations, which may be detected before the establishment of pregnancy to ensure unaffected pregnancy and the birth of a healthy child without an inherited predisposition to malignancy.

Although preimplantation genetic diagnosis (PGD) for inherited cancer predisposition is still a controversial issue [57, 58], the possibility of establishing only mutation-free pregnancies makes PGD an attractive option for the late-onset disorders with genetic predisposition, because of the possibility for preselection of the genetic predisposition-free embryos for transfer, avoiding the risk for pregnancy termination, as only potentially normal pregnancies could be established.

Three couples presented for PGD, two at risk for producing a child with NFI and one with the NF2 mutation. In one of the couples at risk for producing a child with maternally derived NF1, presented in Fig. 3.28, the 23-year-old mother with café-au-lait spots, axillary freckling, and Lisch iris nodules had a nonsense mutation (Trp->Ter) resulting from TGG->TGA substitution in exon 29 of the NF1 gene coding sequence. This was a de novo mutation, as no clinical symptoms of NF1 were known in the extended pedigree of the patient.

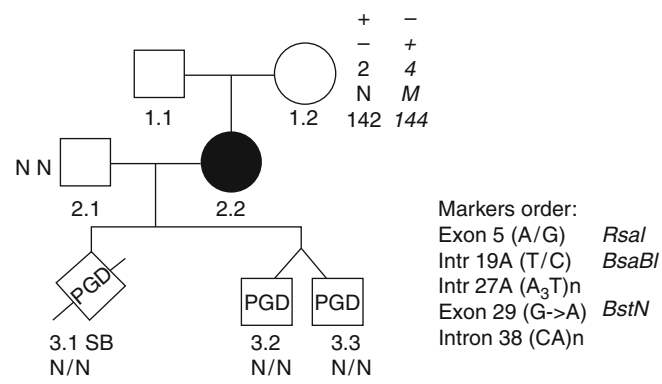

Fig. 3.28 PGD for neurofibromatosis type 1 (NF1): family pedigree. Haplotype analysis in a PGD couple with maternal de novo nonsense NF1 mutation Trp->Ter (TGG->TGA) in exon 29 of NF1 gene (based on sequential polar body analysis) Rsa – in exon 5, Bsa+in intron 19A, and AAATup in intron 27A (*Top*) Patient's parents (1.1 & 1.2) who are normal (*Middle*) markers (2.1 and 2.2) (*Bottom*) Sibling (SB) (3.1) representing a still-born baby born after the first PGD cycle, with confirmed mutation-free status in agreement with linked presented markers, while 3.2 and 3.3 represent unaffected twins resulting from next PGD cycle

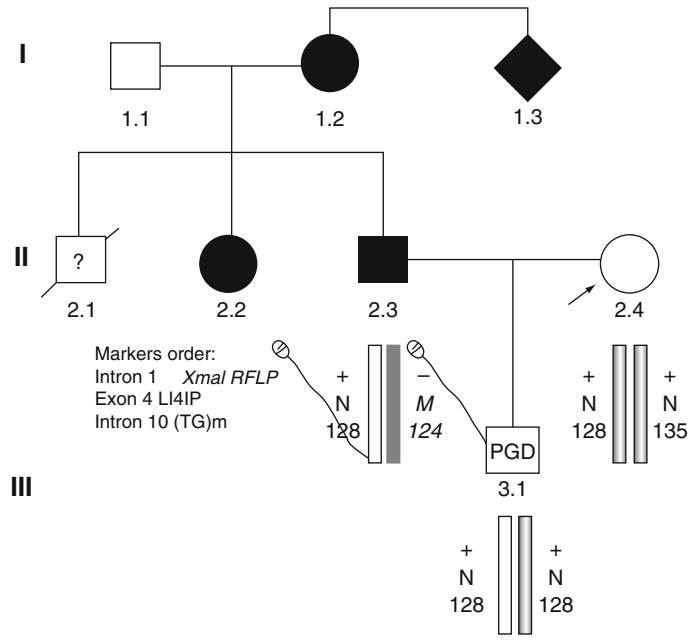

Fig. 3.29 PGD for neurofibromatosis type 2 (*NF2*): Family Pedigree Haplotype Analysis in Couple with Paternal L141P Mutation in Exon 4 of NF2 Gene. Paternal haplotype (2.3) was established by multiplex heminested PCR analysis of single sperm. Maternal haplotype was based on embryo genotypes. PGD cycle resulted in delivery of the normal boy (3.1)

In the couple at risk for producing an offspring with NF2, the 32-year-old father had an NF2 mutation, represented by the DNA sequence alteration at codon 141 of the merlin gene, due to a T–C base substitution in the nucleotide position 422, leading to the change from leucine (L) to proline (P) (Fig 3.29).

For testing of the maternal NF1 mutation, PB1 and PB2 were removed sequentially following maturation and fertilization of oocytes, while single blastomeres were removed from the eight-cell embryos for testing the paternal NF2 mutation. Linkage analysis had been performed for each couple, in order to establish the maternal and paternal haplotypes and to amplify these markers simultaneously with the mutation testing. In the NF1 case, three markers were informative, including Bsa B1 restriction site in intron 19A [59], short tandem repeat (STR) (AAAT) in intron 27A [60], and Rca I restriction site in exon 5 [61]. In the NF2 case, two markers were informative, one representing single nucleotide polymorphism (SNP) in intron 1, following XmaI restriction digestion, and the dinucleotide repeat (TG) in intron 10 [62, 63]. Thus, in both cases, a multiplex nested PCR was performed, amplifying the mutations simultaneously with the linked polymorphic

Table 3.20 Primers and reaction conditions for PGD of NF1 & NF2

Gene/ polymorphism	Upper primer	Lower primer	Annealing T_m (°C)
NF1exon 29 (TGG-TGA) *Bst NI* cuts normal	Outside 5′ GTTTAATTCTTCTCCACTTCACC 3′	5′ CAACACTGCATACCTTCCA 3′	62–45
	Inside 5′ TTCATATCCGGACCCCC 3′	5′ CTTTTGGCCGAATCTTGG 3′	53
NF1 (AAAT)n	Outside 5′ TGGTGGCACATACCTGTAG 3′	5′ TTACAGATTAAGGCAATTCTGA 3′	62–45
	Inside 5′ TGCATTCTAGCCTGAGTGA 3′	5′ AAACAAGCAAGAATAGAAAAAG 3′	48
NF1 SNP *Bsa BI*	Outside 5′ ATTAGTGGGTTTTACTGTG 3′	5′ CTGAGGCTTTATGTATCTTA 3′	62–45
	Inside 5′ TGTGTATTTAAACTTTTGAG 3′	5′ TTCCCAATAACTGTAGAC 3′	53
NF1 SNP Rsa I	Outside 5′ CATGTGGTTCTTTATTTATAGG 3′	5′ TTGACACCAGTTGACAATAG 3′	62–45
	Inside 5′ GGTAGAAAATTATCCAGATGA 3′	5′ AACTTGGAAAACGATGATAG 3′	55
NF2 *Msp I* cuts mutant	Outside: 5′ GGCAGCCCTCATTAGAAC 3′	5′ AGAATACAGAAAACCCAAAG 3′	62–45
	Inside: 5′ AAGATCTACTGCCCTCCTG 3′	5′ TGATCCCATGACCCAAATTA 3′	54
NF2 SNP Xma I	Outside: 5′ AAGAATATTCGCCGTGTGTC 3′	5′ GACTTTCCCGCTCCGTC 3′	62–45
	Inside: 5′ CAACGAAGGACCCAATTCC 3′	5′ AAGCAGGCCTAGGCTCG 3′	54
NF2 Intron 10 (TG)n	Outside: 5′ GGAGAAAATTGGAGAAGAACT 3′	5′ CCACTCTGGTCATACAACG 3′	62–45
	Inside: 5′ TTCACTGTTTTATTGCTTGTC 3′	5′ FamGACTGCTGCTTTTTCTAAATC 3′	

markers [64, 65]. The primers designed for amplification of NF1 and NF2 genes and their linked markers mentioned are listed in Table 3.20.

Testing for NF1 was performed using BstNI restriction digestion, which produces two fragments of 20 and 52 bp in the second-round PCR product of the normal allele, in contrast to a single undigested fragment of 72 bp in the mutant gene. The maternal haplotypes were established by PB1 and PB2 analysis, demonstrating the linkage of the affected allele to Rsa –, Bsa+, and AAATup markers (Fig. 3.30).

Testing for NF2 mutation was done by blastomere analysis, using MspI restriction digestion, which produces two fragments of 36 and 86 bp in the second-round PCR product of the mutant allele, in contrast to a single 122 bp fragment in the normal gene. The single-sperm haplotype analysis demonstrated the linkage of the affected allele to the XmaI undigested fragment, and to the 124 bp dinucleotide repeat in intron 10, the latter being tested using fluorescent PCR (Fig. 3.31).

A total of 57 oocytes were tested in 5 PGD cycles from the patient carrying the NF1 mutation. Based on simultaneous mutation and marker analysis in PB1 and PB2, 20 oocytes with the available PCR results in both PB1 and PB2 were predicted as affected. Of 26 oocytes containing no mutant gene, 8 (two in each cycle) with sufficient marker information available resulted in the embryos of acceptable quality for embryo transfer, and 3 reached blastocyst stage and were frozen. Due to the close location of the gene to the centromere, which might explain the presence of only 2 oocytes with heterozygous PB1, the information on the linked markers was of particular importance to avoid misdiagnosis due to a potential ADO of one of the alleles in PB1.

Two of these transfers resulted in clinical pregnancies. In one of these cycles, of 17 tested oocytes, 9 contained no mutant allele, from which only 2 with sufficient linked marker information to exclude the risk for misdiagnosis resulted in the embryos of acceptable quality for transfer, yielding a singleton clinical pregnancy. Prenatal diagnosis by chorionic villus sampling (CVS)

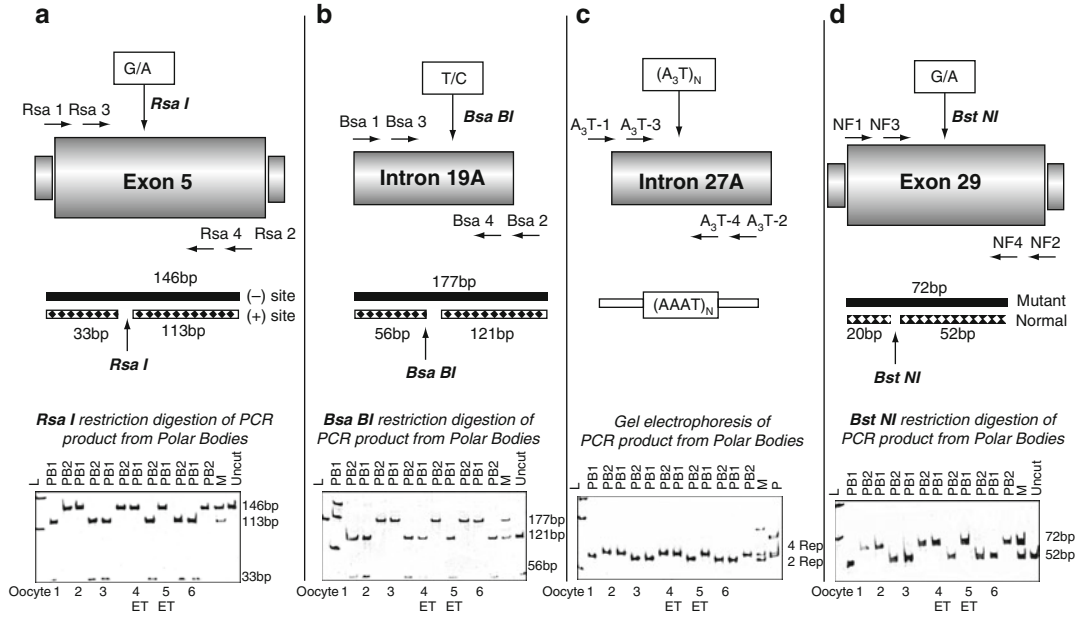

Fig. 3.30 PGD for NF1 nonsense mutation Trp->Ter (TGG->TGA) in exon 29: mutation and polymorphic marker analysis. (*Top*) Schematic diagram of the mutation (**d**) and linked markers (**a**–**c**) on chromosome 17q11.2. (*Middle*) Restriction maps for BstN I (**d**), Rsa I (**a**), and Bsa BI (**b**) restriction fragment-length polymorphism; and short tandem repeat in intron 27A (**c**). (*Bottom*) Polyacrylamide gel electrophoresis of the restriction-digested PCR products of PB1 and PB2 from six oocytes in one of the cycles of PGD for NF1, showing mutation-free oocytes #2, #4, and #5, evidenced by 72 bp undigested fragment in PB1 and a 52 bp digested fragment in PB2 (**d**), in agreement with all three marker analyses (**a**–**c**) (for linkages to mutant and normal alleles)

confirmed the mutation-free status of the fetus, but the pregnancy ended in a stillbirth at 24 weeks. Similar results were obtained in the next cycle, resulting in preselection and transfer of two mutation-free oocytes, yielding a twin pregnancy and the birth of healthy twins (Figs. 3.28 and 3.30). As seen from polyacrylamide gel electrophoresis of the restriction-digested PCR products of PB1 and PB2 from six oocytes from this cycle, mutation-free status of oocytes #2, #4, and #5 is evidenced by 72 bp undigested fragment in PB1 and a 52 bp digested fragment in PB2, in agreement with all three marker analyses. One of the cycles performed for this couple, resulting in the establishment of embryonic stem cell line from the affected NF1 embryos, will be described in Chap. 7.

Of 18 day-3 embryos tested in one cycle from the couple with the paternally derived NF2 mutation, 8 were predicted to be mutation-free including four with no or only one linked marker information available to exclude the risk for misdiagnosis. Three of four normal embryos with both linked markers in agreement with mutation analysis (Fig. 3.31) were transferred back to the patient, resulting in a clinical pregnancy and the birth of a healthy child free from NF2 mutation, following confirmation of PGD by CVS. Three of five remaining mutation-free embryos that continued development were frozen for future possible use by the couple.

The presented data demonstrate the acceptable diagnostic accuracy of both the PB and blastomere analysis for PGD of NF1 and NF2 [66]. As shown by the follow-up analysis of the mutant embryos or those with insufficient marker information, the PGD results were confirmed in all resulting embryos available for the study. As mentioned, in one of the cycles performed for maternally derived NF1 mutation, the pregnancy resulted in a stillbirth, following confirmation of the mutation-free status of the fetus by CVS. Mutation-free status was also confirmed in a baby born following PGD for NF2 (Fig. 3.31).

As seen from the presented cases, together with the other application of PGD to cancer

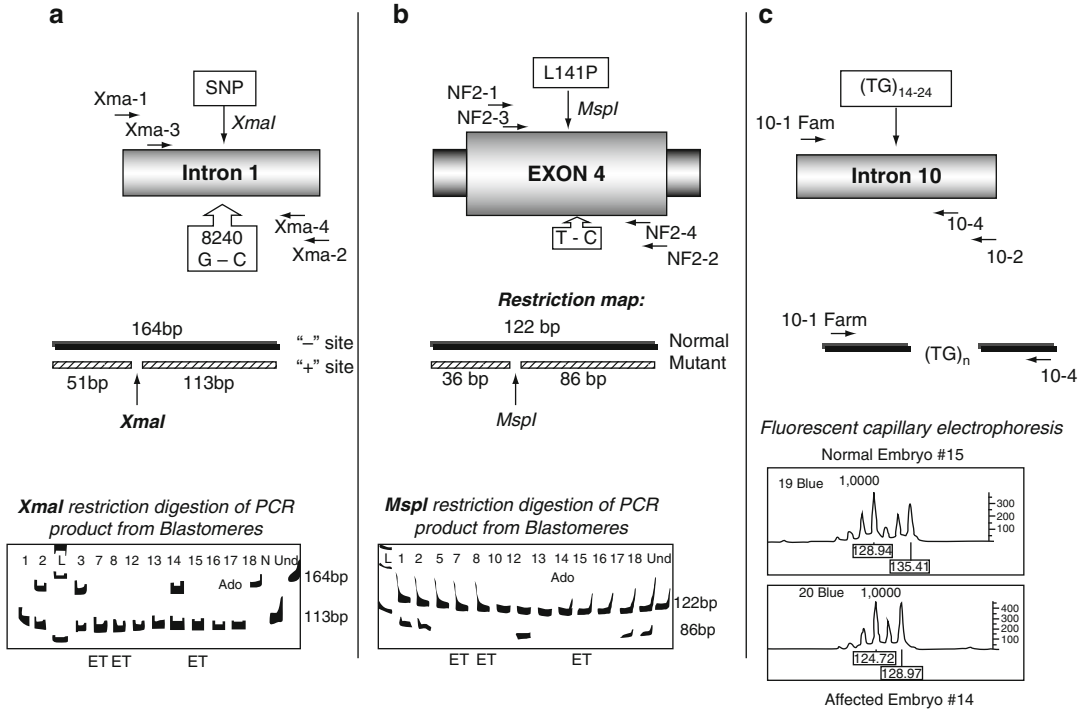

Fig. 3.31 PGD for L141P mutation in exon 4 of NF2 gene: mutation and polymorphic marker analysis. (*Top*) Schematic diagram of the mutation (**b**) and linked markers (**a**, **c**) on chromosome 22q12.2. (*Middle*) Restriction maps for Msp I (**b**) and Xma I (**a**) restriction digestion in exon 4 and intron 1 of NF2 gene, and design for the dinucleotide TG repeat testing in intron 10 (**c**). (*Bottom*) Polyacrylamide gel electrophoresis of the restriction digested PCR products of blastomeres, showing seven mutation-free embryos (#5, #7, #8, #10, #13, #15, and #16), evidenced by the presence of a 122 bp undigested fragment, as compared to the presence of a digested 86 bp fragment in addition to a 122 fragment in the rest of the embryos (**b**), in agreement with XmaI restriction length polymorphism in intron 1 (**a**), and dinucleotide TG repeats in intron 10 (the latter being detected by fluorescent capillary electrophoresis (**c**)) shown for normal embryo #14, as an example (for the linkages to normal and mutant genes, see Fig. 3.29)

predisposition, the approach seems to be acceptable to the couples at risk, despite important ethical implications. So current genetic counseling services may consider informing patients at risk of having children with a strong genetic predisposition to cancers and late-onset disorders about the availability of PGD, without which these couples may remain childless because of their fear to opt for prenatal diagnosis and possible pregnancy termination.

3.7.1.3 Other Cancers

At the present time the most common cancer for which PGD has been performed is inherited breast cancer [52, 67–71]. Almost half of inherited breast cancers are caused by BRCA1 and BRCA2, which were indications for 31 PGD cycles in our experience. A total of 39 embryos free from these mutations were preselected for transfer in 23 cycles, resulting in 10 clinical pregnancies and the birth of 14 children without predisposition to breast cancer. Because of the high prevalence of these conditions, some of the couples were at risk not only of producing offspring with genetic predisposition to breast cancer, but also with other genetic disorders at the same time.

The examples of combined PGD for BRCA1 and SMA, and BRCA2 and MEN1, are presented in Fig. 3.32, the latter also involving aneuploidy testing by FISH analysis. Despite testing for both mutations in each of these cycles, two embryos were identified for transfer in both cases.

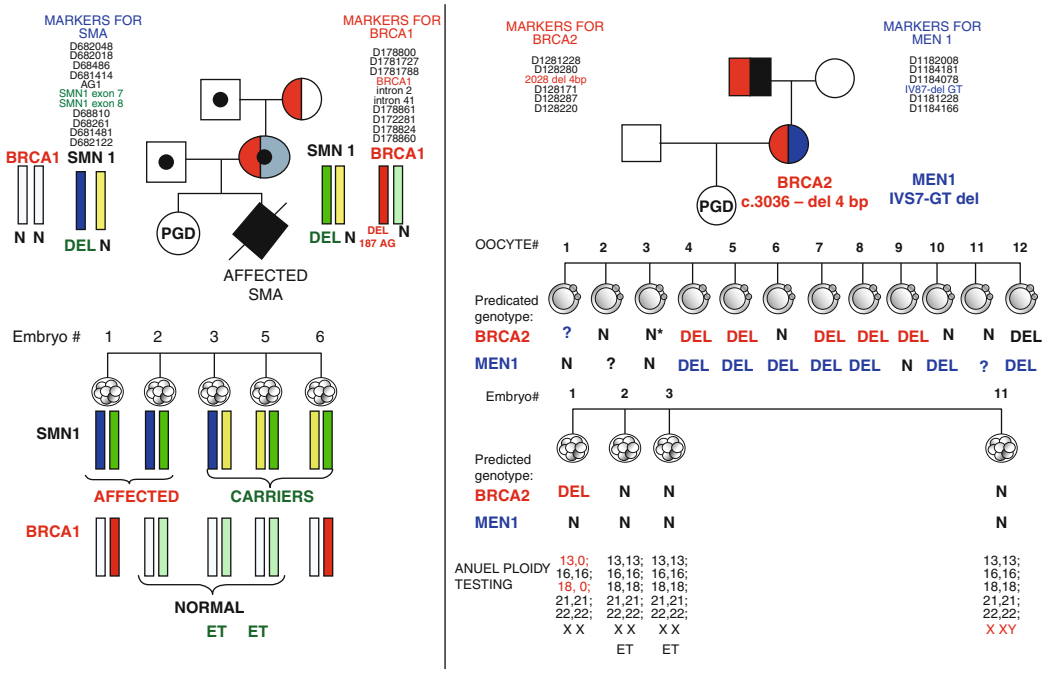

Fig. 3.32 Concomitant PGD for breast cancer, BRCA1 and BRSA2, and SMA and MEN1. (**a**) PGD for BRCA1 and SMA in the same couple. (*Upper panel*) Pedigree showing that the patient and her mother are carriers of BRCA1 mutation (Del 187 AG; shown in *red*) – linked markers are listed on the *right*. The patient is also a carrier of SMN1 mutation (deletion, shown in *green*), inherited from her father. The male partner (the father) is also an unaffected carrier of the same deletion in SMN gene (shown in *blue*). The couple had one previous pregnancy resulting in the birth of an affected child with SMA who died (linked polymorphic markers for SMN1 mutation are listed on the *left*). (*Lower panel*) Five embryos were tested for both SMN1 and BRCA1 in the same reaction, showing that embryos #1 and #2 contained deletion in SMNA from both parents (*blue and green*), and the remaining three embryos were carriers of either maternal (embryos #4 and #5) or paternal (embryo #3) deletion. Two of these embryos (embryos #1 and #5) were also carriers of BRCA1 mutation, so three embryos (embryos #2, #3, and #4) were predicted to be free of BRCA 1 mutation and unaffected by SMA. Two of these embryos (embryos #3 and #4) were transferred, resulting in the birth of an unaffected child, shown in pedigree as PGD (*ET* embryo transfer). (**b**) Combined PGD for BRCA2, MEN1, and aneuploidy. (*Upper panel*) Pedigree showing that the patient and her father are carriers of BRCA2 (c.3036-del4 bp, shown in *red*) and MEN1 (IVS7-GT del, shown in *blue*) mutations. Polymorphic markers for testing of BRCA2 mutation are shown on the *left*, and for MEN1 deletion on the *right*. (*Middle panel 1*) Twelve oocytes were tested by sequential PB1 and PB2 analysis simultaneously for both mutations, which detected only one oocyte (oocyte #3) to be free of both mutations (in addition, oocyte #2 had insufficient marker information to confirm a normal allele for MEN1), so the resulting four embryos (embryos #1, #2, #3, and #11) were further tested by blastomere biopsy, presented in the *middle panel 2*. (*Middle panel 2*) Blastomere analysis of embryos #1, #2, #3, and #11, showing that all but one (embryo #1) are free of both mutations. (*Lower panel*) Two of these embryos were chromosomally abnormal (embryos #1 monosomic for chromosomes 13 and 18; and embryo #11 with extra chromosome X), while the other two (embryos #2 and #3) were euploid. These two embryos were transferred, resulting in an unaffected singleton pregnancy and the birth of a healthy child (shown in pedigree as PGD) free of both BRCA2 and MEN1 mutations

As seen from Table 3.18, the second most frequent indication was *FAP*. Patients with FAP usually present with colorectal cancer in early adult life, secondary to extensive adenomatous polyps of the colon, determined by mutation of the adenomatous polyposis coli (APC) gene located on chromosome 5 (5q21-q22). Over 826 germ-line mutations have been found in families with FAP, causing a premature truncation of the APC protein, through single amino acid substitutions or frameshifts, with the most common mutation being a 5 bp deletion resulting in a frameshift

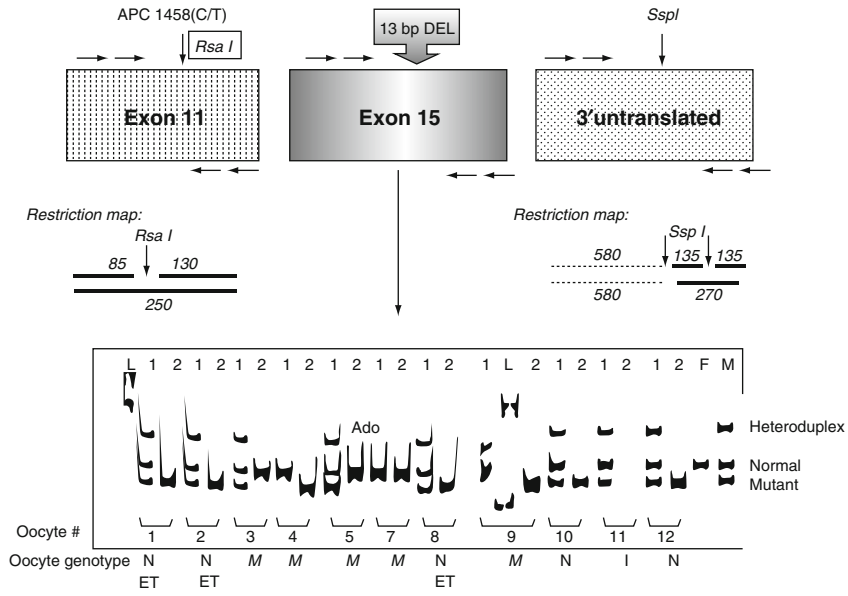

Fig. 3.33 PGD for 13 bp deletion in APC gene resulted in the birth of a normal child. (*Top*) Schematic diagram of the mutation, and linked markers on chromosome 5q21. (*Middle*) Restriction map for Rsa I and Ssp I restriction digestion in exon 1 and untranslated area of APC gene. (*Bottom*) Polyacrylamide gel electrophoresis of the PCR products of PB1 and PB2 from 11 oocytes in one of the cycles of PGD for FAP, showing mutation-free oocytes #1, #2, #8, #10, and #12, evidenced by normal and mutant fragments in PB1 and a mutant fragment in PB2, in agreement with both marker analyses

mutation at codon 1309. The APC mutations lead to a premalignant disease with one or more polyps progressing through dysplasia to malignancy with a median age at diagnosis of 40 years. Because the mutations in the APC gene are almost completely penetrant, although with striking variation in expression, even presymptomatic diagnosis and treatment of carriers cannot exclude the progression of polyps to malignancy, making PGD an attractive approach for couples carrying APC mutations [72].

The example of the PGD strategy for FAP mutations in the APC gene is presented in Fig. 3.33, showing PGD for the maternally derived mutation resulting from the 13 bp deletion in exon 15 of the gene. DNA testing in all the PGD cycles was performed by the multiplex nested PCR analysis, amplifying mutations simultaneously with linked markers both in blastomere and PB1 and PB2, with the set of primers listed in Table 3.21. Linkage analysis had been performed for each couple, and the maternal and paternal haplotypes were established to avoid a possible misdiagnosis, which still requires special attention because of the phenomena of allele-drop out (ADO) and preferential amplification, known to be frequent in a single-cell DNA analysis. For example, in a couple with FAP, two linked markers were found to be informative, including Rsa I restriction site in intron 11, and SspI restriction site in 3′ untranslated area of the APC gene (Fig. 3.33). As seen from this figure, three mutation-free oocytes were detected for transfer, resulting in an unaffected pregnancy, confirmed by follow-up prenatal diagnosis and a blood test after delivery of a child. However, a cord blood sample was not appropriate for confirmation analysis, as it was contaminated by maternal blood, clearly demonstrated by the presence of the mutant allele, as well as both maternal polymorphic markers in the cord blood sample. The fact that the baby has no mutant allele was further confirmed by testing of a heel stick blood from the child, which contained no trace of the mutant gene, also in agreement with the analysis of polymorphic markers.

Table 3.21 Primers and reaction conditions for PGD of cancer predisposition

Gene/ polymorphism	Upper primer	Lower primer	Annealing T_m (°C)
APC 13 bp deletion	Outside		62–55
	5′ TCGACATGATGATAATAGGTC 3′	5′ TTTCTGTTGCTGGATGGTAG 3′	
	Inside		58
	5′ GACAATTTTAATACTGGCAACA 3′	5′ TCCAAACTTCTATCTTTTTCAGA 3′	
APC RFLP *RsaI*	Outside		62–55
	5′ GGTACCAGTTTGTTTTATTTTAG 3′	5′ CACAGGTTTTTATCAGTCATTG 3′	
	Inside		62
	5′ GATGATTGTCTTTTTCCTCTTGC 3′	5′ CTGAGCTATCTTAAGAAATACATG 3′	
APC RFLP *Ssp I*	Outside		62–55
	CTATGCATTAAGAGTAAAATTCC 3′	5′ GTATTACCCTATCTGAGTGCC 3′	
	Inside		62
	5′ CATTGAAGAAGACTGTTGCCAC 3′	5′ AAAAGGTTTTCCTCCCCAAATAC 3′	
VHL (Nt 482) Creates *MboII* site	Outside		62–55
	5′ ACGGCGGGGAGGAGTCG 3′	5′ CTCAAGGGGCCTCAGTTC 3′	
	Inside		58
	5′ GCGCCGAGGAGGAGATG 3′	5′ GGGGCTTCAGACCGTGC 3′	
VHL D3S100	Outside		62–55
	5′ GTCTGGTGGCCTGTGAAC 3′	5′ CTTTCTCTTCGGAATGGGAG 3′	
	Inside		58
	5′ GAAAATGTGTTCATCATCCTC 3′	5′ TTATCTTATCCCTGCCTCAC 3′	
hSNF5 (Nt443) Creates *Hpy188 I* site	Outside		62–55
	5′ GGGGGAGTTTGTCACCAC 3′	5′ GGAGGACGGAGCAAACAC 3′	
	Inside		54
	5′ CCACCATCGCATACAGCA 3′	5′ GGAGGACGGAGCAAACAC 3′	
D22S1144 (heminested)	Outside		62–55
	5′ AAATAGGCAGATGCTGAAA 3′	5′ ACAGAGCCTCTGGTCCTC 3′	
	Inside		50
	5′ Hex GGAAAGCAACTTTGGTAAA 3′	5′ ACAGAGCCTCTGGTCCTC 3′	
D22S1174 (heminested)	Outside		62–55
	5′ GGACATAGCAAACTCTTAGGG 3′	5′ GAATCTGCTGCTTGCTTTT 3′	
	Inside		50
	5′ FamCACTTCTGAGTTGTTTGAATCTC 3′	5′ GAATCTGCTGCTTGCTTTT 3′	
RB (GA del)	Outside		62–55
	5′ GTAGGCTTGAGTTTGAAGA 3′	5′ TGAAGTTGTTTTTAAAATGAGA	
	Inside		55
	5′ Fam TGATTTTACTGCATTATGTCAG 3′	5′ CTTACCAATACTCCATCCAC 3′	
RB Intron 20 STR (CTTT)n	Outside		62–55
	5′ GACAGGCATTTGGACCAAG 3′	5′ GCAGTGAGCCGAGATTGC 3′	
	Inside		56
	5′ Hex CCCTACTTACTTGTTAACTG 3′	5′ GGTAACAGAGTGAGACTCTA 3′	

Five cycles were performed for *VHL*, which is a cancer syndrome with age-related penetrance, characterized by hemangiomablastomas of the brain, spinal cord, and retina; bilateral renal cysts and renal carcinoma; pheochromocytoma; and pancreatic cysts. Depending on the combination of these clinical features, four different types of the disease have been described. The gene responsible for VHL syndrome consists of three exons and is located on chromosome 3 (3p26-p25), with specific VHL gene mutations correlating with the clinical phenotype. Its normal gene product is a

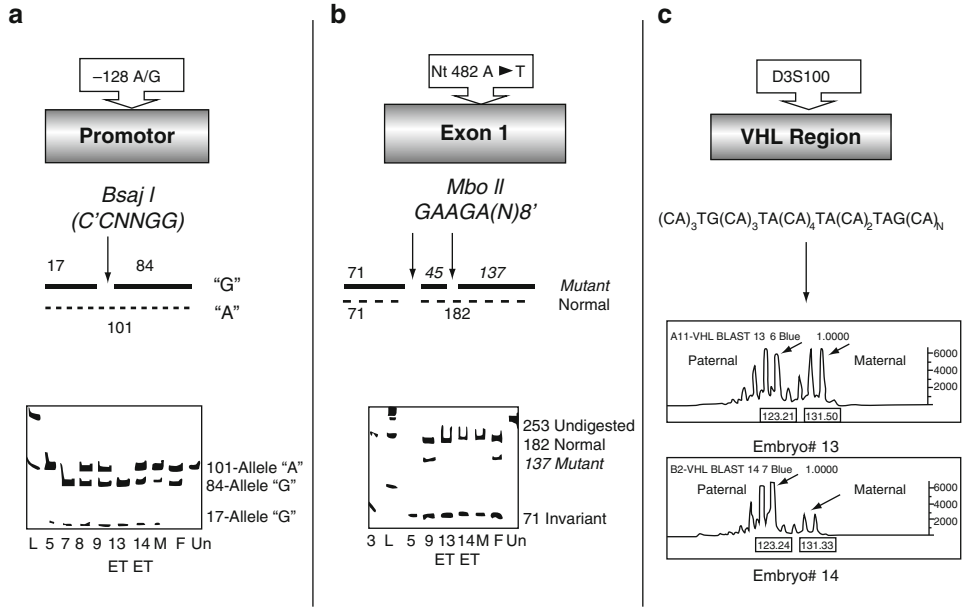

Fig. 3.34 PGD for Nt 482 A-T mutation in exon 1 of VHL gene. (*Top*) Schematic diagram of the mutation, and linked markers; (**a**) Position of G/A SNP in promoter area of the gene and the restriction map, and the restriction digestion with *Bsaj*I enzyme differentiated "A" and "G" sequences (*middle*). (**b**) Position of nt482 A-T mutation in exon 1 of VHL gene and the restriction map (*middle*). Amplified sequence has invariant restriction fragment (71 bp). Enzyme *Mbo*II-digested mutant sequence into two fragments of 45 bp and 137 bp, with the size of the normal allele being 182 bp. (*Bottom*) Polyacrylamide gel electrophoresis of the *Mbo*II restriction-digested PCR products of blastomeres detected mutation-free embryos #13 and #14, evidenced by the presence of a 182 bp undigested fragment, as compared to the presence of a digested 137 bp fragment in the affected embryos. This is in agreement of the results of SNP analysis in the promoter (**a** *bottom*). (**c**) Position and sequence of D3S100 dinucleotide repeat in VHL region. Capillary electrophoregrams of fluorescently labeled dinucleotide repeat PCR products scored by Genotyper™. The presence of 123 bp paternal allele in embryos #13 and #14 confirmed the normal status of these embryos predicted by mutation analysis. *ET* embryo transfer, *M* maternal DNA, *P* paternal DNA containing the mutation, *L* 100 bp standard

tumor suppressor protein, which is expressed in most cells and has a variety of functions, including transcriptional and posttranscriptional regulation. More than 300 germ-line mutations have been identified in families with VHL syndrome, consisting of partial or complete gene deletions, and frameshift, nonsense, missense, and splice site mutations, most commonly affecting codon 167. Mutations in the VHL gene either prevent its expression completely or lead to the expression of an abnormal protein. Because only 20% of cases of VHL are sporadic, with the remaining 80% being familial, PGD is clearly an attractive option for couples carrying these mutations to avoid the inheritance of these tumor suppressor gene mutations to their potential children and have a mutation-free child, with no risk of developing cancer.

The example of PGD for paternally derived mutation causing VHL is shown in Fig. 3.34, performed for the male partner carrying A to T substitution in nucleotide 482 of exon 1. As seen from this figure, only one of four embryos in this cycle contained the mutant gene (embryo #9), the remaining three being normal. The haplotype analysis, an obligatory part of PGD for paternally derived dominant mutations, confirmed the presence of a normal paternal gene. As seen from Fig. 3.34, both embryos transferred in this cycle contained the polymorphic 123 bp marker, representing a dinucleotide repeat (CA)3TG(CA)3TA (CA)3TA(CA)2TAG(CA)n, which is strongly linked to the normal paternal gene, and therefore absolutely essential to be able to confirm the presence of the normal paternal gene in the

embryos selected for transfer, confirming the results of the mutation analysis. The transfer of these two normal embryos back to the patient, however, did not result in a clinical pregnancy. The affected embryo was reanalyzed, confirming the prediction of the Nt 482 (A-T) mutation in the embryo.

Four cycles were done because of inherited predisposition to *RB*, caused by the germ-line mutations in the RB1 gene, located on chromosome 13 (q14.1-q14.2), and represents a malignant tumor of the retina, which occurs in cells with cancer-predisposing mutations usually before the age of 5 years. More than half of the patients have unilateral RB, which may be diagnosed at 24 months, while bilateral RB is recognizable as early as 15 months, using direct ophthalmoscopy. The majority of cases are due to a point mutation in the coding regions of the RB1 gene, while partial deletions of the gene were also described. Over 200 distinct mutations have been reported, with the majority resulting in premature termination codon, usually through single base substitutions, frameshift, or splice mutations, scattered throughout exon 1 to exon 25 of the RB1 gene and its promoter region. The mutations lead to the loss of the cell cycle regulation function of the RB1 protein, and are nearly completely penetrant in nonsense and frameshift mutations, making PGD and important option for couples at risk.

In each of the four cycles performed for three patients at risk for producing offspring predisposed to RB, nine unaffected embryos were preselected, resulting in clinical pregnancies in each cycle, with the birth of three healthy children free from the mutant gene predisposing to RB.

A single PGD cycle was performed for the patient carrying the *hSNF5* mutation predisposing to brain tumor, which is very rare, found in sporadic rhabdoid tumors of the central nervous system. Rhabdoid tumors are known to be highly malignant neoplasms usually occurring in children under 2 years of age. Although rhabdoid tumors determined by truncating mutations of the hSNF5 gene are mainly sporadic and have never been previously found in the parents of affected children, a first familial case of posterior fossa brain tumor has recently been described in two generations [73]. The proband presented at the age of 18 months with a cerebellar malignant rhabdoid tumor. Although the parents were healthy, the child's maternal uncle died at age 2 years from a posterior fossa choroids plexux carcinoma, and her grandfather's sibling also died as an infant from a brain tumor, suggesting the presence of a germ-line mutation. The couple presented for PGD in order to have a pregnancy free from the hSNF5 mutation, also avoiding the birth of a second child with brain tumor. As seen from Fig. 3.35, the mutation is due to G to A substitution in a donor splice site of exon 7, which alters the conserved GT sequence at the beginning of the intron violating the GT rule for splice site recognition. In this unique case, the mother was unaffected but her daughter who inherited the mutation had a brain tumor [51]. Because the mutation was also detected in DNA from her uncle's tumor, suggesting the risk of transmitting the mutation to the next child, PB1 and PB2 were removed in this case to preselect mutation-free oocytes in a standard IVF cycle.

Of only four oocytes available for testing, three have results of both PB1 and PB2 analysis, showing that only one oocyte (oocyte #4) could be predicted to be free of mutation, based on the heterozygous status of PB1 and homozygous mutant PB2. Of the remaining two oocytes, oocyte #2 was clearly mutant as evidenced by the heterozygous PB1 and homozygous normal PB2, suggesting that only the normal allele was left in the resulting oocyte. The results of mutation analysis in oocytes #2 and #4 were in agreement with both markers in PB1 and PB2 tested. On the other hand, while based on mutation analysis, oocyte #3 could have also been predicted as normal and transferred, as evidenced from the homozygous mutant status of PB1 and homozygous normal status of PB2, the presence of both alleles of D22s1144 marker linked to both the normal and mutant gene in the corresponding PB1 suggested a completely opposite (mutant) genotype of oocyte #3, despite the second polymorphic marker D22s1174 showing a correspondence with the mutation analysis. So the availability of

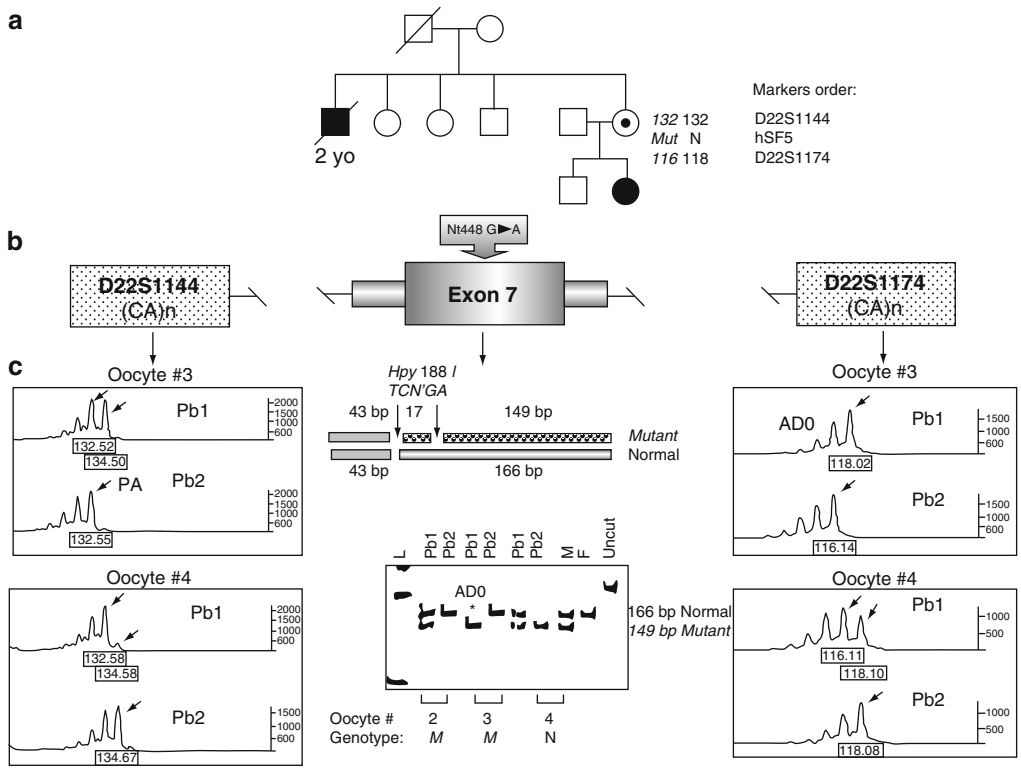

Fig. 3.35 PGD for familial posterior fossa brain tumor (hSNF5). (**a**) Family pedigree with posterior fossa tumors in two generations: an unaffected carrier haplotype was determined by sequential PB1 and PB2 analysis. (**b**) Position of the Nt 443G--A mutation in exon 7 of hSNF5 gene and tightly linked dinucleotide polymorphic markers *D22s1144* and *D22s1174*. (**c**) (*Left*) Fluorescent PCR results of the sequential PB1 and PB2 analysis. One of the second-round PCR primers was labeled with Hex fluorescent dye. Oocyte #3 is predicted to be affected based on heterozygous (132/134) PB1 and 132 bp PCR product linked to normal maternal allele in PB2. Preferential amplification (PA) of 132 bp allele was detected in PB1 from oocyte #4 in agreement with mutation analysis and the second *D22s1174* marker, suggesting that the oocyte #4 may be predicted to be normal. (*Middle*) Restriction map and polyacrylamide gel analysis of *Hpy188 I* restriction digestion of PCR product from PB1 and PB2. Based on this analysis oocyte #2 is normal based on heterozygous PB1 and mutant PB2. Allele dropout (*ADO*) was detected in PB1 from oocyte #3 by polymorphic markers *D22s1144* and *D22s1174*. Without these markers, oocyte #3 genotype would have been predicted normal based on homozygous mutant PB1 and hemizygous normal PB2, which might have led to misdiagnosis. Oocyte #4 is predicted to be normal based on heterozygote PB1 and mutant PB2, in agreement with marker analysis as mentioned (*Right*) Fluorescent PCR (FL-PCR) results of sequential PB1 and PB2 analysis. One of the second-round PCR primers was labeled with Fam fluorescent dye. ADO of 116 bp allele was detected in PB1 from oocyte #3 by mutation analysis and *D22s1144* marker study. Heterozygous PB1 from oocyte #4 confirmed PA suspected during the *D22s1144* analysis. *N* normal, *M* mutant, *F* paternal DNA, *Mo* maternal DNA, *U* uncut PCR product, *Nt* nucleotide

the two polymorphic markers made it possible to avoid the transfer of the additional embryo, which may have led to misdiagnosis. Unfortunately, the transfer of only one unaffected embryo back to the patient yielded no clinical pregnancy. The follow-up testing of embryos resulting from oocytes #2 and #3 confirmed the diagnosis, further supporting the need for a simultaneous mutation and linked marker analysis for avoiding misdiagnosis in PB-based PGD. Therefore, as previously suggested, the priority in the preselection of mutation-free oocytes should be given to those with heterozygous PB1 and homozygous mutant PB2. If no such oocytes are available, at least three linked polymorphic markers are required to exclude ADO of one of the alleles in apparently

homozygous PB1, which is currently the major potential source of misdiagnosis due to ADO and preferential amplification in PB-based PGD.

With current progress in understanding of the molecular basis of cancers, and sequencing of the genes involved in malignancy, the inherited cancer predisposition will become one of the major emerging PGD indications, presently already representing approximately 10% of all PGD experience for Mendelian disorders. As mentioned, despite extensive discussions of the ethical and legal issues involved in PGD for late-onset disorders with genetic predisposition, an increasing number of patients regard the procedure not only as their favorable option but also the only possible reason for forgoing the pregnancy, which can be established free of mutation from the onset, avoiding their potentially difficult decision to have a pregnancy at high risk of being affected with the option of prenatal diagnosis and termination of pregnancy if the fetus would be diagnosed to carry a mutant gene. So the genetic counseling services may consider informing patients at risk of having children with a strong genetic predisposition to cancers about the presently available option for PGD, without which these couples may remain childless because of their fear to opt for prenatal diagnosis and possible pregnancy termination.

Because such diseases present beyond early childhood and even later may not be expressed in 100% of the cases, the application of PGD for this group of disorders is still highly controversial. However, initial experience in offering PGD for this indication shows that the availability of PGD allows couples forgoing pregnancy, which otherwise would never be attempted. This may be further demonstrated by the first case of PGD performed for genetic predisposition to Alzheimer disease (AD) [74].

3.7.2 Alzheimer Disease

Alzheimer disease (AD) is a rare autosomal-dominant familial predisposition to a presenile form of dementia. Three different genes were found to be involved in this form of AD, including presenilin 1 (PS1) located on chromosome 14 [75], presenilin 2 (PS2) on chromosome 1 [76], and amyloid precursor protein (APP) gene on chromosome 21 [77], which is well known for its role in the formation of amyloid deposits found in the characteristic senile plaques of patients with AD. The early-onset dementias associated with βAPP mutations are nearly completely penetrant, and, therefore, are potential candidates not only for predictive testing but also for PGD. Of ten APP mutations presently described, mutations in exons 16 and 17 were reported in the familial cases with the earliest onset. One of such mutations with as early onset as the mid- or late 30s has been reported to be due to a single G to C nucleotide substitution in exon 17, resulting in a valine-to-leucine amino acid change at codon 717 (V717L) [78]. This mutation was identified in three of five family members (siblings) tested, one of whom presented to PGD, described in this chapter, which resulted in a pregnancy and the birth of a healthy child free from the APP mutation.

The patient that presented for PGD was a 30-year-old woman with no signs of AD, carrying a V717L mutation, resulting from G to C substitution in exon 17 of the APP gene. The predictive testing in the patient was done because of the early onset of AD in her sister carrying this mutation, who developed symptoms of AD at the age of 38 [78]. This sister is still alive, but her cognitive problems progressed to the point that she was placed in an assisted living facility. Her father had died at the age of 42 and had also a history of psychological difficulties and marked memory problems. The V717L mutation was also detected in one of her brothers, who experienced mild short-term memory problems as early as the age of 35, with a moderate decline in memory, new learning, and sequential tracking in the next 2–3 years. The other family members, including one brother and two sisters, were asymptomatic, although predictive testing was done only in sisters, who appeared to be free from mutation in the APP gene (Fig. 3.36).

Two PGD cycles were performed, by testing for the maternal mutation using DNA analysis of PB1 and PB2. A multiplex nested PCR was

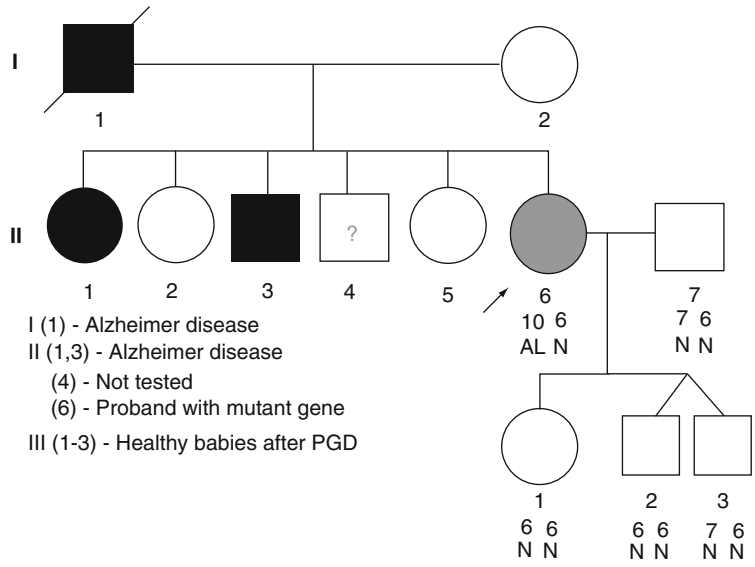

Fig. 3.36 PGD for early-onset Alzheimer disease caused by mutation V717L: *Pedigree*. I Patient's parents, showing that her father was affecetd (I;1). The sister (II;1) and brother (II;3) were affected by early-onset AD, as well as the father (I;1). Two PGD cycles for asymptomatic carriers of the mutant gene (II;6), both resulting in the birth of unaffected children (III). Haplotype analysis shows that these children inherited normal maternal allele linked to the six repeats.

Table 3.22 Primers and reaction conditions for PGD of Alzheimer disease

Gene/ polymorphism	Upper primer	Lower primer	Annealing T_m (°C)
APP V717L	Outside: APP-1	APP-2	55
	5′ GTGTTCTTTGCAGAAGATG 3′	5′ CATGGAAGCACACTGATTC 3′	
	Inside		55
	5′ GTTCAAACAAAGGTGCAATC 3′	5′ TCTTAGCAAAAAGCTAAGCC	
Intron 1 (GA) n(GT)n	Outside		55
	5′ CCTTATTTCAAATTCCCTAC 3′	5′ GATTGGAGGTTAAGTTTCTG 3′	
	Inside		55
	5′ CAGCATCTGTCACTCAAG 3′	5′ AATATTTGTTACATTCCTCTC 3′	

performed, involving mutation testing simultaneously with the linked polymorphic marker, representing the short tandem repeat (STR) in intron 1 [(GA)n… (GT)n] [79].

The first-round amplification cocktail for the multiplex nested PCR system contained outer primers for both the APP gene and the linked marker, while the second-round PCR used inner primers for each gene. We designed the outer primers APP-1 and APP-102 (see primers in Table 3.22) for performing the first-round amplification, and the inner primers APP-101 and APP-103 for the second round of PCR. As shown in Fig. 3.36, second-round PCR produces a 115-base pair (bp) product, undigested by Mnl I restriction enzyme, corresponding to the normal allele, and two restriction fragments of 72 and 43 bp, corresponding to the mutant allele. There was also invariant fragment of 84 bp produced in both normal and mutant alleles, used as a control.

To perform nested PCR for specific amplification of the linked marker (GA)n… (GT)n in intron 1, we designed the outer primers In1–1 and In1–2 for the first round and the inner primers In1–3 and In1–4 for the second round of amplification. The haplotype analysis, based on the polar body genotyping, demonstrated that the affected allele was linked to the ten repeats, and the normal one to the six repeats.

A total of 23 oocytes were available for testing in two cycles, of which 15 were tested by both PB1 and PB2 (13 in one cycle and 2 in the other). The mutation and linked marker analysis in intron 1 revealed six normal oocytes, all in one cycle,

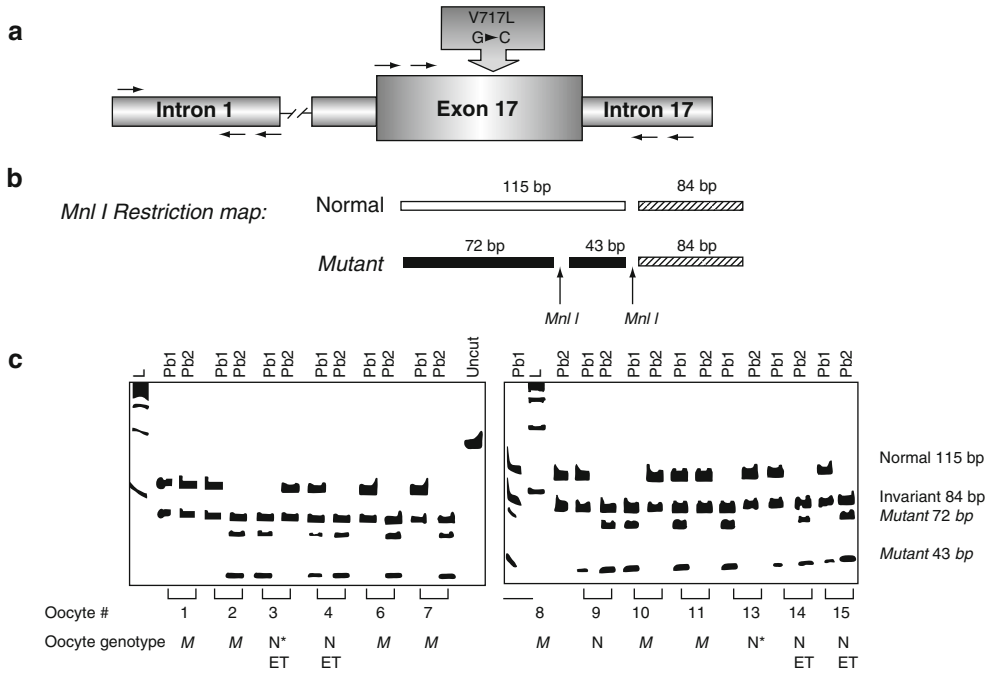

Fig. 3.37 Preimplantation diagnosis for V717L mutation in the amyloid precursor protein gene, causing early-onset Alzheimer disease by polar body analysis. (**a**) Map of human APP gene, showing sites and location of V17L G-C mutation and polymorphic markers. (**b**) Restriction map for normal and abnormal alleles. (**c**) Polyacrylamide gel analysis of Mnl I restriction digestion, showing six unaffected (*N*) oocytes (#3, #4, #9, #13, #14, and #15), and seven mutant (*M*) oocytes (#1, #2, #6, #7, #8, #10, and #11). Four of 6 embryos resulting from unaffected oocytes (#3, #4, #14, and #15) were transferred back to the patient, resulting in an unaffected pregnancy. Three of these oocytes were with heterozygous PB1 and mutant PB2 (noted as *N*), and only one (#3) was with homozygous mutant PB1 and normal PB2, leaving 5% probability for misdiagnosis, noted as *N**. *ET* embryo transfer, *L* ladder (size standard), *Uncut* the undigested PCR product. *Arrows* indicate fully nested primer sets

and nine affected oocytes, including two in one cycle and seven in the other. The results of one of the cycles, resulting in the transfer, are presented in Fig. 3.37. As seen from this figure, oocytes #4, #9, #14, and #15 were clearly normal, because both mutant and normal genes were present in their PB1, with the mutant gene further being extruded with the corresponding PB2, leaving only the normal gene in the resulting oocyte. In addition, oocytes #3 and #13 were also normal, because their corresponding PB1s were homozygous mutant, suggesting, therefore, that the resulting oocytes should have been normal, as further confirmed by the presence of the normal gene in the extruded PB2s, also in agreement with the linked markers analysis. However, because only one linked marker was available for testing, a 5% probability for ADO of the normal gene in the corresponding PB1 could not be excluded in this particular PB1.

The remaining oocytes were predicted to be mutant, based on heterozygous PB1 and normal PB2 in five of them (oocytes #1, #2, #8, #10, and #11), and homozygous normal PB1 and mutant PB2 in two (oocytes #6 and #7). The follow-up study of the embryos resulting from these oocytes confirmed their affected status in all but one (oocyte #7). The latter may be explained by ADO of the mutant allele in the apparently heterozygous PB1, which was left undetected because of the amplification failure of the linked marker in this case.

To exclude any probability of misdiagnosis, the priority in the embryo transfer was given to the four of six normal embryos, resulting from the oocytes with heterozygous PB2 and mutant PB2.

However, only three of these embryos developed into the cleavage stage and could be transferred (#4, #14, and #15), so the additional embryo (#3) was preselected, originating from the oocyte with homozygous mutant PB1 and the normal PB2, as these results were also confirmed by the linked marker analysis. These four embryos were transferred back to the patient, yielding a singleton clinical pregnancy and the birth of an unaffected mutation-free child.

The presented results demonstrate feasibility of PGD for early-onset AD, providing a nontraditional option for patients who may wish to avoid the transmission of the mutant gene predisposing to the early AD in their potential children. This may appear for some patients the only reason of undertaking pregnancy, as the pregnancy may be established free from an inherited predisposition to AD from the very onset. Because the disease never presents at birth or early childhood and even later may not be expressed in 100% of the cases, the application of PGD for AD is still controversial. However, with no current prospect for treatment of AD, which may arise despite presymptomatic diagnosis and follow-up, PGD seems to be the only relief for the at-risk couples, such as in the presented case, and the cases of PGD for cancer predisposition described above.

Therefore, prospective parents with risk for AD and other relevant conditions should be informed about this emerging new technology, so they could make their choice between seizing their reproduction, and forgoing pregnancy free from AD. This seems to be ethically more acceptable than a denial of the information on the availability of PGD. Presented results of PGD for early-onset AD, together with previously described cases of PGD for the late-onset disorders with genetic predisposition and HLA typing (see below), demonstrate the extended practical implications of PGD, providing prospective couples at genetic risk with wider reproductive options for having unaffected children of their own.

So, for the diseases with genetic predisposition and with no current prospect for treatment, arising despite presymptomatic diagnosis and follow-up, PGD may be offered as the only relief for the at-risk couples.

3.7.3 Inherited Cardiac Diseases

As mentioned, PGD application has been expanding beyond traditional indications of prenatal diagnosis and currently includes common disorders with genetic predisposition described in detail in the previous section. This applies also to the diseases with no current prospect of treatment, such as inherited cardiac diseases, which may manifest despite presymptomatic diagnosis and follow-up, when PGD may provide the only relief for the at-risk couples to reproduce.

The first case of PGD for inherited cardiac disease was described for a couple at risk for producing offspring with Holt-Oram syndrome (HOS), which is an autosomal-dominant condition determined by mutation in the *TBX5* gene [80]. HOS is characterized by atrial septal defect and cardiac conduction disease, together with upper extremity malformations, although these clinical manifestations may be extremely variable, not usually being presented at birth, or presented only with a sinus bradycardia, as the only clinical sign which might be also left unnoticed.

As in PGD for other common disorders, the fact that inherited cardiac disorders may not be realized even during a lifetime makes the application of PGD controversial, perhaps explaining the limited application of PGD for inherited cardiac diseases at the present time. The majority of inherited cardiac disorders are dominant, for which no cure may be administered, because their first and only clinical occurrence may be a premature or sudden death. One of such conditions is the familiar hypertrophic cardiomyopathy (HCM), which clinically manifests at different ages, with no symptoms observed for years until provoked by different factors, such as excessive exercise. Different conditions leading to HCM have been reported, two of which, HCM4 and HCM7, will be described in this chapter. HCM4 is caused by mutation in the *MYBPC3* gene located on chromosome 11 (11p11.2), encoding the cardiac isoform of myosin-binding protein C, exclusively in the heart muscle (MIM ID#115197). HCM7 is caused by a mutation in the *TNNI3* gene located on chromosome 19 (19q13.4), leading to an asymmetric ventricular hypertrophy and defect in the

interventricular septum, with high risk of cardiac failure and sudden death (MIM ID#613690).

Hypertrophic cardyomyopathy is also one of the clinical manifestations of fatal infantile cytochrome C oxidase deficiency (MIM ID#604377), for which PGD is strongly indicated, as described below. In contrast to the above conditions, this is an autosomal-recessive cardiac disease, presented within the first month after birth and characterized by a generalized congenital muscular dystrophy, similar to spinal muscular atrophy (SMA), but with significant reduction or lack of cytochrome C oxidase in the muscles [81]. This devastating disease is caused by a defect in the *SCO2* gene located on chromosome 22 (22q13), although the same condition may be also determined by mutations in at least ten other genes involved in Cox activity.

The other condition, for which PGD is strongly indicated, is dilated cardiomyopathy (CMD), which is an autosomal-dominant disease, caused by different mutations in the *LMNA* gene located on chromosome 1 (1q21.2; MIM ID#115200). This cardiac disease is characterized by ventricular dilation and impaired systolic function, resulting in heart failure and arrhythmia, which causes premature or sudden death. While the large phenotypic variability of patients may be determined by different mutations in the *LMNA* gene, differences from one family to another may be observed within the same mutation, with possible involvement of skeletal muscles that leads to muscle weakness, similar to that in Emery-Dreifuss muscular dystrophy (EMD), which is an X-linked disease, also characterized by cardiomyopathy, although presented within the first year after birth (MIM ID# 310300).

The first cumulative experience of the PGD application is presented below for 18 cycles of inherited cardiac disorders that resulted in the birth of 7 healthy children free of the above predisposing gene mutation, demonstrating the utility of PGD for inherited cardiac disease. These 18 PGD cycles were performed for 9 couples at risk for producing an affected progeny with the above conditions, including 9 cycles for CMD, 3 for CMH4, 1 for CMH7, 3 for cardioencephalomyopathy, and 2 for EDMD (Table 3.23).

The couple at risk for producing a progeny with CMD, presented in Fig. 3.38, requested PGD prospectively, with no previous pregnancies attempted, because the male partner was the carrier of the *LMNA* mutation predisposing to CMD. He first experienced cardiac symptoms, such as palpitations, at the age of 22, and then was diagnosed to have a ventricular tachycardia in a 48-h Halter monitoring at the age of 26. To prevent the risk for the development of cardiomyopathy and arrhythmias, which can lead to sudden death, a cardioverter defibrillator had been implanted. As seen from Fig. 3.38, the patient's father passed away from sudden death at age 32, after experiencing heart failure due to cardiomyopathy. His father's side aunt also had been diagnosed with cardiomyopathy at the age 49, and his grandfather and great aunt and her son died at the age of 49–50 from cardiovascular complications.

The patient had dominant mutation in the *LMNA* gene as a result of C to T change in codon 1033 (c.1033C>T), leading to amino acid change from Arg to Trp in position 335 of the proteins lamin A and lamin B, involved in the heart muscles' work. This mutation was detected by *Msp*I digestion, which creates two fragments of 90 and 95 bp in the PCR product of the normal *LMNA* allele, leaving the mutant one uncut. As seen from Table 3.23, four polymorphic markers were also tested simultaneously with the mutation analysis, including *D1S2714*, *D1S82777*, *D1S2624*, and *D1S506*, to avoid misdiagnosis due to preferential amplification or allele drop out (ADO) of the genes tested.

Nine cycles were performed for four patients with CMH4 and CMH7, determined by mutation in *MYBPC3* and *TNNI3* genes respectively. Neither of these couples had previous progeny, but had a family history of premature or sudden death. As seen from Fig. 3.39a, CMH4 in one of the families was due to frameshift mutation *D1076 fs* in the *MYBPC3* gene, while CMH7 in the other family was caused by *A157V* mutation in the *TNNI3* gene (Fig. 3.39b). The *D1076 fs* mutation in the *MYBPC3* gene was detected by *RSA*I and *BsaH*I digestion, the first cutting the mutant gene into two fragments of 72 and 60 bp, and the second cutting the normal one into two fragments of

Table 3.23 Reproductive outcome of PGD for cardiac diseases

Disease	Gene (mutation)	Patient/cycle	Embryos				Number of transfers	Number of embryos transferred	Pregnancies	Births
			Total received/ amplified	Normal/ carrier	Abnormal[a]	Inconclusive[b]				
Cardioencephalomyopathy (AR)	SCO2 (*R262delCA*; *E140K*)	1/3	33/32	16	13	3	3	7	2	1
Cardiomyopathy dilated; CMD1(AD)	LMNA (*K270K*)	1/ 4	51/ 47	20	26	1	4	9	2	3[c]
	LMNA (*R335T*)	1/1	11/11	7	2	2	1	2	1	1
	LMNA (*R189P*)	1/1	2/2	1	1	0	1	1	0	0
	LMNA (*T528K*)	1/3	44/34	9	19	6	2	3	1	0
Cardiomyopathy familial, hypertrophic 4; CMH4 (AD)	MYBPC3 (*D1076fs*)	1/1	7/6	3	3	0	1	2	1	0
	MYBPC3 (*IVS11–10C-A*)	1/2	10/8	1	6	1	0	0	0	0
Cardiomyopathy familial, hypertrophic 7; CMH7 (AD)	TNNI3 (*A157V*)	1/1	11/10	3	7	0	1	1	0	0
Emery–Dreifuss muscular dystrophy 1, X-linked	EMD	1/2	31/31	17	14	0	2	5	2	2
Total		9/18	190/181	77	91	13	15	30	9	7

[a]Including aneuploidies
[b]Shared markers in parents, making it impossible to exclude ADO
[c]Including one pair of twins

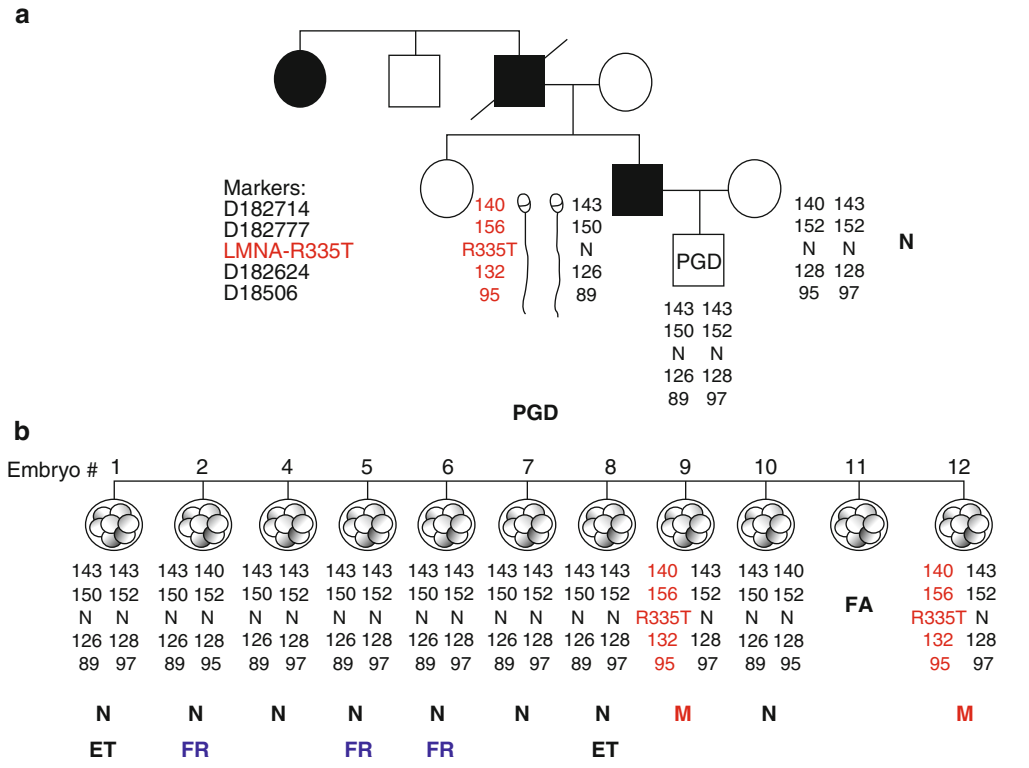

Fig. 3.38 PGD for dilated cardiomyopathy (*CMD*), determined by dominant mutation in *LMNA* gene. (**a**) Family pedigree of a couple with affected husband carrying *R335T* mutation in *LMNA* gene. Paternal linked polymorphic markers are shown on the *left*, and maternal on the *right*, and the order of the markers and mutation in *LMNA* gene are shown on the *upper left*. (**b**) Blastomere results revealed two embryos carrying *R335T* mutation in *LMNA* gene (embryos #9 and #12), while the remaining nine were free of *R335T* mutation. Two of these embryos (#1 and #8) were transferred, resulting in a singleton pregnancy and the birth of a healthy child without the predisposing gene to CMD (as indicated in the family pedigree by PGD). *ET* embryo transfer, *FR* frozen embryos

the same size. In addition, five polymorphic markers were also used to exclude the possibility of ADO, including *D11S1978*, *D11S1344*, *D11S4117*, *D11S1350*, and *D11S4147*. The *A157V* mutation in the *TNNI3* gene was detected by the use of the two enzymes, *Hae*II, cutting the normal, and *Bsp*MI, cutting the mutant gene into two fragments, as presented in Table 3.24.

Two cycles were performed for cardioencephalomyopathy in the couple with a previous affected child with left ventricular hypertrophic cardyomyopathy, whose first symptoms were manifested as early as at 1.5 months, with a severe respiratory attack. Maternal mutation *E140K* of the *SCO2* gene in this case was detected by *Hind* III and *BsrB*I digestion, the first cutting the mutant and the second cutting the normal gene (see Table 3.24). The paternal mutation *R262* del (CA) was tested by sequencing, which resulted in detection of 139 bp fragment in normal and 137 bp fragment in the mutant gene. Five polymorphic markers, *D22S1153*, *D22S1160*, *D22S1161*, *D22S922*, and *SNP Nla*III, were also tested simultaneously, to avoid misdiagnosis due to ADO (Table 3.24).

Finally, two cycles were performed for a couple at risk for producing offspring with EMD, through testing for maternal mutation *IVS2+1G-T*, using *BpM*I digestion, which cuts the normal gene into two fragments of 115 and 6 bp, with the mutant one left uncut. In addition, five polymorphic markers, *DXS8103*, *DX1684*, *DXS8087*, *DXS1073*, and *DYS154*, were tested to exclude the presence of ADO (see Table 3.24).

All PGD cycles were performed using a standard IVF protocol coupled with

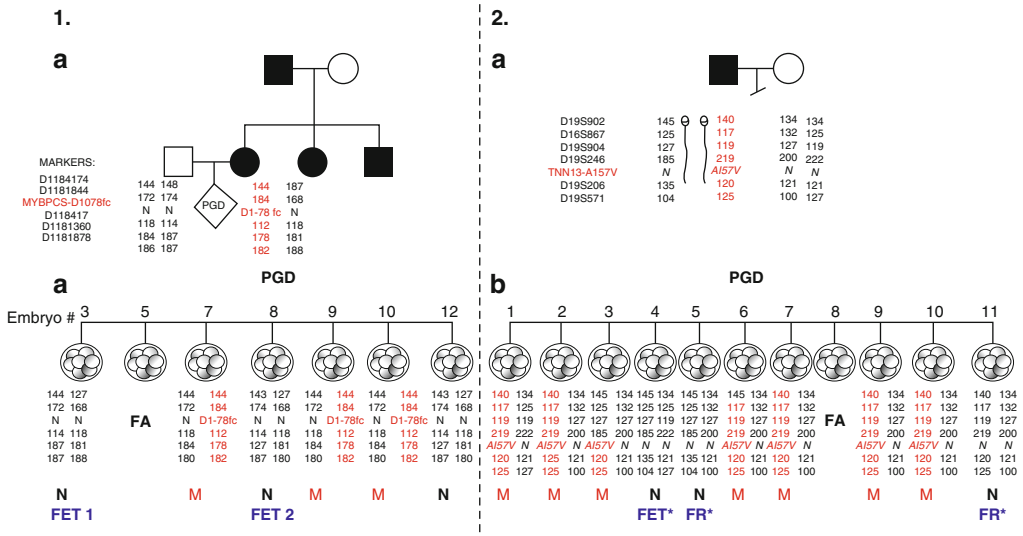

Fig. 3.39 PGD for hypertrophic cardiomyopathy (CMH). (1) PGD for CMH4. (**a**) Family pedigree of a couple with affected mother carrying frameshift mutation *D1076 fs* in *MYBPC3* gene. Paternal linked polymorphic markers are shown on the *left*, and maternal on the *right*, and the order of the markers and frameshift mutation in *MYBPC3*gene are shown on the *upper left*. (**b**) Blastomere results revealed three embryos (embryos #7, #9, and #10) carrying the frameshift mutation *D1078*fr in *MYBPC3* gene, four unaffected, and 1 did not amplify. Two of the normal embryos were transferred (embryos #3 and #8), following the freezing (frozen embryo transfer (*FET*)), resulting in an unaffected pregnancy (as indicated in the family pedigree by PGD). (2) PGD for CMH7. (**a**) Family pedigree of a couple with affected father carrying *A157V* mutation in *TNNI3* gene. Paternal linked polymorphic markers are shown on the *left*, and maternal on the *right*, and the order of the markers and mutation in *A157V* mutation in *TNNI3* gene are shown on the *upper left*. (**b**) Blastomere results revealed three mutation-free embryos, based on the testing of the mutation and six polymorphic markers (embryos #4, #5, and #11), seven mutant ones, and one did not amplify. Unaffected embryos were tested for 24-chromosome aneuploidy at the blastocyst stage, of which one (embryo #4) was euploid and was transferred in the subsequent cycle. *FR* frozen, *FET* frozen embryo transfer, *FA* failed amplification

micromanipulation procedures for PB1 and PB2 sampling, and/or embryo biopsy, described in Chap. 2. The biopsied PBs and blastomeres were tested by the multiplex nested PCR analysis, involving the above-mentioned mutation and linked marker analysis in a multiplex heminested system. Except for the case of EMD for which PB biopsy procedure was performed, all others were tested by embryo biopsy at the cleavage stage. In cases of advanced reproductive age, aneuploidy testing by FISH analysis, described previously, or by microarray technique for 24 chromosomes, using array-CGH (see Chap. 2) was performed, the latter requiring a blastocyst biopsy and embryo freezing, with their transfer in a subsequent cycle.

As seen from Table 3.23, of 18 cycles performed for 9 at-risk couples, the cardiac disease predisposition-free embryos were preselected for transfer in 15 of them, resulting in 9 pregnancies and the birth of 7 disease-free or disease predisposition-free children.

In nine cycles performed for four patients with CMD, 15 mutation-free embryos were preselected for transfer in eight cycles, yielding the birth of three healthy children free from predisposition to sudden death. One of the cases of PGD for CMD, determined by dominant mutation in the *LMNA* gene, is demonstrated in Fig. 3.38, showing that of 10 of 11 embryos tested for mutation and four linked polymorphic markers, 2 were found to carry the *R335T* mutation in the *LMNA* gene, while the remaining 8 were free of the *R335T* mutation. Two of these embryos were transferred, resulting in a singleton pregnancy and the birth of a healthy child without a predisposing gene to CMD.

Table 3.24 Primers and reaction conditions for PGD of cardiac diseases

Disease	Gene/mutation polymorphism	Upper primer	Lower primer	Product size (bp)	Annealing T_m (°C)
cardiomyopathy, dilated, CMD1A	LMNA- R335T	Outside: R335T-1 5′ GTCTCCTACACCGACCCACGT 3′ Inside: R335T-3 5′ GCTCACCAAACCCTCCCAC 3′	Outside: R335T-2 5′ CGTGGATCTCCATGTCCAGG 3′ Inside: R335T-4 5′ GTCCAGAAGCTCCTGGTACTCGT 3′	*Msp1* cuts Normal allele:90+95 bp; Mutant: 185 bp	62–45
	D1S2714 *Heminested*	Outside: 2714-1 5′ TGTGGGGGCTGAGATGAAT 3′ Inside:2714-3 Hex 5′ CCCAGGATTTTAAGACCAGC 3′	2714-2 5′ AGACTCTGGAGTAGCAGGGACTA 3′ 2714-2 5′ AGACTCTGGAGTAGCAGGGACTA 3′	140–150	62–45 55
	D1S2777 Heminested	Outside: 2777-1 5′ CACCACGGAACTCCAGTAT 3′ Inside 2777-1 5′ CACCACGGAACTCCAGTAT 3′	2777-2 5′ CAAGTAATCCTCCTGCCTCAG 3′ 2777-3 Hex 5′ TGTTGGGATTACAGGTGTGAG 3′	140–150	62–45 55
	D1S2624 Heminested	Outside: 2624-1 5′ GAGGCAGAGGCAGACACAGATG 3′ Inside:2624-3 Hex 5′ ATGGGGCTGACACTCTATGAGG 3′	2624-2 5′ GACTCAGCGTCCTGCACAGAGT 3′ 2624-2 5′ GACTCAGCGTCCTGCACAGAGT 3′	120–130	62–45 55
	D1S506 Heminested	Outside: 506-1 5′ CTGGACTCAGCCTGAGAAGAATATG 3′ Inside: 506-3 Fam 5′ AGAAAGGGAGGGATCGTTCAG 3′	506-2 5′ GCTATGCTGGGGCAAGGG 3′ 506-2 5′ GCTATGCTGGGGCAAGGG 3′	80–100	62–45 55

(continued)

Table 3.24 (continued)

Disease	Gene/mutation polymorphism	Upper primer	Lower primer	Product size (bp)	Annealing T_m (°C)
Cardiomyopathy, familial hypertrophic, CMH4	MYBPC3 D1076fs	Outside:D1076fs-1 5′ CTGGTTGGCAGGGTGG 3′ Inside: D1076fs-3 5′ AGGCGTGGTGACCCAACTG 3′	D1076fs-2 5′ TCTTCTTGTCGGCTTTCTGCA 3′ D1076fs-4 5′ TCCGTGTTGCCGACATCCT 3′	*RsaI* cuts *Mutant*: *72+60 bp*; Normal –132 bp; BsaHI cuts normal: 72+60 bp; *Mutant – 132 bp*	62–45 55
	D11S1978 Heminested	Outside: 1978-1 5′ TGCACTCCACAAATACACACAATT 3′ Inside:1978-3 Hex5′ CAGAATGTTAGTATAAGTGTGCATGTG 3′	1978-2 5′ ACTTAGATGTCCATCGACAGATGAA 3′ 1978-2 5′ ACTTAGATGTCCATCGACAGATGAA 3′	160–190	62–45 55
	D11S1344 Heminested	Outside:1344-1 5′ GCCTCCTGTTCTGTTATTTCACTTA 3′ Inside:1344-3 Fam5′ TGACTTTAGCCTTGTGCTGAACTG 3′	1344-2 5′ CAGCGCCTGGCTTGTACATAT 3′ 1344-2 5′ CAGCGCCTGGCTTGTACATAT 3′	130–180	62–45 55
	D11S4117 Heminested	Outside: 4117-1 5′ TTGTCTTCTTTCTAATCTTCCTTCCA 3′ Inside:4117-1 5′ TTGTCTTCTTTCTAATCTTCCTTCCA 3′	4117-2 5′ GTGAGCAAGAGATCACGCCAC 3′ 4117-3 Fam 5′ TGACAGAGCGAGACTCCATCTAAAA 3′	100–120	62–45 55
	D11S1350 Heminested	Outside:1350-1 5′ CAAATTAAATCATTCTGGGGTCTTT 3′ Inside:1350-3 Fam 5′ AAACACCTGCTCTCCAAGAATATC 3′	1350-2 5′ AAACTACCAGCAGTAGAGCACACCT 3′ 1350-2 5′ AAACTACCAGCAGTAGAGCACACCT 3′	180–200	62–45 55
	D11S4147 Heminested	Outside: 4147-1 5′ AGCTTTTCCCTTGTGGGTGTT 3′ Inside:4147-3 Fam 5′ AAGGGGAAGACGGACATAAAAC 3′	4147-2 5′ GCCAGCCTATCTAAACTGTATAATT 3′ 4147-2 5′ GCCAGCCTATCTAAACTGTATAATT 3′	130–150	62–45 55

Cardiomyopathy, familial hypertrophic, CMH7	TNNI 3 A157V	Outside: A157V-1 5′ AAAAAGGAGTGTAGGATGGAGGAGT 3′ Inside: A157V-3 5′ GGTGTGCGGGAAATGGAAG 3′	A157V-2 5′ TTCCCCTCAGCATCCTCTTTC 3′ A157V-4 5′ TTCTCGGTGTCCTCCTTCTTCA 3′	*HaeII cuts* Normal: 150+26; Mutant: 226; *BspMI cuts* Mutant: 190+35+1; Normal: 134+56+35+1	62–45 55
	D19S867	Outside:867-1 5′ CAATGAAAATGCTTTGTAAAACTCTT 3′ Inside: 867-1 5′ CAATGAAAATGCTTTGTAAAACTCTT 3′	867-2 5′ TTGGTTTCCTTCTGTCATGTCATC 3′ 867-3 Fam 5′ TCAGAGGTGACCAGTTCTTTCATAC 3′	110–130	62–45 55
	D19S 904	Outside:904-1 AATCACACCATTGTACTCCAGCC Inside:904-3 HEX 5′ AGGGCAAGACTCCGTTTCAA 3′	904-2 TCGGAGATGTTAAAATGTGAAAAAC 904-2 TCGGAGATGTTAAAATGTGAAAAAC	115–130	62–45 55
	D19S 246	Outside:246-1 5′ GTGAGCCAAGACTACGCCACT Inside: 246-3 Fam 5′ AGAGTGAGATTCCACCTTTCAAAAA 3′	246-2 5′ CCAGAAACACATCATTTACCCACTT 3′ 246-2 5′ CCAGAAACACATCATTTACCCACTT 3′	200–230	62–45 55
	D19S 206	Outside:206-1 5′ TTTTCCTATTTTATCTGGCGGG 3′ Inside:206-3 FAM 5′ AAGTGAAAGCCGAAGTCTTTTCA 3′	206-2 5′ TCATCAAGTCTGTTCCAGCCAA 3′ 206-2 5′ TCATCAAGTCTGTTCCAGCCAA 3′	120–140	62–45 55
	D19S 571	Outside:571-1 5′ TGAACTCCAGCCTGGGTGAG 3′ Inside:571-1	571-2 TTGACAGCATGTATTTGAAATATGG 571-3HEX	100–130	62–45 55

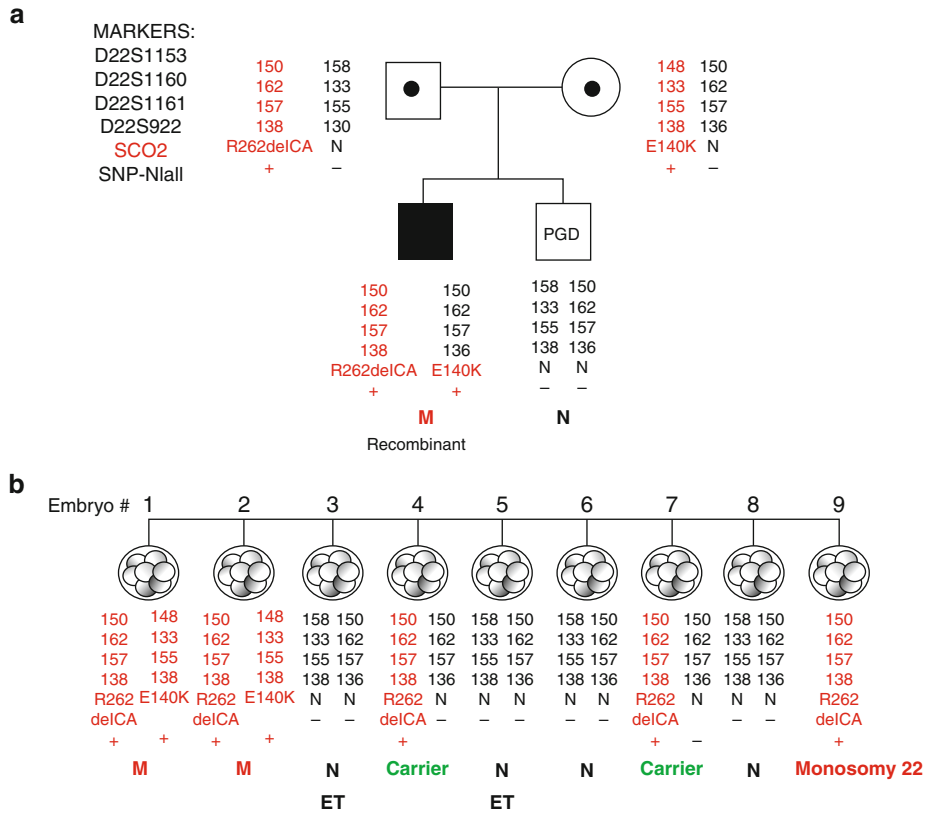

Fig. 3.40 PGD for cardioencephalomyopathy. (**a**) Family pedigree of a couple with a previous affected child, who was double-heterozygous for *E140K* and *R262* del (CA) in the *SCO2* gene. Paternal polymorphic markers are shown on the *left*, and maternal on the *right*, with the order of the markers and mutation shown on the *upper left*. (**b**) Blastomere results revealed two embryos (embryo #1 and #2) homozygous affected, two (embryos #4 and #7) carriers of the paternal mutation, four mutation-free embryos (embryos #3, #5, #6, and #8), and one monosomic for chromosome 22, based on the testing of the mutation and 6 polymorphic markers. Two mutation-free embryos (embryos#3 and #5) were transferred, resulting in a singleton pregnancy and the birth of an unaffected child (as indicated in the family pedigree by PGD). *ET* embryo transfer

Of four cycles performed for three couples at risk for producing offspring with CMH, three embryos were preselected for transfer in two cycles, resulting in a singleton pregnancy, which is presented in Fig. 3.39-1. Of seven embryos tested, three (embryos #7, #9, and #10) were carriers of the frameshift mutation *D1078*fr in the *MYBPC3* gene, three were unaffected, and one did not amplify. Two of the normal embryos were transferred following freezing, resulting in an unaffected pregnancy.

The results of the PGD cycle for the patient at risk for producing the offspring with CMH7 is presented in Fig. 3.39-2. Of 11 tested embryos, 10 amplified, of which 3 (embryos #4, #5, and #11) were unaffected, based on the testing of the mutation and 6 polymorphic markers. Because these embryos were also tested for 24 chromosome aneuploidy by array-CGH analysis at the blastocyst stage, the embryos were frozen and one of them (embryo #3), which was also aneuploidy-free, was transferred in the subsequent cycle.

Of three cycles performed for cardioencephalopathy, seven unaffected embryos were found unaffected and transferred, resulting in two unaffected pregnancies and the birth of a healthy child free from cardioencephalopathy. The results of one of these cycles are shown in Fig. 3.40, showing that of nine embryos tested, two embryos

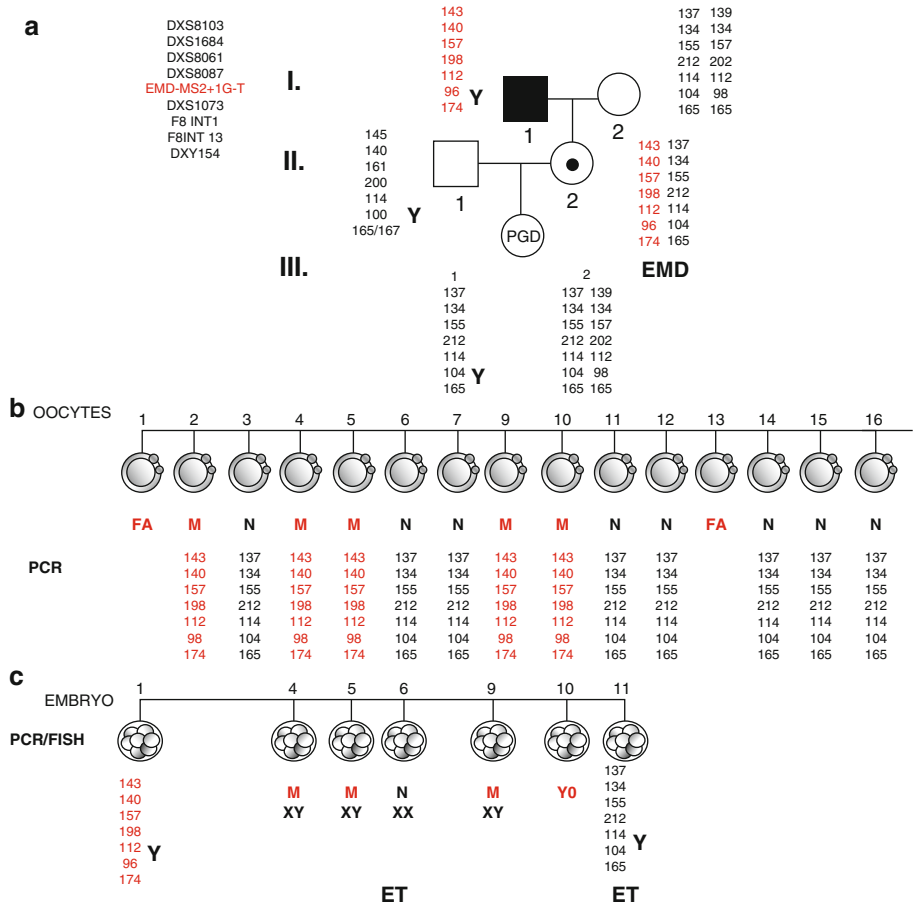

Fig. 3.41 PGD for Emery–Dreiffus muscular dystrophy (*EMD*). (**a**) Family pedigree of a couple with the mother (II-2) carrying an X-linked EMD- IVS2+1G-T mutation, inherited from her father (I-1). Maternal polymorphic markers are shown on the *right*, paternal on the *left*, with the order of the markers and mutation shown on the *upper left*. The haplotypes for the patient's father (I-1) are also shown on the *left*. (**b**) Sequential first and second polar body analysis results in eight mutation-free oocytes, five mutant (#2, #4, #5, #9, and #10) and two did not amplify (#1 and #13). (**c**) Blastomere results of seven resulting embryos for gender determination by FISH and PCR showed that embryos resulting from mutant oocytes #4, #5, and #9 were males, and therefore affected, so only embryos #6 and #11, originating from mutation-free oocytes, regardless of XY genotype, were transferred, resulting in a singleton pregnancy and the birth of an unaffected child (as indicated in the family pedigree by PGD). *ET* embryo transfer

(embryo #1 and #2) were homozygous affected, two (embryos #4 and #7) carriers of the mutant gene, one (embryo #9) monosomic for chromosome 22, and four (embryos #3, #5, #6, and #8) free of the mutation. Two of these embryos (embryos #3 and #5) were transferred, resulting in a singleton pregnancy and the birth of an unaffected child.

Of two PGD cycles performed for EMD, five disease-free embryos were preselected for transfer, yielding an unaffected pregnancy in each cycle and the birth of two EMD-free children. One of these cycles is presented in Fig. 3.41, demonstrating the results of sequential PB1 and PB2 analysis for IVS2+1G-T mutation, followed by mutation and aneuploidy testing at the cleavage stage. Only one of these embryos was free of mutation and aneuploidy (embryo #12) and was transferred, resulting in the birth of an unaffected child.

The presented results show that PGD may be a realistic option for couples at risk for producing offspring with cardiac disease, determined by

inherited predisposition. Inheritance of such susceptibility factors places the individual at risk of serious cardiac disease, clinically manifested from as early as the first year of life such as in cardioencephalopathy, to as late as later in life, with the only clinical realization of premature or sudden death, as in CMD and CMH.

Among the conditions in the family history of the couples at risk that may indicate a possible need of PGD may be a heart attack and sudden death at young age, family members with pacemakers or internal cardiac defibrillators, arrhythmia, and heart surgery. The chances that the offspring of these patients will develop the same heart disease will differ depending on the mode of inheritance, but their penetrance is difficult to predict, because many inherited cardiac conditions are difficult to diagnose and will develop with age and may be induced by certain medications or activities, such as excessive exercise, which may lead to cardiac arrest or sudden death, justifying the parents' requests for PGD.

In fact, in some cases a common, apparently "milder" disease susceptibility gene may contribute to premature death, major disability, or hardship in a family. However, only personal experience may alter a family's perception of severity of the condition, as the basis for their decision to undertake PGD. Many couples already going through IVF for fertility treatment may have questions about the implications of genetic susceptibility factors for offspring, the option to test embryos, and the appropriateness of using PGD in testing for susceptibility to inherited cardiac disease.

Because the symptoms of inherited cardiac disease may be easily overlooked, as seen from the description of the cases above, the family history may be the only reason to test for the presence of predisposing gene mutations and consideration about the need for PGD, which may appear as the life-saving procedure for individuals at risk. So with the future identification of the genes predisposing to inherited cardiac disease, PGD might appear as a useful tool for couples at risk to avoid the risk for producing offspring with inherited cardiac diseases with high probability of premature or sudden death during their life span.

3.8 Blood Group Incompatibility

Although the at-risk pregnancies for blood group incompatibility, including that caused by Kell (KI) genotype or RhD, may be detected by prenatal diagnosis, in order to be treated by an intrauterine transfusion, the potential complication for the fetus cannot be completely excluded even after the procedure. Pregnancy termination in such cases will also be unacceptable, as the antibodies to K1, for example, are developed only in 5% of persons obtaining incompatible blood. On the other hand, some of the at-risk couples have had so unfortunate an experience of hemolytic disease of the newborn (HDN), resulting in neonatal death, that they regard PGD as their only option to plan another pregnancy. This makes PGD attractive for patients at risk for alloimmunization, although such conditions have rarely been an indication for prenatal diagnosis.

We performed the first PGD for maternal fetal incompatibility caused by K1 genotype, which is presented below.

The K1 system is one of the major antigenic systems in human red blood cells, comparable in importance to RhD, as it may cause maternofetal incompatibility leading to severe hemolytic disease of the newborn (HDN) in sensitized mothers. The K1 allele is present in 9% of the populations, in contrast to its highly prevalent allelic variant K2. The gene is located on chromosome 7 (7q33), consisting of 19 exons, with the only C to T base substitution in exon 6 in K1 compared to the K2 antigen, which leads to a threonine to methionine change at amino acid residue 193, preventing *N*-glucosylation [82, 83]. C to T base substitution also creates a BsmI restriction enzyme site, providing a reliable DNA test for diagnosis of KEL genotype.

In case of pregnancy by the K1 fetus in the K2 mother, antibodies to K1 may be developed leading to maternofetal incompatibility causing severe HDN. Although prenatal diagnosis is available for identification of pregnancies at risk for HDN, this may not always prevent the potential complications for the fetus, stillbirth, or neonatal death, making PGD a possible option for preventing both Kell and Rhesus hemolytic diseases.

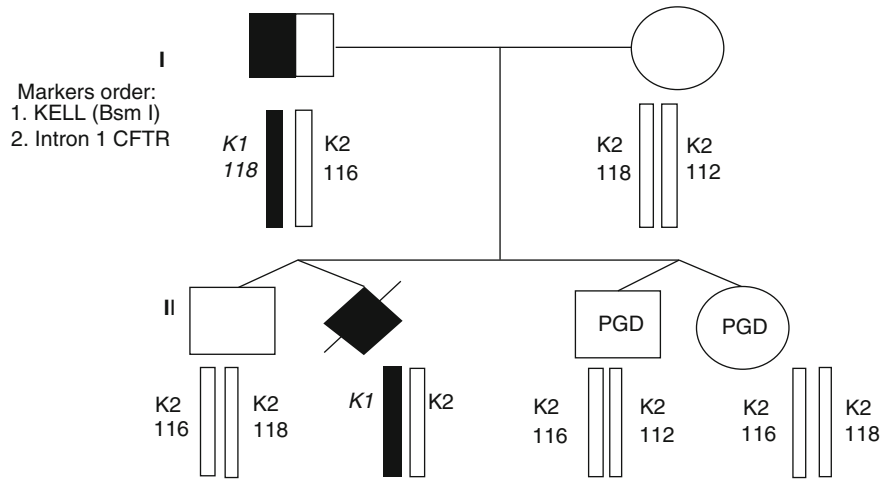

Fig. 3.42 Preimplantation genetic diagnosis for Kell genotype: family pedigree. (*Upper panel*) The father (*upper left*) has *K1*/*K2* genotype, *K1* allele linked to 118 bp repeats, and *K2* allele to 116 bp repeats of intron 1 of *CFTR* polymorphic marker, while the mother (*upper right*) has *K2*/*K2* genotype, one allele linked to 118 bp repeats, and the other to 112 bp repeats of intron 1 of *CFTR* polymorphic marker. (*Lower panel*) Reproductive outcomes of this couple, including previous twin pregnancy resulting in the death of one of the twins near birth due to HDN. Two healthy twins with *K2*/*K2* genotype resulting from PGD were born confirmed also by linked polymorphic markers

Two couples presented for PGD, both with paternal K1/K2 genotype, that is, heterozygous for C to T base substitution in exon 6, creating a BsmI restriction enzyme site. In one couple, a 36-year-old mother had a previous dizygotic twin pregnancy, resulting in the death of one of the twins carrying the K1 allele near birth, due to HDN (Fig. 3.42).

In the second couple, a 37-year-old mother had three previous pregnancies, of which the first resulted in the birth of a healthy boy, carrying the K1 allele, the second in the birth of a normal K2/K2 boy, and the third in a premature delivery of a 32-week female carrying the K1 allele, who died the next day after birth with the clinical features of a severe HDN.

To establish paternal haplotypes, a single-sperm analysis was performed, to be able to undertake the linked marker analysis, in addition to KEL genotyping. Short tandem repeats (STR) associated with the cystic fibrosis (CFTR) gene were used, which are known to be located close to the K1 and K2 alleles, with extremely rare recombination rates [84]. This analysis showed the presence of one informative linked marker (CFTR Intron 1) in the first and three (D7S550, CFTR Intron 6, and CFTR Intron 8) in the second couple. The K1 allele was linked to 118 (CFTR Intron 1) repeat in the first (Fig. 3.43), and to the 158 (D7S550), 7 (CFTR Intron 6), and 124 (CFTR Intron 8) repeats in the second couple. Thus, in PGD cycles for both couples, multiplex nested PCR analysis was performed, by testing the BsmI restriction site simultaneously with the linked polymorphic markers, including the CFTR Intron 1 in the first, and the D7S550, CFTR Intron 6, and CFTR Intron 8 in the second couple. Outside and inside primer sequences and primer melting temperatures for DNA analysis in both couples are shown in Table 3.25 [85–87]. PCR products were identified by restriction digestion using BsmI for Kell gene (Fig. 3.43), and by capillary electrophoresis and scoring by GynotyperTM for STRs.

Overall, five PGD cycles were performed, including one for the first and four for the second couple, using blastomere biopsy. Based on both BsmI restriction digestion and STR analysis, K1 allele-free embryos were preselected for transfer back to patients, while those predicted to contain the K1 allele were exposed to confirmatory analysis using genomic DNA from these embryos, in order to evaluate the PGD accuracy.

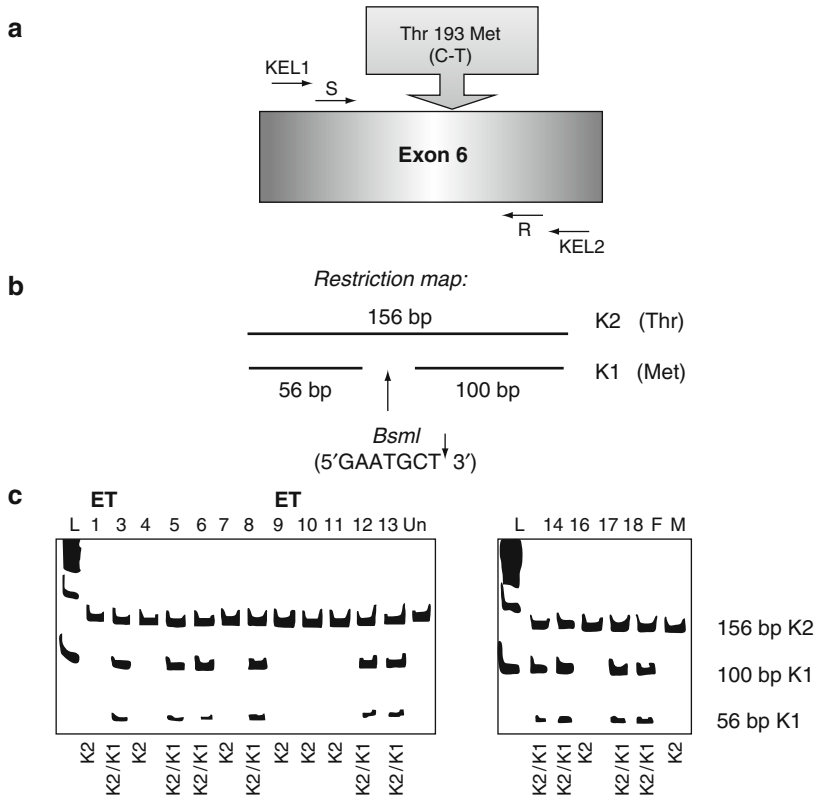

Fig. 3.43 Preimplantation genetic diagnosis for Kell genotype. (**a**) Schematic diagram showing C>T substitution in exon 6 of *KEL* gene on chromosome 7: *black arrows* demonstrate the positions of nested primers. (**b**) Restriction map for *Bsm*I digestion, showing the gain of *Bsm*I site by the *K1* allele (*lower line*). (**c**) Polyacrylamide gel electrophoresis of the *Bsm*I digested PCR products of 16 blastomeres from the first PGD couple, demonstrating *K1* allele-free genotype in embryos #1, #4, #7, #9, #10, #11, and #17, from which embryos #1 and #9 were transferred, resulting in a twin pregnancy and the birth of healthy *K1* allele-free children. The remaining nine embryos have *K1*/*K2* genotype. *L* standard, *F* paternal DNA amplified from sperm, *M* maternal normal amplified DNA, *Un* undigested PCR product, *K1*/*K2* affected blastomere, *K2*/*K2* normal blastomere

In a single PGD cycle for the first couple, 16 embryos at day 3 were tested, of which 9 were excluded from transfer due to the presence of the K1 allele (Fig. 3.43). The remaining 7 embryos did not contain the K1 allele (embryos #1, #4, #7, #9, #10, #11, and #17), also in agreement with the absence of the linked intron 1 CFTR (118 repeats) marker, but showed the presence of the paternal K2 allele, evidenced also by the presence of the intron 1 CFTR (116 repeats) marker, linked to the paternal K2 allele. One of the K1 allele-free embryos (embryo #11) did not develop, 4 were frozen (embryos #4, #7, #10, and #17), while the remaining 2K1 allele-free embryos (embryos #1 and #9) were transferred back to the patient, resulting in a clinical twin pregnancy and the birth of a healthy boy and girl homozygous for K2 genotype (Fig. 3.42).

In the second couple, a total of 20 embryos at day 3 were tested for the K1 allele in four PGD cycles (8 in the first, 5 in the second, 3 in the third, and 4 in the fourth cycle). Nine of these embryos were heterozygous for K1 allele, that is, unsuitable for transfer, while the remaining 11 embryos were predicted to be free from this allele. Seven of these embryos were transferred, including 2 in the first, 1 in the second, 1 in the third, and 3 in the fourth cycle, however, yielding no clinical pregnancy.

The follow-up analysis of the K1 allele-containing embryos, excluded from transfer, was possible in a total of nine cases from both couples. Although the predicted genotypes were

Table 3.25 Primers and reaction conditions for PGD of Kell genotype

Gene/ polymorphism	Upper primer	Lower primer	Annealing T_m (°C)
Kell gene (NESTED PCR)	Outside		62–55
	5′ TCAGCCCCCTCTCTCTCCTT 3′	5′ GTGTCTTCGCCAGTGCATCC 3′	
	Inside [63]		50
	5′ AAGCTTGGAGGCTGGCGCAT 3′	5′ CCTCACCTGGATGACTGGTG 3′	
D7s550 (Heminested PCR)	Outside:	Outside:	62–55
	5′ ACTATCATCCACAATCCACTCC 3′	5′ GCAGTTGGGTTATTTCAAGTCT 3′	
	Inside:	Inside:	56
	5′ ACTATCATCCACAATCCACTCC 3′	5′ HexGATGTTGTGATTAGAGTTGCTGTA 3′	

confirmed overall, six cases of recombination between K alleles and two linked markers (CFTR Intron 6 and CFTR Intron 8) was observed, suggesting a limited value of these two markers on their own. However, no recombination was observed between the gene and one linked marker in both cases (intron 1 CFTR in the first and D7S550 in the second couple), which allowed verifying the absence of the KI allele and detecting both maternal and paternal K2 alleles in the embryo, thus improving considerably the reliability of the diagnosis. For example, the preselection of the K1-free embryos shown in Fig. 3.42 was based not only on the absence of the K1 allele, which may be also explained by ADO, but also on the absence of the linked intron 1 CFTR (118 repeats) marker, and the presence of both the paternally and maternally derived K2 alleles, evidenced by the presence of polymorphic markers linked to the paternal and maternal K2 alleles. In other words, the absence of the K1 allele together with the presence of both paternal and maternal K2 alleles allowed reliably preselecting the KI allele-free embryos for transfer.

The presented cases are the only PGD cycles resulting in the birth of unaffected K1-free children in the worldwide PGD experience. A number of attempts have been undertaken also to perform PGD for Rhesus disease, which initially did not resulted in a clinical pregnancy [88]. The most recent attempt, however, yielded a clinical pregnancy and the birth of a healthy girl confirmed to be blood type Rh-negative [89]. A couple with Rh-negative mother and RhD-positive father had two children, one of whom was affected by HDN, with hyperbilirubinemia and neonatal jaundice, as well as significant hemolitic anemia. Because of RhD alloimmunization, the couple was presented with the dilemma of whether to attempt further pregnancy, as there is a tendency for rhesus disease to worsen with each subsequent rhesus-incompatible pregnancy in sensitized women. Using blastomere biopsy and direct PCR amplification with analysis by capillary electrophoresis of fluorescently labelled amplicons, RhD-negative embryos were preselected for transfer, yielding an unaffected pregnancy and the birth of a healthy child.

Both Kell and Rh disease are quite prevalent in the populations, taking into consideration approximately 15% frequency for RhD and 9% for KEL antigen, presenting the risk for alloimmunization that may lead to HDN in some of the at-risk couples. Therefore, PGD may be a practically useful option for these couples to avoid the establishment of the RhD or K1 pregnancy in the sensitized mothers.

Thus, PGD for Kell genotype and other red blood group systems is feasible, providing a novel approach for sensitized mothers to avoid the risk of having children with HDN [90]. Therefore, PGD may be a useful option for these couples to avoid the establishment of the RhD or K1 pregnancy in sensitized mothers.

3.9 Congenital Malformations

Congenital malformations are highly prevalent (29.3/1,000 live births) and are usually sporadic. As described in Chap. 1, the major reduction of congenital malformations may be expected from population-based preventive measures, such as folic acid fortification of major foodstuffs, which may result in prevention of birth of tens of

thousands of children with congenital malformations in North America. However, this will not have sufficient impact on the prevention of inherited forms, for which PGD might be an important option. In fact, with the progress of the human genome project, an increasing number of inherited forms are being described, which, therefore, may be avoided through PGD. One example of the first application of PGD for congenital diseases was PGD for the sonic hedgehog (SHH) gene mutation, which is presented below.

The SHH gene is a human homolog of the Drosophila gene encoding inductive signals involved in patterning the early embryo, known to be (functionally) highly conserved in many species. The gene was mapped to chromosome 7 (7q36), previously designated as the locus for the gene involved in holoprosencephaly (HPE3) [91].

The available data provide the evidence that SHH mutations may cause the failure of cerebral hemispheres to separate into distinct left and right halves, leading to HPE, which is one of the most common developmental anomalies of the forebrain and midface [92]. Although the majority of HPE are sporadic, familial cases are not rare, with clear autosomal-dominant inheritance.

A great intrafamilial clinical variability of HPE from alobar HPE and cyclopia to cleft lip and palate, microcephaly, ocular hypertelorism, and even normal phenotype suggests the interaction of the SHH gene with other genes expressed during craniofacial development and the possible involvement of environmental factors. This may explain the fact that almost one-third of the carriers of SHH mutations may be clinically unaffected. Therefore, even in familial cases, the detection of SHH mutations in prenatal diagnosis might not justify pregnancy termination, making preimplantation genetic diagnosis (PGD) a more attractive option for couples at risk for producing a progeny with HPE.

In our first case, the couple presented for PGD with two children showing the clinical signs of HPE [93] (Fig. 3.44). One of them, a female with severe HPE and cleft lip and palate died shortly after birth. The chromosomal analysis performed using peripheral blood lymphocytes of both this

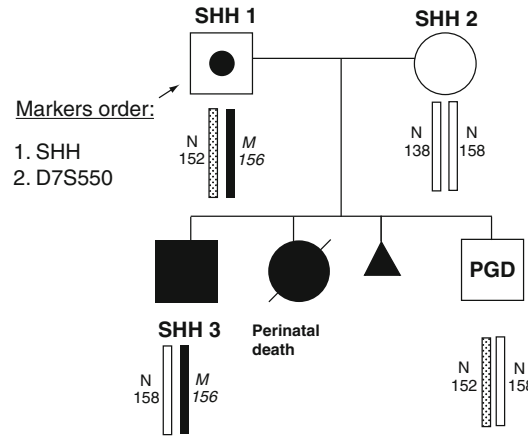

Fig. 3.44 Preimplantation diagnosis for sonic hedgehog (*SHH*) mutation: family pedigree. (*Upper panel*) The father has a gonadal mosaicism for SHH mutation, which is linked to 156 bp dinucleotide C-A repeat allele of D7S550 polymorphic marker, while the mother is normal, with one normal allele linked to 158 bp repeat and the other to 138 bp repeat alleles. (*Lower panel*) Reproductive outcomes of this couple, including three previous pregnancies, one resulting in the birth of an affected child with holoprosencephaly, carrying the mutant gene (*lower left*), one in perinatal death, also carrying the mutant gene (*lower middle* (*circle*)), and one in a spontaneously aborted fetus with Turner syndrome, free from SHH mutation (*lower middle* (*triangle*)). The *lower right* (PGD) shows the outcome of preimplantation diagnosis, resulting in an unaffected clinical pregnancy and the birth of a healthy child, following confirmation of the mutation-free status by amniocentesis

child and the parents was normal, but DNA analysis in the child's autopsy material demonstrated the presence of SHH nonsense mutation due to GAG>TAG sequence change leading to premature termination of the protein at position 256 (Glu256→stop) [92] (Fig. 3.45). SHH protein is an intercellular signalling molecule, which is synthesized as a precursor undergoing autocatalytic internal cleavage into a highly conserved domain (SHH-N) with signaling activity, and a more divergent domain (SHH-C), which in addition to precursor processing acts as an intramolecular cholesterol transferase crucial for proper patterning activity in animal development. Although the effect of the above nonsense mutation on SHH function is unknown, the resulting protein may fail fulfilling the expected signaling function in early morphogenesis [16, 92].

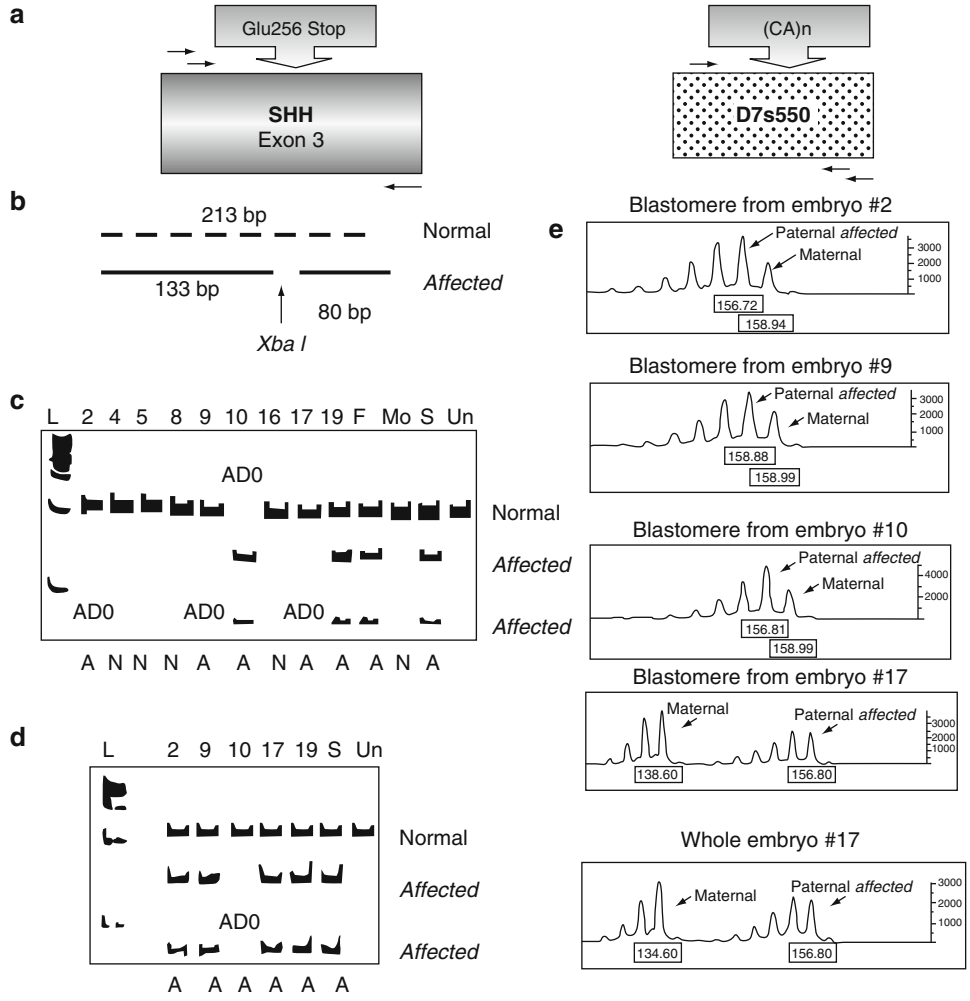

Fig. 3.45 PGD for sonic hedgehog (*SHH*) mutation involving confirmation of the presence of both maternal and paternal normal genes in preselected mutation-free embryo. (**a**) Schematic diagram of the mutation and D7S550 linked marker on chromosome 7. *Black arrows* demonstrate the positions of heminested primers. (**b**) Restriction map for *Xba*I digestion, showing the gain of *Xba*I site by the mutant allele (*lower line*). (**c**) Polyacrylamide gel electrophoresis of the *Xba*I digested PCR products of nine blastomeres from PGD cycle. (**d**) Follow-up DNA analysis of genomic DNA from five embryos predicted to be affected by blastomere testing. (**e**) Capillary electrophoregrams of fluorescently labeled PCR product of tightly linked marker D7S550. Paternally derived 156 bp dinucleotide C-A repeat linked to SHH mutation are shown by arrow (noted as "paternal affected") in blastomeres of embryos #2, #9, #10, and #17 and the genomic DNA of the whole embryo #10, in which ADO of mutant gene was seen in the follow-up study (see *panel* **b**, embryo #10). Maternally derived 158 bp dinucleotide C-A repeats of D7S550 polymorphic marker are shown by *arrow* (noted as "maternal") in blastomeres of embryos #2, #9, and #10, while the other maternally derived 138 bp repeats of D7S550 are shown in blastomeres of embryo #17. *L* 100 bp standard, *ADO* allele dropout, *F* paternal DNA amplified from sperm, *Mo* maternal normal amplified DNA, *S* amplified DNA from affected baby, *Un* undigested PCR product, *A* affected blastomere, *N* normal blastomere

The same mutation was found in their 5-year-old son, who was born after a full-term normal pregnancy weighing 6 lb, with a birth length of 18 1/3 inches. This child has less severe facial dismorphisms, which included microcephaly, Rathke's pouch cyst, single central incisor, and choanal stenosis (the latter was treated surgically after birth with dilatation). There was also

Table 3.26 Primers and reaction conditions for the detection of Glu256Stop mutation in sonic hedgehog gene and linked marker D7S550

Gene/polymorphism	Upper primer	Lower primer	Annealing T_m (°C)
SSH (heminested)	Outside:	Outside:	62–55
	GAGCAGGGCGGCACCAA	GGCCGAGTCGTTGTGC	
	Inside:	Inside:	56
	GGCACCAAGCTGGTGAAG	GGCCGAGTCGTTGTGC	
D7S550 (heminested)	Outside:	Outside:	62–55
	ACTATCATCCACAATCCACTCC	GCAGTTGGGTTATTTCAAGTCT	
	Inside:	Inside:	56
	ACTATCATCCACAATCCACTCC	GATGTTGTGATTAGAGTTGCTGTA	

clinodactily of the fifth fingers and incurved fourth toes bilaterally. The child's growth was slow in the first 2 years, but then he has been maintaining a reasonably good growth and presently has normal social and cognitive development.

The couple had another pregnancy, which has ended in spontaneous abortion due to Turner syndrome (45, X), showing no inheritance of the SHH mutation. The mutation was not found in either parent's genomic DNA, although the paternity testing showed that the father was in fact a biological father of both affected children. This clearly suggested a de novo gonadal mutation in one of the parents, which has been identified by a single-sperm genotyping in the present study (see below).

Two PGD cycles were performed based on single blastomere analysis removed from the 8-cell embryos and tested by multiplex nested PCR analysis, involving specific mutation testing simultaneously with linked marker analysis. Of 15 embryos in the first cycle, 12 were available for blastomere biopsy at the 8-cell stage. Blastomeres from four embryos failed to amplify, leaving eight with available data for mutation analysis. Seven of these eight embryos appeared to contain the mutant allele, while only one embryo was mutation-free and transferred, yielding no clinical pregnancy.

The second PGD cycle was performed in 1 year's time, in which 19 embryos were available, of which 10 were acceptable for blastomere biopsy and DNA analysis. Of these 10 biopsied single blastomeres, only one failed to amplify, the remaining 9 being with available data for the SHH gene and the marker, to identify the mutation-free embryos for transfer (Fig. 3.45).

Prior to PGD cycles, a single-sperm testing was performed, which identified mosaicism for SHH mutation. As the mutation was shown to lead to the gain of an XbaI restriction site [92], the normal allele was identified as undigested PCR product, the mutant allele being represented by two fragments, as a result of XbaI digestion (Fig. 3.45).

To avoid misdiagnosis in mutation analysis due to ADO, which exceeds 10% in single blastomere DNA analysis, a closely linked microsatellite DNA marker D7S550 was tested in the same reaction as the internal control. The list of primes used in the first- and second-round PCR for mutation and linked marker analysis and reaction conditions are presented in Table 3.26. A haplotype analysis showed that the mutant allele was linked to 156 bp dinucleotide CA repeat, while the normal gene was linked to 152 bp repeat allele in 7q36 (Figs. 3.44 and 3.45). Although other linked markers have also been described [91], they were not informative in the present couple.

As seen from Fig. 3.45, four ADOs were observed in the mutation analysis, including ADO of the mutant allele in embryos #2, #9, and #17, and ADO of the normal allele in embryo #10. This was based on the marker analysis, showing that in all four cases the embryos were heterozygous. In other words, three of these four embryos (#2, #9, and #17) could have been misdiagnosed as normal without linked marker analysis. In addition to these three embryos, embryo #19 also contained the mutant gene.

The remaining four embryos were free of the mutant gene, as confirmed by marker analysis,

showing that all these embryos contained two normal alleles, including the paternal one linked to 152 repeat, and either normal maternal allele linked to 138 repeat (embryos #4 and #5) or the other normal maternal allele linked to 158 bp repeat (embryos #8 and #16). Two of these embryos (embryos #4 and #5) were transferred back to the patient, resulting in a singleton pregnancy and the birth of a healthy child following confirmation of the mutation-free status by amniocentesis. The other two mutation-free embryos (embryos #8 and #16) were frozen for further use by the couple.

The presented data demonstrate a diagnostic accuracy of the multiplex PCR-based blastomere analysis, despite the well-known high ADO rate in this type of single cells. As mentioned, ADO is an important limitation of PCR analysis in single cells, due to allele-specific amplification failure, which is particularly high in single-blastomere analysis shown to be at least two times higher than in single fibroblasts and polar bodies. As shown by the follow-up analysis of the preselected mutant embryos, PGD results were confirmed in all resulting embryos available for study, which is in accordance with extensive data, described above, based on testing of hundreds of oocytes and embryos for different single-gene disorders. Although ideally three linked markers are needed to completely exclude the risk for misdiagnosis due to ADO, the use of only one linked marker in the present study was quite reliable, probably because the preselection of mutation-free embryos was based not only on the presence of the paternally derived normal allele, but also on the presence of the second normal allele linked to the maternal-linked marker. In other words, the absence on the mutant gene together with the presence of the two normal alleles, identified by different linked makers, led in this case to the correct identification of embryos as normal or carrying the SHH mutation.

The presented case demonstrates the clinical relevance of PGD for familial HPE [93]. Because of the high prevalence of congenital craniofacial anomalies, this approach may have practical implications for at-risk couples. A great intrafamilial clinical variability of HPE from alobar HPE and cyclopia to cleft lip and palate, microcephaly, ocular hypertelorism, and even normal phenotype suggests the interaction of the SHH gene with other genes expressed during craniofacial development and the possible involvement of environmental factors. This may explain the fact that almost one-third of carriers of SHH mutations may be clinically unaffected. Therefore, even in familial cases, the detection of SHH mutations in prenatal diagnosis might not justify pregnancy termination, making PGD a more attractive option for couples at risk for producing a progeny with HPE, as demonstrated by the first PGD for this mutation mentioned, which resulted in the birth of a healthy mutation-free baby.

Of other congenital malformations, PGD was performed for Currarino triad, Crouson and Holt-Oram syndrome [94, 95], all resulting in the birth of mutation-free children. In these cases the application of prenatal diagnosis may be limited by the factors that modify clinical manifestations and confound prediction of an individuals' phenotype making PGD an attractive choice, as shown in the example of PGD for Crouson syndrome and Currarino triad [95], presented below.

Currarino Triad. Currarino syndrome (CS) is a severe autosomal-dominant disorder caused by homeobox gene HLXB9 mutation, involving partial sacral agenesis, presacral mass, and anorectal malformations, which are one of the commonest digestive anomalies requiring neonatal surgery [16, 17]. This homeobox gene is located on chromosome 7q36, between microsatellite DNA markers D7S559 and D7S2423 [96]. The abnormalities observed in CS are caused by the disturbances in early embryonic development of the human tail bud, leading to the formation or positioning defects of neural tube, notochord, somites, and hindgut. More than two dozens of different HLXB9 intragenic mutations and microdeletions were detected in patients with CS, including frameshift and nonsense mutations in intron 1 and missense mutations in homeodomain, resulting in a nonconservative substitution of a highly conserved amino acid [16, 97–99].

Although a carrier screening and prenatal diagnosis of CS is currently available, the decision

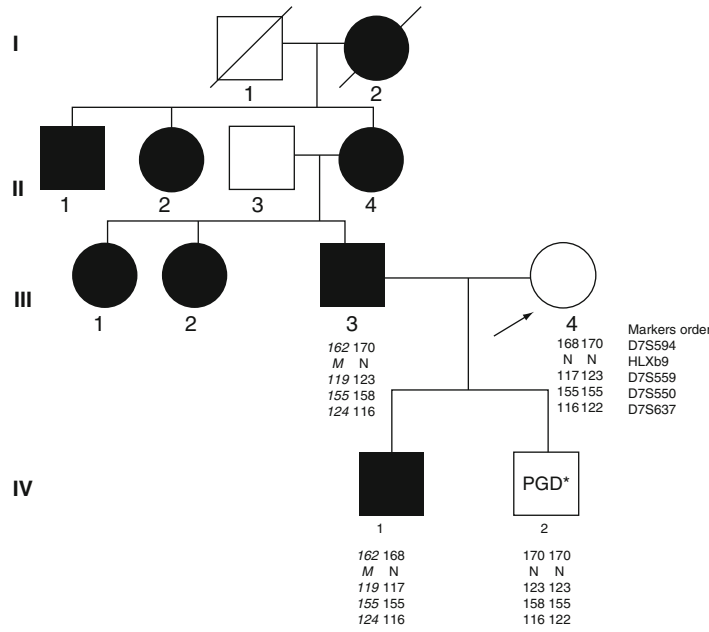

Fig. 3.46 Preimplantation diagnosis for Currarino syndrome: Family pedigree. I & II Patient's parents & grand parents with signs of symptoms of the disease in his mother and grand father. Affected father (III, 3) has two affected sisters; homeobox gene HLXB 9 mutation was inherited from their mother (II, 4), who also had two affected siblings (brother II, 1, and sister II. 2). Reproductive outcome is shown in *lower panel*, with the previous affected child (IV. 1) and the healthy baby boy born after PGD (IV. 2)

about termination of pregnancy will be controversial, as approximately half of the carriers of the mutation are asymptomatic [99]. Therefore, the absence of the genotype–phenotype correlation and an extremely high variability of phenotype in the carriers, from the above severe triad to minor sacral abnormalities undetectable without X-ray or even a completely asymptomatic carrier status, make PGD an important alternative for the at-risk couples wishing to avoid CS in their offspring.

A couple presented for PGD with a previous child diagnosed to have CS. The child was born with imperforate anus, an anterior meningocele, and a typical sickle-shaped hemisacrum revealed by X-ray of the sacrum region (Fig. 3.46; *IV 1*). The father was also born with an anal stricture (Fig. 3.46; *III 3*), requiring anal dilatation, and also had sacral defect detected by X-ray, involving a central anomaly from S2 downward. One of his two sisters (Fig. 3.46; *III 1*) was born with imperforate anus and anterior meningocele and also had rectovaginal fistula, and a vesico-ureteric reflux resulting in the need of renal transplantation; a sacral X-ray showed the same central defect with absence of the distal one-third of the sacrum. The other sister (Fig. 3.46; III 2) was clinically asymptomatic, but sacral X-ray revealed no coccyx and a MRI scan disclosed an anterior meningocele. His mother had an undeveloped coccyx and urinary tract bilateral ureteropelvic junction obstruction (Fig. 3.46; *II 4*). Of her three siblings, only one of two brothers had anal stricture (Fig. 3.46; *II 1*), while the asymptomatic sister (Fig. 3.46; *II 2*) was identified as a carrier of the mutation because of the finding of an imperforate anus in her grandson. As seen from the pedigree, the father inherited the mutation from his grandmother (Fig. 3.46; *I 2*), who was probably the first affected member of the family, known to have constipation but normal sacral X-ray.

DNA analysis in this family demonstrated the presence of homeobox HLXB9 mutation due to frameshift insertion of a cytosine into a stretch of six cytosines at positions 125–130 in exon 1 of the gene, leading to the introduction of premature termination codon [96]. The primer sequences for mutation testing and their positions are presented in Fig. 3.47 and listed in Table 3.27.

A PGD cycle was performed using single blastomeres, removed from the 8-cell embryos and tested by multiplex nested PCR analysis, involving specific mutation testing simultaneously with linked marker analysis. The PCR product was identified by fragment-length analysis using capillary elecrophoresis (Fig. 3.47).

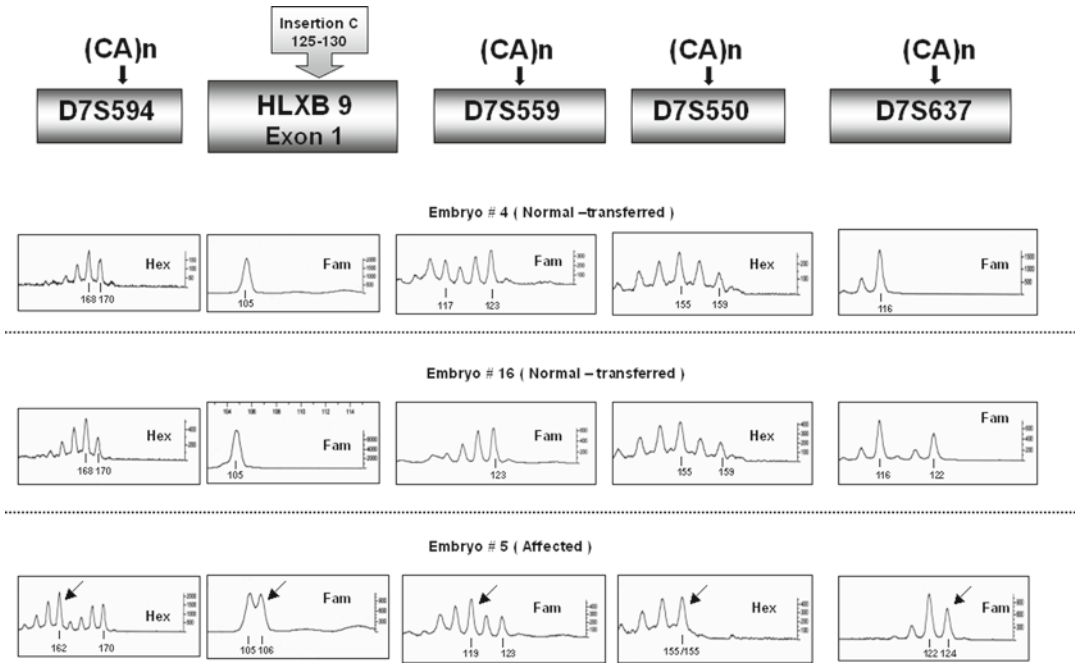

Fig. 3.47 Preimplantation diagnosis for homeobox gene HLXB 9 mutation in Exon 1 causing Currarino syndrome. *Upper panel* shows the location of the mutation in HLXB9 gene and linked markers on chromosome 7. The *other three panels* show capillary elecrophoregrams of fluorescently labeled PCR products of HLXB9 alleles and each of the four linked markers. Paternally derived mutant allele is shown by *arrow* in embryos #5 (*lower panel*), in agreement with paternally derived markers (CA repeats) linked to the mutant gene. The mutant allele is absent in embryos # 4 and #16 (*middle panels*), also in agreement with all four markers. These embryos have been transferred back to the patient resulting in the birth of mutation-free baby. According to marker analysis the baby originates from the transfer of embryo #16

Prior to initiating PGD cycles a single-sperm testing was performed to establish paternal haplotypes. To be able to identify a possible allele drop out (ADO) in the mutation analysis, four closely linked microsatellite dinucleotide DNA markers, D7S559, D7S550, D7S637, and D7S594, were tested in the same reaction with the HLXB9 gene [96]. As seen from Fig. 3.47 and Table 3.27, the mutant allele was linked to 119, 155, 124, and 162 bp, and the normal allele to 123, 159, 116, and 168 bp repeats of D7S559, D7S550, D7S637, and D7S594 markers, respectively. Testing for these markers in the affected child and the mother showed that the parents shared the same size of two of four markers linked to the normal allele, making theses markers of limited value for preselection of mutation-free embryos for transfer.

A total of 17 embryos were available for testing in a single PGD cycle. Single blastomeres were removed from these embryos, of which 3 failed to amplify either HLXB9 alleles or polymorphic markers (embryos #1, #9, and #14), suggesting the lack of a nucleus in these blastomeres, and 2 showed amplification of polymorphic markers only with no signal detected for the HLXB9 gene (embryos #8 and #12) (Table 3.28). Of a total of 12 embryos with results for the mutation and linked marker analysis, 11 were with conclusive results, of which 5 were predicted to contain the mutant allele in agreement with the presence of repeat markers (embryos #3, #5, #6, #11, and #13). One of these embryos contained only paternal alleles (embryo #13), which may be explained by the absence of the maternal chromosome 7, which may be due to mosaicism, known to be very frequent at the cleavage stage.

The remaining six embryos were predicted to be free of mutation, but only in three of them (embryos #2, #4, and #16) ADO of the mutant allele may have been excluded based on the linked marker analysis (Table 3.28; Fig. 3.47). Two of these embryos were transferred, yielding a

Table 3.27 Primers and reaction conditions for PGD of Currarino triad

Gene/polymorphism	Upper primer	Lower primer	Annealing T_m (°C)
HLXb9 Insertion C 125–130 (Heminested PCR)	Outside: 5′ TGGCAAATAACCACCATAACAA 3′	5′ CGAGCGACGTGACCAAGG 3′	62–55
	Inside: 5′ FamCGAGCCGATGGAAAAATCC 3′	5′ CGAGCGACGTGACCAAGG 3′	55
D7s559 (Heminested PCR)	Outside: 5′ GACCACAGTAAGAAATAACCCATTA 3′	5′ AAAAATAATAAAACAGAAGATGCCA 3′	62–55
	Inside: 5′ GACCACAGTAAGAAATAACCCATTA 3′	5′ FamAAGTACTGTCTTGTTAAATTTTTGC 3′	55
D7S637 (Heminested PCR)	Outside: 5′ GCACAGAACTAAATACACCCCAT 3′	5′ CTTCCCCTAAAGTTAACATCTTG 3′	62–55
	Inside: 5′ GCACAGAACTAAATACACCCCAT 3′	5′ FamAACTATAGTACAATATCAAAACCAAGA 3′	55
D7s594 (Heminested PCR)	Outside: 5′ CAGCCTGTGTATGGTTACTTTTTA 3′	5′ GAAGTTCTACAGGCTGAAATCAA 3′	62–55
	Inside: 5′ HexAAAAGTATGCATTTATGTATTTTTT 3′	5′ GAAGTTCTACAGGCTGAAATCAA 3′	55
D7s550 (Heminested PCR)	Outside: 5′ ACTATCATCCACAATCCACTCC 3′	5′ GCAGTTGGGTTATTTCAAGTCT 3′	62–55
	Inside: 5′ ACTATCATCCACAATCCACTCC 3′	5′ HexGATGTTGTGATTAGAGTTGCTGTA 3′	55

Table 3.28 Summary of results of PGD for Currarino triad

Blastomere number	D7S594	HLXb9	D7S559	D7S550	D7S637	Predicted genotype	ET
1	**FA**	FA	**FA**	**FA**	FA	Embryo: INCONCLUSIVE	**NO**
2	170	N	**123**	159/155	**116/122**	**Embryo: NORMAL**	**YES**
3	**162**/170	M/**N**	**119**/123	**155**/155	**124**/122	**Embryo:** AFFECTED	**NO**
4	170/168	**N**	123/117	159/155	116/116	**Embryo: NORMAL**	**YES**[a]
5	**162**/170	M/**N**	**119**/123	**155**/155	**124**/122	**Embryo:** AFFECTED	**NO**
6	**162**/168	**M/N**	**119**/117	**155**/155	ADO/116	**Embryo:** AFFECTED	**NO**
7	170	N	123	159/155	116/122	**Embryo: NORMAL**	**YES**[b]
8	170	FA	123	**155**/155	**124**/122	Embryo: INCONCLUSIVE	**NO**
9	**FA**	FA	**FA**	FA	**FA**	Embryo: INCONCLUSIVE	**NO**
10	170	N	123	159/155	116/122	**Embryo: NORMAL**	**YES**[b]
11	**162**/168	**M/N**	**119**/117	**155**/155	**124**/116	**Embryo: AFFECTED**	**NO**
12	170/168	FA	**119**/117	**155**/155	**124**/116	Embryo: INCONCLUSIVE	**NO**
13	**162**	**M**	**119**	**155**	**124**	**Embryo: AFFECTED**	**NO**
14	**FA**	**FA**	**FA**	**FA**	**FA**	Embryo: INCONCLUSIVE	**NO**
15	170	N	123	155	116/122	**Embryo: NORMAL**	**YES**[b]
16	170/168	FA	123/ADO	159/155	116/122	**Embryo: NORMAL**	**YES**[a]
17	170	FA	FA	159/155	116/122	**Embryo: INCONCLUSIVE**	**NO**
Father	**162**/170	**M**/N	**119**/123	**155**/159	**124**/116		
Mother	168/170	N/N	117/123	155/155	116/122		
Affected child	**162**/168	**M** / N	**119**/117	**155**/155	**124**/116		

ADO allele dropout, *FA* failed amplification, *ET* embryo transfer, *M* mutant allele, *N* normal
Affected haplotype is bolded
[a]Transferred embryos
[b]Chance of misdiagnosis due to potential ADO or recombination

singleton pregnancy and the birth of a mutation-free child, following confirmation of diagnosis by amniocentesis (Fig. 3.48). In the other three embryos predicted to contain the normal allele (embryos #7, #10, and #15), ADO of the mutant gene could not be excluded, because of the parents' sharing the same size of polymorphic markers linked to the normal allele. For example, one of these embryos (embryo #15) was informative only for one linked marker, D7S637 (116/122 bp), which may have suggested the presence of both paternal and maternal normal alleles, assuming that both of these alleles could not be of maternal origin. However, this may have been also due to the uniparental disomy 7 of maternal origin, which was not supported by the other linked markers.

The probability of ADO of the mutant gene in the other two embryos (embryos #7 and #10) could have not been excluded either, despite the fact that these embryos were heterozygous for the two linked markers, D7S637 (116/122) and D7S550 (159/155), because the detected alleles (116 and 159 bp), linked to the paternal normal gene, may have also derived from the mother who shares the same size of linked marker, linked to the normal allele. Finally, one of the embryos (embryo #12) showed the failure of amplification of HLXB9 alleles, but may have been predicted to be mutant, based on the presence three of four polymorphic markers linked to the mutant gene. However, this was not in agreement with the presence of 170 bp repeat of the D7S594 marker, linked to the normal paternal allele, which may probably be due to recombination of the paternal alleles.

Unfortunately, due to the parents sharing two of four markers, linked to the normal allele, only three of six potentially normal embryos could have been preselected for transfer, because of the inability to completely exclude the risk for misdiagnosis due to ADO of the mutant paternal allele.

The presented case is the first PGD for homeobox-containing gene mutations, demonstrating

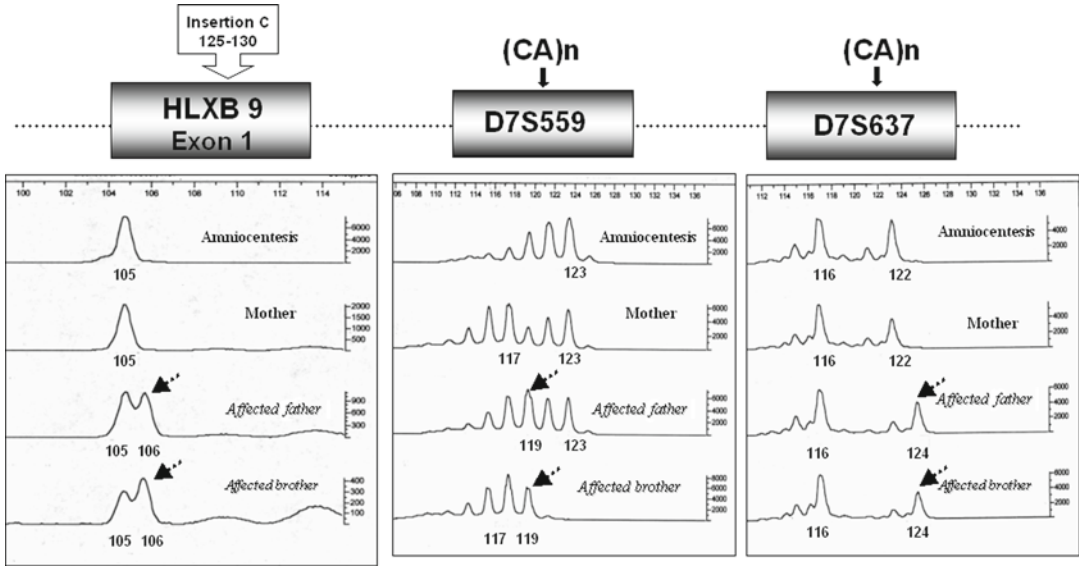

Fig. 3.48 Confirmation of Currarino triad free pregnancy by amniocentesis. *Upper panel* shows capillary electrophoregrams of fluorescently labeled PCR products of HLXB9 gene and two linked markers in amniotic fluid, evidencing the mutation-free status of the fetus, confirming the results of PGD. *Two lower panels* show patterns for affected father and the first affected child, in which paternal mutant allele is shown by arrow, in agreement with paternally derived markers (CA repeats) linked to the mutant gene. The *second panel from the top* shows the normal pattern for the mother

Table 3.29 Results and outcomes of PGD for congenital malformations

Disease	Number of patients	Number of cycles	Cycle by PB	Cycle by PB & BL	Cycle by BL	Number of ET	Number of embryos	Pregnancy	Birth
Craniofacial dysostosis, type I (CFD1)	2	3	0	2	1	3	8	2 (1)[a]	1
Currarino syndrome	1	1	0	0	1	1	2	1	1
Sonic hedgehog (SHH)	1	2	0	0	2	2	3	1	1
Treacher–Collins–Franceschetti syndrome (TCOF)	1	1	1	0	0	1	2	1 (1)[a]	0
Total	5	7	1	2	4	7	15	5 (2)[a]	3

[a]Ongoing pregnancies; number of fetuses is shown in parentheses

the clinical relevance of PGD for this group of genes involved in transcriptional regulation during early embryonic development. Because of the high prevalence of congenital anomalies determined by the mutations causing the formation and positioning defects, this approach may have practical implications for the at-risk couples carrying such mutations, and also mutations causing other groups of familial dysmorphologies, as a principally new option for a large group of couples to avoid the risk of having children with a wide range of the formation and positioning abnormalities at different stages of embryogenesis. The data on the stage-specific expression of homeobox genes observed in CS will be also of relevance for the development of PGD for these transcriptionally relevant anomalies to offer different options for the couples at risk for producing progeny with inherited predisposition to congenital malformations.

Our experience of PGD for congenital malformations (Table 3.29) also includes Crouson syndrome (CFD1), which is described below. It is a dominantly inherited craniosynostosis

caused by mutations in the fibroblast growth factor receptor 2 gene (*FGFR2*) on chromosome 10q [16, 100]. It is quite rare, with birth prevalence of 15–16 per million [101]. PGD was previously applied to testing of G/A base substitution at codon 568 in a couple with one affected child who died aged 18 months during corrective surgery. Of two PGD cycles performed, one resulted in the birth of an unaffected child [94]. We performed three PGD cycles for two couples at risk of producing offspring with Crouson syndrome, of which two resulted in unaffected clinical pregnancies (primers and reaction conditions are presented in Table 3.30). In one of these cases, the mother was a carrier of the C3422Y mutation in exon B of the FGFR2 gene and had also one previous affected child with Crouson syndrome (Fig. 3.49). Two clinical cycles were performed for this patient, using PB1 and PB2 testing, based on restriction digestion with HpyCH4 V, cutting the normal allele into 74 and 20 bp fragments and leaving the mutant allele intact. Two informative linked markers, D10S190 and Msp I polymorphism, were amplified simultaneously with the causative gene for testing PB1 and PB2, allowing the preselection of mutation-free oocytes for transfer. Of nine oocytes tested in the first cycle, five appeared to be mutation-free, but the transfer did not result in clinical pregnancy. In the other cycle, 22 oocytes were available for testing, of which 9 were mutation-free (Fig. 3.50). The transfer of 2 of these embryos resulted in a singleton pregnancy and the birth of an unaffected child, confirmed to be free of the causative gene.

3.10 Dynamic Mutations

Dynamic mutations, which represent trinucleotide repeat expansion, are currently among the most frequent indications for PGD, following X-linked disorders, *CF*, and hemoglobin disorders, although PGD for this group of diseases was introduced only in 1995, initially offered to the couples at risk for producing offspring with myotonic dystrophy (DM) [102, 103]. PGD for XRM1, another important example of the dynamic mutations, was described in Sect. 3.3, demonstrating the complexity of performing PGD for this group of diseases [104, 105].

In addition to DM and FRAXA, the current PGD practices include PGD for Huntington disease (HD), spinal and bulbar muscular atrophy (SBMA), and spino-cerebellar ataxia (SCA) type 2, 3, 6, and 7. The majority of these cases were done for DM, XRM1, and HD. The accuracy of PGD for dynamic mutations has reported to be improved with the application of fluorescent PCR with the expanded long template (ELT) kit, which enabled reducing the ADO rate from 30% to 35% in both conventional and fluorescent PCR to as low as 5% in the testing for DM [104]. The other attractive approach for improving the accuracy of PCR analysis for this group of disease, similar to those mentioned in Chap. 2, involved the application of real-time PCR, which was found to reduce the ADO rate by half, in comparison to conventional or fluorescent PCR. The application of these approaches together with the simultaneous testing of a sufficient number of linked markers may allow avoiding the risk for misdiagnosis completely in PGD for dynamic mutations.

Table 3.31 presents the first 95 PGD cycles of our initial experience for 60 couples at risk for producing offspring with DM, FRAXA, Huntington disease (HD), SCA2, SCA3, SCA6, and SCA7, which is representative of our overall experience. Among these conditions, almost half (43 cycles) were performed for FRAXA, also described in Sect. 3.3, which resulted in 37 embryo transfers yielding 16 unaffected pregnancies and 15 healthy children born. The second largest group was DM, involving 33 PGD cycles performed for 19 at-risk couples, of which 22 resulted in the transfer of the mutation-free embryos, yielding 11 clinical pregnancies and 8 births of healthy children. Overall, 168 (2.3 per transfer on an average) unaffected embryos were selected for transfer in 74 (77.8%) of 95 cycles, resulting in 32 (43%) unaffected pregnancies and the birth of 25 healthy children.

As the expanded alleles are usually not amplified in single-cell PCR, PGD for dynamic mutation is mainly based on the identification of normal alleles based on the testing of a sufficient number of linked markers. To avoid misdiagnosis, at least three closely linked markers should be

Table 3.30 Primer sequences and reaction conditions for PGD of Crouzon syndrome

Gene/polymorphism	Upper primer	Lower primer	Annealing Tm (°C)
FGFR2 Cys 342 Tyr (G—A) (Heminested; mismatched inside primer; Hpy CH4V cuts normal allele)	Outside		62–45
	5′ TAACACCACGGACAAAGAGA 3′	5′ ACCCAGAGAGAAAGAACAGTAT 3′	
	Inside		50
	5′ TAACACCACGGACAAAGAGA 3′	5′ AATAGAATTACCCGCCA*T*G 3′	
D10S190 (Heminested)	Outside		62–45
	5′ AGTGTATGGTTCCTTCCCCTG 3′	5′ CAGGCATGTAACACAGCAAAAG 3′	
	Inside		55
	5′ HexCTGGTTGTTTAAGTGTATGGTTCC 3′	5′ CAGGCATGTAACACAGCAAAAG 3′	
D10S 1483 (Heminested)	Outside		62–45
	5′ CCAATGCTATCCCGGCTAT 3′	5′ AAGCGTGTAACATTTGGTATGC 3′	
	Inside		55
	5′ CCAATGCTATCCCGGCTAT 3′	5′ HexCAAATGCAATAACATTAAACCATT 3′	
D10S 209 (Heminested)	Outside		62–45
	5′ TCATATCCTGCTAACATTACCAACA 3′	5′ CCCACAGGTCACTATGCTTACTT 3′	
	Inside		55
	5′ FamCTGAGCCAGTGGGATGAGAG 3′	5′ CCCACAGGTCACTATGCTTACTT 3′	
D10S 1230 (Nested)	Outside		62–45
	5′ GCTCTGGTTATTTGCTGCCT 3′	5′ GCAGCAGCTTTGTTTTCCA 3′	
	Inside		55
	5′ HexTTTCACCTGACTTTCCTAATAATCC 3′	5′ AGAGCAAGCAACTAAATTATTTTTC 3′	
D10S 1757 (Heminested)	Outside		62–45
	5′ CAAAGACAATTTAGGAAATTCAAAA 3′	5′ CATTCCCTCGTGTATCAGCC 3′	
	Inside		55
	5′ CAAAGACAATTTAGGAAATTCAAAA 3′	5′ Fam CTTTCTGCCTAAAACATATCCCT 3′	
D10S 1679 (Heminested)	5′ GCAGTGCCTGAGGCTTGTG 3′	5′ CCATGAGGGTACTATAGAAAGTTG 3′	62–45
	5′ Hex CCATGAGGGTACTATAGAAAGTTG 3′	5′ CCATGAGGGTACTATAGAAAGTTG 3′	55

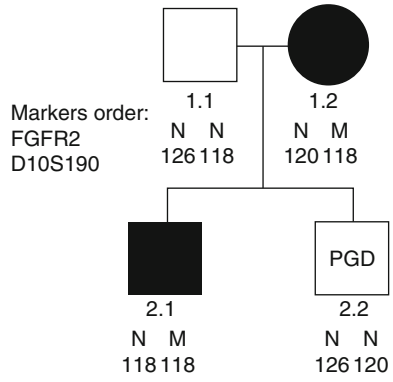

Fig. 3.49 PGD for Crouson syndrome: family pedigree. The mother (1.2) is the carrier of a mutation in FGFR2 gene and had a previous child with Crouson syndrome (2.1). PGD resulted in the birth of a healthy unaffected boy (2.2)

present, confirming the inheritance of the normal allele from the affected parents. In practice, the presence of normal alleles from both parents should be confirmed by the analysis of the maternal and paternal haplotypes, as demonstrated by the example of PGD for DM and Machado-Joseph disease (SCA3), presented in Figs. 3.51 and 3.52.

As seen from Fig. 3.51, the affected mother with DM (*DMPK*) has an expanded allele linked to 159 and 151 repeat markers. Of six embryos tested, using three closely linked markers, three were affected (embryos #2, #9, and #15), including one with trisomy 19 (embryo #2), evidenced by the presence of both mutant and normal maternal alleles, and one set of paternally derived mark-

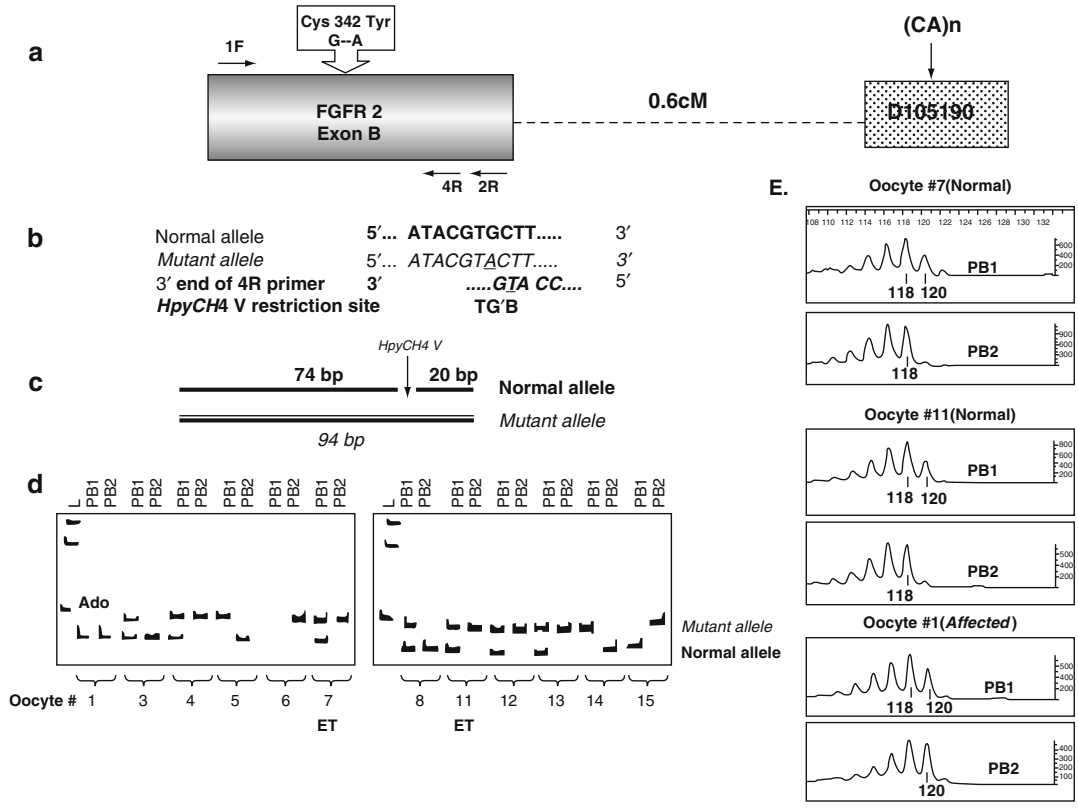

Fig. 3.50 PGD for mutation in FGFR2 gene causing Crouson syndrome. (**a**) Map of human FGFR2 gene, showing sites and location of C342Y mutation and position of linked D10s190 dinucleotide STR. Horizontal arrows show primer sets for heminested PCR. (**b**) Primer design and (**c**) restriction map for normal and abnormal alleles. (**d**) Mutation analysis of 12 oocytes by sequential first (PB1) and second (PB2) polar bodies. Allele dropout (*ADO*) of the mutant allele (*) was detected both by sequential PB1 and PB2 study (identical genotype of both) and linked marker analysis (presence of 118 bp and 120 bp bands). STR profile for PB1 and PB2 from oocytes #1, #7, and #11 confirmed the results of mutation analysis (**e**), suggesting that the latter two are normal and may be transferred. *L* size standard, *bp* base pair, *ET* embryo transfer

Table 3.31 Results and outcomes of PGD for dynamic mutations

Disease	Number of patients	Number of cycles	Number of cycles performed by PBs	Number of cycles performed by PB + Blast	Number of cycles performed by Blast	Number of ET	Number of embryos	Pregnancy	Birth
DM	19	33	6	13	14	22	48	11	8
FRA X	29	43	16	24	3	37	86	16	15
HD	6	10	0	1	9	8	17	3	0 (1)[a]
SCA2	3	4	1	3	0	4	11	1	2
SCA3	1	2	1	0	1	1	2	1	2
SCA6	1	2	1	1	0	1	2	0	0
SCA7	1	1	1	0	0	1	2	1	0
Total	60	95	26	42	27	74	168	33	27

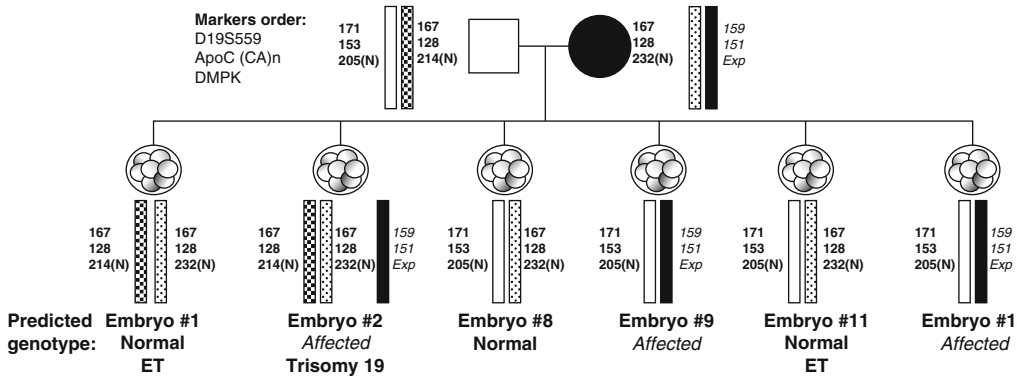

Fig. 3.51 PGD for myotonic dystrophy combined with chromosome 19 aneuploidy testing. (*Top*) Maternal haplotype based on PB1 and PB2 multiplex DNA amplification of the normal allele of DMPK gene (19q13.2–13.3) and linked markers (*right*). Paternal haplotype based on blastomere analysis (*open and darker*). As the expansion of $(CTG)^n$ repeat in DMPK gene is not detectable at single-cell level (*darker bar* in maternal haplotype corresponds to the affected allele), linked polymorphic markers are used for PGD; *clearer bar* represents the normal allele and tightly linked markers. (*Bottom*) Six embryos tested for the presence of the normal number of $(CTG)^n$ repeat in DMPK gene using polymorphic marker pattern. Embryos #1, #8, and #11 were predicted normal based on the presence of the normal maternal chromosome (haplotype) (*clearer bar*) and one paternal chromosome 19. Embryos #2, #9, and #15 were affected evidenced by the presence of the maternal affected haplotype (*darker bar*). Embryo #2 contains two sets of maternal and one set of paternal polymorphic markers, suggesting trisomy 19 of maternal origin. Therefore, amplification of only $(CTG)^n$ repeat in DMPK gene would have revealed the normal status based on the presence of only normal maternal and paternal alleles, which would have led to misdiagnosis. The follow-up FISH analysis confirmed trisomy 19, as predicted, and also incidental trisomy 13 (data not shown). *DMPK* dystrophic myotonia protein kinase gene, *ET* embryo transfer

ers. The fact that this embryo is trisomic for chromosome 19, to which the gene for *DMPK* is assigned (19q13.2–q13.30), was also confirmed by FISH analysis using a specific fluorescent probe for chromosome 19 and 13, showing three signals for this chromosome as well as three signals for chromosome 13, suggesting double trisomy 13 and 19. The remaining three embryos (embryos #1, #8, and #11) were normal, in which all three markers were in agreement with the presence of the maternal normal allele, together with the presence of one of the paternal alleles. So two of these embryos (embryo #1 and #11) were transferred, resulting in an unaffected clinical pregnancy.

The other condition caused by dynamic mutation, Machado-Joseph disease, for which PGD is shown in Fig. 3.52, is a neurodegenerative disorder characterized by cerebellar ataxia

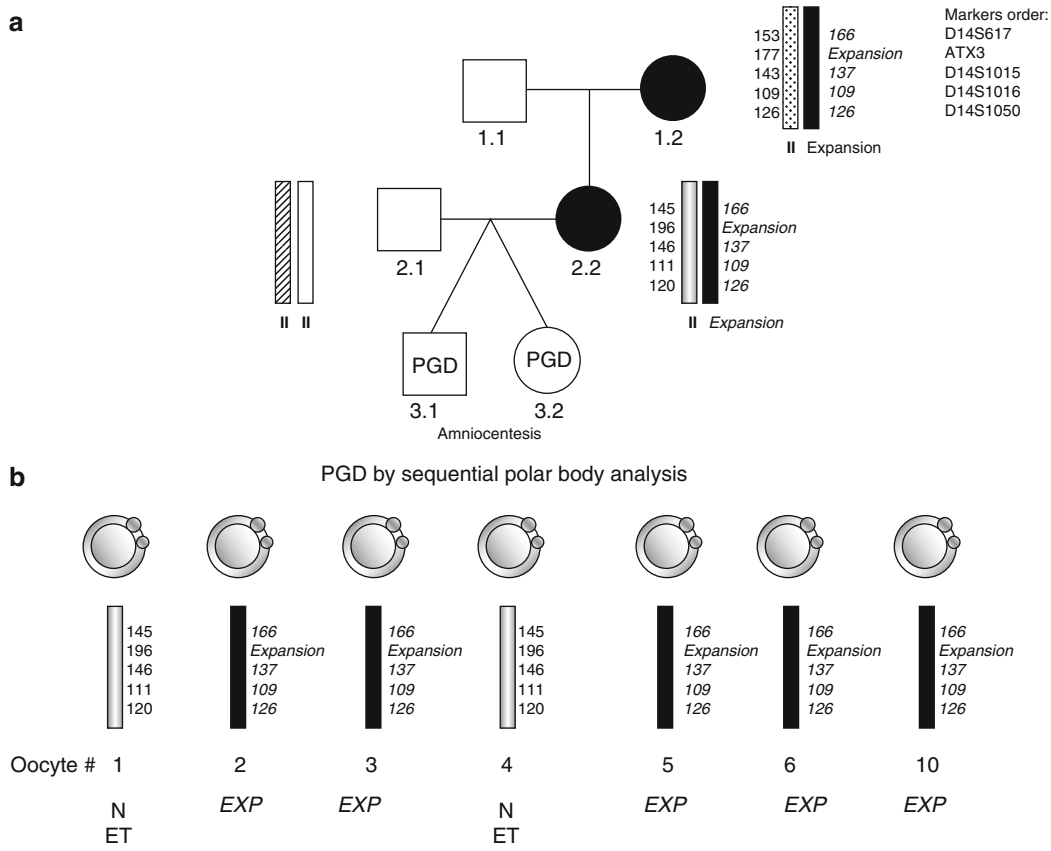

Fig. 3.52 PGD for Machado–Joseph disease (SCA3) resulted in the birth of healthy twins. (**a**) Family pedigree with haplotype analysis, showing that the mother (2.2) inherited the expanded allele (*darker bar*) from her mother (1.2). PGD resulted in the birth of two unaffected twins (3.1 and 3.2), following amniocentesis. (**b**) Seven oocytes were tested for the presence of the expanded allele by sequential PB1 and PB2 analysis, showing that only two oocytes (oocyte #1 and #4) were free of the expansion. Both embryos resulting from these mutation-free oocytes were transferred yielding the birth of unaffected children

3 (SCA3), pyramidal and extapyramidal signs, peripheral nerve palsy, external ophthalmoplegia, facial and lingual fasciculation, and bulging. The mother was a carrier of the expanded allele, inherited from her mother, closely linked to 166, 137, 109, and 126 repeat markers of D14S617, D14S1015, D14S1016, and D14S1050, respectively. PGD was performed by sequential PB1 and PB2 analysis (primer sequences are listed in Table 3.32) in 7 oocytes, 5 of which appeared to be affected and only two without expansion, which were transferred back to patients, yielding an unaffected twin pregnancy and the birth of healthy children, following confirmation of PGD by amniocentesis.

Finally, a nondisclosure PGD has been considered for couples at risk for HD, involving the transfer of the disease-free embryos while the prospective parents do not learn their own status. Parents receive no information about the number of oocytes obtained after hormonal stimulation, the number of embryos formed, and the number of embryos available for transfer. However, there might be no unaffected embryos for transfer, or no affected embryos might be found, suggesting the parent is genetically normal. The other alternative in HD is an exclusion-PGD testing, but embryos with a detected grandparental allele would be excluded from transfer notwithstanding that only half of these embryos would contain the

Table 3.32 Primers and reaction conditions for PGD of Machado-Joseph Disease

Gene/polymorphism	Upper primer	Lower primer	Annealing Tm (°C)
Mutation in ATX3 gene	Outside		62–45
	5′ TACCAGTGACTACTTTGATTCGTGA 3′	5′ GCTCCTGAACTGGTGGCTG 3′	
	Inside		55
	5′ TACCAGTGACTACTTTGATTCGTGA 3′	5′ FamTCTGTCCTGATAGGTCCCCC 3′	
D14S995 (Heminested)	Outside		62–45
	5′ TCTGGAAGGCAGAGAGGTTG 3′	5′ GTAGATAATATGTTTGGCGAGGG 3′	
	Inside		58
	5′ HexCCACTGCACTCCAGCCTG 3′	5′ GTAGATAATATGTTTGGCGAGGG 3′	
D14S1050 (Heminested)	Outside		62–45
	5′ AGACAGGAGTGGGCAGAAAT 3′	5′ ATCTCCCATACTGACTCTCCCT 3′	
	Inside		58
	5′ AGACAGGAGTGGGCAGAAAT 3′	5′ HexGTGACAATTTAGAGGGGGGAC 3′	
D14S1015 (Heminested)	Outside		62–45
	5′ TATTTTGTCCTTTTTTATGGCTG 3′	5′ AACTACAGAAAAAATTGAAAGTAGAAC 3′	
	Inside		58
	5′ TATTTTGTCCTTTTTTATGGCTG 3′	5′ HexCTATTTGATTCAGAAATCCCATTAC 3′	
D14S1016 (Heminested)	Outside		62–45
	5′ TAAAAAGGGAAAGTAGTTAGAATGG 3′	5′ GAAGATGAACCTGAACATGGC 3′	
	Inside 5′		58
	HexGTTATGACATATATTTTTTCCCCAC 3′	5′ GAAGATGAACCTGAACATGGC 3′	
D14S617 (Heminested)	Outside		62–45
	5′ ATTCTCCTCTTATTATAGGACTTTA 3′	5′ GCAACAGAACAAGATCTGTCTC 3′	
	Inside		58
	5′ FamTGTGGAGAAATTAAGTTTTAGGTG 3′	5′ GCAACAGAACAAGATCTGTCTC 3′	

affected allele. However, in our experience, a direct testing of embryos from known disease gene carriers was performed, currently including ten PGD cycles for six couples at risk, resulting in the transfer of 17 mutation-free embryos in eight cycles, yielding three unaffected clinical pregnancies.

3.11 Overall Experience of PGD for Mendelian Disorders

The presented experience is the world's largest series of PGD for Mendelian disorders, presented in Tables 3.1, 3.2, and 3.3, which comprises 2,158 PGD cycles performed in the period of over 20 years. The number of conditions for which PGD is being performed is expanding gradually, with the present number being within 300. As can be seen from Tables 3.2 and 3.3, the outcome of PGD for single-gene disorders was even more favorable than in a routine IVF, resulting in 733 pregnancies (41.2% pregnancy rate), despite transfer of only two embryos per cycle on an average. It is of note that unaffected embryos for transfer were available in 1,778 of 2,158 PGD cycles (82.4%), so only in 380 cycles (17.6%) either no unaffected embryos could have been detected or the embryos predicted to be normal did not develop properly to consider their transfer on day 3 or day 5. Overall, 731 children were born following the procedure, with only three misdiagnoses (0.2%) observed during the whole period of over 20 years, all due to ADO, one in PGD for CFTR, involving one misdiagnosis of compound heterozygote embryos as heterozygous at the very beginning of the introduction of PGD, when the phenomenon of ADO was not yet appreciated, and the other two in PGD for FRM1 and myotonic dystrophy, involving the transfer of the embryos with the predicted over 5% risk of misdiagnosis, which the couple decided to transfer in addition to others with 100% accuracy, to improve their chances to become pregnant. Assuming that the overall experience has involved the genetic testing of more than 20,000 oocytes and embryos, which resulted in preselection and transfer of 3,437 unaffected embryos in 1,778 cycles, the applied technique may be considered to be highly accurate and reliable. The distribution of different conditions for which PGD was performed have been changing gradually, with an increase in the proportion of common diseases with genetic predisposition and non-disease testing, including preimplantation HLA matching, described below in Chap. 4.

Although some of the cases have been done exclusively by PB approach, as it is sufficient to perform PGD with high accuracy, other approaches, such as single-blastomere removal at the cleavage stage, or blastocyst biopsy, should be available to ensure PGD application in complex cases, and to avoid the transfer of affected embryos, determined by paternally derived mutations. In addition, these methods also provide a confirmatory diagnosis following the PB diagnosis. The choice of additional methods will differ depending on circumstances, and a reliable diagnosis may require using two or even three different methods, especially when there is more than one indication for PGD, such as PGD for single-gene disorders together with HLA typing, or preimplantation HLA typing together with aneuploidy testing. The combined testing is required with the expanding range of PGD indications when testing is performed for causative gene, linked markers, HLA typing, and aneuploidy in the same case (see Chap. 4 and 5).

The above overall experience also includes the world's largest PB-based PGD series of *938* PGD cycles for Mendelian disorders performed for 553 patients at risk for producing offspring with inherited disorders. These PB-based PGD cycles were performed for 146 monogenic conditions (Table 3.33), resulting in the preselection and transfer of 1,578 unaffected embryos originating from mutation-free oocytes in 790 of 988 cycles (84%), demonstrating the safety, reliability, and extremely high accuracy of the procedure. While PB sampling was sufficient for making decisions on embryo transfer in 188 of 237 of these cycles, additional blastomere and/or blastocyst biopsy was required in the remaining 602 of 701 cycles involved. A total of 9,036 oocytes were tested, of which 7,841 (86.8%) were with both PB1 and PB2, with the results of sequential PB1 and PB2

testing obtained in 97.6% of these oocytes. This made it possible to preselect for transfer as many as 1,578 embryos originating from these oocytes (1.99 on the average), in 790 (84.2%) cycles, resulting in 329 pregnancies (41.6%) and the birth of 342 healthy children.

Additional embryo biopsy was applied in 701 of these cases, to confirm the diagnosis when necessary, or identify unaffected embryos for transfer in the absence of embryos originating from mutation-free oocytes, such as heterozygous carrier embryos, originating from mutant oocytes.

Of a total of 9,036 oocytes tested, amplification of both PB1 and PB2 was successful in 7,650 PB1/PB2 sets, suggesting an extremely high (97.6%) amplification efficiency. This allowed transferring embryos in 84.2% of initiated cycles, with the priority in preselection of mutation-free oocytes given to the oocytes with heterozygous PB1, that is, with both normal and mutant genes amplified, ideal for further testing, despite the fact that their potential transfer depended entirely on the identification of the mutant gene in the sequential analysis of PB2. In the absence of DNA contamination, this indicates the absence of ADO of either normal or mutant allele, and allows avoiding the potential misdiagnosis due to ADO. Although most of the transferred embryos were preselected using this particular strategy, the embryos originating from homozygous normal oocytes, inferred from homozygous mutant status of PB1 and hemizygous normal status of PB2, may be also transferred, provided that ADO could be excluded using a sufficient number of linked polymorphic markers. In our experience of PB-based PGD, we observed only two misdiagnoses in 790PB-based PGD transfer cycles, suggesting an extremely high accuracy rate of 99,7%.

As seen from Tables 3.3 and 3.33, autosomal-recessive disorders were the most frequent indication for PGD by PB analysis, performed for 81 recessive conditions in 504 (53.7%) of an

Table 3.33 List of Mendelian disorders for which PGD was performed by PB-based approach

Genetic disorder	Gene	Inheritance
ACYL-CoA dehydrogenase, medium-chain, deficiency	ACADM	AR
ACYL-CoA dehydrogenase, long-chain, deficiency	ACADL	AR
ACYL-CoA dehydrogenase, very long-chain (ACADVL)	ACADVL	AR
Argininosuccinic aciduria	ASL	AR
Ceroid lipofuscinosis, neuronal 2, late infantile (CLN2)	CLN2	AR
Citrullinemia	ASS	AR
Congenital adrenal hyperplasia (CAH)	CYP21A2	AR
Deafness, neurosensory, autosomal-recessive 1 (DFNB1)	GJB2	AR
Cystic fibrosis (CF)	CFTR	AR
Cystinosis, nephropathic (CTNS)	CTNS	AR
Ectodermal dysplasia, hypohidrotic	EDA	AR
Epidermolysis bullosa dystrophica	COL7A1	AR
Fanconi anemia, complementation group A	FANCA	AR
Fanconi anemia, complementation group F	FANCF	AR
Fanconi anemia, complementation group J	FANCJ	AR
Gaucher disease, type I	GBA	AR
Glutathione synthetase deficiency	GSS	AR
Glycogen storage disease II	GAA	AR
Hemoglobin-alpha locus 1 (HBA1)	HBA1	AR
Hemoglobin-beta locus (HBB)	HBB	AR
Hurler syndrome	IDUA	AR
Hypophosphatasia, infantile	ALPL	AR
Isovaleric acidemia (IVA)	IVD	AR
Krabbe disease	GALC	AR

Table 3.33 (continued)

Genetic disorder	Gene	Inheritance
Leukoencephalopathy with vanishing white matter (VWM)	EIF2B2	AR
Homocystinuria due to deficiency of N(5, 10)-methylenetetrahydrofolate reductase activity	MTHFR	AR
Nephrosis 1, congenital, Finnish type (NPHS1)	NPHS1	AR
Neuropathy, hereditary sensory and autonomic, type III; HSAN3	IKBKAP	AR
Oculocutaneous albinism, type I; OCA1	TYR	AR
Osteopetrosis, autosomal-recessive	TCIRG1	AR
Polycystic kidney disease, autosomal-recessive; ARPKD	PKHD1	AR
Propionic acidemia	PCCA	AR
Sandhoff disease	HEXB	AR
Sickle cell anemia	HBB	AR
Smith-Lemli-Opitz syndrome (SLOS)	DHCR7	AR
Spinal muscular atrophy, type I (SMA1)	SMN1	AR
Tay-Sachs disease (TSD)	HEXA	AR
Thrombotic thrombocytopenic purpura, congenital (TTP)	ADAMTS13	AR
Tyrosinemia, type I	FAH	AR
Zellweger syndrome (ZS)	PEX1	AR
Ataxia telangiectasia (AT)	ATM	AR
Adenomatous polyposis of the colon (APC)	APC	AD
Angioedema, hereditary (HAE)	AD	AD
Brain tumor, posterior fossa of infancy, familial	SMARCB1	AD
Breast cancer, familial	BRCA1	AD
Breast-ovarian cancer, familial	BRCA2	AD
Cardiomyopathy, dilated, 1A (CMD1A)	LMNA	AD
Charcot-Marie-Tooth disease, axonal, type 2E	NEFL	AD
Charcot-Marie-Tooth disease, demyelinating, type 1A	PMP22	AD
Charcot-Marie-Tooth disease, demyelinating, type 1B	MPZ	AD
Craniofacial dysostosis, type I (CFD1)	FGFR2	AD
Darier-White disease (DAR)	ATP2A2	AD
Diamond-Blackfan anemia (DBA)	RPS19	AD
Dystrophia myotonica 1	DMPK	AD
Epiphyseal dysplasia, multiple, 1 (EDM1)	COMP	AD
Huntington disease (HD)	HTT	AD
Li-Fraumeni syndrome 1 (LFS1)	TP53	AD
Loeys-Dietz syndrome (LDS)	TGFBR2	AD
Machado-Joseph disease (MJD)	ATX3	AD
Marfan syndrome (MFS)	FBN1	AD
Migraine, familial hemiplegic, 1 (FHM1)	CACNA1A	AD
Multiple endocrine neoplasia, type I (MEN1)	MEN1	AD
Neurofibromatosis, type I (NF1)	NF1	AD
Neurofibromatosis, type II (NF2)	NF2	AD
Oculocutaneous albinism, type II (OCA2)	OCA2	AD
Omenn syndrome	RAG1	AD
Optic atrophy 1 (OPA1)	OPA1	AD
Osteogenesis imperfecta congenita (OIC)	COL1A1	AD
Polycystic kidney disease 1 (PKD1)	PKD1	AD
Popliteal pterygium syndrome (PPS)	IRF6	AD
Retinoblastoma (RB1)	RB1	AD

(continued)

Table 3.33 (continued)

Genetic disorder	Gene	Inheritance
Spinocerebellar ataxia 1 (SCA1)	ATXN1	AD
Spinocerebellar ataxia 2 (SCA2)	ATX2	AD
Spinocerebellar ataxia 6 (SCA6)	CACNA1A	AD
Spinocerebellar ataxia 7 (SCA7)	SCA7	AD
Stickler syndrome, type I (STL1)	COL2A1	AD
Symphalangism, proximal (SYM1)	NOG	AD
Torsion dystonia 1, autosomal-dominant (DYT1)	DYT1	AD
Treacher Collins-Franceschetti syndrome (TCOF)	TCOF	AD
Tuberous sclerosis type 1	TSC1	AD
Tuberous sclerosis type 2	TSC2	AD
Von Hippel-Lindau syndrome (VHL)	VHL	AD
Adrenoleukodystrophy (ALD)	ABCD1	XL
Agammaglobulinemia, X-linked (XLA)	BTK	XL
Albinism, ocular, type I (OA1)	OA1	XL
Alport syndrome, X-linked (ATS)	AMMECR1	XL
Charcot-Marie-Tooth disease, X-linked, 1 (CMTX1)	GJB1	XL
Choroideremia (CHM)	CHM	XL
Emery-Dreifuss muscular dystrophy, X-linked (EDMD)	EMD	XL
Fabry disease	GLA	XL
Fragile site mental retardation 1	FMR1	XL
Granulomatous disease, chronic, X-linked (CGD)	CYBB	XL
Hemophilia A	F8	XL
Hemophilia B	F9	XL
Hydrocephalus, X-linked (L1CAM)	L1CAM	XL
Immunodeficiency with hyper-IgM, type 1 (HIGM1)	CD40LG	XL
Immunodysregulation, polyendocrinopathy, and enteropathy, X-linked (IPEX)	FOXP3	XL
Incontinentia pigmenti (IP)	IKBKG	XL
Mucopolysaccharidosis type II (Hunter)	IDS	XL
Muscular dystrophy, Duchenne type (DMD)	DMD	XL
Myotubular myopathy 1 (MTM1)	MTM1	XL
Norrie disease (NDP)	NDP	XL
Ornithine transcarbamylase deficiency	OTC	XL
Pelizaeus-Merzbacher-like disease (PMLD)	PLP1	XL
Rett syndrome (RTT)	MECP2	XL
Wiskott-Aldrich syndrome (WAS)	WAS	XL

overall 938 PB cycles. PB analysis is the method of choice for autosomal-recessive disorders, because for avoiding the transfer of embryos with autosomal-recessive conditions, it is sufficient to preselect the embryos originating from the mutation-free oocytes. The largest group of autosomal-recessive disorders performed by PB analysis were hemoglobinopathies, applied extensively in Cyprus [9, 10].

As a result of PB testing performed in 504 PGD cycles for recessive conditions, a total of 882 (2.1 embryos on the average) unaffected embryos were preselected for transfer in 428 (84.9%) of these cycles, yielding 168 (39.3%) clinical pregnancies and 187 healthy children born, with no misdiagnosis (Table 3.3). As can be seen from Fig. 3.53, presenting PB-based PGD for congenital disorder of glycosylation (mutation in PMM2 gene), the sequential PB1 and PB2 analysis provides a robust procedure for selection of embryos originating from mutation-free oocytes (oocytes #2, #5, #9, #13, and #15). The

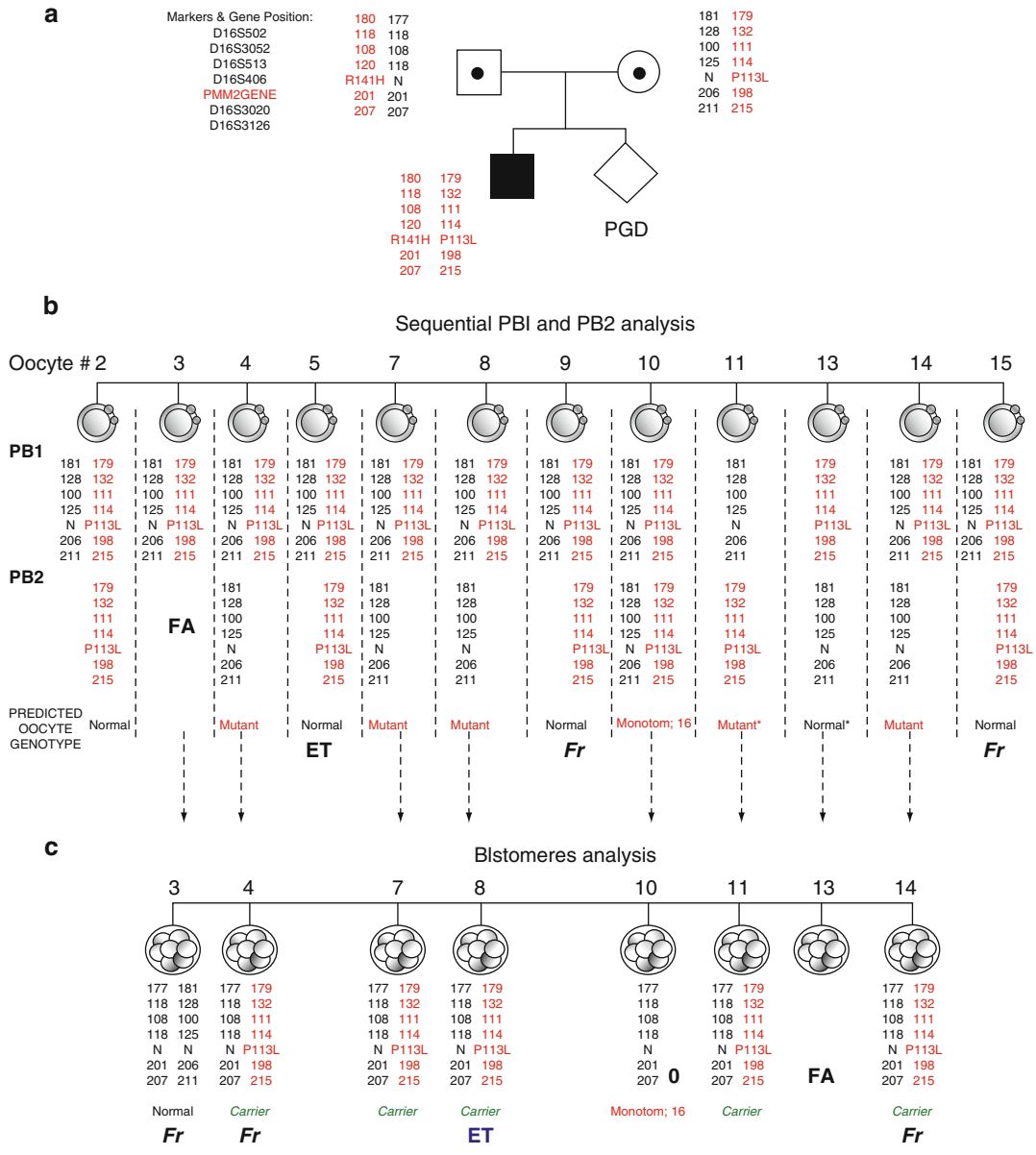

Fig. 3.53 PGD by sequential PB1 and PB2 and blastomere analysis for congenital disorder of glycosylation (PMM2 gene). (**a**) Pedigree and table with PGD results of testing for PMM2 gene and six linked markers. As can be seen from the pedigree, the mother and father are carriers of different mutations (P113L and R141H, respectively), their affected child being double-heterozygous for PMM2 mutation. (**b**) Sequential PB1 and PB2 analysis of 12 oocytes available for testing, resulted in prediction of oocyte status in 11 of them (PB2 of oocyte #3 failed to amplify). Of 12 PB1s tested, oocyte #11 appeared to be homozygous normal, and oocyte #13 homozygous mutant, confirmed by PB2 testing, and further testing by blastomere analysis. The remaining oocytes were heterozygous, so based on the sequential testing of PB2 mutant, four of them (oocytes #2, #5, #9, and #15) were predicted free of PMM2 mutation, requiring no further blastomere testing. (**c**) A follow-up blastomere testing of embryos originating from mutant oocytes or the oocyte with failed amplification of PB2, showing the preselection of additional six unaffected embryos, of which carrier embryo #8 and embryo originating from oocyte 5, with heterozygous PB1 and mutant PB2, were transferred, resulting in unaffected ongoing pregnancy

case also shows the utility of additional blastomere testing to identify the unaffected embryos originating from the mutant oocytes, such as embryos #4, #7, #8, #11, and #14. One of these embryos (carrier embryo #8) was transferred, together with embryo #5, originating from oocytes with heterozygous PB1 and mutant PB2, resulting in an unaffected ongoing singleton pregnancy.

X-linked conditions were the second largest group of indications for performing PB analysis, involving PGD for 24 different conditions (Table 3.3 and 3.33). A total of 270 cycles were performed, which resulted in the transfer of 411 unaffected embryos (1.9 embryos on an average) in 220 (81.5%) cycles, yielding 94 (42.7%) clinical pregnancies and the birth of 91 children (Table 3.3), with one misdiagnosis for FMR1 mentioned. This involved indirect testing using linkage analysis, as no test is available for direct analysis of the expanded alleles. So the mutation-free oocytes in this case were inferred from the presence of the linked markers for the normal allele, and misdiagnosis was due to the fact that a number of markers amplified were not of sufficiently high accuracy for diagnosis. However, despite the predicted 10% error rate in one of the embryos, the couple selected transferring this particular embryo, in addition to two embryos diagnosed with higher accuracy, which in fact turned out to be heterozygous because of an undetected ADO of both alleles linked to the normal gene (see Sect. 3.3).

PB analysis is obviously the method of choice in PGD for X-linked disorders, because preselection of oocytes free of X-linked disorders allows avoiding any micromanipulation of the embryo. As seen from Fig. 3.54, demonstrating PB-based PGD for X-linked adrenoleukodystrophy, embryo #3, originating from the oocyte with mutant PB1 and normal PB2, confirmed with simultaneous testing of six linked markers, required no further testing and was transferred irrespective of gender or the paternal genetic contribution, resulting in the birth of an unaffected child.

In contrast to autosomal-recessive and X-linked disorders, the PB-based approach is applicable to only maternally derived dominant disorders. As listed in Tables 3.3 and 3.33, we performed PB-based PGD for 41 different dominant conditions of maternal origin, for which PB analysis was concentrated in detection and transfer of embryos deriving from oocytes with heterozygous PB1 and hemizygous mutant PB2. The example is demonstrated in Fig. 3.55, presenting PB-based PGD for myotonic dystrophy, in which the embryo originating from oocyte #23 was predicted to be free from the expanded allele, based on the presence of both normal and expanded alleles in PB1 and an expanded allele in PB2. ADO of the normal allele could not be totally excluded in cases of oocytes with homozygous mutant PB1 in oocytes #3, #5, and #6, so to transfer the embryos originating from these oocytes, a follow-up embryo biopsy was required, involving tracing of the maternal and paternal normal haplotypes.

The PB approach was applied in a total of 164 PGD cycles for dominant disorders, which resulted in the transfer of 285 unaffected embryos (2.0 embryos on the average) in 142 (86.6%) of cases, yielding 65 (45.8%) clinical pregnancies and the birth of 64 children (Table 3.3), with one misdiagnosis. The latter represented PGD for myotonic dystrophy, which is always a challenge, because the diagnosis is based on indirect testing, requiring a sufficient number of linked markers, while only one such marker was available for testing.

The presented data show that the PB-based approach is an integral part of PGD, which makes it possible to perform preselection of mutation-free oocytes and complete PGD prior to fertilization. This provides the possibility for pre-embryonic diagnosis for couples objecting to embryo biopsy because of their social or religious attitudes, as described in Chap. 2. Although the approach is currently limited to PGD for autosomal-recessive conditions, X-linked disorders, and dominant mutations of maternal origin, the future progress in testing of paternal mutations prior to fertilization may allow performing pre-embryonic diagnosis for any disease. On the other hand, the PB approach is a component of PGD for couples with two or more PGD indications and should be available for testing of

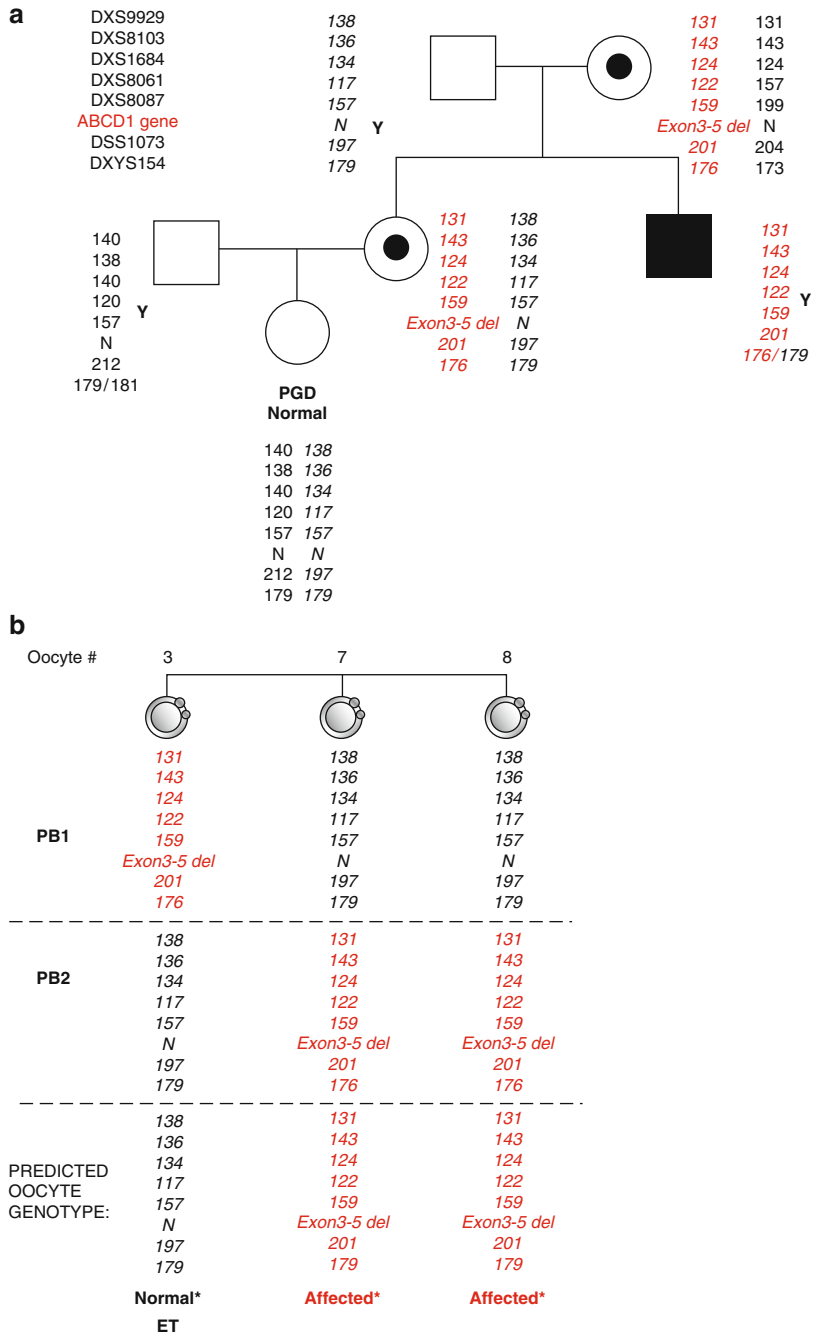

Fig. 3.54 PB-based PGD for X- linked adrenoleukodystrophy (ABCD1 gene). (**a**) Pedigree and table with PGD results of testing for ABCD1 gene and seven linked markers. Haplotypes of the mother and grandmother carrying a mutation are shown in red in the *left column* and the normal haplotypes shown in black on the *right column*. The only maternal brother is affected with mutant allele inherited from their mother (shown in *red*). On the left of the pedigree, an unaffected child, born as a result of PGD, is shown carrying only a normal maternal allele (linked to seven markers). (**b**) As can be seen from the sequential analysis of PB1 and PB2, oocyte #7 and #9 were diagnosed as affected, based on homozygous normal PB1 and mutant PB2, while oocyte #3 was predicted as normal, as evidenced by mutant PB1, confirmed by all seven linked markers, and normal PB2, in agreement with all the linked markers. This embryo was transferred, resulting in a normal singleton pregnancy and the birth of an unaffected child, mentioned

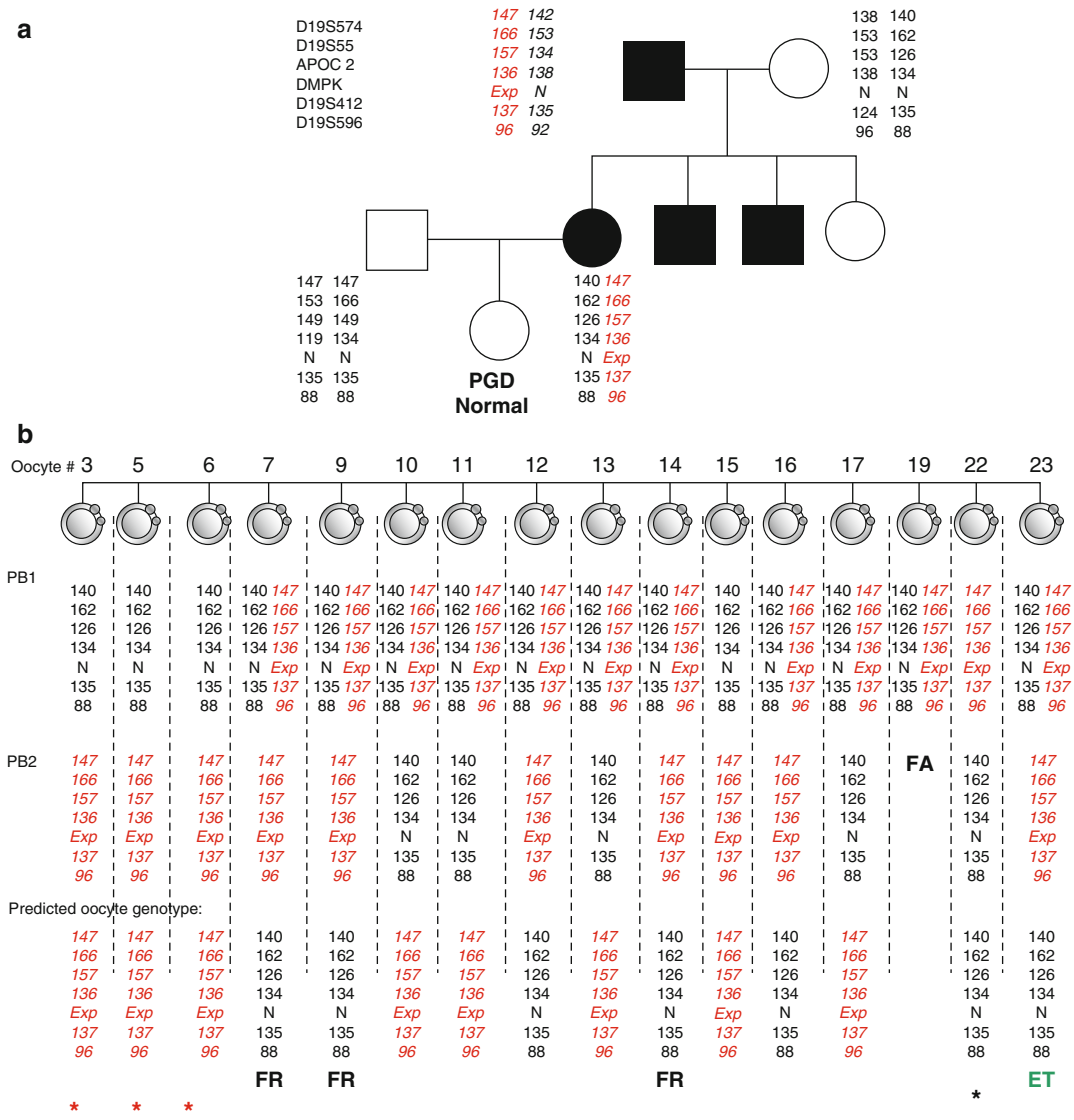

Fig. 3.55 PGD for myotonic dystrophy by sequential PB1 and PB2 analysis. (**a**) Pedigree showing haplotypes of the mother, who inherited an expanded allele of DMPK gene (shown in *red*) from her father (normal haplotype is shown in *black*). Her two brothers are also affected, while the only sister is normal. (**b**) Sixteen oocytes were tested by PB1 (*top*) and PB2 (*middle*) analysis for the presence of the expanded allele in DMPK gene by six polymorphic markers. Embryos, originating from oocytes #7, #9, #12, #14, #16, #22, and #23 were predicted normal based on the presence of the normal maternal chromosome (haplotype) (*black bar*). Embryos #3, #5, #6, #10, #11, #13, #15, and #17 were affected evidenced by the presence of the maternal affected haplotype (*red bar*). PB1 in oocyte #19 was heterozygous, but PB2 did not amplify, so genotype of this oocyte could not be predicted. One embryo originating from oocyte #23 predicted free of expanded allele, based on the presence of heterozygous PB1 and hemizygous affected PB2, was transferred, resulting in a singleton pregnancy and the birth of a normal child (see pedigree)

complex conditions, including Mendelian disorders and chromosomal aneuploidy, originating predominantly from female meiosis. A wider application of the PB approach to PGD of single-gene disorders may be expected with the present tendency of using PB biopsy for testing of chromosomal aneuploidy by microarray technology [106–108], which makes it possible to

perform PGD simultaneously for multiple conditions, including chromosomal aneuploidy and single-gene disorders. So the presented results demonstrate that the PB approach is highly efficient and reliable, providing an extremely high accuracy of PGD for Mendelian disorders. This together with the application of embryo biopsy technique provides a comprehensive diagnostic package, which allows efficient and reliable PGD with extremely high accuracy. As described in Chap. 2, and demonstrated above in the description of our experience, this will in future be applied together with 24-chromosome aneuploidy testing, to ensure the improvement of reproductive outcome of PGD for Mendelian disorders.

References

1. Handyside AH, Kontogiani EH, Hardy K, Winston RML. Pregnancies from biopsied human preimplantation embryos sexed by Y-specific DNA amplification. Nature. 1990;344:768–70.
2. Verlinsky Y, Ginsberg N, Lifchez A, Valle J, Moise J, Strom CM. Analysis of the first polar body: preconception genetic diagnosis. Hum Reprod. 1990;5:826–9.
3. Preimplantation Genetic Diagnosis International Society (PGDIS). 10th International congress on preimplantation genetic diagnosis. Reprod Biomed Online. 2010;20:S1–42.
4. Harper J, Coonen E, De Rycke M, et al. ESHRE preimplantation genetic diagnosis (PGD) consortium data collecttion X: cycles from January to December 2007 with pregnancy follow up to October 2008. Hum Reprod. 2010;25:2685–797.
5. Verlinsky Y, Munne S, Cohen J, et al. Over a decade of preimplantation genetic diagnosis experience – a multi-center report. Fertil Steril. 2004;82:292–4.
6. Kuliev A, Verlinsky Y. Thirteen years' experience of preimplantation diagnosis: report of the fifth international symposium on preimplantation genetics. Reprod Biomed Online. 2004;8:229–35.
7. Kuliev A, Verlinsky Y. Current feature of preimplantation genetic disgnosis. Reprod Biomed Online. 2002;5:296–301.
8. Kuliev A. Expanding indications for PGD. Expert Review of Obstet Gynecol. 2011;6:599–607.
9. Kuliev A, Rechitsky S, Verlinsky O, et al. Preimplantation diagnosis of thalassemia. J Assist Reprod Genet. 1998;15:219–25.
10. Kuliev A, Rechitsky S, Verlinsky O, et al. Birth of healthy children following preimplantation diagnosis for thalassemias. J Assist Reprod Genet. 1999;16:219–25.
11. Kuliev A, Packalchuk T, Verlinsky O, Rechitsky S. Preimplantation diagnosis for hemoglobinopathies. Hemoglobin. 2011;35 5(6:5)47–55. doi: 10.3109/03630269.2011.608457. Epub 2011 Sep 12.
12. Verlinsky Y, Milayeva S, Evsikov S, et al. Preconception and preimplantation diagnosis for cystic fibrosis. Prenat Diagn. 1992;12:103–10.
13. Handyside AH, Lesko JG, Tarin JJ, Winston RM, Hughes MR. Birth of a normal girl after in vitro fertilization and preimplantation diagnosis testing for cystic fibrosis. N Engl J Med. 1992;327:905–9.
14. Goossens V, Sermon K, Lissens W, et al. Clinical application of preimplantation genetic diagnosis for cystic fibrosis. Prenat Diagn. 2000;20:571–81.
15. ESHRE PGD Consortium Steering Committee. ESHRE preimplantation genetic diagnosis (PGD) consortium. Data collecttion II (May 2002). Hum Reprod. 2000;15:2673–83.
16. Online Mendelian Inheritance in Man (OMIM). John Hopkins University. 2001. http://www.ncbi.nlm.nih.gov/Omim.
17. Online Human Gene Mutation Database (HGMD). CELERA. 2004. http://archive.uwcm.ac.uk/uwcm/mg/search/1119297.html.
18. Slaugenhaupt SA, Blumenfekl A, Gill SP, et al. Tissue-specific expression of a splicing mutation in the IKBKAP gene causes familial dysautonomia. Am J Hum Genet. 2001;68:598–605.
19. Blumenfeld A, Slaugenhaupt SA, Liebert CB, et al. Precise genetic mapping and haplotype analysis of the familial dysautonomia gene on human chromosome 9q31. Am J Hum Genet. 1999;64:1110–8.
20. Rechitsky S, Verlinsky O, Kuliev A, Ozen S, Masciangelo C, Lifchez A, Verlinsky Y. Preimplantation genetic diagnsis for familial dysautonomia. Reprod Biomed Online. 2003;6:488–93.
21. Fallon MS, Harton BS, Sisson BS, et al. Preimplantation genetic diagnosis for spinal muscular atrophy type 1. Neurology. 1999;53:1087–90.
22. Daniels G, Pettigrew R, Thornhill A, et al. Six unaffected livebirths following preimplantation diagnosis for spinal muscular atrophy. Mol Hum Reprod. 2001;7:995–1000.
23. Ozelius L, Hewett J, Page CE, et al. The early-onset torsion dystonia gene (DYT1) encodes an AATP-binding protein. Nat Genet. 1997;17:40–8.
24. Ozelius L, Klein C, et al. The TOR1A (DYT1) gene family and its role in early onset torsion dystonia. Genomics. 1999;62:377–84.
25. Valente EM, Povey S, Waener TT, Wood NW, Davis MB. Detailed haplotype analysis in Ashkenazi Jewish and non-Jewish British dystonic patients carrying the GAG deletion in the DYT1 gene: evidence for a limited number of founder mutations. Ann Hum Genet. 1999;63:1–8.
26. Kwiatkovski DJ, Nygaard TG, Schuback DE, et al. Identification of a highly polymprphic microsatellite VNTR within the argininosuccinate synthetase locuc: exclusion of the dystonia gene on 9q32–34 as the cause of dopa-responsive dystonia in a large kindred. Am J Hum Genet. 1991;48:121–8.
27. Risch NJ, De Leon D, Ozelius L, et al. Genetic analysis of idiopathic torsion dystonia in Ashkenazi Jews

and their recent descent from a small founder population. Nat Genet. 1995;9:152–9.
28. Rechitsky S, Strom C, Verlinsky O, et al. Allele drop out in polar bodies and blastemeres. J Assist Reprod Genet. 1998;15:253–7.
29. Rechitsky S, Verlinsky O, Kuliev A, et al. Preimplantation genetic diagnosis for early onset torsion dystonia. Reprod BioMed Online. 2004;8:224–8.
30. De Vos A, Sermon K, De Rijcke M, et al. Preimplantation genetic diagnosis for Charcot-Marie-Tooth disease type 1A. Mol Hum Reprod. 2003;9:429–35.
31. Verlinsky Y, Rechitsky S, Verlinsky O, Strom C. Kuliev A PGD for ornithine transcarbamilase deficiency. Reprod Biomed Online. 2000;1:45–7.
32. Platteau P, Sermon K, Seneca S, et al. Preimplantation genetic diagnosis for Fragile Xa syndrome: difficult but possible. Hum Reprod. 2002;17:2807–12.
33. Garbern J, Hobson G. Prenatal diagnosis of Pelizaeus-Merzbacher disease. Prenat Diagn. 2002;22:1033–5.
34. Garbern J, Krajewski K, Hobson G. PLP1-related disorders. Geneclinics. 2004. Available at http://www.geneclinics.org/profiles/pm.
35. Niemitz EL, Feinberg AP. Epigenetics and assisted reproductive technology: a call for investigation. Am J Hum Genet. 2004;74:599–609.
36. Ray PF, Gigarel N, Bonnefont JP, Attie T, Hamamah S, Frydman N, Vekemans M, Frydman R, Munnich A. First specific preimplantation genetic diagnosis for ornithine transcarbamilase deficiency. Prenat Diagn. 2000;20:1048–54.
37. Verlinsky Y, Rechitsky S, Verlinsky O, Strom C, Kuliev A. Preimplantation testing for pnenylketonuria. Fertil Steril. 2001;76:346–9.
38. Harris PC, Thomas S, Ratcliffe PJ, Breuning MH, Coto E, Lopez-Larrea C. Rapid genetic analysis of families with polycystic kidney disease 1 by means of a microsatellite marker. Lancet. 1991;338:1484–7.
39. Peral B, Ward CJ, San Milan JL, Thomas S, Stalings RL, Moreno F, Harris P. Evidence of linkage desequilibrium in the Spanish polycystic kidney disease I population. Am J Hum Genet. 1994;54:899–908.
40. Snarey A, Thomas S, Shneider MC, Pound SE, Barton N, Wright AF, et al. Linkage desequilibrium in the region of the autosomal dominant polycystic kidney disease gene (PKDI). Am J Hum Genet. 1994;55:365–71.
41. Verlinsky Y, Rechitsky S, Verlinsky O, Ozen S, Beck R, Kuliev A. Preimplantation genetic diagnosis for polycystic kidney disease. Fertil Steril. 2004;82:926–9.
42. Renwick P, Trussler J, Braude P, Ogilvie CM. Preimplantation genetic haplotyping: 127 diagnostic cycles demonstrating a robust, efficient alternative to direct mutation testing on single cells. Reprod Biomed Online. 2010;20:470–6.
43. Altarescu GPI, Brooks BC, Margalioth EC, EldarGeva TC, Levy-Lahad EC, Renbaum PPI. Simultaneous preimplantation genetic diagnosis for Tay-Sachs and Gaucher disease. Reprod Biomed Online. 2007;15:83–8.
44. Rechitsky S, Pomerantseva K, Pakhalchuk T, Polling D, Verlinsky O, Kuliev A. First systematic experience of preimplantation genetic diagnosis for de novo mutations. Reprod BioMed Online. 2011;22:350–61.
45. Cohn DH, Rtartman BJ, Blumberg B, Bayers PH. Recurrence of lethal osteogenesis imperfecta due to paternal mosaicism for a dominant mutation in a type I collagene gene (COLIAI). Am J Hum Genet. 1990;64:1632–7.
46. Kirchman TT, Levy ML, Lewis RA, Kanzler MH, Nelson DL, Scheuerle AE. Gonadal mosaicism fir incontinentia pigmenti in a healthy male. J Med Genet. 1995;32:887–90.
47. Verhoef S, Bakker L, Tempelaars AMP, et al. High rate of mosaicism in tuberous sclerosis complex. Am J Hum Genet. 1999;64:1632–7.
48. Carlson EA, Desnick RJ, Opitz JM. Mutational mosaicism and genetic counseling in retinoblastoma. Am J Med Genet. 2005;4:365–81.
49. Consoli C, Moss C, Green S, Balderson D, Cooper D, Upadhyaya M. Gonosomal mosaicism for a nonsence mutation (R1947X) in the NF1 gene in segmental neurofibromatosis type 1. J Invest Dermatol. 2005;125:463–6.
50. Schwab AL, Tuohy TMF, Condie M, Neklason DW, Burt RW. Gonadal mosaicism and familial adenomatous polyposis. Fam Cancer. 2008;7:173–7.
51. Rechitsky S, Verlinsky O, Chistokhina A, et al. Preimplantation genetic diagnosis for cancer predisposition. Reprod Biomed Online. 2002;4:148–55.
52. Rechitsky S, Kuliev A. Novel indications for preimplantation genetic diagnosis. 10th annual international congress on preimplantation genetic disgnosis, 5–8 May 2010, Montpellier, France. Reprod Biomed Online. 2010;20(Suppl):S1–2.
53. Verlinsky Y, Rechitsky S, Verlinsky O, et al. Preimplantation diagnosis for p53 tumor suppressor gene mutations. Reprod Biomed Online. 2001;2:102–5.
54. Holstein M. p53 mutations in human cancers. Science. 1991;253:49–53.
55. Huson SM, Compston DAS, Clark P, Harper PS. A genetic study of von Recklinghausen neurofibromatosis in Southeast Wales I prevalence, fitness, mutation rate, and the effect of parental transmission on severity. J Med Genet. 1989;26:704–11.
56. Clementi M, Barbujani G, Trolla L, Tenconi R. Neurofibromatosis −1: maximum likelihood estimation of mutation rate. Hum Genet. 1990;84:116–8.
57. Simpson JL. Celebrating preimplantation genetic diagnosis of p53 mutations in Li-Fraumeni syndrome. Reprod Biomed Online. 2001;3:2–3.
58. Cram D. Preimplantation genetic diagnosis for familial cancer. Reprod Biomed Online. 2001;3:3–4.
59. Klose A, Robins PN, Gewies A, et al. Two novel mutations in exon 19a and 20 and BsaI polymorphism in a newly characterized intron of the neurofibromatosis type 1 gene. Hum Genet. 1998;102:367–71.
60. Xu G, Nelson L, O'Connell P, White R. An Alu polymorphism intragenic to the neurofobromatosis type 1 gene. Nucleic Acids Res. 1992;19:3764.

61. Hoffmeyer S, Assum G. An Rsa I polymorphism in the transcribed region of the neurofibromatosis (NF1) – gene. Hum Genet. 1994;93:481–2.
62. Weissenbach J, Gyapay G, Dib C, Vignal A, Morisetti J, Milasseau P, Vaysseix G, Lathrop M. A second-generation linkage map of the human genome. Nature. 1992;359:794–801.
63. Legoix P, Legrand M-F, Ollagnon E, Lenoir G, Thomas G, Zucman-Rossi J. Characterization of 16 polymorphic markers in the NF2 gene: application to hemizygosity detection. Hum Mutat. 1999;13:290–3.
64. Rechitsky S, Strom C, Verlinsky O, et al. Accuracy of preimplantation diagnosis of single-gene disorders by polar body analysis of oocytes. J Assist Reprod Genet. 1999;16:192–8.
65. Rechitsky S, Verlinsky O, Strom C, et al. Experience with single-cell PCR in preimplantation genetic diagnosis: how to avoid pitfalls. In: Hahn S, Holzgreve W, editors. Fetal cells in maternal blood. New developments for a new millennium. 11th Fetal cell workshop. Basel: Karger; 2000. p. 8–15.
66. Verlinsky Y, Rechitsky S, Verlinsky O, et al. Preimplantation diagnosis for newrofibromatosis. Reprod Biomed Online. 2002;4:102–5.
67. Jasper MJ, Liebelt J, Hussey ND. Preimplantation genetic diagnosis for cancer predisposition syndromes. Prenat Diagn. 2007;27:447–56.
68. Sagi M, Weinberg N, Eilat A, et al. Preimplantation genetic diagnosis for BRCA1 exon 13 duplication mutation using linked polymorphic markers resulting in a live birth. Prenat Diagn. 2008;28:292–8.
69. Moutou C, Gardes N, Nicod JC, Viville S. Preimplantation genetic diagnosis for BRCA1/2 – a novel clinical experience. Eur J Obstet Gynecol Reprod Biol. 2009;45:9–13.
70. Vadaparampil ST, Quinn GP, Knapp C, Malo TL, Friedman S. Factors associated with preimplantation genetic diagnosis acceptance among women concerned about hereditary breast and ovarian cancer. Genet Med. 2009;11:757–65.
71. Quinn GP, Vadaparampil ST, King LM, Miree CA, Friedman S. Familial cancer. Conflict between values and technology: perceptions of preimplantation genetic diagnosis among women at increased risk for hereditary breast and ovarian cancer. Fam Cancer. 2009;8:441–9.
72. Ao A, Wells D, Handyside A, Winston R, Delhanty J. Preimplantation genetic diagnosis of inherited cancer: familial adenomatous polyposis coli. J Assist Reprod Genet. 1998;15:140–4.
73. Taylor MD, Gokgoz N, Andrulis IL, et al. Familial posterior fossa brain tumors of infancy secondaty to germline mutation of the hSNF5 gene. Am J Hum Genet. 2000;66:1403–6.
74. Verlinsky Y, Rechitsky S, Verlinsky O, et al. Preimplantation diagnosis for early onset Alzheimer disease caused by V717L mutation. JAMA. 2002;287:1018–21.
75. Sherington R, Rogaev EI, Liang Y, et al. Cloning of the gene bearing missense mutations in early onset familial Alzheimer disease. Nature. 1995;375:754–60.
76. Levy-Lehad E, Wasco W, Poorkaj P, et al. Candidate gene for the chromosome 1 familial Alzheimer's disease locus. Science. 1995;269:973–7.
77. Goate AM, Chantier-Harlin MC, Mullan M, et al. Segregation of missense mutation in the amyloid precursor protein gene with familial Alzheimer disease. Nature. 1991;349:704–6.
78. Murrel J, Hake AM, Quaid KA, Farlow MR, Ghetti B. Early-onset Alzheimer disease caused by a new mutation (V717L) in the amiloid precursor proteen gene. Arch Neurol. 2000;57:885–7.
79. Tupler R, Rogaeva E, Vaula G, et al. A highly informative microsatellite repeat polymorphism in intron 1 of the human amyloid precursor protein (APP) gene. Hum Mol Genet. 1993;2:620–1.
80. He J, McDermont DA, Song Y, Gilbert F, Kligman I, Basson C. Preimplantation genetic diagnosis of human congenital heart disease and Holt-Oram syndrome. Am J Med Genet. 2004;126A:93–8.
81. Papadopoulou LC, Sue CM, Davidson MM, et al. Fatal infantile cardioencephalomyopathy with COX deficiency and mutations in SCO2, a COX assembly gene. Nat Genet. 1999;23:333–7.
82. Lee S, Zambas E, Wu X, Reid M, Zelinsky T, Redman C. Molecular basis of the kell (K1) phenotype. Blood. 1995;85:912–6.
83. Lee S, Zambas E, Green ED, Redman C. Organization of the gene for encoding the human kell group protein. Blood. 1995;85:1364–70.
84. Purohit KR, Weber JL, Ward LJ, Keats JB. The kell blood group locus is close to the cyctic fibrosis locus on chromosome 7. Hum Genet. 1992;89:457–8.
85. Reid ME, Rios M, Powell VI, Charles-Pierre D, Malavade V. DNA from blood samples can be used to genotype patients who have recently received a transfusion. Transfusion. 2000;40:48–53.
86. Zielenski J, Rozmahel R, Bozon D, Kerem BS, Grzelczak Z, Riordan J, Rommens J, Tsui L-H. Genomic DNA sequence of the cystic fibrosis transmembrane conductance regulator (CFTR) gene. Genomics. 1991;10:214–28.
87. Chehab FF, Johnson J, Louie E, Goossens M, Kawasaki E, Elrich H. A dimorphic 4-bp repeat in the cystic fibrosis gene is in absolute linkage disequilibrium with the delta F508 mutation: implications for prenatal diagnosis and mutation origin. Am J Hum Genet. 1991;48:223–6.
88. Van Den Veyver IB, Chong SS, Cota J, et al. Fetus-placenta-newborn: single cell analysis of the RhD blood type for use in preimplantation diagnosis in the prevention of severe haemolitic disease of the newborn. Am J Obstet Gynecol. 1995;172:533–40.
89. Secho SKM, Burton G, Leigh D, Marshall JT, Pearsson JW, Morris JM. The role of PGD in the management of severe alloimmunization: first unaffected pregnancy. Case report. Hum Reprod. 2005;20:697–701.
90. Verlinsky Y, Rechitsky S, Seckin O, Masciangelo C, Ayers J, Kuliev A. Preimplantation diagnosis for kell genotype. Fertil Steril. 2003;80:1047–51.

91. Muenke M, Gurrieri F, Bay C, et al. Linkage of a human brain malformation, familial holoprosencephaly, to chromosome 7 and evidence for genetic heterogeneity. Proc Natl Acad Sci USA. 1994;91:8102–6.
92. Nanni L, Ming JE, Bocian M, et al. The mutational spectrum of the sonic hedgehoc gene in holoprosencephaly: SHH mutations cause a significant proportion of autosomal dominant holoprosencephaly. Hum Mol Genet. 1999;8:2479–88.
93. Verlinsky Y, Rechitsky S, Verlinsky O, et al. Preimplantation diagnosis for sonic hedgehog mutation causing familial holoprosencephaly. N Engl J Med. 2003;348:1449–54.
94. Abou-Sleiman PM, Apessos A, Harper JC, Serhal P, Delhanty JDA. Pregnancy following preimplantation genetic diagnosis for Crouson syndrome. Mol Hum Reprod. 2002;8:304–9.
95. Verlinsky Y, Rechitsky S, Schoolcraft, Kuliev A. Preimplantation diagnosis for homeobox Gene HLXB9 mutation causing currarino syndrome. Am J Med Genet. 2005. Part A, 134A:103–104.
96. Ross AJ, Rui-Perez V, Wang Y, Hagan DM, Scherer SW, Lynch SA, Lindssy S, Custard E, Belloni E, Wilson DI, Wadey R, Goodman F, Orstavic KH, Monclair T, Robson S, Reardon W, Burn J, Scambler P, Strachan T. A homeobox gene, HLXB9, is the major locus for dominantly inherited sacral agenesis. Nat Genet. 1998;20:358–61.
97. Belloni E, Martucciello G, Verderio D, Ponti E, Seri M, Jasonni V, Torre M, Ferrari M, Tsui L-C, Scherer SW, et al. Involvement of the HLXB9 homeobox gene in Currarino syndrome. Am J Hum Genet. 2000; 66:312–9.
98. Hagan DM, Ross AJ, Strachan T, Lynch SA, Ruiz-Perez V, Wang YM, Scambler P, et al. Mutation analysis and embryonic expression of the HLXB9 Currarino syndrome gene. Am J Hum Genet. 2000;66: 1504–15.
99. Kochling J, Karbasiyan M, Reis A. Spectrum of mutations and genotype-phenotype analysis in Currarino syndrome. Eur J Hum Genet. 2001;9: 599–605.
100. Reardon W, Winter RM, Rutland P, et al. Mutations in the fibroblast growth factor gene cause Crouzon syndrome. Nat Genet. 1994;8:98–103.
101. Cohen MM, Kreiborg S. Birth prevalence studies of the Crouzon syndrome: comparison of direct and indirect methods. Clin Genet. 1992;41:12–5.
102. Sermon K, Lissens W, Joris H, et al. Clinical application of preimplantation diagnosis for myotonic dystrophy. Prenat Diagn. 1997;17:925–32.
103. Sermon K, Seneca S, Vanderfaeillie A, et al. Preimplantation diagnosis for fragile X syndrome based on the detection of the non-expanded paternal and maternal CGG. Prenat Diagn. 1999;19: 1223–30.
104. Sermon K, Seneca S, De Rycke M, et al. PGD in the lab for triplet diseases-myotonic dystrophy, Huntington's disease and Fragile-X syndrome. Mol Cell Endocrinol. 2001;183:S77–85.
105. Verlinsky Y, Rechitsky S, Verlinsky O, Strom C, Kuliev A. Polar body based preimplantation diagnosis for X-linked genetic disorders. Reprod Biomed Online. 2002;4:38–42.
106. Geraedts J, Collins J, Gianaroli L, et al. What next for preimplantation genetic screening? A polar body approach. Hum Reprod. 2010;25:575–7.
107. Geraedts J, Montag M, Magli C, et al. Polar body array CGH for prediction of the status of the corresponding oocyte. Part I: clinical results. Hum Reprod. 2011;26:3172–80.
108. Magli C, Montag M, Koster M, et al. Polar body array CGH for prediction of the status of the corresponding oocyte. Part II: technical aspects. Hum Reprod. 2011;26(11):3181–5. doi: 10.1093/humrep/der295. Epub 2011 Sep 9.